MONASH University

AN INVESTIGATION OF THE GENETIC AND NEURAL CORRELATES OF EXECUTIVE DYSFUNCTION IN FEMALE FRAGILE X PREMUTATION CARRIERS

Annie Shelton BBNSc (Hons)

A thesis submitted for the degree of *Doctor of Philosophy* (PhD)
September, 2016.

School of Psychological Sciences and Monash Institute of
Cognitive and Clinical Neurosciences
Faculty of Medicine, Nursing and Health Science
Monash University, Victoria

© Annie L Shelton (2016)

I certify that I have made all reasonable efforts to secure copyright permissions for third-party content included in this thesis and have not knowingly added copyright content to my work without the owner's permission.

TABLE OF CONTENTS

ABSTRACT

Fragile X syndrome is a neurodevelopmental disorder which represents one of the most common genetic risk factors for autism. Fragile X syndrome is the consequence of a large (>200) trinucleotide CGG repeat expansion, in the 5' UTR region of the Fragile X mental retardation gene 1 (*FMR1*), located on the X chromosome. However, smaller *FMR1* premutation (PM) expansions (55-199 CGG repeats) are more common (approximately 1 in 209 females and 1 in 430 males), and confer a risk of a number of medical, psychiatric and cognitive conditions, as well as Fragile X tremor-ataxia syndrome (FXTAS). Estimated to effect up to 40% of PM males, and up to 16% of PM females over 50 years of age, FXTAS is characterised by intention tremor, cerebellar gait ataxia, and cognitive dysfunction (specifically executive dysfunction and dementia), corresponding with changes in neuroanatomy (generalised atrophy as well as hyperintensities in the middle cerebellar peduncles, brainstem and corpus callosum). It is hypothesised that FXTAS is the consequence of an *FMR1* mRNA toxic-gain of function, given that PM individuals tend to exhibit increased levels of *FMR1* mRNA, compared to those with normal *FMR1* alleles (<45 CGG repeats). However, there is increasing evidence of both neuroanatomical changes and cognitive dysfunction in PM-carriers without FXTAS. Specifically, cortical and subcortical atrophy, a reduction in white matter integrity, and compensatory patterns of neural activation, have been well documented in PM males without FXTAS, as well as executive dysfunction on tasks reliant on response inhibition and working memory processes. These changes indicate disruption to cortico-cerebellar processing. It does however; remain unclear whether PM females without FXTAS experience analogous deficits and whether genetic and neural changes (within the cortico-cerebellar network) influence PM-related dysfunction.

Accordingly, the principal aim of this thesis was to investigate whether PM females without FXTAS, like their male counterparts, experience executive dysfunction on tasks reliant on response inhibition and working memory processes. To establish this, a range of

neuropsychological and ocular motor saccadic paradigms were employed. Saccadic paradigms are a sensitive neuromotor tool for investigating cognitive function, with well-defined sensorimotor processes that produce precise and stereotyped output with known neural correlates. Inter-relationships between executive (dys)function, genetic (CGG, DNA methylation and *FMR1* mRNA) and neural (structural and functional) markers were also explored, facilitating inferences concerning the biological source of cortico-cerebellar disruption.

Herein, a series of six experimental chapters provide a comprehensive assessment of the biological correlates of executive dysfunction in PM females without FXTAS. Results revealed deficits of executive function were most prevalent in tasks requiring rapid resolution of responses (**Chapter 2**). This was most evident for saccade paradigms examining response inhibition and working memory processes, for which we reveal correlations between performance and genetic indices (**Chapter 3 and 4**). Correlations were also revealed between executive dysfunction (measures derived from an executive control saccade task), and *FMR1* intron 1 methylation markers. These methylation markers can influence gene function through expression of long non-coding RNAs, and were also found to correspond with measures of cortical grey matter (**Chapter 6**). Meanwhile *FMR1* mRNA levels were found to correlate with measures of white matter integrity (**Chapter 7**). Finally, clear dissociations were revealed between PM females without FXTAS and controls with respect to i) grey matter neural activation (**Chapter 5**); ii) grey matter structure (**Chapter 6**) and iii) white matter microstructure (**Chapter 7**) and executive dysfunction.

Collectively, the biological findings from this work suggest two possible molecular mechanisms for cortico-cerebellar pathway disruption: i) changes in *FMR1* intron 1 methylation which affect grey matter structure through long non-coding RNAs, and ii) increased *FMR1* mRNA which alters white matter microstructure. This second pathway, in particular, may represent early FXTAS-related changes.

GENERAL DECLARATION

This thesis contains no material which has been accepted for the award of any other degree or diploma at any university or equivalent institution and that, to the best of my knowledge and belief, this thesis contains no material previously published or written by another person, except where due reference is made in the text of the thesis.

Signature: ……

Print Name: ……

Date: ……..

THESIS OVERVIEW

In accordance with Monash University Doctorate Regulation 17 the following declarations are made:

I hereby declare that this thesis contains no material which has been accepted for the award of any other degree or diploma at any university or equivalent institution and that, to the best of my knowledge and belief, this thesis contains no material previously published or written by another person, except where due reference is made in the text of the thesis.

This thesis includes three original papers published in peer reviewed journals and three manuscripts submitted and under review. The core theme of the thesis is to investigate the biological correlates of executive dysfunction in *FMR1* premutation females without FXTAS. The ideas, development and writing up of all the papers in the thesis were the principal responsibility of myself, the student, working within the Ocular Motor Research Laboratory under the supervision of Associate Professor Joanne Fielding and Professor Kim Cornish.

The inclusion of co-authors reflects the fact that the work came from active collaboration between researchers and acknowledges input into team-based research.

In the case of Chapters 2-7 my contribution to the work involved the following:

Chapter	Publication Title	Status	% of student contribution	Co-author name(s)
2	Executive dysfunction in female *FMR1* premutation carriers	In press	80%	Kim Cornish, Claudine Kraan, Reymundo Lozano, Minh Bui, & Joanne Fielding
3	Exploring inhibitory deficits in female carriers of fragile X syndrome: through eye movements	Published	80%	Kim Cornish, Claudine Kraan, Darren R. Hocking, Nellie Georgiou-Karistianis, Sylvia A. Metcalfe, John L Bradshaw, Alison D. Archibald, Jonathan Cohen, Julian N. Troller, & Joanne Fielding
4	Delineation of the working memory profile in female *FMR1* premutation carriers: The effect of cognitive load on ocular motor responses	Published	80%	Kim Cornish, David Godler, Meaghan Clough, Claudine Kraan, Minh Bui, & Joanne Fielding
5	Disassociation between brain activation and executive function in Fragile X premutation females	Published	75%	Kim Cornish, Meaghan Clough, Sanuji Gajamange, Scott Kolbe, & Joanne Fielding
6	Brain structure and intragenic DNA methylation are correlated, and predict executive dysfunction in fragile X premutation females	Published	70%	Kim Cornish, Scott Kolbe, Meaghan Clough, Howard R. Slater, Xin Li, Claudine Kraan, Minh Bui, David E. Godler, & Joanne Fielding
7	White matter microstructure relates to cognition and *FMR1* mRNA in Fragile X premutation Females	Under review	80%	Kim Cornish, David E. Godler, Minh Bui, Scott Kolbe, & Joanne Fielding

I have renumbered sections of submitted or published papers, and combined citations into a single reference list, in order to generate a consistent presentation within the thesis.

Student signature:  Date: 15.9.16

The undersigned hereby certify that the above declaration correctly reflects the nature and extent of the student's and co-authors' contributions to this work.

Main Supervisor signature:  Date: 15.9.16

PUBLICATION AND PRESENTATIONS

JOURNAL PUBLICATIONS

Shelton, A. L., Cornish, K., Clough, M., Gajamange, S., Kolbe, S., & Fielding, J. (2016) Disassociation between brain activation and executive function in fragile X permutation females. *Human Brain Mapping,* In press.

Shelton, A. L., Cornish, K. M., Kolbe, S., Clough, M., Slater, H. R., Li, X., Kraan, C. M., Bui, Q. M., Godler, D. E., & Fielding J. (2016). Brain structure and intragenic DNA methylation are correlated, and predict executive dysfunction in fragile X permutation females. *Translational Psychiatry,* 6 (12), e984.

Shelton, A. L., Cornish, K. M., Kraan, C. M, Lozano, R., Bui, M., Fielding, J. (2016) Executive Dysfunction in Female *FMR1* Premutation Carriers. *Cerebellum,* 15 (5), 565-569.

Hall, D. A., Robertson, E., **Shelton, A. L.**, Losh, M. C., Milá, M., Granell Moreo, E., Gomez-Anson, B., Martinex-Cerdeño, V., Grigsby, J., Lozano, R., Hagerman, R., Santa Maria, L., Berry-Kravis, E., O'Keefe, J. A. (2016). Update on the Clinical, Radiographic, and Pathological Manifestations in FXTAS and FMR1 Premutation Carriers. *Cerebellum,* 15 (5), 578-586.

Shelton, A. L., K. M. Cornish, D. E. Godler, M. Clough, C. Kraan, M. Q. Bui and J. Fielding. (2015). Delineation of the Working Memory Profile in Female Fmr1 Premutation Carriers: The Effect of Cognitive Load on Ocular Motor Responses. *Behavioural Brain Research,* 282 (1), 194-200.

Shelton, A. L., K. Cornish, C. Kraan, N. Georgiou-Karistianis, S. A. Metcalfe, J. L. Bradshaw, D. R. Hocking, A. D. Archibald, J. Cohen, J. N. Troller and J. Fielding. (2014). Exploring Inhibitory Deficits in Female Premutation Carriers of Fragile X Syndrome: Through Eye Movements. *Brain and Cognition*, 85, 201-208.

Shelton, A., Kraan, C., Cornish, K., & Fielding, J. (2012). The use of eye movements to detect cognitive changes in carriers of medium expansions of the *FMR1* gene. *Frontiers in Human Neuroscience*. Conference Abstract: ACNS-2012 Australasian Cognitive Neuroscience Conference.

PROFESSIONAL PRESENTATIONS

Shelton, A., Cornish, K., Godler, D., Kolbe, S., Vera, S., Kraan, C., & Fielding, J. (2016). Cortical and cerebellar links to reductions in *FMR1* mRNA expression in female premutation carriers. *Oral Presentation: 15th International Fragile X Conference,* San Antonio, United States.

Gajamange, S., Raffelt, D., Dhollander, T., **Shelton, A. L.**, White, O., Kilpatrick, T., Connelly, A., Fielding, J. Kolbe, S. C. (2016). Apparent Fiber Density: A novel method to detect axonal degeneration in patients with MS. *Poster Presentation: 32nd European Committee for Treatment and Research in Multiple Sclerosis,* London, United Kingdom.

Shelton, A., Cornish, K., Godler, D., Bui, M., Kraan, C., & Fielding, J. (2015). RNA toxicity and brain imaging in *FMR1* premutation carrier women. *Invited Speaker: Fragile X Related Disorders Symposium*, Melbourne, Australia.

Shelton, A. L., K. Cornish, D. E. Godler, C. Kraan and J. Fielding. (2015). Processing speed deficits are significantly correlated with reduced cortical and cerebellar structural volumes in *FMR1* Premutation Women. *Oral Presentation: 2nd International Conference on FMR1 Premutation: Basic Mechanisms and Clinical Involvement*, Sitges, Spain.

Boonstra, F., Gajamange, S., **Shelton, A.** Clough, M. White, C. Fielding, J. & Kolbe, S. (2015). Neural correlates of cognitive variation in patients with clinically isolated syndrome. *Poster Presentation: ECTRIMS European Committee for Treatment and Research in Multiple Sclerosis*, Barcelona, Spain.

Shelton, A., Cornish, K., Godler, D., Vera, S., Kraan, C., Kolbe, S., & Fielding, J. (2015). An integrative gene-brain-behaviour approach to understanding the *FMR1* premutation phenotype. *Poster Presentation: Students of Brain Research Student Symposium*, Melbourne, Australia.

Gajamanage, S., Raffelt, D., Connelly, A., **Shelton, A.,** White, O., Kilpatrick, T., Fielding, J., & Kolbe, S. (2015) Apparent Fibre Density: A novel method to detect axonal degeneration in patients with clinically isolated syndromes. *Poster Presentation: Students of Brain Research Student Symposium*, Melbourne, Australia.

Shelton, A., Cornish, K., Kraan, C., & Fielding, J. (2012). The use of eye movements to detect cognitive changes in carriers of medium expansions of the FMR1 gene. *Oral Presentation: ACNS-2012 Australasian Cognitive Neuroscience Conference*, Brisbane, Australia.

AWARDS AND DISTINCTIONS

Monash Postgraduate Publication Award 2016
Australian Postgraduate Award 2013 – 2016
Award for Best Presentation ECR/PhD at the 2nd International Conference on *FMR1* Premutation: Basic Mechanisms and Clinical Involvement, Sitges, Spain, 2015.
Postgraduate Travel Grant 2015

PROFESSIONAL MEMBERSHIPS

Australian Cognitive Neuroscience Society student member
Royal Society of Victoria member

SOCIETAL CONTRIBUTIONS AND PROFESSIONAL DEVELOPMENT

PSY3180 Human neuropsychology – Developmental and neurodegenerative disorders (Fragile X-Associated Disorders) (2016). Specific contribution: Guest lecturer

Completed the Melbourne Neuroscience Institute Advanced Neuroscience Workshop in MRI (2015).

ACKNOWLEDGEMENTS

This thesis is the culmination of a four-and-a-half-year partnership with my supervisors, Associate Professor Joanne Fielding and Professor Kim Cornish, who truly believed I was capable to take on this project, and all of its challenges. Throughout our journey, they have constantly shared and instilled their expertise, wisdom and passion for research in me. More importantly, they have shown me that a career in research, and maintaining a work-life balance, is possible and within my reach.

In particular to Jo, who has been so generous with her time and support. Whether it was responding to my emails within minutes, providing feedback within days (if not hours), or our chats about research and life in general – it has all been invaluable, and I could never thank her enough.

I would also like to thank my collaborators. Firstly, to Dr David Godler, whose energy and enthusiasm for genetics is contagious, and I sincerely thank him for all his insights and suggestions. Secondly, to Dr Scott Kolbe, who patiently taught me how to analyse MRI data, keeping me focused on the big picture, and welcoming me into the Neuroimaging Lab.

My thanks also goes to the members of the Neuroimaging Lab, and in particular to Sanuji, for sharing their skills, knowledge, and above all else, friendship with me over the last two years.

I would also like to express my sincere appreciation to the Fragile X Association of Australia and the women who kindly gave up their time to participate and share their stories with me. They are truly a remarkable group of women who provided endless inspiration to me for which I am very thankful.

I am also truly grateful to my friends, in particular to Georgia, Hannah, Hannah, Kate, Margherita, Melissa and last but not least Mikaela. The excitement, interest and never-ending support they have shown for me and my research has been overwhelming. Thank you for the laughs, prep-talks and most of all – for keeping me sane.

Above all, I would like to thank my family, for the endless support and encouragement. In particular to my parents, thank you taking this journey with me, for keeping my life in order and always believing in me. Finally, to Dave, who is the most patient person I know, and ever tolerant and supportive – thank you.

ABBREVIATIONS

AR	Activation ratio
BDS	Behavioural dyscontrol scale
CC	Corpus Collosum
CGG	Cytosine-Guanine-Guanine
COWAT	Controlled oral word association test
CpG	Cytosine - phosphate - Guanine
DLPFC	Dorsolateral prefrontal cortex
DTI	Diffusion tensor imaging
FA	Fractional anisotropy
FEF	Frontal eye fields
FEP	Final eye position
FM	Full mutation (>200 CGG repeats)
FMR1	Fragile X mental retardation 1 gene
fMRI	Functional magnetic resonance imaging
FMRP	Fragile X mental retardation protein
FREE2	Fragile X-related epigenetic element 2
FXPOI	Fragile X-associated primary ovarian insufficiency
FXS	Fragile X syndrome
FXTAS	Fragile X-associated tremor/ataxia syndrome
ICP	Inferior cerebellar peduncle
IPS	Intraparietal sulcus
MCP	Middle cerebellar peduncle
MD	Mean diffusivity

MRI	Magnetic resonance imaging
mRNA	Messenger RNA
PASAT	Paced auditory serial addition test
PCR	Polymerase chain reaction
PM	Premutation (55-199 CGG repeats)
PM-carrier	Premutation carrier
ROI	Region of interest
SCP	Superior cerebellar peduncle
SDMT	Symbol digit modalities test
SEF	Supplementary eye fields
SMG	Supramarginal gyrus
TBSS	Tract based spatial statistics
VLPFC	Ventrolateral prefrontal cortex
WASI	Weschler abbreviated scale of intelligence
WMeffect	Working memory effect
XCI	X-chromosome inactivation

CHAPTER 1: LITERATURE REVIEW

UNDERSTANDING THE *FMR1* PREMUTATION CARRIER PHENOTYPE

There are over 150 X-chromosome linked syndromes known to affect intellectual, neuromotor, somatic, metabolic and behavioural functioning (Stevenson *et al.*, 2012). The X-chromosome contains approximately 5% of the mammalian genome, and is sex determining - females have two X-chromosomes, while males have one X-chromosome and one Y-chromosome (Schaffner, 2004). Due to X-chromosome inactivation (XCI), or the silencing of one X-chromosome in females, the prevalence of X-linked disorders varies between genders. This is the case for Fragile X syndrome (FXS), where the incidence rate is higher in males (approximately 1 in 2,500-4000) than females (approximately 1 in 5,000-8,000) (Coffee *et al.*, 2009; McLennan *et al.*, 2011).

FXS is the result of a large trinucleotide (CGG) full mutation (FM) expansion (>200 CGG repeats) in the 5' UTR region of the Fragile X mental retardation gene 1 (*FMR1*), located on the X chromosome. This large expansion results in allelic silencing, a loss (complete or near complete) of the Fragile X mental retardation protein (FMRP), and a clinical phenotype characterised by developmental delay, physical features, psychological and behavioural/cognitive affects. Indeed, FXS is the most commonly inheritable form of intellectual disability, and a monogenetic risk factor for autism.

However, smaller premutation expansions (PM) of *FMR1* (55-199 CGG repeats) are more common than FM, affecting approximately 1 in 209 females and 1 in 430 males (Tassone *et al.*, 2012). It was originally thought that carriers of PM expansions (PM-carriers) were unaffected by the gene's mutation, and that they simply bore the risk of transmitting an expanded allele to offspring. This is no longer considered to be the case, and PM-carriers

confer a risk of a further two other Fragile X-associated disorders (FXDs): Fragile X-associated tremor/ataxia syndrome (FXTAS) and Fragile X-associated primary ovarian insufficiency (FXPOI), as well as a number of medically related disorders. The expression of these distinct syndromes (FXS, FXTAS, FXPOI) provides the ideal opportunity to understand how changes in genomic structure can result in diverse, yet well documented clinical phenotypes.

This section of the review will provide a general overview of the genetic and molecular changes associated with the *FMR1* gene, as well as providing evidence for, a clinical, neural and cognitive phenotype associated with carrying a PM.

1.1 GENETICS AND EPIGENETICS

FMR1 CGG repeat lengths are classified into four categories: i) normal, ii) grey-zone, iii) PM and iv) FM, each featuring different levels of promotor methylation, *FMR1* mRNA, FMRP and ultimately resulting in differing phenotypes (Table 1.1). With respect to the relationships between these characteristics, there is an inverse relationship between increasing CGG repeat size and decreasing (to the point of silencing) FMRP levels across the *FMR1* continuum of repeat lengths from normal to FM. However, this relationship does not hold for *FMR1* mRNA levels and thus transcription of FMRP. In the FM, methylation of the *FMR1* promotor site results in reduced *FMR1* mRNA and an absence of, or limited transcription of, FMRP, the cause of FXS symptomology [see (Oostra and Willemsen, 2009) for a full review].

Conversely, PM expansions result in a 3-8 fold *increase* in *FMR1* mRNA levels, compared with normal *FMR1* alleles (Tassone *et al.*, 2000; Hagerman and Hagerman, 2013), yet due to translational inefficiency, a slight decrease in FMRP levels in high repeat PM-carriers (Tassone *et al.*, 2000).

Table 1.1: *FMR1* allele categories and associated genetic, epigenetic and clinical phenotype features

	Normal Allele	Grey-Zone Allele	PM Allele	FM Allele
CGG repeat	Less than 44	45 - 54	55 - 199	Over 200
Methylation	Unmethylated promotor	Unmethylated promotor	Unmethylated promotor	Most have a methylated promotor
FMR1 mRNA	Normal	Unknown	Elevated 3-8 fold	Low-absent
FMRP	Normal	Unknown	Reduced	Low-absent
Phenotype	-	Risk for FXPOI, FXTAS and parkinsonism	Risk for FXPOI, FXTAS and other clinical symptoms	Mild to severe features of Fragile X syndrome

Offspring may inherit a FM from either a FXS parent or a PM mother. The *FMR1* trinucleotide repeat is somewhat unstable, and may expand from a PM to a FM within one generation, during oogenesis (Moutou *et al.*, 1997). The risk of expansion to a FM is influenced by CGG repeat length and AGG interruptions (Nolin *et al.*, 2011; Yrigollen *et al.*, 2012; Nolin *et al.*, 2013). AGG interruptions within the *FMR1* CGG sequence are thought to help *stabilise* the gene, in that the risk of expansion from a PM to a FM decreases by approximately 60% in PM females with a CGG of 75 and 2 or 3 AGG interruptions compared to a PM female with a CGG of 75 and 0 AGG interruptions (Yrigollen *et al.*, 2014a; Yrigollen *et al.*, 2014b). Finally, maternal age also increases the risk of genetic expansion (Yrigollen *et al.*, 2014a). Hence, maternal age, CGG repeat length and AGG interruptions should be considered when evaluating the risk of *FMR1* genetic expansion.

FMR1 messenger RNA (*FMR1* mRNA)

Although the specific molecular changes that result in PM-related clinical phenotypes (FXTAS and FXPOI) are not yet definitive, it has been hypothesised that increased levels of *FMR1* mRNA drive a RNA-toxic gain of function. The increase in *FMR1* mRNA levels, leads to an excess of RNA-protein binding within the nucleus. This ultimately leads to the sequestration of other proteins which bind together to form protein aggregates (ubiquitin-positive intracellular inclusion bodies, likely due to repeat associated non-AUG initiated translation) and reduced neuronal cell function, due to the reduced availability of necessary proteins (Willemsen *et al.*, 2003; Arocena *et al.*, 2005; Todd *et al.*, 2013). Further, these ubiquitin-positive intracellular inclusion bodies are a neuropathological hallmark of FXTAS.

Fragile X mental retardation protein (FMRP)

The resulting protein from *FMR1* mRNA translation is FMRP. FMRP is a selective mRNA binding protein and is critical for protein synthesis-dependent synaptic plasticity in neural cells [See Callan and Zarnescu (2011) for a full review]. Specifically, FMRP binds its own RNA, among other RNA species, and transports messages to the synapse (Ashley, Wilkinson, Reines, & Warren 1993). FMRP plays a critical role in synaptic maturation through the inhibition of genetic translation of genes known to be important for synaptic plasticity, through RNA sequestration. Thus when there is an absence of FMRP, there is an upregulation of translation of these synaptic plasticity genes, which leads to an increase in long and immature dendritic spines, as seen in FXS (Willemsen *et al.*, 2011). In the embryonic brain, FMRP is thought to predominantly affect neurogenesis of glutamatergic neurons in the subventricular zone of the cortex (Tervonen *et al.*, 2009; Luo *et al.*, 2010). Within FXS mice models, subventricular zones (and dendate gyrus) are most susceptible to loss of FMRP during neurogenesis, resulting in an increase in density of subventircular zones (and size of the dentate gyrus) (Tervonen *et al.*, 2009; Luo *et al.*, 2010). This neuronal regional specificity

is also seen in adult FXS primate models, with relative FMRP expression levels highest in the cerebellum, hippocampus and caudate (Zangenehpour *et al.*, 2009). Therefore it appears that reduced FMRP during neurogenesis leads to alterations in neuronal structure that persist throughout development. Interestingly, a reduction in FMRP levels has also been demonstrated in autism, schizophrenia, bipolar disorder, and major depressive disorder, as well as FXDs (Fatemi and Folsom, 2011).

FMR1 epigenetics

It is important to consider epigenetics, or changes in gene expression, exclusive of underlying changes to the genetic code, which may affect both FM and PM alleles. Methylation, or the addition of methyl groups to the DNA sequence, is an important epigenetic consideration when evaluating PM and FXS specific phenotypes. Methylation of the *FMR1* promotor region has been found to negatively correlate with FMRP and X-activation in FXS females (Godler *et al.*, 2010a), and for FM alleles results in allelic inactivation.

Additionally, methylation of *FMR1* intron 1 has been associated with executive dysfunction (both working memory and response inhibition) in FXS and PM females (Godler *et al.*, 2011; Cornish *et al.*, 2015). Hence, methylation of the *FMR1* epigenetic elements 1 (FREE1) and 2 (FREE2), are seen to be an important biomarker for determining clinical and cognitive functions (Godler *et al.*, 2010a; Pastori *et al.*, 2014).

X-Chromosome inactivation

FMR1 exhibits a mosaic type expression through the body, with the highest concentrations found in the brain and gonads, and differences in penetrance between the genders exist, due to the presence a second X-chromosome in females (Koukoui and Chaudhuri, 2007). In PM and FM females, the activation ratio (AR) characterises the number of cells that carry the

normal *FMR1* allele (less than 45 CGG repeats), and is calculated by dividing the sum of the intensities of normal unmethylated bands over the sum of the intensities of the PM or FM (un)methylated bands (Tassone *et al.*, 1999). Given that PM and FM females often exhibit a relatively high AR value, expressing a greater proportion of the *normal* allele and therefore close to *normal* levels of *FMR1* mRNA and FMRP, the symptoms of FXDs are often less severe in females (Hall *et al.*, 2014; Wheeler *et al.*, 2014).

1.2 CLINICAL PHENOTYPES

In 1994, the deleterious effect of PM expansions was first recognised in PM females who were found to have a higher incidence of early menopause. This is now recognised as Fragile X-associated premature ovarian failure (FXPOI) (Sherman, 2000). In 1999, a neurodegenerative motor disorder, Fragile X-associated tremor/ataxia syndrome (FXTAS), was subsequently reported in PM male relatives of FXS patients (Hagerman *et al.*, 2001; Hagerman *et al.*, 2004).

Fragile X primary ovarian insufficiency (FXPOI)

In FXPOI, ovarian functionality is reduced. Symptoms may include i) alteration to the menstrual cycle; ii) hormonal changes (hypergonadotropic hypogonadism); iii) infertility; and/or iv) symptoms of early menopause. FXPOI related menopause symptoms often begin around 46 years of age for PM females, which is around 5 years earlier than the general population. Approximately 20% of PM females will develop FXPOI symptoms, compared to 1% of the general population (Sullivan *et al.*, 2005).

The decrease in ovarian function is associated with decreased levels of anti-Müllerian hormone and increased levels of follicle-stimulating hormone, which can cause infertility (Murray *et al.*, 2000; Sullivan *et al.*, 2005; Allen *et al.*, 2007; Streuli *et al.*, 2009; Sherman *et*

al., 2014). These hormonal changes, specifically impacting levels of oestrogen, are known to increase the risk of osteoporosis (including low bone density and fractures), endothelial function and heart disease in the general population, and are therefore often more prevalent in PM females with FXPOI (Hundscheid *et al.*, 2003; Kalantaridou *et al.*, 2004; Atsma *et al.*, 2006; Allen *et al.*, 2007; Gallagher, 2007). Indeed, endocrine dysfunction is the most recognised aspect of the PM female phenotype (Coffey *et al.*, 2008), with changes in oestrogen levels and early menopause potentially exacerbating the incidence of anxiety, depression, somatization, sensitivity, as well as immune-related disorders (Wheeler *et al.*, 2014).

The exact molecular mechanism(s) that cause FXPOI are not well understood. Although there are conflicting opinions, there is evidence that CGG repeat length, *FMR1* mRNA levels, *FMR1* non-coding RNAs (FMR6), background genes and environmental factors (smoking), are important considerations when evaluating the risk of FXPOI and its incomplete penetrance among PM females (Wittenberger *et al.*, 2007; Sherman *et al.*, 2014). Indeed, a curvilinear relationship exists between CGG repeat size and risk for FXPOI, suggesting that PM females with a CGG repeat length of 80-100 CGG repeats are most at risk (Sullivan *et al.*, 2005; Allen *et al.*, 2007; Tejada *et al.*, 2008; Elizur *et al.*, 2015). Further, expression of FMR6, a long non-coding antisense transcript overlapping the 3' *FMR1* region, has been found to have a curvilinear relationship with both CGG repeat length (highest correlation with CGG repeats 80-100), and number of oocytes in PM females (Elizur *et al.*, 2015). Interestingly, AR has not been shown to increase the risk of FXPOI (Murray *et al.*, 2000; Sullivan *et al.*, 2005; Tejada *et al.*, 2008; Spath *et al.*, 2010).

Fragile X-associated tremor/ataxia syndrome (FXTAS)

A second PM-related clinical phenotype, known as FXTAS, was first described as a neurodegenerative disorder associated with progressive intention tremor, ataxia and generalised brain atrophy in older PM male relatives of FXS patients (Hagerman *et al.*, 2001). Diagnostic criteria for FXTAS relies on a combination of clinical, radiological, and pathological hallmarks (Table 1.2). However, with ongoing research, phenotypic characteristics of the disorder have expanded to include cognitive, autonomic, psychiatric, other medical disorders, as well as a greater spread of neurological hallmarks (Hall *et al.*, 2014; Hagerman and Hagerman, 2016).

Table 1.2: Revised Fragile X-associated tremor/ataxia syndrome (FXTAS) diagnostic criteria

Hallmark	Degree	Observation
Clinical	Major	Intention tremor
	Major	Cerebellar Gait ataxia
	Minor	Parkinsonism
	Minor	Moderate to severe short-term memory deficiency
	Minor	Executive function deficit
Radiological	Major	MRI white matter lesions in middle cerebellar peduncles and/or brain stem
	Major	MRI white matter lesions in splenium of the corpus callosum
	Minor	MRI white matter lesions in cerebral white matter
	Minor	Moderate to severe generalized atrophy
Pathological	Major	Classic FXTAS CNS intranuclear inclusions
FXTAS category*	Definite	One major clinical, and one major radiological or pathological
	Probable	i) Two major clinical ii) One major radiological and one minor clinical
	Possible	One major clinical, and one minor radiological

Note: Based on (Hall *et al.*, 2014); * For all FXTAS categories, the patient must be a *FMR1* PM-carrier (CGG 55-199).

FXTAS is thought to affect 40% of PM males, and 8-16% of PM females over the age of 50 years (Rodriguez-Revenga *et al.*, 2009). Whether definite, probable or possible, FXTAS diagnosis requires a degree of clinical impairment. Although the clinical presentation of FXTAS is variable, motor deficits (intention tremor or cerebellar gait ataxia) are required for a definite FXTAS diagnosis. The initial presenting tremor may be classified as either essential, cerebellar or parkinsonism tremor (Apartis *et al.*, 2012). Other motor features of Parkinsonism (bradykinesia and resting tremor) and neurological symptomology (neuropathy and vestibular dysfunction) are also common (Hagerman *et al.*, 2007; Coffey *et al.*, 2008; Soontarapornchair *et al.*, 2008; Loesch *et al.*, 2009; Juncos *et al.*, 2011; Schneider *et al.*, 2012; Hagerman and Hagerman, 2013; Niu *et al.*, 2014). Cerebellar gait ataxia, including balance and gait deficits, place patients at risk of increased falls and progressive mobility disability, impacting their quality of life (O'Keefe *et al.*, 2015b).

The clinical presentation of FXTAS also includes executive dysfunction as a minor criterion (Table 1.2). FXTAS related executive dysfunction may range from mild to dementia-like in severity, and often presents later in the disease course, up to four years after initial motor symptoms (Seritan *et al.*, 2008). Here, dysfunction is evident using tasks assessing response time, working memory and visuospatial processing, but is not seen to affect generalised IQ scores (Grigsby *et al.*, 2006; Grigsby *et al.*, 2007; Brega *et al.*, 2008; Grigsby *et al.*, 2008). Not surprisingly, a milder dysexecutive phenotype has been seen for FXTAS females (Sterling *et al.*, 2013; Yang *et al.*, 2013).

The second fundamental diagnostic criterion for FXTAS is radiological change. Although an extensive review of the radiological features in FXTAS is beyond the scope of this thesis (see Rivera, Stebbins and Grigsby (2010) for a full review), the most notable changes are cerebellar. These include middle cerebral peduncle (MCP) hyperintense lesions (known as the MCP sign) and volumetric reductions in the cerebellar vermis (except lobules VII and IX) and cerebellar hemispheres (except lobule VII and right lobule XI) (Cohen *et al.*, 2006; Hashimoto *et al.*, 2011b; Battistella *et al.*, 2013).

FXTAS is also viewed as a white matter neurodegenerative disease. Besides the MCP sign, widespread alterations in white matter diffusivity measures have been found in FXTAS (Cohen *et al.*, 2006; Hashimoto *et al.*, 2011c; Apartis *et al.*, 2012; Wang *et al.*, 2012b; Battistella *et al.*, 2013; Wang *et al.*, 2013b). White matter abnormalities have been reported in the periventricular, subcortical, corpus callosum splenium, and deep white matter of the cerebellum (likely due to Purkinje cellular loss and ubiquitin-positive intracellular inclusions) (Brunberg *et al.*, 2002; Cohen *et al.*, 2006; Greco *et al.*, 2006; Jacquemont *et al.*, 2007; Loesch *et al.*, 2007; Apartis *et al.*, 2012). Interestingly, corpus callosum hyperintensities are reported as frequently as, if not more commonly than, MCP hyperintensities (Apartis *et al.*, 2012; Renaud *et al.*, 2015b), and there is growing evidence for the inclusion of corpus callosum splenium hyperintensities as a radiological diagnostic marker of FXTAS (Apartis *et al.*, 2012; Hall *et al.*, 2014; Renaud *et al.*, 2015a).

As discussed earlier, ubiquitin-positive intracellular inclusion bodies are a pathological hallmark of the disorder, thought be the result of a toxic-gain of function, a consequence of increased *FMR1* mRNA (see 1.1 Genetics and Epigenetics: *FMR1* messenger RNA). However, alterations to protein titration, non-AUG translation, antisense transcription, mitochondrial function and FMRP levels have also been found in individuals with FXTAS and may represent differing modes of molecular involvement that may collectively contribute to FXTAS aetiology (Hagerman and Hagerman, 2013; Sellier *et al.*, 2014).

Further, there are a number of factors that influence the age of onset and severity of FXTAS. Firstly, CGG repeat length has been shown to be associated (inversely) with age of symptom onset (both tremor and ataxia individually) (Tassone *et al.*, 2007a), as well as the overall severity of clinical involvement (Leehey *et al.*, 2008). Secondly, greater XCI (greater expression of the PM allele compared to the second, most likely normal *FMR1* allele) is also seen to increase the risk (Alvarez-Mora *et al.*, 2015) and severity of FXTAS for PM females (Hall *et al.*, 2016a). Finally, environmental effects (i.e. substance abuse) (Muzar *et al.*, 2014) and concomitant neurodegenerative diseases (Parkinson's disease) (De Pablo-Fernandez *et*

al., 2014) decrease the age of onset and increase degeneration, resulting in severe FXTAS symptomology.

Importantly, not all FXTAS patients show these radiological hallmarks suggestive of FXTAS, but still meet the criteria for clinical diagnosis (Adams *et al.*, 2007; Capelli *et al.*, 2007; Loesch *et al.*, 2008; Oyama *et al.*, 2014). The FXTAS diagnostic criteria is evolving, with current research identifying a number of FXTAS-related phenotypes which may lead to advanced diagnostic markers for FXTAS.

Other medical concerns

Not all PM-carriers develop FXPOI or FXTAS, although they have a heightened risk for a range of medical and psychiatric issues compared to the general population (Wheeler *et al.*, 2014; Hagerman and Hagerman, 2016). These conditions appear with unequal penetrance between genders, and differ according to FXTAS status (Table 1.3). Moreover, vestibular (including dizziness) and balance issues, which may be early signs of ataxia, have also been identified in PM-carriers without FXTAS (Chonchaiya *et al.*, 2010; Seltzer *et al.*, 2012a; O'Keefe *et al.*, 2015a).

Although the rates of depression and anxiety reported in PM cohorts are not seen to be greater than that reported in the DSM-5 (SCID-5), both depressive symptoms and anxiety have been associated with CGG repeat length and number of negative life events in PM females with a child with FXS (Seltzer *et al.*, 2012b). Further, a large study on the life-time prevalence of mood and anxiety reported that social anxiety was seen to be heightened in PM-carriers without FXTAS compared to controls (Bourgeois *et al.*, 2007; Bourgeois, 2016). Significantly, Adams and colleagues (2009) as well as Hessl and colleagues (2007; 2011) have reported smaller hippocampal size and amygdala dysfunction in PM cohorts without FXTAS, brain regions associated with emotion regulation. These subcortical regions are

known to have a relatively high expression of FMRP (Zangenehpour *et al.*, 2009), and are therefore more dramatically affected by altered FMRP levels, as in PM.

Table 1.3: Summary of the medical issues for which PM-carriers have a heightened risk compared to the general population

Medical Issue	**FXTAS**		**Non-FXTAS**	
	Females	Males	Females	Males
Immune-mediated disorders (i.e. Graves' disease) [1]	73%		45%	
Thyroid disease [1-3]	53%		18%	
Fibromyalgia [1, 2, 4-6]	25-44%		8%	
Hypertension [2-7]	61%	67%	16%	42%
Migraines [8-9]	53%	81%	12%	27%
Sleep disturbances [10-11]	63%#		63%#	
Restless leg syndrome [11]	33.1%*	33.1%*	33.1%*	33.1%*
Sleep apnoea [12]	31.4%^	31.4%^		
Neuropathy [2, 9, 13, 14]	53%	88%	12%	36%
Muscle pain [2]	77%		26%	
Tremor history [2]	89%		12%	
Sensory loss [2]	83%		45%	
Central pain sensitivity syndrome [6, 9]	75%			
Tandem gait abnormalities [9, 15]	30%	100%		

Note: Prevalence rates are approximate figures only; Blank spaces indicate that prevalence rates have not been determined as yet; *Indicates figures were obtained from a mixed sample of PM males and females with and without FXTAS; ^Indicates figures were obtained from a mixed sample of PM males and females with FXTAS; #Indicates figures were obtained from a mixed sample of PM females with and without FXTAS. References: 1: (Winarni *et al.*, 2012), 2: (Coffey *et al.*, 2008), 3: (Rodriguez-Revenga *et al.*, 2009), 4: (Martorell *et al.*, 2012), 5: (Rodriguez-Revenga *et al.*, 2013), 6: (Leehey *et al.*, 2011), 7: (Hamlin *et al.*, 2012), 8: (Au *et al.*, 2013), 9: (Hall *et al.*, 2015), 10: (Chonchaiya *et al.*, 2010), 11: (Summers *et al.*, 2014), 12: (Hamlin *et al.*, 2011), 13: (Hagerman *et al.*, 2004), 14: (Berry-Kravis *et al.*, 2007), 15: (Jacquemont *et al.*, 2003).

Further increased prevalence of autism spectrum disorders and traits have been reported for PM-carrier children (Clifford *et al.*, 2007), and PM-carrier adults compared to the general population (Hunter *et al.*, 2012a).

Overall, a clear PM clinical phenotype is absent, although a range of symptomology and severity is evident. Therefore, further investigation of the molecular mechanisms that may contribute to each of the PM-related FXD is warranted.

1.3 COGNITIVE AND BEHAVIOURAL PHENOTYPES

FXTAS, FXPOI and clinical disorders alone do not account for the full spectrum of involvement in PM-carriers, which also includes a range of cognitive and behavioural impairments. Cognition refers to a set of mental processes which enable the acquisition and understanding of thoughts, experiences and sensations.

Although general intelligence quotient (IQ) scores are typically normal in PM-carriers (Moore *et al.*, 2004a; Cornish *et al.*, 2008b; Grigsby *et al.*, 2008; Hunter *et al.*, 2008; Cornish *et al.*, 2009; Allen *et al.*, 2011; Cornish *et al.*, 2011; Filley *et al.*, 2015), cognitive deficits can be anywhere from mild to severe (dementia like), and affect a broad range of skills such as memory, linguistic, athematic, sensory, social and mental control/planning (Grigsby *et al.*, 2014). Interestingly, the majority of investigations in PM-carriers have focused on cognitive aspects that are impaired in FXS, i.e visuospatial processing, verbal skills, perceptual organisation, inattention and processing speed (Schneider *et al.*, 2009). The following discussion describes our current understanding of the cognitive profile of PM-carriers *without* FXTAS, including studies in which FXTAS status is not specified, and concludes with a summary of the behavioural disturbances found.

Memory

Memory functionality, or the ability to recall information previously stored, appears to be relatively unaffected in PM-carriers without FXTAS (Franke *et al.*, 1999; Hunter *et al.*, 2008; Yang *et al.*, 2013). However, deficits in memory encoding (Wang *et al.*, 2012a), and recall

(Grigsby *et al.*, 2008; Koldewyn *et al.*, 2008) have been found for PM males without FXTAS. Moreover, these changes in memory encoding and recall may be associated with functional magnetic resonance imaging (fMRI) changes in blood-oxygen-level-dependent neural activation within hippocampal and prefrontal regions (full description of changes in Neurological Phenotype: Functional studies section below) (Koldewyn *et al.*, 2008; Wang *et al.*, 2012a).

Language

Although generalised IQ scores are within the average range, a few studies have found lower *verbal* IQ scores in PM male and females without FXTAS (Franke *et al.*, 1999; Allen *et al.*, 2005; Adams *et al.*, 2007; Allen *et al.*, 2011). Further, deficits in verbal fluency and verbal long term memory have been demonstrated (Moore *et al.*, 2004a; Moore *et al.*, 2004b; Grigsby *et al.*, 2008; Hippolyte *et al.*, 2014; Kraan *et al.*, 2014b), albeit not consistently (Hunter *et al.*, 2012a; Yang *et al.*, 2013).

Language dysfluencies, particularly in the organisation and planning of speech have also been reported in PM females (Sterling *et al.*, 2013), as have elevated rates of pragmatic language and conversational difficulties (Losh *et al.*, 2012). However, neither of these functional language studies assessed PM male performance or specified FXTAS status.

Arithmetic

Anecdotal reports of mathematical difficulties are common amongst PM and FXS females. Such reports were confirmed by Lachiewicz *et al.* (2006), who demonstrated that PM females scored below average on arithmetic skills on an achievement skills test. More recently, Semenza and colleagues (2012) found that PM females had a specific, yet subtle, weakness on tests of basic number processing and understanding, although calculation was spared.

Even if subtle, difficulties with arithmetic processing are likely to impact everyday activities. To date, linguistic and arithmetic skills have only been characterised in PM females, and not PM males.

Visuospatial processing

Deficits in visuospatial processing, both low-level and higher-order cognitively driven, have been found in PM-carriers (Kéri and Benedek, 2009; Kéri and Benedek, 2010; Goodrich-Hunsaker *et al.*, 2011a; Keri and Benedek, 2012; Wong *et al.*, 2012; Gallego *et al.*, 2014; Wong *et al.*, 2015). For example, PM females have been shown to experience visuospatial processing deficits (Kéri & Benedek, 2009); these deficits also correlated with increasing CGG length in a quantitative magnitude comparison task (Goodrich-Hunsaker *et al.*, 2011a). Visuospatial impairment has also been seen in PM males without FXTAS (>100 CGG repeats) using the Cube Analysis Task Visual Object and Space Perception Battery and the Dot Test of Visuospatial Working Memory, when compared to controls (Hocking *et al.*, 2012). Interestingly, the correlations detected between CGG length and visuospatial performance in PM-carriers are the same as those seen in FXS (Cornish, Munir, & Cross, 1998), where it has been proposed that performance reflects abnormalities in the magnocellular pathway and early visual processing.

Although not necessarily directly linked to visuospatial processing, social cognition, based on the interpretation of black and white photographs, is also impaired in PM males, albeit milder than is seen in FXS (Cornish *et al.*, 2005).

Executive function

A range of deficits linked to executive function have been found in PM-carriers without FXTAS. Although there is no clear consensus concerning the set of processes that collectively

underlie executive function, throughout this thesis the term will encompass attention, processing speed (initiation), inhibition, planning, and the ability to manipulate and maintain information for a short period of time (Collette *et al.*, 2006; Niendam *et al.*, 2012). These processes require highly integrative neural networks, spanning cortical (mainly prefrontal) and subcortical regions, that are vulnerable to a range of pathological processes. The following discussion will review studies that assess executive function more generally in PM-carriers *without* FXTAS before dissociating domain specific weaknesses.

The Behavioural Dyscontrol Scale (BDS) is a test of executive function commonly used in PM-carriers and includes simple motor, verbal and complex working memory test items (Brega et al., 2008). Importantly, the BDS has revealed executive dysfunction in a number of PM studies. While impairment is generally more evident in PM males than PM females (Loesch *et al.*, 2003; Brega *et al.*, 2008; Hunter *et al.*, 2012c), similar deficits have been found across genders for Test Items 5 and 6, which assess purposeful movement control (Loesch *et al.*, 2003).

Attention and processing speed

Studies using objective measures of attention, specifically of sustained attention or the ability to remain focused on a *simple* task, have yielded mixed results among PM-carrier cohorts (Franke *et al.*, 1999; Steyaert *et al.*, 2003a). However, for PM females without FXTAS, increasing age and CGG repeat length has been shown to correlate with worsening attentional performance on an enumeration (magnitude estimation) task (Goodrich-Hunsaker *et al.*, 2011b). Similarly, increasing age correlates negatively with selective attention in PM males (Cornish *et al.*, 2008b).

Self-reported attentional problems (specifically of inattention, impulsivity and lowered interest levels) are high in PM-carriers (Steyaert *et al.*, 2003a; Bailey *et al.*, 2008; Hunter *et al.*, 2008). Like objective measures of attention, self-reported attentional complaints increase

with increasing CGG repeat length, as well as processing speed measures for PM males and females without FXTAS (Hunter *et al.*, 2008). Increased response time, or slowed processing speed, has also been found for PM-carriers using selective and divided tasks of attention, visuospatial tasks, simple motor tasks (finger tapping and others) and saccade paradigms examining endogenous and exogenous visual cues (Steyaert *et al.*, 2003a; Goodrich-Hunsaker *et al.*, 2011a; Goodrich-Hunsaker *et al.*, 2011b; Narcisa *et al.*, 2011; Wong *et al.*, 2012; Wong *et al.*, 2015). It may be that PM-related attentional difficulties and slowed processing speeds are affected in a gene-dosage manner.

Response inhibition

Impairments of response inhibition, or the ability to withhold a prepotent response, were first reported by Cornish and colleagues (2008b). Specifically, scores from the Haylings sentence completion and Stroop-colour Word tests were found to be adversely affected by increasing age in PM males (Cornish *et al.*, 2008b; Cornish *et al.*, 2011). Subsequently, when controlling for age, no differences in Stroop-Colour Word test scores were found (Grigsby *et al.*, 2008). Deficits on the Haylings sentence completion but not Stroop-colour word test have been reported in PM females without FXTAS (Kraan *et al.*, 2014b; Kraan *et al.*, 2014c; Cornish *et al.*, 2015).

Working memory

Generally, intact working memory has been reported for both PM males and females without FXTAS (Hashimoto *et al.*, 2011a; Kraan *et al.*, 2014b; Cornish *et al.*, 2015). However, working memory, deficits have been linked to increasing age in PM males (Cornish *et al.*, 2009), and CGG repeat length linked to letter number sequencing scores in PM males (Cornish *et al.*, 2011), as well as temporal working memory in PM mice (CGG > 72 repeats) (Hunsaker *et al.*, 2010). This suggests that any decrement in working memory processes may be modulated

by age and CGG-dosage, and may potentially represent early markers of FXTAS related neurodegeneration. However, a greater understanding of the nature and development of working memory weakness in PM-carriers is clearly needed.

Multiple studies have delineated aspects of the executive function profile in PM males and females. Systematic examination of attentional deficits for PM females exists, however few studies have investigated whether or not PM females have analogous response inhibition and working memory deficits as PM males.

Neurobehavioral disturbances

Behavioural disturbances related to FXTAS symptomology (cerebellar gait and balance predominantly) have also been investigated in PM-carriers without FXTAS. Balance deficits were first reported in knock in (KI) PM mice using the ladder rung task, where KI male and female mice recorded an increase in the number of foot slips compared to wildtype mice (Hunsaker *et al.*, 2011). Further, a CGG-dosage effect was found for increasing foot slips (Hunsaker *et al.*, 2011).

Studies in humans have also revealed deficits in balance and gait performance in PM-carriers without FXTAS. PM males without FXTAS have been shown to have less severe postural sway and gait variability than those with FXTAS (Aguilar *et al.*, 2008; Narcisa *et al.*, 2011; O'Keefe *et al.*, 2015b), but more severe vestibular and somatosensory sway than controls (O'Keefe *et al.*, 2015a). PM males without FXTAS had greater impairment during a motor control test (evaluating balance) than PM females without FXTAS, with PM female performance impacted by increased age and CGG repeat length, and reduced AR (O'Keefe *et al.*, 2015a). However, PM females without FXTAS are shown to be more variable on gait and balance parameters when concurrently completing an executive function task (dual-task condition involving either the excluded verbal fluency or counting backwards by 3s or 7s) (Kraan *et al.*, 2013b; Kraan *et al.*, 2014a; Hocking *et al.*, 2015). Similarly, tests of executive function have been

shown to correlate with greater postural sway, delayed postural reflexes, reduced stability, gait speed and cadence among PM-carriers with and without FXTAS (Hall *et al.*, 2016b). Gait and vestibular issues in PM-carriers without FXTAS indicate cerebellar impairment, and tend to be exacerbated by cognitive load.

Although not definitive, the developing cognitive and neurobehavioural phenotype of PM-carriers without FXTAS, suggests disruption to cortico-cerebellar networks, with impairments generally exacerbated with advancing age and greater CGG repeat length. However, it remains unclear whether the impairments seen are a) preclinical markers of FXTAS, or b) common amongst all PM-carriers and not indicative of further FXTAS risk. Therefore, as suggested by Kraan *et al.* (2013a), targeted, domain specific tests may help to delineate these developing phenotypes. Finally, it is clear that a larger body of work exists for the PM males without FXTAS and thus we have a greater understanding the dysexecutive phenotype(s) associated with PM males without FXTAS. Greater emphasis should now be placed on understanding the phenotype of PM females without FXTAS, particularly in relation to the executive dysfunction associated with FXTAS.

1.4 NEUROLOGICAL PHENOTYPE

Although a clear radiological profile has been suggested for FXTAS, a range of neurological changes have been revealed for PM-carriers without FXTAS, albeit less severe (Cohen *et al.*, 2006; Adams *et al.*, 2007). Generalised atrophy of the whole brain, cerebral and cerebellum regions as well as increased ventricle size, have been reported for male and female PM-carriers without FXTAS (Murphy *et al.*, 1999; Brunberg *et al.*, 2002; Moore *et al.*, 2004b; Loesch *et al.*, 2005a), although not consistently (Cohen *et al.*, 2006; Adams *et al.*, 2007; Hessl *et al.*, 2007). However regional atrophy is commonly found in prefrontal, hippocampal, and cerebellar regions of PM-carriers without FXTAS, which are regions known to have high FMRP expression (Wilson *et al.*, 2009). The following discussion will evaluate neurological

features in PM-carriers *without* FXTAS, as well as how *FMR1* genetic measures relate to such changes.

Grey matter structure

Cerebral cortical grey matter atrophy has been reported in PM males without FXTAS, bilaterally in the insula, in the left inferior temporal gyrus, right precentral and postcentral gyri, and right inferior parietal cortex (Moore *et al.*, 2004b; Loesch *et al.*, 2005a), although not consistently (Cohen *et al.*, 2006; Koldewyn *et al.*, 2008; Hashimoto *et al.*, 2011b; Hessl *et al.*, 2011). Greater CGG repeat length has been found to correlate with decreased prefrontal volumes in PM males without FXTAS (Hashimoto *et al.*, 2011b) – indicating the presence of a gene-dosage effect. However, only a single study has examined grey matter cortical volumes in PM females (*n*=8), in which cortical atrophy and altered cortical glucose metabolism were revealed (Murphy *et al.*, 1999).

Subcortical grey matter alterations have also been found, although again without consistency. For example, while some studies reveal increased amygdalo-hippocampal size (Murphy *et al.*, 1999; Loesch *et al.*, 2005a), others report decreased (Jäkälä *et al.*, 1997; Moore *et al.*, 2004b), or no volumetric differences between PM-carriers and controls (Selmeczy *et al.*, 2011; Wang *et al.*, 2012a). However, higher CGG repeat length (between 55-85 CGG repeats) and lower FMRP levels have been shown to correlate with smaller amygdalo-hippocampal complexes in PM males (Moore *et al.*, 2004b; Selmeczy *et al.*, 2011). More consistent reports for volumetric reductions in the caudate and thalamus have been found in PM males and females without FXTAS (Murphy *et al.*, 1999; Battistella *et al.*, 2013). Atrophy within the brainstem has also been revealed for PM males without FXTAS (Cohen *et al.*, 2006; Leow *et al.*, 2014), with increasing age and CGG repeat length, as well as decreased FMRP seen to associate with greater volumetric reductions (Moore *et al.*, 2004b; Cohen *et al.*, 2006).

Global reduction in cerebellar volumes have not been found for PM-carriers (Cohen *et al.*, 2006). However, compared to controls, regional cerebellar grey matter atrophy was revealed for PM males without FXTAS within cerebellar vermis lobules I/II, and cerebellar lobule III of the left hemisphere (Hashimoto *et al.*, 2011b), as well as cerebellar lobule VI (Battistella *et al.*, 2013). It appears that grey matter atrophy may not be limited to those with FXTAS, but rather affect a subset of PM males without FXTAS. Whether these changes extend to PM females without FXTAS is less clear.

White matter structure

Although FXTAS is predominately seen as a neurodegenerative white matter disease (Filley, 2016), changes in white matter integrity have been found in PM-carriers without FXTAS. White matter hyperintensities are a radiological feature of FXTAS, and have been found in PM-carriers without FXTAS, albeit less severe (Cohen *et al.*, 2006; Adams *et al.*, 2007). Further, no differences in global connectome efficiency, yet altered nodal efficiency in right fusiform and ventral diencephalon have been reported in PM-carriers without FXTAS (Leow *et al.*, 2014). Together, these studies suggest that white matter changes in PM-carriers without FXTAS appear to be regional rather than global in nature.

Increased radial diffusivity (RD) has also been reported for PM males without FXTAS in the hippocampal fimbria/fornix, bilateral stria terminalis and MCP tracts (Battistella *et al.*, 2013). Accelerated age-related changes in diffusion coefficients (mean diffusivity (MD) and RD) have also been revealed for PM males without FXTAS in frontal white matter and corticospinal tracts (posterior and superior corona radiate) (Battistella *et al.*, 2013), in the absence of changes to tractography variability and diffusivity measures (fractional anisotropy (FA), MD, and RD) (Battistella *et al.*, 2013; Wang *et al.*, 2013b).

Focal changes in cerebellar peduncle diffusivity measures have yielded inconsistent findings in PM-carriers without FXTAS. Reduced axial diffusivity (AD) and RD have been reported for

PM males without FXTAS in the left cerebellar peduncle (Hashimoto *et al.*, 2011c), and MCP (Hashimoto *et al.*, 2011c; Battistella *et al.*, 2013). Further an inverted U-shaped relationship with CGG repeat length was found for MCP AD and RD (Hashimoto *et al.*, 2011c). However, Wang *et al.* (2013b) failed to find differences between PM males without FXTAS and controls for more coarse measures of diffusivity (FA and MD) within the MCP, SCP and corpus callosum. This discrepancy is likely due to the different analytical approaches and diffusivity coefficients employed by these studies.

Cortical diffusivity measures have also been shown to correlate with cognitive performance. For example, total scores on the Californian Verbal Learning Task negatively correlated with MD values in the white matter under the motor cortex, supplementary motor area and dorsolateral prefrontal cortex (DLPFC) of PM males without FXTAS (Hippolyte *et al.*, 2014). Similar negative correlations were also found between verbal retrieval scores and MD of the left hippocampal fimbria/fornix and stria terminalis (Hippolyte *et al.*, 2014). Finally, measures of executive function (BDS and the controlled oral word association task (COWAT)) have been shown to correlate with FA of the MCP and corpus callosum genu and splenium in a combined cohort of PM males with and without FXTAS (Filley *et al.*, 2015).

Together, these studies investigating white matter microstructure reinforce that, even in the absence of overt neuropathology, there may be a genetic basis for attenuated white matter structure, leading to cognitive and executive function impairment in PM males without FXTAS. Whether or not this is true for PM females is yet to be determined.

Functional studies

Although structural differences are uncertain for PM-carriers without FXTAS, evidence of attenuated functionality of neural networks during specific cognitive tasks is emerging. A total of six fMRI studies examining PM-carriers have been reported. Three of these have focused on the amygdala-hippocampal complex regions through memory recall and

emotion-matching tasks for PM males without FXTAS (Hessl *et al.*, 2007; Koldewyn *et al.*, 2008; Wang *et al.*, 2012a), and the other three have used a range of paradigms to probe working memory processing for combined groups of male and female PM-carriers without FXTAS (Hashimoto *et al.*, 2011a; Kim *et al.*, 2013; Kim *et al.*, 2014). A further two studies have used electrophysiological approaches to examine specific neural responses to stimuli (Conde *et al.*, 2013; Yang *et al.*, 2013). Each of these studies will now be described.

The first functional study in PM-carriers without FXTAS investigated amygdala functionality when viewing fearful faces (Hessl *et al.*, 2007). Compared to controls, neural activity in PM males without FXTAS was found to be reduced in the amygdala, bilateral intraparietal sulci (IPS), right cingulate sulcus (insula and amygdala included), right orbital gryus, left superior temporal gyrus and the left cerebellar lobule VI. Additionally, decreased amygdala neural activity was found to significantly correlate with higher self-reported psychological symptoms and *FMR1* mRNA levels (Hessl *et al.*, 2007).

The functional activity of the amygdala-hippocampal complex has also been assessed for its role in memory processing in PM males without FXTAS. Firstly, during a colour choice memory task, PM males without FXTAS exhibited equivalent memory performance, yet greater neural activation in the right IPS, supramarginal gyrus, angular gyrus and caudate, yet reduced neural activation in the left parahippocampal gyrus, hippocamapal gyrus, right cuneus, right lingual gyrus and right caudate, compared to controls (Koldewyn *et al.*, 2008). Further, increased *FMR1* mRNA levels were found to correlate with increased right parietal activity and decreased left hippocampal activity, suggesting that the altered neuronal pattern of activity may by modulated according to a RNA toxic gain of function. A second study of hippocampal functionality during a memory-encoding processing task in PM males without FXTAS, found equivalent neural activation patterns and memory performance compared to controls (Wang *et al.*, 2012a). However, increased *FMR1* mRNA levels correlated with decreased task-related activity in the left DLPFC (accuracy contrast), while increased levels of FMRP associated with increased task-related activity in the ventrolateral prefrontal cortex

(accuracy contrast) and reduced left parahippocampal activity (encoding contrast). Additionally, reduced connectivity between i) bilateral hippocampal gyri and bilateral ventrolateral prefrontal cortex, as well as between ii) right hippocampal gyrus and right DLPFC was revealed for PM males without FXTAS compared to controls. A positive relationship between FMRP levels and connectivity between the right hippocampus and right DLPFC regions was found for PM males without FXTAS (Wang *et al.*, 2012a).

Altered prefrontal neural activation has also been observed during a fMRI working memory tasks for PM-carriers without FXTAS. Firstly, during a verbal working memory task, PM males and females without FXTAS were found to have reduced neural activation in the right ventral inferior frontal cortex and left dorsal inferior frontal cortex/premotor cortex, compared to controls (Hashimoto *et al.*, 2011a). Reduced right ventral inferior frontal cortex activation in PM-carriers without FXTAS was found to correlate with increased *FMR1* mRNA levels. In a second working memory fMRI study, reduced neuronal activation in the left frontal gyrus and IPS bilaterally was found for PM males and females without FXTAS compared to controls (Kim *et al.*, 2013). Interestingly, higher CGG repeat length (when controlling for *FMR1* mRNA levels), but not vice-versa, correlated with decreased neural activation bilaterally in the IPS and middle frontal gyrus, as well as right inferior and superior frontal gyri (Kim *et al.*, 2013).

A third fMRI working memory study found that compared to controls, a cohort of male and female PM-carriers without FXTAS recorded slower reaction times during a temporal working memory task compared to a spatial working memory task. This behavioural difference is likely driven by reduced neural activity in the 'when' pathway for PM-carriers compared to controls (specifically in the right temporoparietal junction, left posterior cingulate, left middle temporal gyrus and their surrounding areas) (Kim *et al.*, 2014). Increased *FMR1* mRNA levels were found to correlate with reduced activation in the right temporoparietal junction for PM-carriers without FXTAS (Kim *et al.*, 2014). Together, these

three fMRI working memory studies reveal attenuated cortical activation, in which *FMR1* gene expression is seen to relate to foci regions of neuronal activation difference.

In addition to these fMRI studies, other techniques for measuring neural activity have been employed in PM-carriers. Using transcranial magnetic stimulation (TMS), Conde *et al.* (2013) found that PM females with and without FXTAS had reduced cortical inhibition in GABA and cortico-cerebellar motor networks. Further, during an auditory oddball paradigm, higher count-hit ratio and a reduction in the amplitude of the frontal P300, an event related potential component associated with decision making, were found for PM females without FXTAS compared to controls (Yang *et al.*, 2013). However, the P300 amplitude data was not found to correlate with CGG length (Yang *et al.*, 2013).

A range of neurophysiological (fMRI, TMS and event related potential) tasks have shown attenuated neural activity in PM-carriers without FXTAS. Attenuation was commonly found within fronto-parietal and hippocampal regions, and often correlated with *FMR1* mRNA levels. Together, these functional studies suggest that PM-carriers use compensatory neural mechanisms, to achieve equivalent cognitive performance as controls.

Overall, an altered neurological profile is emerging for PM-carriers without FXTAS, yet many questions remain regarding the origin of these findings – whether neurodevelopmental or neurodegenerative in nature. Both structural and functional changes identified in PM-carriers without FXTAS converge on prefrontal, hippocampal and cerebellar regions, with apparent laterality. However, the extent of these changes is less clear for PM females without FXTAS compared to PM males without FXTAS. Given the extensive and sometimes confounding structural and functional alterations found, particularly in relation to grey matter atrophy, it is critically important to assess the inter-relationships between *FMR1* genetic markers, neuroanatomical structure and function, and behaviour, to fully delineate the PM-carrier neurological phenotype.

1.5 SUMMARY

The clinical, cognitive, behavioural and neurological phenotype of PM-carriers points to disruption within the cortico-cerebellar pathways, particularly in prefrontal and cerebellar regions. While there are parallels between the neural and cognitive phenotype of PM males with and without FXTAS there is a clear gap in our understanding of PM females with and without FXTAS. Understanding the specific females PM-carriers phenotypes is critically important given the relatively high prevalence of PM females (1 in every 209 females), and their heightened risk of a range of medical and hormone associated conditions. Given the suspected involvement of cortico-cerebellar network, it is proposed that ocular motor assessment might provide an ideal tool to investigate both behavioural and neurological dysfunction in PM females without FXTAS.

THE OCULAR MOTOR SYSTEM

One of the most sensitive behavioural methods for investigating neural (dys)function is the assessment of ocular motility. Ocular motility encompasses a range of eye movement types including saccades, smooth pursuit, vergence as well as optokinetic and vestibular-ocular reflexes. Ocular motor paradigms, particularly saccadic, have been used extensively in a range of neurodevelopmental and neurodegenerative conditions to examine not only the control of lower level motor processes, but also higher order executive control processes (Shafiq-Antonacci *et al.*, 2003; Reuter and Kathmann, 2004; Fielding *et al.*, 2006; Franke *et al.*, 2007; Lasker *et al.*, 2007; Fielding *et al.*, 2010; Yugeta *et al.*, 2010; Boxer *et al.*, 2012).

Following preliminary visual processing in the retina, lateral geniculate nuclei, and occipital cortex, top-down cognitive processing of saccades utilises complex circuitry traversing the cortex, subcortical, cerebellum, and brain stem regions (Figure 1.1) (Munoz and Everling, 2004). The neural overlap of the saccade network with those regions controlling cognition, make the ocular motor system ideal for investigating the cognitive control of behaviour. Other advantages of using eye movement analysis are the limited degrees of freedom of movement (restricted to two rather than three planes), the isolated nature of saccade generation (free from balance, inertia of heavy limb, mechanical stiffness, and handedness), and few recording artefacts.

Specifically, for this thesis, saccades will be examined to assess reflexive and cognitively driven (volitional) behaviours. The neural networks and nodes required for saccade generation are well characterised (Figure 1.1). In addition, a close relationship between sensory input and motor output facilitates precise measurement, and provides an exquisitely sensitive behavioural measure of sensorimotor processing. This section of the review will provide a general overview of the cortical and subcortical regions responsible for the generation of saccadic eye movements, as well as the use of ocular motor assessment within the context of the *FMR1* gene.

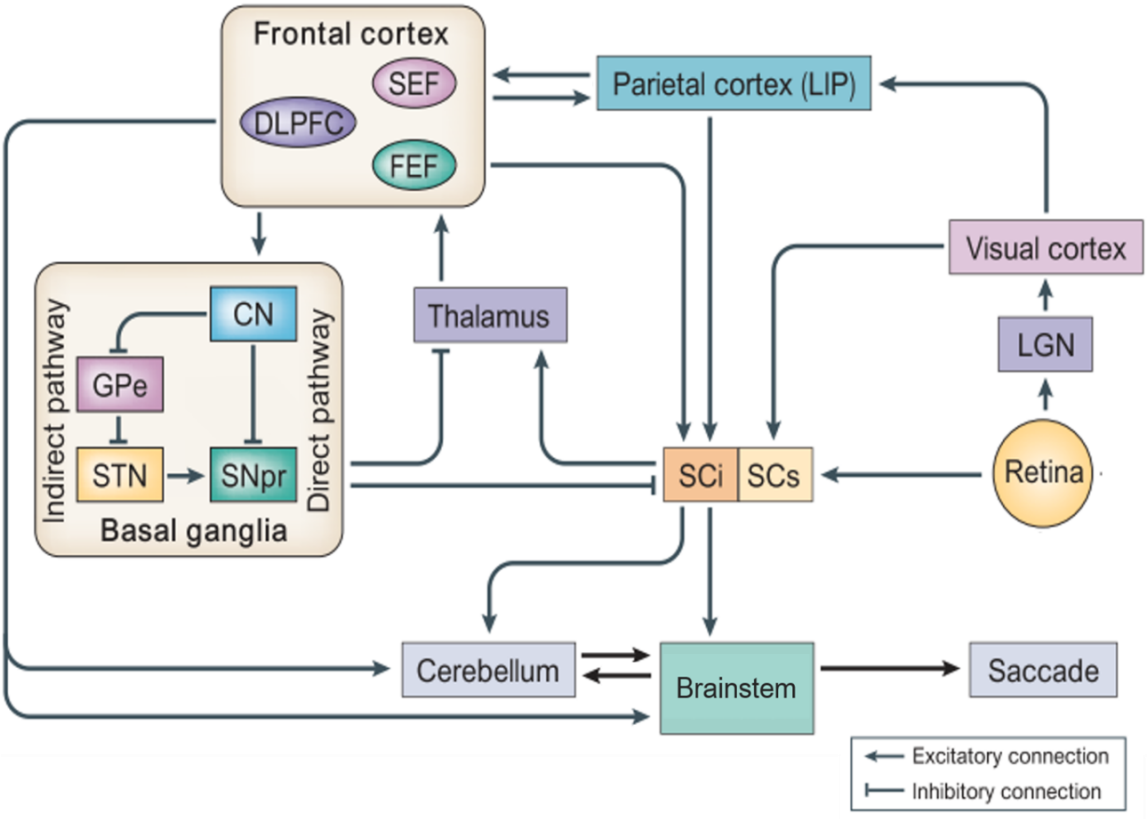

Figure 1.1: The ocular motor neural network

CN: Caudate nucleus, DLPFC: Dorsolateral prefrontal cortex, FEF: Frontal eye fields, LIP: Lateral intraparietal sulcus, GPe: Globlus pallidus external segment, LGN: Lateral geniculate nucleus, SCi: Superior colliculus intermediate layers, SCs: Superior colliculus superficial layers, SEF: Supplementary eye fields, SNpr: Substantia nigra pars reticulata, and STN: Subthalamic nucleus (Adapted from Munoz & Everling 2004).

1.6 SACCADIC EYE MOVEMENTS

A saccade is a rapid eye movement, which allows us to direct our focus on a visual stimulus by aligning it with the fovea. This typically occurs within 200ms (Carpenter, 1988). Saccades can be classified as i) reflexive (or prosaccades), where there is a direct sensorimotor transformation to an external stimuli, or ii) volitional, where the eye movement response is intentionally generated, governed by higher-order top-down cognitive control processes. Both reflexive and volitional saccades are easily quantifiable in terms of latency, accuracy

(amplitude), velocity, duration, and response error, with a linear relationship between peak velocity and amplitude (Becker, 1989).

The basic neural circuitry for the execution of a saccade does not substantially differ between reflexive and volitional saccades. Visual information is detected in the retina, and sent to the primary visual cortex (100-120ms after presentation of stimuli) via the optic tract and lateral geniculate nucleus (Clementz *et al.*, 2007; McDowell *et al.*, 2008). The information then passes through the visual cortical regions (V2 and V3), to the posterior parietal regions, and then on to the frontal cortex. From these cortical regions, the multiple pathways converge upon the superior colliculus (SC) and premotor neurons within the brainstem, with a feedback loop involving to the cerebellum, prior to saccade generation from the brainstem premotor burst neurones (Figure 1.1). These regions will now be discussed in turn.

1.7 SACCADIC CORTICAL NETWORK

Parietal cortex

From the visual cortex, information for the position and ocular motor output travels via the dorsal stream to the parietal cortex. The parietal cortex appears to influence saccadic behaviour in two ways. Firstly, the parietal cortex has a direct role in the programming and initiation of saccades to visual targets (via direct projections to the SC). Both lesions and reduced neural activation within the parietal cortex, specifically the IPS, are seen to result in increased prosaccade latencies (Heide and Kompf, 1998; Anderson *et al.*, 2008). The lateral region of the intraparietal sulcus (LIP) are known as the parietal eye fields (PEF), and are thought to be involved in the triggering of reflexive saccades and programming saccades to visual targets (Bisley and Goldberg, 2003; Nyffeler *et al.*, 2005; Anderson *et al.*, 2008).

Secondly, the parietal cortex has an indirect influence by virtue of its role in directing visual attention to objects; in that the superior parietal cortex has reciprocal connections to the

frontal (FEF) and supplementary eye fields (SEF) (Corbetta and Shulman, 2002; Godijn and Pratt, 2002).

Frontal eye fields

The FEF lie in the lateral section of the precentral sulcus, and include regions of the precentral, middle frontal, and superior frontal gyri. The FEF are integral to the planning and preparation of saccades, both reflexive and volitional (Pierrot-Deseilligny *et al.*, 2003). Afferent inputs to the FEF arrive from the PEF, SEF, prefrontal cortex, cingulate gyrus, superior temporal cortex and thalamus (Barbas and Mesulam, 1981; Schall *et al.*, 1993). Projections from the FEF reach the SC, basal ganglia, cerebellum, brainstem nuclei, as well as the PEF and SEF (via reciprocal connections) (Lynch and Tian, 2006; Cieslik *et al.*, 2016).

From primate studies, the FEF is shown to be topographically organised, in that larger saccades are triggered by activation from the dorsomedial portion of the FEF, while smaller saccades are evoked from ventrolateral portions (Bruce *et al.*, 1985). Thus, the discharge of neurons within this regions, approximately 40-50ms prior to saccade onset, is related to saccade amplitude and direction (Leigh and Zee, 2006). The FEF have also been shown to contribute to inhibiting unwanted saccades during antisaccade (Curtis and D'Esposito, 2003; Clementz *et al.*, 2007) and memory-guided tasks (Curtis and D'Esposito, 2006). In a study of antisaccades, which require participants to suppress a reflexive saccade to the target and initiate a volitional saccade to the opposite location, participants with hemispheric stroke or seizure disorder affecting the FEF, revealed a greater percentage of inhibition errors and responses to distractor stimuli than controls (Van der Stigchel *et al.*, 2012).

Supplementary eye fields

The SEF are located anteriorly to the supplementary motor cortex in the upper part of the paracentral sulcus (Grosbras *et al.*, 1999). Similar to the FEF, the SEF have an encoding map, in that the rostral SEF encodes saccades in an eye-centred frame, whereas the caudal SEF encodes saccades in a head-centred frame (Leigh and Zee, 2006). The SEF projects to the SC and brainstem premotor nuclei (Tehovnik *et al.*, 1994). Tasks of learning and motor planning, specifically in the triggering and amplitude of memory-guided saccades, double-step paradigms, and saccade sequences require SEF involvement (Pierrot-Deseilligny *et al.*, 1995; Schlag-Rey *et al.*, 1997)

Dorsolateral prefrontal cortex

The dorsolateral prefrontal cortex (DLPFC), does not play a critical role in the generation of reflexive saccades, but rather integrates into the ocular motor system when cognitive control is required (Muri and Nyffeler, 2008). Specifically, it performs an executive role, involved in saccade inhibition as well as short-term spatial working memory (Pierrot-Deseilligny *et al.*, 2003). For example, individuals with ADHD and frontal lobe lesions affecting the DLPFC, exhibited increased saccade latencies, poorer spatial accuracy and more anticipatory errors compared to controls during a memory-guided task, which requires a target to be remembered prior to saccade execution (Goto *et al.*, 2010). Moreover, the DLPFC and ventrolateral prefrontal cortices have been found to be more active in cognitively driven antisaccade tasks, rather than reflexive prosaccade tasks (Jamadar *et al.*, 2013).

Overall, the cortical regions are critically important for i) visual attention (specifically in the parietal cortex), and ii) motor planning of saccades (the prefrontal regions in particular).

1.8 SACCADIC SUB-CORTICAL NETWORK

Basal ganglia

For saccades, the basal ganglia nuclei play a role in appropriate response selection (McDowell *et al.*, 2008), mediating the behavioural context of all saccades (Hikosaka *et al.*, 1989; Shimo and Hikosaka, 2001). Input from the prefrontal regions is received by the caudate nucleus. The caudate then sends inhibitory projections to the substantia nigra pars reticular (SNpr) either directly or indirectly (via the globus pallidus and subthalamic nuclei) prior to saccade onset (Hikosaka *et al.*, 2000). These projections result in the cessation of tonic inhibitory discharge of the SNpr to the SC. Therefore, altering the tonic discharge of the SNpr enables saccade initiation (due to a pause in the inhibitory output of the basal ganglia), or saccade suppression (due to sustained inhibitory output from the SNpr).

Superior colliculus

The SC is situated in the midbrain and is central to the execution of eye movements through its role in the integration and organisation of cortical and subcortical ocular motor inputs (Figure 1.1). The SC is divided into two functional regions: i) the superficial layers (visual region) (SCs) and ii) the intermediate and deep layers (ocular motor region) (SCi) (Johnston and Everling, 2008).

The SCs receives projections from the retina and visual cortex, which are mapped according to the contralateral visual field (Cynader and Berman, 1972). Output from this region is sent to the lateral geniculate body, thalamus and SCi (Mays and Sparks, 1980).

The SCi receives afferent input from the visual, parietal, and frontal cortices, SCs, as well as the basal ganglia (which provides a continuous tonic inhibitory input). The SCi is organised retinotopically, corresponding with the required saccade amplitude and direction. The rostral pole is primarily concerned with fixation and small saccades, and the caudal regions

with target selection and initiation of large saccades (Leigh and Zee, 2006). Thus, the SCi encodes for the saccade target in the contralateral visual field, but does not pertain to information relevant to directly innervate the extraocular muscles (Krauzlis, 2005). Further, the SCi contains both i) build-up neurones which fire prior to saccade initiation, and ii) burst neurones which have a short, high frequency discharge during saccade execution (Munoz and Wurtz, 1995). Output from the SCi projects to i) the brainstem to generate the premotor response, and ii) the cerebellum which forms part of a feedback loop.

Cerebellum

The core function of the dorsal vermis cerebellum (lobules V-VII) in ocular motility is to revise and modify programmed movements for optimal and accurate eye movements (Zee and Walker, 2009; Herzfeld *et al.*, 2015). Input from the frontal cortex and SCi, travels via the nuclus reticularis tegmenti pontis (NRTP), and MCP before disseminating within the cerebellum dorsal vermis (Scudder *et al.*, 1996).

The cerebellum vermis is topographically organised and Purkinje cells in this region discharge approximately 15ms prior to saccade onset (Ohtsuka and Noda, 1995). Output from the vermis travels via the fastigial nucleus to the brainstem premotor nuclei (via the SCP), and is involved in the modification of saccade trajectories (Noda *et al.*, 1990; Scudder, 2002; Leigh and Zee, 2006). Neurones within the fastigial nuclei discharge approximately 8ms before saccade onset (although this is modulated by the saccade size and velocity) (Fuchs *et al.*, 1993; Leigh and Zee, 2006). The caudal fastigial nucleus provides inhibitory input to the SCi and brainstem premotor neurones to slow/stop a saccade. Damage to the oculomotor vermis can affect the burst of neuronal discharge, altering the size and timing of saccadic eye movements and errors in planned motor output are often not detected (Kheradmand and Zee, 2011).

Brainstem premotor neurons

The brainstem contains three main groups of premotor neurons, which ultimately innervate the extraocular muscles (Girard and Berthoz, 2005). Firstly, long-lead burst neurones are located within the NRTP. The NRTP encodes the 3D eye displacement vectors for the upcoming saccade, and is important for saccadic feedback given its connections with the SCi, cortical eye fields and cerebellum (Leigh and Zee, 2006). The NRTP discharges approximately 40ms prior to saccade onset (Noda *et al.*, 1990; Van Opstal *et al.*, 1996).

Secondly, omnipause neurons receive projections from the SCi, FEF, SEF, cerebellum and other neurons within the reticular formation, pons and midbrain (Scudder *et al.*, 2002). Omnipause neurones have continuous tonic discharges which cease approximately 16ms before and throughout saccade generation (Leigh and Zee, 2006). Omnipause neurons project to the third group of premotor neurones, known as premotor burst neurones. Similar to the gating mechanism of the SNpr on the SCi, the omnipause neurones must be *paused* to enable activation of these premotor burst neurones.

The premotor burst neurones may be either excitatory or inhibitory in nature, and discharge at high frequencies approximately 12ms prior to and during saccades. The location of the premotor burst neurones is dependent on the direction of the saccade – either horizontal or vertical. Horizontal burst neurons are located within the paramedian pontine reticular formation (excitatory) and rostral interstitial nucleus of the medial longitudinal fasciculus (inhibitory); while vertical burst neurones are located within the medullary reticular formation (excitatory) and rostral interstitial nucleus of the medial longitudinal fasciculus (inhibitor) (Van Gisbergen *et al.*, 1981; Leigh and Zee, 2006). Excitatory burst neurons (EBNs) innervate the medial rectus muscle of the contralateral eye via ipsilateral projections to the abducens motoneurons, internuclear neurons, as well as back to the cerebellum (Scudder *et al.*, 2002; Leigh and Zee, 2006). EBNs also project to the ipsilateral inhibitory burst neurons (IBNs). IBNs suppress the innervation of antagonist muscles during saccades through projections to the contralateral abducens nucleus to inhibit the contralateral

motoneurons and interneurons (Scudder *et al.*, 2002). Therefore, activation of these EBNs and IBNs ultimately leads to the innervation of the extraocular muscles, and ultimately saccade generation.

1.9 OCULAR MOTOR ANALYSIS AND THE *FMR1* GENE

Prior to commencing the current investigation, only a single study has examined ocular motility in individuals with *FMR1* expansions. The study found that FXS females (CGG>200) experienced greater difficulty generating accurate and timely saccades on during gap/overlap and memory-guided tasks, the latter suggestive of compromised working memory capabilities (Lasker *et al.*, 2007). In the interim, Wong *et al.* (2014) examined ocular motor performance in a cohort of 21 PM males without FXTAS and 22 age matched controls. Equivalent behavioural measures were found during fixation, smooth pursuit and visually guided paradigms. However, PM males without FXTAS showed slower antisaccade responses, and increased inhibitory cost (mean latency of antisaccade – mean latency of prosaccade) compared to controls. Inhibitory cost was found to correlate with the volume of cerebellar vermis lobules VI-VII and CGG repeat length in PM males without FXTAS. Moreover, age-related decline was seen for controls (an increase in prosaccade and antisaccade anticipatory saccades, and antisaccade error rate) which was absent for PM males without FXTAS (Wong *et al.*, 2014). Finally, a short series of case reports has found progressive supranuclear gaze palsy-like ocular motor abnormalities (square wave jerk intrusions during fixation) in five FXTAS patients (Hall *et al.*, 2016b).

1.10 SUMMARY

The saccadic neural network descends from cortical regions involved in the initial perceptual integration, across parietal and frontal regions (critical for cognitive control), down to subcortical structures in the midbrain, cerebellum, and ultimately the brainstem. The cortico-cerebellar connections within this saccadic neural network are central to the accurate performance of cognitively driven saccades. Thus, utilising saccadic paradigms to probe and disseminate the executive function phenotype of PM carriers without FXTAS is advantageous as it enables i) sensitive measure of sensorimotor cognitive processing, ii) clear and defined neural correlations related to easily measurable stereotyped outcomes, iii) targets cortical and cerebellar nodes and pathways known to be weakened by FXTAS, and iv) they have currently been underutilised in *FMR1* expansions and provide a fruitful tool for future investigations.

RATIONALE FOR THESIS

It is clear that PM females without FXTAS are at risk for a number of medical disorders and impaired cognitive skills (language and mathematical abilities), however the extent of executive dysfunction and neural abnormalities is less clear compared to PM males without FXTAS. Understanding the intricacies and complexities of the PM female without FXTAS dysexecutive profile is important, as it may represent preclinical markers related to FXTAS. Further, the expected prevalence of PM females is anticipated to rise by 30%, affecting an estimated 114,000 Australian women by 2030 (Brown, 2010). Therefore delineating the executive dysfunction and neural phenotype of PM females without FXTAS will be critical for the development of gender specific early interventions (cognitive and medical) for future generations of PM women.

1.11 AIMS

The principal aim of this thesis was to determine the extent and nature of executive dysfunction in PM females without FXTAS. Saccadic paradigms were employed, amongst a range of other neuropsychological tasks, to sensitively assess executive function weakness and the integrity of the cortico-cerebellar neural network. A secondary aim was to examine the biological sources of predicted cortico-cerebellar disruption, through the examination of the inter-relationships between executive (dys)function, genetic (CGG, DNA methylation and *FMR1* mRNA), and neural markers. To do this, comprehensive genetic and molecular analyses, as well as sophisticated neuroimaging techniques were adopted. This has allowed for an integrative analytical approach in the assessment of executive dysfunction, utilising a gene – brain – behaviour model.

CHAPTER 2: NEUROPSYCHOLOGICAL ASSESSMENT OF EXECUTIVE DYSFUNCTION

Chapter 1 provided an overview of the PM-carrier phenotypes, proposing that the delineation of the female specific executive dysfunction phenotype is required. Chapter 2 provides the first of a series of experiments exploring executive function in PM females without FXTAS. It provides a comprehensive analysis of dysfunction across five neuropsychological tasks which assess attention, processing speed, response inhibition, working memory and executive function more generally. Age-related changes are also examined using regression analyses, to identify whether, like PM males, PM females without FXTAS experience an age-related decline in executive function (Cornish *et al.*, 2008b; Cornish *et al.*, 2009; Cornish *et al.*, 2011).

This Chapter is written as a manuscript for publication: *Executive dysfunction in female FMR1 premutation carriers*. It was published in *Cerebellum,* Volume 15, Issue 5 2016. To maintain consistency throughout this thesis, changes have been made to formatting.

Declaration by candidate

In the case of Chapter 2, the nature and extent of my contribution to the work was the following:

Nature of contribution	Extent of contribution (%)
Conceptualisation, project design and programming of paradigms, data collection, data analysis and interpretation, and manuscript preparation	80%

The following co-authors contributed to the work. If co-authors are students at Monash University, the extent of their contribution in percentage terms must be stated:

Name	Nature of contribution	Extent of contribution (%) for student co-authors only
Kim Cornish	Conceptualisation, project design and manuscript preparation	
Claudine Kraan	Manuscript preparation	
Reymundo Lozano	Manuscript preparation	
Minh Bui	Statistical analysis and manuscript preparation	
Joanne Fielding	Conceptualisation, project design, data interpretation, and manuscript preparation	

The undersigned hereby certify that the above declaration correctly reflects the nature and extent of the candidate's and co-authors' contributions to this work.

Candidate's Signature	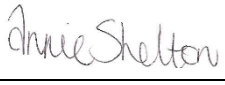	Date
Main Supervisor's Signature		Date

EXECUTIVE DYSFUNCTION IN FEMALE *FMR1* PREMUTATION CARRIERS

Annie L. Shelton, Kim M. Cornish, Claudine Kraan, Reymundo Lozano, Minh Bui, & Joanne Fielding

2.1 ABSTRACT

There is now growing evidence of cognitive weakness in female premutation carriers (between 55 and 199 CGG repeats) of the Fragile X mental retardation gene, including impairments associated with executive function. While an age-related decline in assessments of executive function has been found for male premutation carriers, few studies have explored whether female carriers show a similar trajectory with age. A total of 20 female premutation carriers and 21 age- and IQ-matched healthy controls completed a battery of tasks assessing executive function tasks, including the Behavioural Dyscontrol Scale (BDS), Symbol Digit Modalities Test (SDMT), Paced Auditory Serial Addition Test (PASAT), Haylings sentence completion test and the digit span task (forward and backward). Performance was compared between premutation carriers and healthy controls, and the association between task performance and age ascertained. Compared to controls, female premutation carriers were found to be impaired on the BDS, SDMT, PASAT, and Haylings sentence completion tasks, all of which rely on quick, or timed, responses. Further analyses revealed no significant association between age and task performance for either premutation carriers or controls. This study demonstrates that a cohort of female premutation carriers have deficits on a range of tasks of executive function that require the rapid temporal resolution of responses. We propose that the understanding of the phenotype of permutation carriers will be advanced through use of such measures.

2.2 INTRODUCTION

Executive dysfunction is amongst a range of deficits associated with CGG trinucleotide expansions of the Fragile X mental retardation (*FMR1*) gene, located on the long arm of the X chromosome at position Xq23.11. While deficits in executive function are evident in those with Fragile X syndrome (FXS), a consequence of full mutation expansions of over 200 CGG repeats (Kemper *et al.*, 1988), carriers of premutation expansions (55 to 199 CGG repeats) who have Fragile X-tremor ataxia syndrome (FXTAS) are also at risk (Loesch *et al.*, 2003). FXTAS has a penetrance rate of approximately 45% in male and 16% of female premutation carriers over 50 years of age (Rodriguez-Revenga *et al.*, 2009), and is a severe progressive neurodegenerative disorder (Hall *et al.*, 2014) (for updates on the FXTAS phenotype see the review by Hall et al in this edition). There is now, however, increasing evidence of executive dysfunction amongst premutation carriers without FXTAS (see reviews (Loesch and Hagerman, 2012; Kraan *et al.*, 2013a; Grigsby *et al.*, 2014)).

Executive functions refer to the set of skills used to organise and act on information, including the initiation of behaviour, inhibiting a prepotent response, planning, cognitive flexibility and retaining information in working memory (Collette *et al.*, 2006; Niendam *et al.*, 2012). Premutation males without FXTAS have executive function deficits, which have been found in tasks assessing processing speed, working memory and inhibition (Grigsby *et al.*, 2006; Cornish *et al.*, 2008b; Cornish *et al.*, 2009; Cornish *et al.*, 2011; Hunter *et al.*, 2012c). Moreover, an age-related decline in performance on response inhibition (Cornish *et al.*, 2008b) and working memory (Cornish *et al.*, 2009) tasks has been found in male permutation carriers, during the third and fourth decades of life, respectively. This suggests that for male premutation carriers, executive dysfunction could be an early biomarker of neuropathology and progression to FXTAS.

Deficits of executive functions have also been reported in female premutation carriers, specifically during processing speed (Yang *et al.*, 2013; Shelton *et al.*, 2015) and response inhibition tasks (Kraan *et al.*, 2014c; Shelton *et al.*, 2014; Cornish *et al.*, 2015). There is also

preliminary evidence of working memory impairments (Shelton *et al.*, 2015), yet this has not been consistently found. However, few studies have employed a comprehensive battery of testing to examine executive dysfunction in female premutation carriers. Thus, the full extent of executive dysfunction, across multiple executive function skills, in female premutation carriers is currently unknown.

Whether there is a decline with age in cognitive function more generally in female premutation carriers is also unclear. Our previous report found that response inhibition (assessed through the Haylings sentence completion test) was correlated with increasing age, but this did not survive Bonferonni correction (Kraan *et al.*, 2014c). However, age-related cognitive decline has been found in measures of visuospatial perception (during a quantitative magnitude comparison task), even though performance was equivalent for female premutation carriers and controls (Goodrich-Hunsaker *et al.*, 2011a), and for a range of language dysfluencies (Sterling *et al.*, 2013). Given that female premutation carriers appear to have similar executive deficits as males, yet a lower prevalence rate of FXTAS; little is known about the effect of ageing of executive functions for female premutation carriers.

This study aims to expand understanding of the phenotypic characteristics of executive function in female premutation carriers, by using a battery of tests of executive functions targeting attention, processing speed, response inhibition and working memory processes. Furthermore, this study aims to ascertain the consequence of ageing on these functions. This will provide preliminary evidence for the utility of executive function tasks as early biomarkers of FXTAS.

2.3 METHODS

A total of 41 female participants between the ages of 22 and 54 years (20 premutation carriers, 21 healthy controls) were recruited from support groups, population-based Fragile X carrier screening studies (Metcalfe *et al.*, 2008), as well as local networks and via online

advertisements. This sample included 16 premutation carriers and 14 healthy controls who had completed prior cognitive investigation (Kraan *et al.*, 2014b; Kraan *et al.*, 2014c). Five families were included (4 with 2 premutation carriers, and 1 with 2 premutation carriers and 1 healthy control).

All participants were English speaking with no history of any serious neurological damage/disease, and had normal (or corrected) vision and hearing. No participant reported any signs of symptoms indicative of FXTAS and this was confirmed with all participants being screened with the FXTAS Rating Scale (Leehey, 2009). CGG repeat size was analysed for all participants to confirm premutation status (CGG between 55 to 199 repeats) and normal allele size in healthy controls (less than 45 CGG repeats), using DNA from peripheral blood and the Asuragen® AmplideX™ *FMR1* PCR Kit (Asuragen: Austin, TX, USA). Participants were matched for age [Premutation carriers: M=40.10, SD=9.77; controls: M=39.76 SD=9.00; t(39)=0.115, p=0.901] and full scale IQ [Premutation carriers: M=110.85, SD=9.56; controls: M=114.62 SD=8.87; t(39)=-0.131, p=0.198] as determined using the Wechsler Abbreviated Scale of Intelligence (WASI) (Wechsler, 1999). Ethics approval for this study was granted by Monash University and Southern Health Human Research Committees (Project Number 10147B); all participants gave their informed consent prior to inclusion in the study in accordance with the declaration of Helsinki.

Executive function tasks

A range of cognitive tasks were selected to examine executive dysfunction. The Behavioural Dyscontrol Scale (BDS) (Grigsby and Kaye, 1996) was used to provide a global measure of executive dysfunction. The BDS has nine test items that assess simple motor responses, procedural motor learning, working memory, attention and self-insight. Each item is scored individually (0-3), and then combined to create a total BDS score.

The Haylings sentence completion test (Burgess and Shallice, 1997) was used to evaluate response inhibition. Participants are required to provide a word to finish 15 sentences, which had the last word omitted, as quickly as possible. Responses were classified as either correct (the word provided was completely unconnected to the sentence), a category 'A' error (the word provided logically completed the sentence) or as a category 'B' error (the word provided was somewhat connected to the sentence). A total error score (Hayling AB error) was calculated by combining the raw scores of category A and category B errors together, thus providing a measure of response inhibition.

The Symbol Digit Modality Test (SDMT) written version was used to assess attention and processing speed (Smith, 1973). The SDMT required participants to pair abstract symbols with specific numbers, as quickly and as accurately as possible (Smith, 1973). The total number of correctly paired numbers was calculated for each participant during 90s.

The Paced Auditory Serial Addition Test (PASAT) was used to measure processing speed, as well as to assess working memory capability (Gronwall, 1977). During the PASAT, participants were audibly presented with a series of numbers at a rate of one every 3s. They were instructed to add the two most recently spoken words together and vocalise the number, before the next number was said.

The digit span task was used to further examine verbal working memory ability (Wechsler, 1997). It required participants to repeat a sequence of numbers aloud, either as they heard it (forward condition) or in reserve order (backward condition) (Wechsler, 1997). The total number of correct responses for both conditions was combined to form a total digit span score.

Lower scores on all tasks except for the Haylings sentence completion task indicate impaired executive functionality.

Statistical analysis

Statistical analysis was performed using Stata Statistical Software, Release 14 2015. Each cognitive variable for controls and premutation carriers was assessed separately for normality distribution (via skewness and kurtosis tests) – for all non-normally distributed variables an appropriate transformation was applied (square root). Levene's test of equal variance was then assessed for each task. To assess whether scores were related to age, least squares regression analyses were used for all participants combined. If age was not related to a particular score, an independent samples t-test was used (equal or unequal variances), to assess group differences. When age was related to a score, ANCOVA analysis was used, where age was the covariate. Finally, least squares regression analyses with 10,000 permutations were used to assess the relationship of age on test score performance for both control and premutation carriers separately. A significance level of $p<0.05$ was set for all analyses.

2.4 RESULTS

The test scores of female premutation carriers were compared to controls (see Table 2.1 for statistics). Independent samples *t*-tests found that premutation carriers exhibited impaired performance compared to controls for the BDS ($p=0.001$), Haylings AB score ($p=0.034$), and PASAT ($p=0.030$), but not for the digit span total score ($p=0.566$). Age was found to associate with the SDMT, whereby increasing age was related to decreased processing speed through reduced test item completion for all participants ($r=-0.39$, $p=0.045$). Therefore, when covarying for age in a between group analysis (ANCOVA), no interaction between group (premutation or control) and age was seen ($p=0.69$). However, significant effects for group ($p=0.019$) (see Table 2.1) and age ($p=0.015$) were revealed. Thus, premutation carriers made fewer correct number-symbol matches in the allocated time of the SDMT, showing impaired performance compared to controls.

Analysis of age amongst premutation carriers yielded no significant associations between increasing age and scores on the BDS (p=0.983), SDMT (p=0.108), PASAT (p=0.297), Haylings AB (p= 0.353) and digit span (p=0.517) tasks (see Table 2.2 for statistics). Similarly, age was not found to significantly predict scores on any tasks for controls: BDS (p=0.992), SDMT (p=0.070), PASAT (p=0.798), Haylings AB error (p=0.079) and digit span (p=0.383) (see Table 2.2).

Table 2.1: Summarised statistics (mean and standard deviation) and comparison (p-value) between controls and premutation carriers.

	Control		Premutation Carriers		
	Mean	SD	Mean	SD	*p*
BDS	25.619	1.071	23.500	2.395	**0.001**[++]
Haylings AB error*	4.650	4.987	8.900	7.907	**0.034**[+]
SDMT	64.952	11.500	57.100	9.851	**0.019**[§]
PASAT	86.905	10.945	74.872	21.037	**0.030**[++]
Digit Span total	19.238	3.859	18.450	4.828	0.566[+]

Note: [*]p-value computed using square root transformation, raw mean and standard deviation values shown. [+]equal variance, [++]unequal variance, [§]Comparison adjusted for age (covariate) using ANCOVA. Figures in red bold show that p<0.05.

Table 2.2 – Least Squares Regression analysis between age (predictor) and executive function tasks (outcome) for healthy controls and premutation carriers.

	Healthy Controls			Premutation Carriers		
	β	S.E	*p*	β	S.E	*p*
BDS	-0.001	0.025	0.992	0.001	0.024	0.983
SDMT	-0.045	0.023	0.070	-0.038	0.022	0.108
PASAT	0.007	0.025	0.798	-0.025	0.023	0.297
Haylings A+B errors*	0.053	0.028	0.079	0.030	0.031	0.353
Digit Span Total	-0.023	0.025	0.383	-0.016	0.024	0.517

Note: [*]p-value computed using square root transformation, β=standardised coefficient, S.E=standard error.

2.5 DISCUSSION

The primary aim of this study was to determine executive function deficits in female premutation carriers, using a battery of tests assessing attention, processing speed, response inhibition and working memory processes. Executive dysfunction was found across a range of cognitive processes previously identified in studies of premutation carriers without FXTAS (Kraan *et al.*, 2013a; Grigsby *et al.*, 2014), specifically reduced processing speed, impaired response inhibition, reduced attention, and working memory. These results indicate that specific deficits in executive functions were best delineated when temporal response stress was involved (SDMT, PASAT, and Haylings), rather than tasks with undefined response time frames, such as the digit span task. Similar deficits in executive functions have been found on tasks that limit response time, namely the Haylings test (Kraan *et al.*, 2014b; Kraan *et al.*, 2014c; Cornish *et al.*, 2015), excluded letter verbal fluency (Kraan *et al.*, 2014b; Cornish *et al.*, 2015), the SDMT (Yang *et al.*, 2013), and an ocular motor n-back task (Shelton *et al.*, 2015), in female premutation carrier cohorts.

Executive functions rely on the integrity of nodes within prefrontal and parietal cortices as well as the cerebellum (see reviews (Middleton and Strick, 2001; Collette *et al.*, 2006; Ramnani, 2012; Stoodley, 2012)), while the integrity of the white matter connecting these regions subserves the speed of processing (Turken *et al.*, 2008; Madden *et al.*, 2009a). Diffuse reductions in white matter integrity within these neural tracts have been found in permutation carriers without FXTAS (Jacquemont *et al.*, 2010; Hashimoto *et al.*, 2011c; Apartis *et al.*, 2012; Battistella *et al.*, 2013; Leow *et al.*, 2014). Temporally limiting responses is likely to exacerbate any underlying executive deficits, due to increased demand on neural resources. Together, these results reinforce the notion that *some* male and female premutation carriers, have a cognitive '*signature*' that is quantifiable in terms of executive dysfunction, which is best studied when tasks are reliant on quick responses.

This proposition is evidenced by the conflicting results on the PASAT and digit span tasks, both explicitly working memory tasks, seen in this study. Previous studies have shown that

number manipulation-repetition tasks that have no temporal limits on responses, such as digit span (Moore *et al.*, 2004a; Cornish *et al.*, 2009; Hunter *et al.*, 2012c; Hippolyte *et al.*, 2014) and letter-number sequencing (Brega *et al.*, 2008; Shelton *et al.*, 2014) tasks, may not be sensitive to impairment in male and female premutation carriers. To our knowledge, this is the first time the PASAT has been used to assess group differences in a premutation cohort. The PASAT is a number calculation task that not only relies on working memory, but also relies on efficient processing speed as well as mathematical ability. We cannot exclude that arithmetic skills may influence PASAT findings; however such skills are not impaired in female premutation carriers (Semenza *et al.*, 2012). The temporal *stress* experienced during the PASAT is likely to exacerbate working memory weaknesses within this population. Especially given that psychological affect (anxiety) and executive dysfunction have been found to be correlated in female premutation carriers (Kraan *et al.*, 2014c; Cornish *et al.*, 2015). Thus, impaired working memory, along with other executive functions, may be best investigated using tasks with high temporal demand, increasing anxiety and stress, amongst premutation carriers.

The second aim of the study was to examine the association between increasing age and executive functions. Regression analysis did not reveal any significant associations between age and task scores for either controls or premutation carriers in this study, yet age was found to be associated with SDMT performance when assessing all participants together. Although ageing has been associated with reduced cognitive ability more generally (Goodrich-Hunsaker *et al.*, 2011a; Sterling *et al.*, 2013), no study has found age-related changes in executive function in female premutation carriers. This is in contrast to findings with male premutation carriers. However, these findings in males comprised participants up to the age of 69 years of age (Cornish *et al.*, 2008b; Cornish *et al.*, 2009; Cornish *et al.*, 2011). We therefore attribute the absence of an age effect in this study to the restricted age of our female participants (all less than 55 years of age), a relatively small sample size and cross-sectional nature of the study. Therefore, it is conceivable that age related decline in executive

function may begin later in female premutation carrier, and hence not detected in this study due to limited statistical power. To rigorously delineate the impact of ageing on executive functions in female premutation carriers, repeating the current study, as well as longitudinal follow-up analysis, with a larger cohort inclusive of participants up to 70 years of age would be advantageous.

Evidence of executive dysfunction in not a novel finding within the premutation literature. However, our results demonstrate that female premutation carriers, like males, may experience a range of executive function impairments, particularly in tasks of attention, processing speed, response inhibition and working memory. To our knowledge, this is the first study to provide evidence that executive function deficits of premutation carriers are best delineated using tasks that require the efficient and rapid temporal resolution of responses. Replicating these findings in a larger sample of male and female premutation carriers will provide further support for the reliance on temporally based cognitive tasks, when assessing the cognitive phenotype of *FMR1* premutation carriers in the future. Together, these preliminary findings provide a comprehensive assessment of executive dysfunction in female premutation carriers, further establishing the cognitive phenotype and demonstrating similar cognitive weakness between male and female premutation carriers. Critically, this study shows the utility of executive functions tasks with limited temporal response time for refining the premutation carrier cognitive phenotype, critical for the development of early biomarkers indicative of FXTAS.

CHAPTER 3: SACADIC EXECUTIVE DYSFUNCTION ASSESSMENT

Chapter 2 reported and discussed a range of deficits in PM females without FXTAS on executive function tasks requiring a rapid resolution of responses. Chapter 3 examines the extent and nature of these deficits, specifically using saccadic paradigms which probe response inhibition and working memory domains of executive function. These saccadic paradigms require rapid and accurate eye movements in response to visual stimuli, and have been utilised in a range of neurological conditions. Results from these paradigms were also correlated with CGG-repeat length in PM females without FXTAS, to ascertain the presence, or otherwise, of a CGG-dosage effect.

This Chapter is written as a manuscript for publication: *Exploring inhibitory deficits in female carriers of Fragile X syndrome: Through eye movements*. It was published in *Brain and Cognition*, Volume 85 2014. To maintain consistency throughout this thesis, changes have been made to formatting.

Declaration by candidate

In the case of Chapter 3, the nature and extent of my contribution to the work was the following:

Nature of contribution	Extent of contribution (%)
Conceptualisation, project design and programming of paradigms, data collection, data analysis and interpretation, and manuscript preparation	80%

The following co-authors contributed to the work. If co-authors are students at Monash University, the extent of their contribution in percentage terms must be stated:

Name	Nature of contribution	Extent of contribution (%) for student co-authors only
Kim Cornish	Conceptualisation, project design and manuscript preparation	
Claudine Kraan	Project design and manuscript preparation	
Darren R. Hocking	Project design and manuscript preparation	
Nellie Georgiou-Karistianis	Manuscript preparation	
Sylvia A. Metcalfe	Manuscript preparation	
John L. Bradshaw	Manuscript preparation	
Alison D. Archibald	Manuscript preparation	
Jonathan Cohen	Manuscript preparation	
Julian N. Trollor	Manuscript preparation	
Joanne Fielding	Conceptualisation, project design, data interpretation, and manuscript preparation	

The undersigned hereby certify that the above declaration correctly reflects the nature and extent of the candidate's and co-authors' contributions to this work.

Candidate's Signature		Date
Main Supervisor's Signature	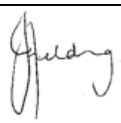	Date

EXPLORING INHIBITORY DEFICITS IN FEMALE CARRIERS OF FRAGILE X SYNDROME: THROUGH EYE MOVEMENTS

Annie L. Shelton, Kim Cornish, Claudine Kraan, Nellie Georgiou-Karistianis, Sylvia A. Metcalfe, John L. Bradshaw, Darren R. Hocking, Alison D. Archibald, Jonathan Cohen, Julian N. Trollor, & Joanne Fielding

3.1 ABSTRACT

There is evidence which demonstrates that a subset of males with a premutation CGG repeat expansion (between 55-200 repeats) of the Fragile X mental retardation 1 gene exhibit subtle deficits of executive function that progressively deteriorate with increasing age and CGG repeat length. However, it remains unclear whether similar deficits, which may indicate the onset of more severe degeneration, are evident in female PM-carriers. In the present study we explore whether female PM-carriers exhibit deficits of executive function which parallel those of male PM-carriers. Fourteen female Fragile X premutation carriers without Fragile X-associated tremor/ataxia syndrome and fourteen age, sex, and IQ matched controls underwent ocular motor and neuropsychological tests of select executive processes, specifically of response inhibition and working memory. Group comparisons revealed poorer inhibitory control for female premutation carriers on ocular motor tasks, in addition to demonstrating some difficulties in behaviour self-regulation, when compared to controls. A negative correlation between CGG repeat length and antisaccade error rates for premutation carriers was also found. Our preliminary findings indicate that impaired inhibitory control may represent a phenotype characteristic which may be a sensitive risk biomarker within this female Fragile X premutation population.

3.2 INTRODUCTION

Fragile X syndrome (FXS), the leading cause of inherited intellectual disability worldwide (Cornish *et al.*, 2008a), is caused by a large CGG repeat expansion (>200 CGG repeats) on the 5' untranslated region of the Fragile X mental retardation 1 (*FMR1*) gene. While those with a CGG repeat expansion of up to 45 are considered free from any deleterious effects, those with expansions from 55-200 CGG repeats, otherwise known as premutation (PM) expansions, are now known to be vulnerable to both neurodevelopmental and neurodegenerative changes (Jacquemont *et al.*, 2007). Approximately 45% of male and 8-17% of female PM-carriers over the age of 50 develop Fragile X-associated tremor/ataxia syndrome (FXTAS) (Rodriguez-Revenga *et al.*, 2009). For female PM-carriers there is also an enhanced risk for Fragile X-associated primary ovarian insufficiency (FXPOI), which can include premature menopause in approximately 20% of PM-carriers compared to 1% in the general population (Sherman, 2000; Rodriguez-Revenga *et al.*, 2009). However, FXTAS and FXPOI alone do not account for the full spectrum of involvement in the PM, which includes a range of specific executive processing impairments (Cornish *et al.*, 2008a; Cornish *et al.*, 2008b; Cornish *et al.*, 2009; Kogan and Cornish, 2010; Cornish *et al.*, 2011; Hocking *et al.*, 2012; Hunter *et al.*, 2012a). Given the most recently documented prevalence rates of PM in males (1:430) and females (1:209) in a North American sample (Tassone *et al.*, 2012), and the possibility that subtle cognitive changes may reflect either neurodevelopmental affects and/or the very earliest signs of neurodegeneration, further investigation of the neurocognitive profiles of PM-carriers is warranted.

Executive dysfunction, a feature of FXTAS, has been demonstrated in male PM-carriers in the absence of clinical features. Specifically, studies have found that the subcomponents of response inhibition (Cornish *et al.*, 2008a; Cornish *et al.*, 2008b; Cornish *et al.*, 2011), and working memory (Cornish *et al.*, 2009; Kogan and Cornish, 2010) are impaired, regardless of FXTAS status, and that there is a relationship between decline in these subcomponents of

executive function and increasing age and CGG-repeat length (Cornish *et al.*, 2008a; Cornish *et al.*, 2008b; Cornish *et al.*, 2009; Cornish *et al.*, 2011; Hocking *et al.*, 2012).

For female PM-carriers, the relationship between executive function and CGG repeat size is more complex due to X-inactivation, the phenotypic expression of only one set of X-linked genes. Increased rates of anxiety and depression symptoms, inattention, impulsivity and problems with self-concept have been self-reported by female PM-carriers, and there is evidence for low-level visuospatial processing deficits (Kéri and Benedek, 2009; Kéri and Benedek, 2010; Hunter *et al.*, 2012a; Hunter *et al.*, 2012b). Attentional, visuospatial, and neuromotor impairments have also been reported, and appear to affect to a greater extent those with CGG-repeat lengths greater than 100 (Hunsaker *et al.*, 2010; Goodrich-Hunsaker *et al.*, 2011a; Hunsaker *et al.*, 2011). However, these studies are yet to specifically and empirically target executive processing subcomponents of inhibition and working memory in female PM-carriers, which may resemble a subtle form of impairment reported in male PM-carriers (Cornish *et al.*, 2008a; Cornish *et al.*, 2008b; Cornish *et al.*, 2009; Kogan and Cornish, 2010; Cornish *et al.*, 2011).

Emerging evidence suggests that PM-carriers exhibit neuroanatomical differences that may underlie these observed deficits. In male PM-carriers without FXTAS, alterations in white matter connectivity were found bilaterally in the cerebellar peduncles, specifically in the middle cerebellar peduncle compared to controls, and in the left fornix when compared to PM-carriers with FXTAS (Hashimoto *et al.*, 2011c). Moreover, regions-of-interest analysis has revealed grey matter volumetric reductions within the cerebellum, particularly within lobule I/II of the vermis, which is implicated in the control of eye movements and balance, as well as in lobule III of the left hemisphere for PM-carriers compared to controls (Hashimoto *et al.*, 2011b). In female PM-carriers without FXTAS, reduced cortical inhibition in GABA and cortico-cerebellar motor networks has been identified using transcranial magnetic stimulation (Conde *et al.*, 2013). Beyond the cerebellum, a combined group of male and female PM-carriers has been found to have reduced cortical activation in inferior prefrontal

areas (right ventral inferior frontal cortex and left dorsal inferior frontal cortex/premotor cortex), regardless of FXTAS status, during a verbal working memory task (Hashimoto *et al.*, 2011a). Collectively, these findings demonstrate structural and functional differences primarily in the prefrontal and cerebellar regions of the brain; which have known links to the control of executive processes (Koziol *et al.*, 2012). While imaging is a compelling and sophisticated method of examining deficits at a neuroanatomical level, reinforcing these studies through a clear understanding of the behavioural phenotype is critical for potential identification of early clinical markers suggestive of cognitive decline.

One of the most sensitive behavioural methods for investigating neural (dys)function is assessment of ocular motility. Ocular motor paradigms have been used extensively in a range of neurodevelopmental and neurodegenerative conditions to examine not only control of lower level motor control processes, but of higher order cognitive control processes, in particular response inhibition and working memory (Fielding *et al.*, 2006; Lasker *et al.*, 2007; Fielding *et al.*, 2010). The networks and nodes implicated in generating saccadic eye movement are well defined, spanning almost the entire brain: distributed throughout the neocortex (particularly prefrontal areas), subcortical and cerebellar regions (Leigh and Zee, 2006). In addition, a close relationship between input and motor output facilitates precise measurement and provides an exquisitely sensitive behavioural measure of sensorimotor processing. To date, only a single study has examined ocular motility within the context of the FXS spectrum. This study found that adolescent females with FXS (CGG>200) had greater difficulty generating accurate and timely saccades on gap/overlap and memory-guided tasks, the latter result suggestive of compromised working memory capabilities (Lasker *et al.*, 2007).

The present study sought to examine the utility of saccadic paradigms to detect subtle cognitive changes in female PM-carriers. It specifically investigated executive dysfunction, focusing on response inhibition and working memory impairments that have previously been reported in male PM-carriers. We also examined the relationships between ocular

motor task errors and performance on neuropsychological tasks. Mindful of the emerging evidence of prefrontal and cerebellar deficits in female PM-carriers, we anticipate specific inhibitory and working memory deficits similar to those previously identified in male PM-carriers.

3.3 METHODS

Participants

Fourteen female PM-carriers (55-200 CGG repeats) were recruited through local and national Fragile X syndrome support groups, via a population-based Fragile X carrier screening pilot study (Metcalfe *et al.*, 2008) and a large carrier screening study currently underway in Victoria and Western Australia (unpublished). Fourteen controls were recruited through the current population-based Fragile X carrier screening study, local networks and via online advertisements. A thorough neurological history was taken for all controls. Female PM-carriers and controls were found to be well-matched on age [$t(20.95)=-.60$, $p=0.56$] and IQ [$t(26)=1.39$, $p=0.18$], as determined using the Wechsler Abbreviated Scale of Intelligence (WASI) (Wechsler, 1999) (see Table 3.1).

Table 3.1: Age, IQ and CGG repeat length for controls and asymptomatic PM-carriers.

	Controls (n=14)		**PM-carriers (n=14)**	
	Mean ± SD	Range	Mean ± SD	Range
Age	39.64 ± 11.94	23-56	41.93 ± 7.00	25-52
Full-scale IQ (WASI)	117.93 ± 9.44	99-133	112.93 ± 8.89	101-127
CGG length			79.36 ± 11.28	61-102

Female PM-carriers were screened for features related to FXTAS (tremor, ataxia or parkinsonism) with the FXTAS Rating Scale (Leehey, 2009), with all PM-carriers found to be asymptomatic for FXTAS related features. All PM-carriers were confirmed with genetic

analysis (see below for protocol) and had CGG repeat sequences within the PM range. No participant demonstrated visual impairment, or a history of serious head injury or neurological dysfunction. This study was approved by Monash University and Southern Health Human Research Ethics Committees. In accordance with this, all participants provided signed informed consent and the study procedures were consistent with the declaration of Helsinki.

DNA was extracted from 2ml whole blood from PM-carrier participants using the Promega Maxwell® 16 instrument and associated Maxwell® 16 Blood DNS Purification Kit (Promega Cat No.: AS1010). PCR was performed using the Asuragen® AmplideX™ *FMR1* PCR Kit as this assay has been shown to detect a full range of Fragile X expanded alleles (Chen *et al.*, 2010). PCR products were assessed via capillary electrophoresis on an Applied Biosystem 3130 Genetic Analyzer with electropherogram analysis conducted using GeneMapper® software. All procedures were performed in accordance with manufacturer's instructions.

Ocular motor testing was completed in a single session lasting approximately one hour, followed by a battery of neuropsychological tasks which lasted approximately forty minutes for control participants. Neuropsychological data for PM-carriers derive from a concurrent study prior to ocular motor assessment (time difference *M*=120 days, *SD*=75.22 days, range=38-301days). All testing was conducted within the Monash Biomedical Imaging facility.

Neuropsychological tasks

Intellectual functioning

A full scale IQ score was evaluated based on four subtests of the WASI (Wechsler, 1999) that evaluated both verbal and performance domains.

Executive functioning

Executive functioning, was firstly evaluated using the Behavioural Dyscontrol Scale (BDS) (Grigsby and Kaye, 1996). This scale comprises nine individual test items assessing simple motor response, motor procedural learning, working memory, attention and self-insight (see Table 3.2 for BDS test item description). Each test item is scored from 0 to 3, 0 indicating poor performance, prior to combining test item scores to form an overall BDS score.

To assess working memory, the Letter Number Sequencing (Wechsler, 1999) task was used. Participants were required to recall a number and letter sequence in numerical then alphabetical order. Responses are scores as either correct or incorrect, and testing was stopped after 3 consecutive incorrect responses. The Stroop Colour and Word (Golden and Freshwater, 2002) task measures response inhibition as a function of cognitive flexibility when separating colour word and ink colour stimuli. Interferences scores were calculated using Golden's equation (Golden, 1978).

Ocular motor apparatus

Horizontal displacement of the eye was binocularly recorded using a SR Research Eyelink 1000 desktop mounted video-oculographic eye tracker. The pupil-corneal-reflection method was used with a sampling rate of 500Hz. A head and chin rest enabled stabilization of the head during recording, and was centered at a distance of 84cm from a display screen. Screen-based stimuli were generated against a black background using SR Research Experiment Builder software version 1.10.165 and displayed on a 22inch LCD monitor with a resolution of 1680x1050pixels. Stimuli comprised green target crosses measuring 25x25mm (with a black cross hair measuring 9x9mm), located at either 5^0 or 10^0 of visual angle left or right from a central fixation point. A white centrally positioned re-fixation stimulus measuring 6x6mm was presented between trials. Preceding each ocular motor task, the SR Research

Eyelink 1000 automated 3-point calibration task, in which dots move at random intervals along the central horizontal plane of the screen, was used.

Ocular motor tasks

Reflexive saccade

The reflexive saccade task was used as a baseline measure of performance, and required participants to shift their gaze to a suddenly appearing target cross as quickly and as accurately as possible. Each trial commenced with participants fixating a central stimulus. After a randomly presented interval of either 750 or 1500msec, a peripheral green target cross appeared at either 5^0 or 10^0/left or right of center. This appeared simultaneously with the offset of the central fixation stimulus (Figure 3.1). Two blocks totalling 60 trials were presented.

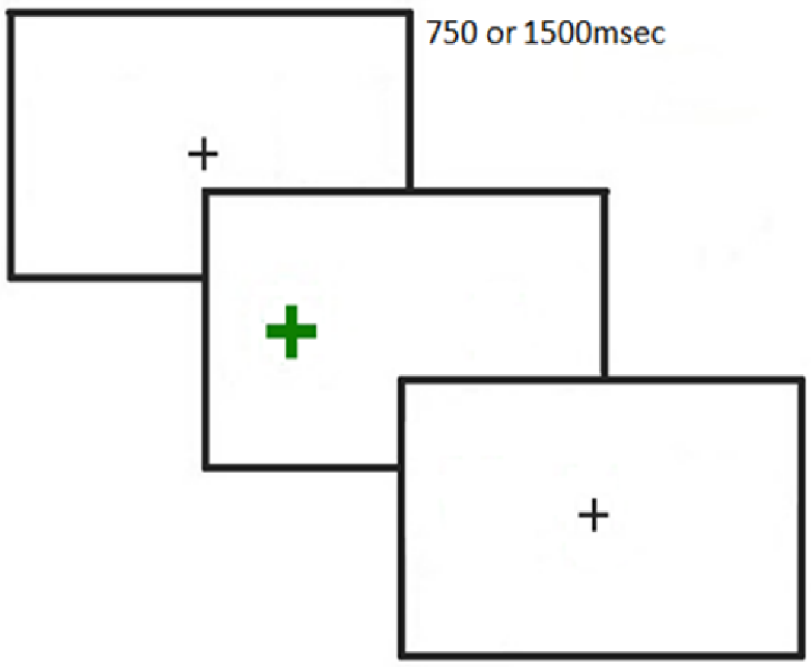

Figure 3.1: Schematic diagram of the reflexive saccade paradigm.

Antisaccade

Inhibition of a reflexive saccade to a suddenly appearing stimulus, and initiation of a volitional saccade are necessary for successful antisaccade task performance. This task required participants to fixate on a central stimulus, which was presented for either 1250 or 1600msec. Subsequently with the extinction of the central stimulus, a green target cross was presented for 1500msec at a location either 5^0 or 10^0/left or right of center. Without directing gaze to the green target cross, participants were instructed to look to the mirror opposite location as quickly and as accurately as possible (Figure 3.2). Two blocks of 24 trials were presented. A directional error was categorized as a saccade made toward the green target cross rather than towards its mirror opposite location.

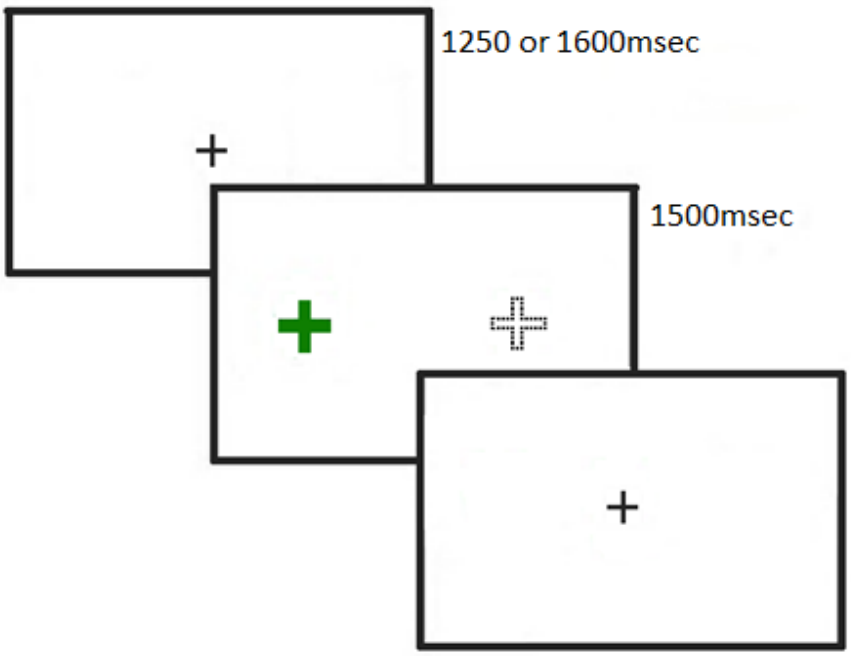

Figure 3.2: Schematic diagram of the antisaccade paradigm

Memory-guided saccade

Inhibition of a reflexive saccade to a suddenly appearing stimulus, as well as initiation of a volitional saccade to its remembered location, are necessary for successful performance on the memory-guided saccade task. Each trial began with the presentation of a central green fixation cross for 1500ms. A red cross (with identical dimensions as the green target cross) was then presented alongside the green fixation cross at either 5^0 or 10^0/left or right of centre for 500ms. Participants were instructed not to look directly at the red cross, but to remember its spatial position. Following extinction of the red cross, the green fixation cross was presented for a further 1500ms or 2500ms. Once the central green cross was extinguished, participants were asked to move their eyes to the remembered spatial position of the previously illuminated red cross (Figure 3.3). Two blocks of 24 trials were presented. A saccade made prior to the extinction of the green target cross was categorized as a timing error.

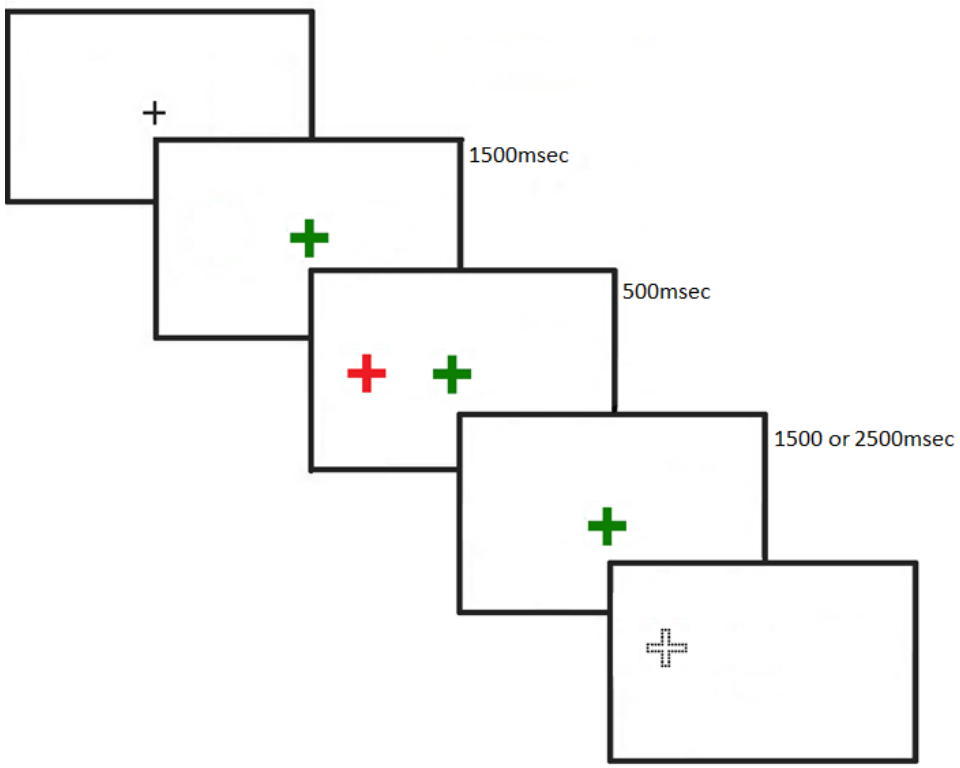

Figure 3.3: Schematic diagram of the memory guided paradigm

Endogenous saccade

The endogenous saccade task requires the suppression of a pre-potent response initiated by a directional cue, and the initiation of a saccade to a suddenly appearing target. Participants were instructed to direct their gaze to a central white fixation cross, and to shift gaze as quickly as possible when a green target cross appeared in one of two peripheral boxes. The centrally positioned fixation cross appeared at the commencement of each trial, prior to the presentation of a horizontally oriented directional arrow. The directional arrow remained on screen for a period of 500ms, and participants were instructed to maintain fixation on the arrow. A peripheral target green cross was subsequently presented for 1500ms, in one of two peripheral boxes located at 10^0 left/right from center, after which time, gaze was redirected to the centre of the screen by the appearance of the white fixation stimulus. Trial type was determined by the type of cue preceding target onset (A) Valid trial: directional arrow at fixation, compatible with side of subsequent target presentation, (B) Invalid trial: directional arrow at fixation, incompatible with side of subsequent target presentation (Figure 3.4). Valid trials comprised 80% of all trials, and invalid 20% of all trials, ensuring that cue type was largely predictive of subsequent target location. Trials were presented randomly. A directional error constituted any saccade in the direction of the arrow, either before or within 100msec of the presentation of the green target cross.

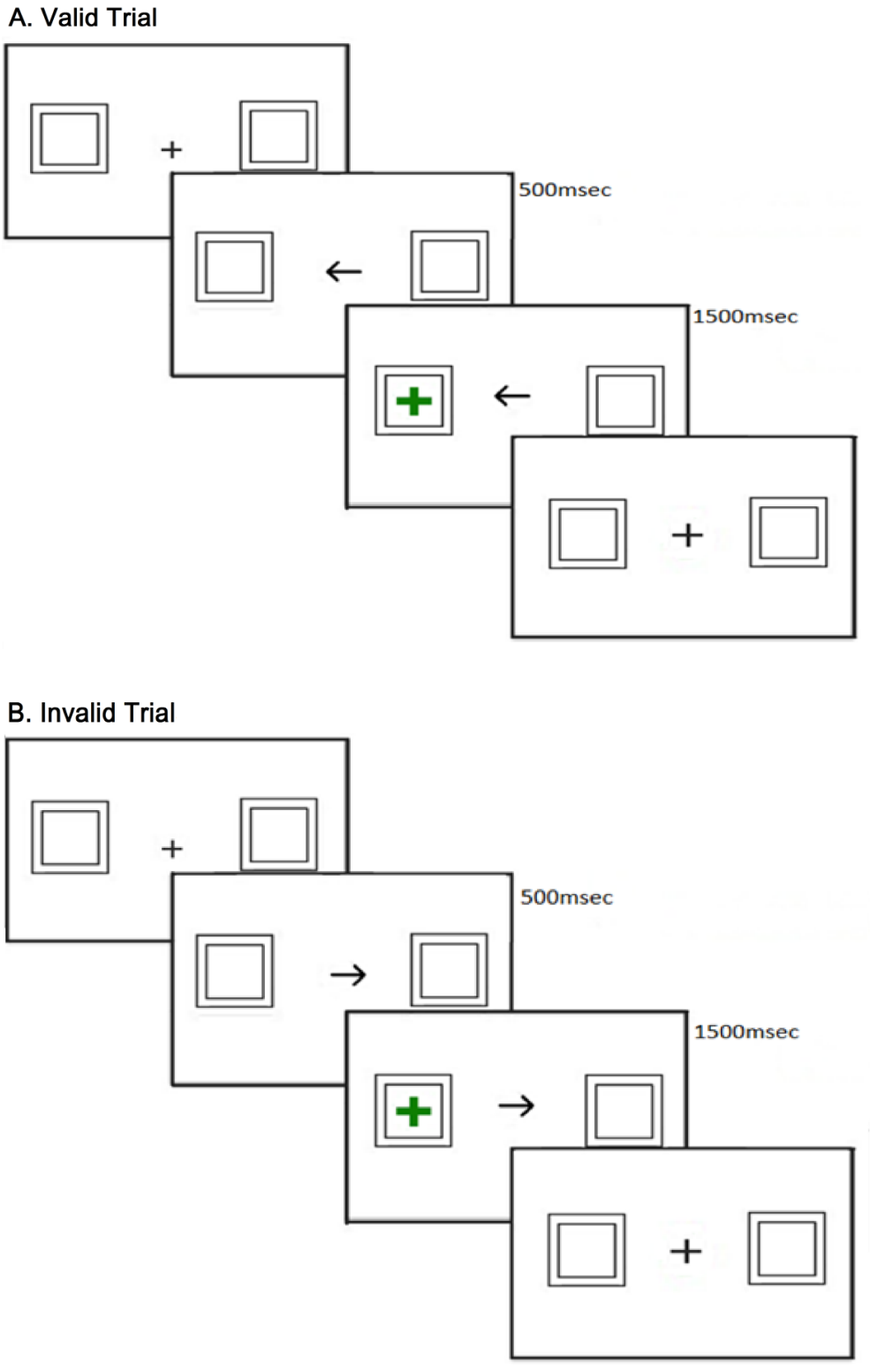

Figure 3.4: Schematic diagram of the endogenous paradigm.

A) Shows the leftward sequence of a validly cued trial. **B)** Shows a leftward invalid sequence, in which the directional arrow at fixation is incompatible with the side of the subsequent target presentation.

Data analysis

Data were analyzed using customized software written in Matlab. Saccade onset and offset were identified using a velocity criterion of +/-30^0/sec. Trials were excluded from analysis if they were degraded by (a) blinks, (b) poor fixation or an anticipatory response (<100ms after target presentation), or (c) saccades less than 3° in amplitude. Mean and coefficient of variability (a ratio of mean and standard deviation scores) were calculated for: latency [time between target onset and saccade onset (ms)], saccade gain (initial saccade amplitude/target amplitude), mean absolute position error {[(FEP−TA)/TA]×100, where FEP is the final eye position and TA is the target amplitude} for all task correct saccades, as well as task error (%, as specified above).

Neuropsychological and ocular motor latency and accuracy scores were compared between PM-carriers and control participants using either *t*-tests (or Mann-Whitney *U* tests where any violation of distribution assumptions was made). Ocular motor error data were transformed (square root transformation for antisaccade and memory guided task errors and a logarithmic transformation for the endogenous task errors) to minimize the inequality of variance between PM-carriers and controls, and analyzed with *t*-tests once assumptions were met. Correlational relationships between neuropsychological task scores, ocular motor error scores (transformed) and CGG repeat lengths were investigated where significant differences were demonstrated between PM-carriers and controls using Pearson's for all associations, except those involving BDS test item analyses, in which Spearman's rho was used. A significance value of $p<0.05$ was set for all between group analyses (adjusted to $p<.025$ for BDS test item comparisons).

3.4 RESULTS

Neuropsychological tasks

There were significant differences between groups for total BDS [$t(26)=2.80$, $p=.009$, $d=.23$] scores as well as for BDS test items 3 [$U=55.00$, $z=-2.50$, $p=.013$, $r=.47$], BDS test item 5 [$U=27.00$, $z=-3.50$, $p=.000$, $r=.66$], and BDS test item 6 [$U=36.50$, $z=-3.09$, $p=.004$, $r=.58$] (see Table 3.2), demonstrating impairments in inhibitory and executive processes for PM-carriers.

Table 3.2: Means and standard deviations for neuropsychological task measures

Measure	Controls	PM-carriers	*p*-value
	Mean ± SD	Mean ± SD	
Stroop Colour and Word	7.71 ± 8.13	9.64 ± 17.41	0.48#
Letter-Number Sequencing	11.86 ± 2.68	13.64 ± 3.48	0.22
BDS Total	24.78 ± 1.52	22.57 ± 2.53	**0.01***
BDS Test Item 1 (simple motor control)	2.86 ± 0.35	2.86 ± 0.35	1.00#
BDS Test Item 2 (simple motor control)	2.79 ± 0.41	2.93 ± 0.26	0.29#
BDS Test Item 3 (inhibition)	2.93 ± 0.26	2.36 ± 0.72	**0.01#^**
BDS Test Item 4 (inhibition)	2.93 ± 0.26	2.79 ± 0.56	0.52#
BDS Test Item 5 (motor learning)	2.64 ± 0.48	1.64 ± 0.61	**0.01#^**
BDS Test Item 6 (motor learning)	2.71 ± 0.59	1.93 ± 0.59	**0.01#^**
BDS Test Item 7 (working memory)	2.93 ± 0.26	2.64 ± 0.48	0.07#
BDS Test Item 8 (control of attention)	2.21 ± 0.67	2.43 ± 0.73	0.37#
BDS Test Item 9 (insight)	3.00 ± 0.00	3.00 ± 0.00	1.00#

Note: Figures in red bold indicate $p<0.05$, and ^$p<.025$; #denotes a violation of the assumption of normality and hence Mann-Whitney U test statistic presented.

Ocular motor latency and accuracy measures

There were no differences revealed between groups for saccade latency, saccade gain or mean absolute position error measures for task specific correct saccades made on any ocular motor task (see Table 3.3).

Table 3.3: Means and standard deviations for saccade profile measures of latency, gain and absolute position error.

Task	Measure	Controls	PM-carriers	*p*-value
		Mean ± SD	Mean ± SD	
Reflexive	Latency (msec)	203.57 ± 22.05	196.36 ± 22.88	.40
		(.15 ±.07)	(1.58 ± 5.38)	(1.00)#
	Gain	.98 ± .08	.98 ± .07	.85
		(.10 ± .04)	(.63 ± 1.98)	(.57)#
	Mean Absolute Position Error	.69 ± .29	.74 ± .25	.51#
		(.73 ±.13)	(.75 ± .26)	(.60)#
Antisaccade	Latency (msec)	304.19 ± 39.62	312.07 ± 48.90	.64
		(.13 ± .03)	(.55 ± 1.50)	(.13)#
	Gain	.98 ± .22	1.24 ± .63	.54#
		(.40 ± .07)	(.69 ± 1.01)	(.40)#
	Mean Absolute Position Error	2.70 ± .50	4.22 ± 3.06	.14#
		(.72 ± .06)	(.81 ± .47)	(.98)#
Memory-Guided	Latency(msec)	304.71 ± 50.36	291.29 ± 48.58	.31#
		(.24 ± .08)	(.37 ± .60)	(.51)#
	Gain	1.30 ± 1.44	.93 ± .09	.87#
		(.21 ± .12)	(.47 ± 1.06)	(.87)#
	Mean Absolute Position Error	1.66 ± 1.57	1.10 ± .46	.33#
		(.69 ± .08)	(.77 ± .19)	(.45)#
Endogenous	Latency (msec)	247.20 ± 43.65	245.87 ± 92.55	.32#
		(.98 ± 2.47)	(.20 ± .05)	(.56)#
	Gain	1.03 ± .07	.95 ± .28	.38#
		(1.68 ± 4.87)	(.07 ± .03)	(.71)#
	Mean Absolute Position Error	.74 ± .54	1.34 ± 2.51	.14#
		(.91 ± .47)	(.70 ± .10)	(.46)#

Note: Figures in parentheses relate to the results of using coefficient of variability. # denotes a violation of the assumption of normality and hence Mann-Whitney U test statistic presented.

Ocular motor errors

Antisaccade task

PM-carriers generated a significantly larger proportion of errors, (M=30.27, SD=23.83 raw data) than controls (M=11.76, SD=7.36 raw data) [$t(21.41)=-2.27$, $p=.034$, $d=.86$ using square root transformed data] (Figure 3.5).

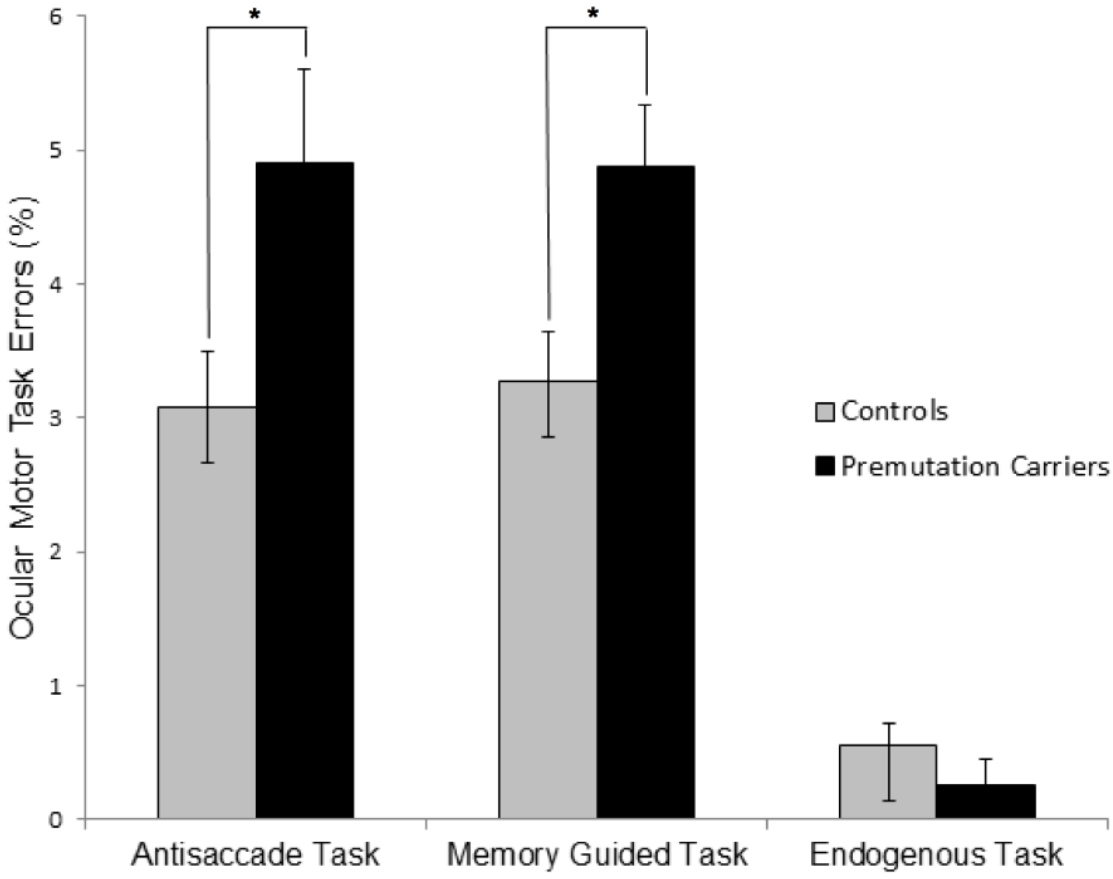

Figure 3.5: Mean Ocular Motor Task Error Percentages.

Percentage errors shown relate to transformed data: Square root transformations for antisaccade and memory guided task errors, and a logarithmic transformation for endogenous task errors. Error bars represent standard error and *p<.05.

Memory-guided task

Compared to the control group (M = 12.53, SD = 7.88 raw data), PM-carriers made a greater number of timing errors (M = 26.59, SD = 18.73 raw data) [t(26) = -2.70, p = .012, d = 1.02 using square root transformed data] (Figure 3.5).

Endogenous task

Directional saccade errors were minimal for both PM carriers (M=8.08, SD=17.22 raw data) and controls (M=7.20, SD=7.49 raw data) [$t(26)=1.17$, $p=.252$, $d=.44$ using logarithmic transformed data] (Figure 3.5).

Correlations

A number of significant correlations were found in this study for female PM-carriers. Firstly, the proportion of antisaccade errors and total BDS scores demonstrated an inverse relationship ($r=-.47$, $p=.012$). Specifically, BDS test item 5 ($r=-.63$, $p=.000$) and test item 6 ($r=-.45$, $p=.016$) correlated significantly with antisaccade error rates. Additionally, BDS test item 5 was found to have a negative correlation with memory guided errors ($r=-.47$, $p=.011$). Further, a significant correlation was found for error rate between the antisaccade and memory-guided tasks ($r=.60$, $p=.000$). Finally a significant one-tailed correlation was found between CGG repeat length and antisaccade error rate ($r=-.52$, $p=.028$) (Figure 3.6).

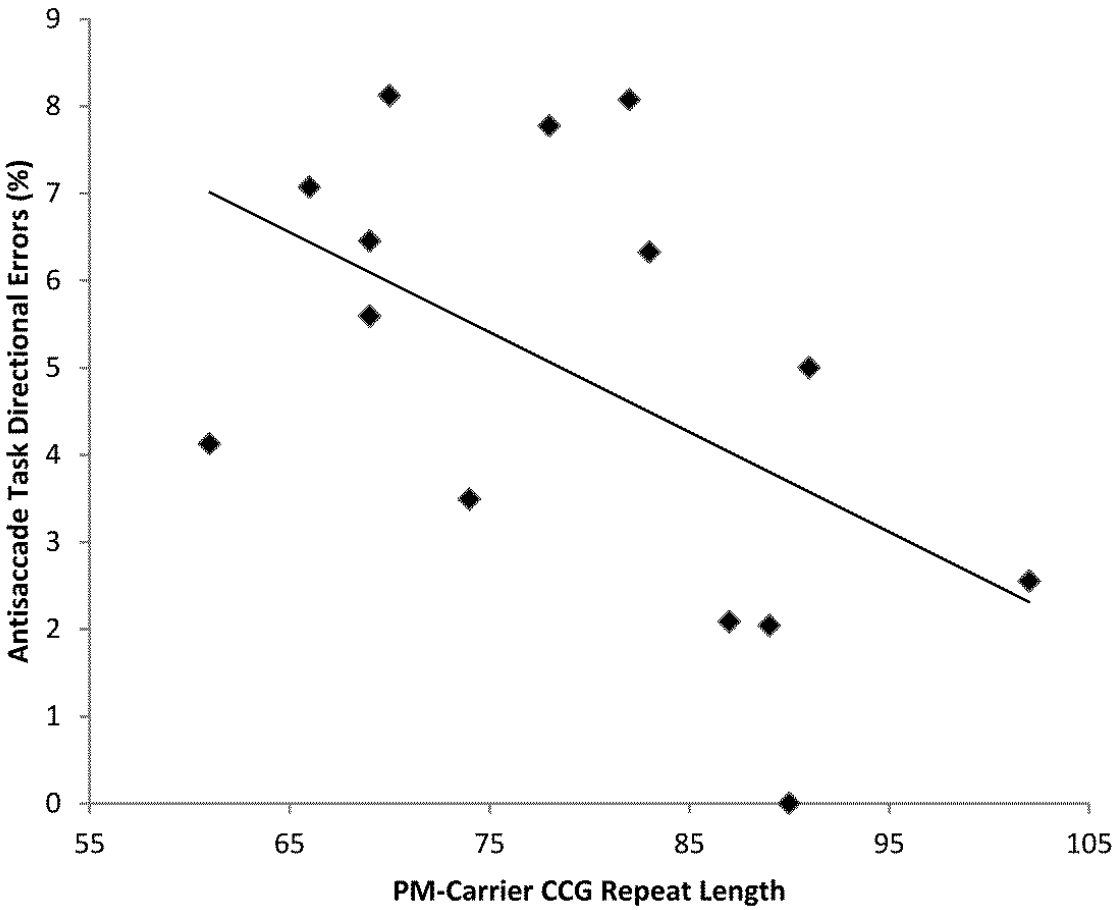

Figure 3.6: PM-carrier Antisaccade and CGG Repeat Length Pearson Correlation. Antisaccade error percentage relates to transformed (square root) data.

3.5 DISCUSSION

This study examined the utility of saccadic paradigms to detect subtle cognitive changes in female PM-carriers, specifically of response inhibition and working memory, where changes have previously been reported as vulnerable in male PM-carriers (Cornish *et al.*, 2008a; Cornish *et al.*, 2008b; Cornish *et al.*, 2009; Kogan and Cornish, 2010; Cornish *et al.*, 2011). The results of this investigation demonstrate specific deficits in response inhibition for this female population using ocular motor tasks. These are important findings, given that these deficits are found in the absence of any clinically significant signs of FXTAS, although it is

unknown at this point whether they represent neurodevelopmental or neurodegeneration changes.

A greater proportion of errors were made by female PM-carriers for both the antisaccade and memory-guided tasks. Both of these tasks require the inhibition of a reflexive saccade, prior to initiating a volitional saccade. As the timing and accuracy of each volitional saccade type was comparable across groups, errors on these tasks by female PM-carriers likely stem from a failure within response inhibition circuitry, a deficit previously identified in male PM-carriers (Cornish *et al.*, 2008a; Cornish *et al.*, 2008b; Cornish *et al.*, 2011).

The dorsolateral prefrontal cortex (DLPFC) is invariably implicated in the inhibition of reflexive saccades (Leigh and Zee, 2006). Indeed it is proposed to play a key inhibitory role across a range of executive functions (Koziol *et al.*, 2012). Notably, reduced DLPFC activation has been demonstrated in PM-carriers during a verbal working memory task, despite exhibiting behavioural scores comparable to controls (Hashimoto *et al.*, 2011a). The cerebellum is also thought to play a role in the regulation of inhibitory behaviour, alongside its role in motor learning and optimization of motor metrics (Leigh and Zee, 2006). Indeed, in our recently published work in multiple sclerosis (Kolbe *et al.*, in press April 2013), we showed that diffusion tensor imaging changes and atrophy in the cerebellum were associated with antisaccade dysfunction. Interestingly, a recent transcranial magnetic stimulation study found that female PM-carriers not only had reduced levels of inhibitory GABA signalling, but also an absence of cerebellar inhibition over primary motor cortex (Conde *et al.*, 2013). Further, PM-carriers are known to have grey matter volumetric reductions in lobules I/II of the anterior vermis and lobule III of the left hemisphere of the cerebellum (Hashimoto *et al.*, 2011b). Moreover, reduced integrity of white matter in the cerebral peduncles, specifically the middle cerebral peduncle, has been reported in PM-carriers without FXTAS (Hashimoto *et al.*, 2011c; Conde *et al.*, 2013). Thus, we postulate that changes within the prefrontal and cerebellar regions and their neural networks may be associated with the behavioural deficits seen in the antisaccade and memory-guided tasks in PM-carriers.

Previous studies have demonstrated that PM-carriers experience difficulty with BDS test items involving procedural learning of motor tasks, in addition to overall deficits in behavioural self-regulation (Loesch *et al.*, 2003; Brega *et al.*, 2008). Not only did our neuromotor BDS results replicate those seen in male PM-carriers (Loesch *et al.*, 2003; Brega *et al.*, 2008), but we also found that female PM-carriers had difficulty in BDS test item 3, a measure of inhibition. Further, although not significant, there was a trend for female PM-carriers to perform more poorly on the Stroop Colour and Word task compared to controls. This along with the BDS test item correlational analyses further suggests that difficulty in behaviour self-regulation may be driven by motor learning difficulties in female PM-carriers, further implicating the cortico-cerebellar connections within the female PM-carrier phenotype.

The relation between CGG repeat length and *FMR1* mRNA is relatively stable for low and medium repeat PM-carriers (<100 CGG repeats) (Kraan *et al.*, 2013a). Although the neurobiological mechanisms associated with Fragile X-associated disorders are not fully understood, it is thought that FXTAS is the result of *FMR1* mRNA toxicity (Jacquemont *et al.*, 2007; Kraan *et al.*, 2013a). However, translation of Fragile X mental retardation protein 1 (FMRP), a selective mRNA binding protein and translational regulator, occurs in both the GABAa and mGluR neural networks (Fatemi and Folsom, 2011), influencing higher-order cognitive pathways. Specifically, progressive FMRP reductions have been associated with executive functioning decline, as measured by the BDS (Loesch *et al.*, 2003). A curvilinear FMRP relation has also been described for male PM-carriers (Peprah *et al.*, 2010). Therefore, we speculate a specific molecular vulnerability exists, dependent on FMRP levels, within a range of female PM-carriers (<100 CGG repeats).

Given the cross-sectional design of this study, we are unable to determine whether these cognitive impairments are a consequence of neurodevelopmental or neurodegenerative processes; although no participant demonstrated clinical signs of FXTAS. Unfortunately, levels of FMRP and *FMR1* mRNA leucocytes were not available, nor was the X-inactivation

ratio. Provision of these markers in future studies would allow for a greater understanding of the relationship between the neurobiological state and these cognitive changes. Moreover, CGG analysis was ascertained via peripheral blood, and some slight tissue variability may exist for neural measures, from PM-carriers only. In addition to this, the extent to which this small sample represents the range of PM CGG in the population is unknown. Specifically, the current sample was small and consisted of only one female PM-carrier with over 100 CGG repeats. A greater sample size and inclusion of higher repeat PM-carriers would provide greater insight into the effect of CGG length on inhibitory control in *FMR1* PM-carriers.

This study presents preliminary yet compelling evidence for a specific cognitive weakness in female PM-carriers. We add to the developing understanding of the female PM-carrier profile, with findings from neuromotor paradigms highlighting deficits in specific executive processing domains. These results endorse a response inhibition deficit which may present as a potential neuromotor marker for neurodevelopmental or preclinical changes associated with Fragile X-associated disorders and neurodegeneration within the *FMR1* PM population.

CHAPTER 4: SACCADIC WORKING MEMORY

In Chapters 2 and 3 it was demonstrated that PM females without FXTAS exhibit deficits across of range of executive function tasks. Chapter 4 focuses specifically on the sub-domain of working memory and utilises a saccadic n-back task. This saccadic n-back task allows for a systematic increase in cognitive load, when recalling the location of a target embedded within a short sequence of visual stimuli via an eye movement to that location. This task has been previously utilised to demonstrate the progressive decline in working memory processes in patients with early and late stage Multiple Sclerosis (Clough *et al.*, 2015). Here, associations between genetic indices and working memory impairment are assessed.

This Chapter is written as a manuscript for publication: *Delineation of the working memory profile in female FMR1 premutation carriers: the effect of cognitive load on ocular motor responses*. It was published in *Behavioural Brain Research*, Volume 282, Issue 1 2015. To maintain consistency throughout this thesis, changes have been made to formatting.

Declaration by candidate

In the case of Chapter 4, the nature and extent of my contribution to the work was the following:

Nature of contribution	Extent of contribution (%)
Conceptualisation, project design and programming of paradigms, data collection, data analysis and interpretation, and manuscript preparation	80%

The following co-authors contributed to the work. If co-authors are students at Monash University, the extent of their contribution in percentage terms must be stated:

Name	Nature of contribution	Extent of contribution (%) for student co-authors only
Kim Cornish	Conceptualisation, project design and manuscript preparation	
David Godler	Genetic analysis and manuscript preparation	
Meaghan Clough	Project design and manuscript preparation	
Claudine Kraan	Manuscript preparation	
Minh Bui	Statistical analysis and manuscript preparation	
Joanne Fielding	Conceptualisation, project design, data interpretation, and manuscript preparation	

The undersigned hereby certify that the above declaration correctly reflects the nature and extent of the candidate's and co-authors' contributions to this work*.

Candidate's Signature		Date
Main Supervisor's Signature		Date

DELINEATION OF THE WORKING MEMORY PROFILE IN FEMALE *FMR1* PREMUTATION CARRIERS: THE EFFECT OF COGNITIVE LOAD ON OCULAR MOTOR RESPONSES

Annie L. Shelton, Kim M. Cornish, David E. Godler, Meaghan Clough, Claudine Kraan, Minh Bui, and Joanne Fielding

4.1 ABSTRACT

Fragile X Mental Retardation 1 (*FMR1*) premutation carriers (PM-carriers) are characterised as having mid-sized expansions of between 55 to 200 CGG repeats in the 5' untranslated region of the *FMR1* gene. While there is evidence of executive dysfunction in PM-carriers, few studies have explicitly explored working memory capabilities in female PM-carriers. 14 female PM-carriers and 13 age- and IQ- matched healthy controls completed an ocular motor n-back working memory paradigm. This task examined working memory ability and the effect of measured increases in cognitive load. Female PM-carriers were found to have attenuated working memory capabilities. Increasing the cognitive load did not elicit the expected reciprocal increase in the task errors for female PM-carriers, as it did in controls. However female PM-carriers took longer to respond than controls, regardless of the cognitive load. Further, *FMR1* mRNA levels were found to significantly predict PM-carrier response time. Although preliminary, these findings provide further evidence of executive dysfunction, specifically disruption to working memory processes, which were found to be associated with increases in *FMR1* mRNA expression in female PM-carriers. With future validation, ocular motor paradigms such as the n-back paradigm will be critical to the development of behavioural biomarkers for identification of PM-carrier cognitive-affective phenotypes.

4.2 INTRODUCTION

The CGG trinucleotide expansions of the Fragile X mental retardation gene (*FMR1*) are associated with a wide spectrum of early and late onset conditions. The full mutation (>200 CGG repeats) causes silencing of the *FMR1* gene and loss of the *FMR1* protein (FMRP), which is essential for normal neurodevelopment (Willemsen *et al.*, 2004; Willemsen *et al.*, 2011), resulting in the neurodevelopmental disorder known as Fragile X syndrome (FXS). In contrast, the medium sized premutation expansions (PM: 55-200 CGGs), found in approximately 1 in 430 males and 1 in 209 females within the general population (Tassone *et al.*, 2012), causes over-expression of the *FMR1* gene. This over-expression results in mRNA "gain-of-function" toxicity accompanied by ubiquitin-positive intracellular inclusion bodies and reduced cell viability in neuronal cells (Willemsen *et al.*, 2003; Arocena *et al.*, 2005). These molecular changes are the postulated cause of a late onset neurodegenerative disorder known as Fragile X-associated tremor/ataxia syndrome (FXTAS). FXTAS affects approximately 45% of male and 8-17% of female PM-carriers over the age of 50 (Rodriguez-Revenga *et al.*, 2009). Besides the characteristic intention tremor, ataxia, and dementia, FXTAS also results in a range of molecular and structural abnormalities throughout the central nervous system, as well as executive functioning deficits (Brunberg *et al.*, 2002; Greco *et al.*, 2002; Tassone *et al.*, 2004a; Tassone *et al.*, 2004b; Loesch *et al.*, 2005a; Cohen *et al.*, 2006; Adams *et al.*, 2007; Hashimoto *et al.*, 2011b; Hashimoto *et al.*, 2011c).

There is strong evidence for the existence of a dysexecutive profile in asymptomatic PM-carriers (those without FXTAS) (Brega *et al.*, 2008; Grigsby *et al.*, 2008; Schneider *et al.*, 2012; Yang *et al.*, 2013). The male asymptomatic PM-carrier phenotype is currently characterised by impairments in executive processing, with specific deficits in tasks reliant upon working memory, inhibitory processing, visuospatial processing and attentional control (Moore *et al.*, 2004a; Cornish *et al.*, 2005; Cornish *et al.*, 2008b; Cornish *et al.*, 2009; Kogan and Cornish, 2010; Cornish *et al.*, 2011; Hocking *et al.*, 2012). Significantly, higher CGG repeat levels (>100) have been associated with impaired working memory and response inhibition

performance in male PM-carriers (Cornish *et al.*, 2008b; Cornish *et al.*, 2009; Cornish *et al.*, 2011; Hocking *et al.*, 2012).

There is also evidence suggesting that there is at-least a sub-group of female PM-carriers demonstrating weakness in executive functioning (i.e attentional and inhibitory control), processing speed, and visuospatial processing (Kéri and Benedek, 2009; Kéri and Benedek, 2010; Goodrich-Hunsaker *et al.*, 2011a; Goodrich-Hunsaker *et al.*, 2011b; Hunter *et al.*, 2012a; Semenza *et al.*, 2012; Kraan *et al.*, 2013b; Sterling *et al.*, 2013; Kraan *et al.*, 2014b; Kraan *et al.*, 2014c; Shelton *et al.*, 2014). The extent to which working memory is affected in female PM-carriers is not well understood. Research indicates that the female PM-carrier phenotype may be less easily resolved and milder in nature than males, a consequence of the protective effects attributed to the presence of a normal allele (CGG <45 repeats) on the second X chromosome (Leehey *et al.*, 2008). Hence a sensitive cognitive measure is required to ascertain whether or not female PM-carriers exhibit impaired working memory functionality, and if this is related to genetic or molecular markers.

Working memory is a limited-capacity system which enables the temporary storage, manipulation, and retrieval of information for use in complex cognitive tasks (Baddeley, 1986). It is a process which relies upon widespread cortical and subcortical involvement (Jonides *et al.*, 1993; Courtney *et al.*, 1996; Osaka *et al.*, 2004; D'Esposito, 2007; Charlton *et al.*, 2010), with the precise network activated dependent on the *type* of information involved (Curtis *et al.*, 2004). Specifically, when visuospatial working memory circuitry is overwhelmed (or near capacity due to increases in cognitive load), neural activation is found to be highest in the frontal eye fields and along the intraparietal sulcus (IPS) (Linden *et al.*, 2003). Both of these are key ocular motor regions, and central to the support of visual attention (Goldberg *et al.*, 2002; Bisley and Goldberg, 2003).

Ocular motor (saccadic) paradigms have been used extensively to assess cognitive (dys)function in a range of disorders; for example multiple sclerosis (Fielding *et al.*, 2012),

Parkinson's (Fielding *et al.*, 2005), and Huntington's (Henderson *et al.*, 2011). Indeed, we have previously utilised ocular motor paradigms, demonstrating reduced capacity to inhibit reflexive eye movements (inhibitory errors) in asymptomatic female PM-carriers, compared to healthy controls (Shelton *et al.*, 2014). Not only did these female PM-carriers perform more inhibitory errors, they also showed greater difficulty responding to and learning motor/hand sequences compared to controls.

The extensive and well defined ocular motor network encompasses cortical (i.e parietal and prefrontal regions), subcortical and cerebellar structures (Leigh and Zee, 2006). Further, the frontal-parietal connections required for cognitively driven saccades are also key networks required for visuospatial working memory tasks (Owen *et al.*, 2005). A range of saccadic paradigms have been developed to investigate working memory. An elegant example of one is the task devised by Jeter *et al.* (2011), which is based on the classic n-back task. The task involves the presentation of a continuous sequence of visual stimuli, and requires participants to identify the location of the stimulus presented 'n' locations -back in the sequence. The greater the 'n' value, the higher the cognitive load. Jeter, Patel and Sereno (2011) have used their ocular motor n-back task to characterise developmental changes in working memory ability, as well as the effects of increasing cognitive load, in neurologically healthy individuals.

This study aimed to further delineate the female PM-carrier cognitive profile by characterising working memory performance under differing and increasing cognitive loads. Given the emerging similarities between the male and female PM-carrier cognitive phenotypes, we anticipated impaired working memory performance in female PM-carriers, with working memory performance being inversely correlated with increases in *FMR1* mRNA levels and CGG expansions. This would provide the first evidence for a role of RNA toxicity as a predictor of impaired working memory performance in female PM-carrier.

4.3 METHODS

Participants

All participants were aged between 18 and 55 years of age at the time of recruitment, were English speaking, had no history of serious head injury, had normal or corrected vision, and had around average IQ (as assessed using the Wechsler Abbreviated Scale of Intelligence). The cohort included 14 female PM-carriers (61-102 CGG repeats; Mean = 79.36 repeats, Standard Deviation (SD) = 11.705) who had previously participated in our earlier studies (Kraan *et al.*, 2013b; Kraan *et al.*, 2014a; Kraan *et al.*, 2014b; Kraan *et al.*, 2014c; Shelton *et al.*, 2014) and a comparison group of 13 healthy control women from our earlier population-based screening study (Metcalfe *et al.*, 2008) as well as local networks and via online advertisements

Ethics approval for this study was granted by Monash University and Southern Health Human Research Committees (Project Number 10147B); with all participants giving their informed consent prior to inclusion in the study in accordance with the declaration of Helsinki.

Molecular analyses

CGG sizing was performed from DNA extracted from whole blood using the Asuragen® AmplideX™ *FMR1* PCR Kit (Asuragen: Austin, TX, USA) as part of our earlier studies (Kraan *et al.*, 2013b; Kraan *et al.*, 2014a; Kraan *et al.*, 2014b; Kraan *et al.*, 2014c). For *FMR1* mRNA analysis RNA was extracted from peripheral blood mononuclear cells (PBMCs) as described in Loesch and colleagues (2011). Reverse transcription real-time PCR (RT-PCR) was then performed on a ViiA™ 7 Real-Time PCR System (Life Technologies, Global) to quantify *FMR1*-5', *FMR1*-3' and three internal control genes with the previously described relative standard curve method (Loesch *et al.*, 2011). *FMR1* mRNA levels were expressed in arbitrary units in relation to the standard curve performed on each plate, standardized to the mean of the three

internal control genes (GUS, EIF4A2, and SDHA). RNA from each sample was reverse-transcribed in 4 separate cDNA reactions, with each cDNA analysed in two separate RT-PCR reactions. The mean of the eight arbitrary unit outputs was used as a summary measure for *FMR1* mRNA expression for each participant.

Ocular motor apparatus and task

The ocular motor n-back task involved the presentation of a serial sequence of visual stimuli, and required participants to identify the location of the stimulus presented 'n' locations back in the sequence through the use of eye movements. The SR Research Eyelink 1000 desktop mounted video-oculographic eye tracker camera detects the pupil-corneal reflection of the eyes, which is created by the infrared illuminator. This reflection is used to determine the horizontal and vertical displacement of the eye, which is recorded at a sample rate of 500Hz.

Participants' heads were stabilised and centred at a distance of 840mm from a display screen using a head and chin rest. Stimuli were displayed on a 22 inch LCD monitor with a resolution of 1680x1050 pixels, and generated using SR Research Experiment Builder software version 1.10.165. Participants completed a nine point calibration prior to testing.

The stimulus display comprised a black background with a white, centrally located fixation cross (15mm x 15mm). Surrounding the fixation cross were six white bordered boxes, two situated 10^0 left and right of the central fixation cross, and four situated at 45^0 angles from the central fixation cross (upper left, lower left, upper right, lower right). Each trial consisted of a series of three identical stimuli (red dots measuring 30mm in diameter) presented sequentially for 250msec, each within a different box. Participants were instructed to remember the order and location of each stimulus within the series. The central fixation cross was then replaced with a cue (1, 2, or 3) which appeared on screen for 500ms. Cues referred participants to the order and box/location in which the red dot stimuli appeared in the sequence. Upon extinction of the cue, participants were instructed to make an eye

movement toward the box that corresponded with the location indicated by the cue, as quickly and as accurately as possible.

The three cues corresponded to three working memory conditions. A '3' cue referred to the location of the final red dot stimulus in the sequence, representing a 0-back condition. A '2' cue referred to the location of the second red dot stimulus, representing a 1-back condition. Finally, a '1' cue corresponded to the location of the first red dot stimulus, representing a 2-back condition (Figure 4.1). A total of 96 trials, divided into three discrete blocks, were presented, with each working memory condition being equally represented. The first block of 32 trials were used as training, and removed from further analysis.

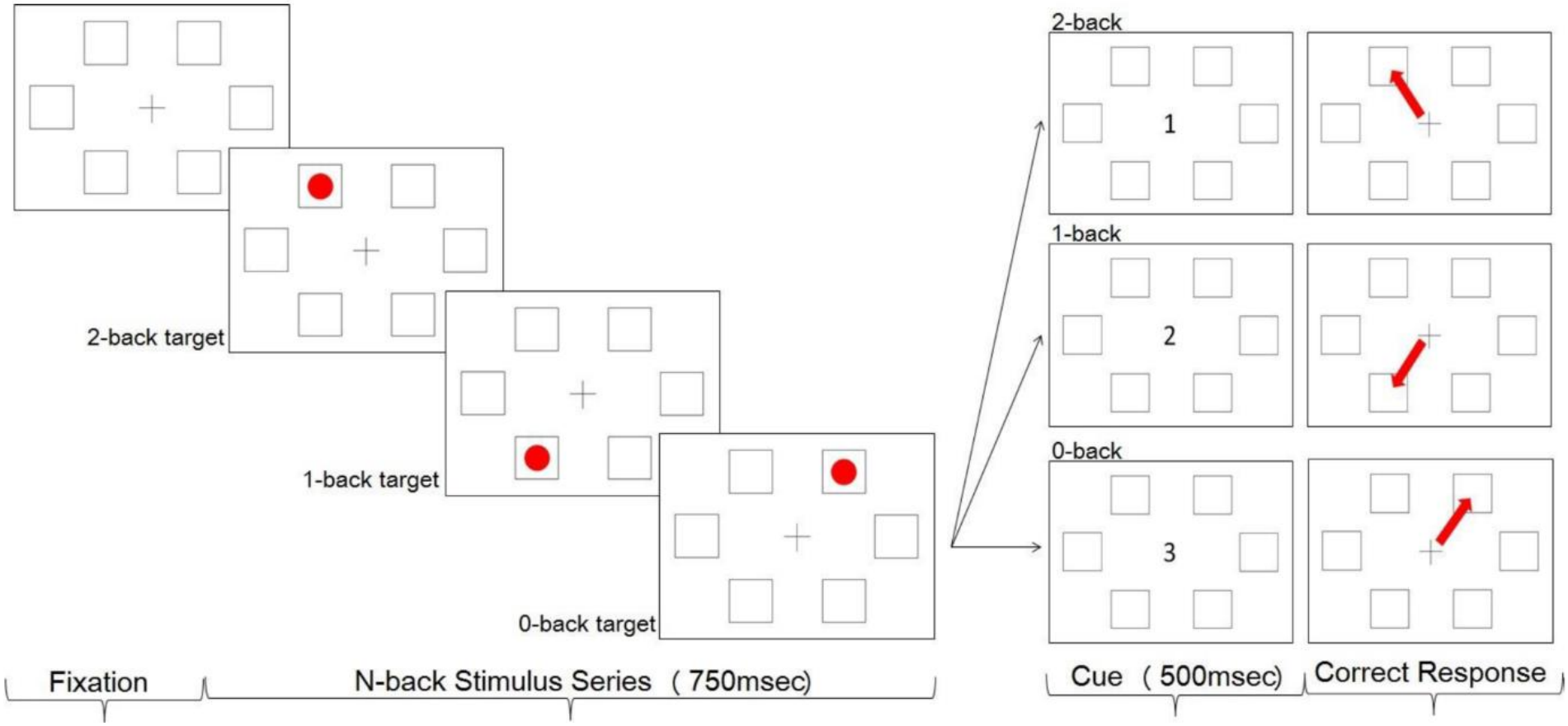

Figure 4.1: Schematic diagram of the ocular motor n-back task.

Red arrows indicate the correct direction of the eye movement required and were not displayed on the screen.

Data analysis

Eye movement data were examined using customized software written in Matlab. Trials corrupted by blinks or poor fixation were excluded from analysis. Saccades were identified using a velocity onset/offset criterion of $+30^0$/sec. Trials were then categorised as either correct or an error. An error was defined by an initial eye movement that was made toward a location other than the target location. The response time for each trial was calculated as the difference between fixation offset and saccade onset.

The total percentage of errors (accuracy) and the response time (RT) for correct saccades were calculated for all conditions. A concurrently run pilot analysis by our group in a different cohort of individuals; found that the 2-back working memory condition did not increase working memory load. Given that this condition did not increase working memory load, all data which was derived from the 2-back condition were subsequently removed from further analysis.

Working memory effect (WMeffect), a measure of the consequence of increasing cognitive load, and an indication of working memory capacity, was calculated as the difference in performance between working memory conditions. A WMeffect score was calculated for each participant for both error percentage [WMeffect (accuracy)], and response time [WMeffect (RT)] using the formula "1-back-0-back". A larger WMeffect score indicated reduced working memory capacity due to increasing cognitive load.

Data were analysed using IBM SPSS Statistics 20.0 software. Normal distribution for a variable was tested using the Shapiro-Wilk test of normality. If the normal distribution was satisfied, independent sample *t*-tests were used to examine the effect of cognitive load between the 0-back and 1-back conditions for both accuracy and RT, separately for controls and PM-carriers. Further independent sample *t*-tests were used to compare groups for age, IQ, 0-back (accuracy, and RT), 1-back (accuracy, and RT), as well as WMeffect (accuracy), and WMeffect (RT), while non-parametric Mann-Whitney was used for non-normal data. Pearson

or Spearman correlation was used to examine correlation in both groups for a speed/accuracy trade off. Finally, the relationships between each PM-carrier WMeffect scores (outcome) and CGG repeat size (predictor), and *FMR1* mRNA levels (predictor) were examined using robust regression. *P*-values less than 0.05 were considered significant in all analyses.

4.4 RESULTS

The two groups were well matched for age (Control: mean = 41.2, SD = 12.6, range 33.00; PM-carrier: mean = 41.9, SD = 7.26, range = 27.00; p = 0.859). There was no significant difference in full scale IQ scores for these two groups (Control: mean = 115.4, SD = 12.9, range = 44.00; PM-carrier: mean = 112.9, SD = 9.23, range = 27.00; p = 0.671), with all participants demonstrating IQ's within the normal/average population range.

Accuracy

No difference in overall error percentage was found between controls (Mean = 33.2, SD = 18.50, range = 34.09) and PM-carriers (Mean = 40.91, SD = 26.20, range = 50.00) (p = 0.383). The control group of participants were found to generate a significantly higher proportion of errors for the 1-back compared to the 0-back working memory condition, as anticipated by the increased cognitive load for the 1-back condition [0-back: Mean = 10.8%, SD = 8.4%, range = 32.00; 1-back: Mean = 22.4%, SD = 13.1%, range = 41.00, $t(24)$= 2.680, p=0.013]. This was not found for PM-carriers, who generated a similar proportion of errors for both conditions, and hence no effect of working memory load was seen [0-back: Mean = 18.8%, SD = 14.1%, range = 55.00; 1-back: Mean = 22.1%, SD = 16.0%, range = 55.00, p = 0.575]. No significant difference was found for WMeffect (accuracy) between PM-carriers (Mean =

0.032, SD = 0.151, range = 50.00) and controls (Mean = 0.115, SD = 0.118, range = 36.36) (p = 0.126), presumably a function of within group variability (Figure 4.2).

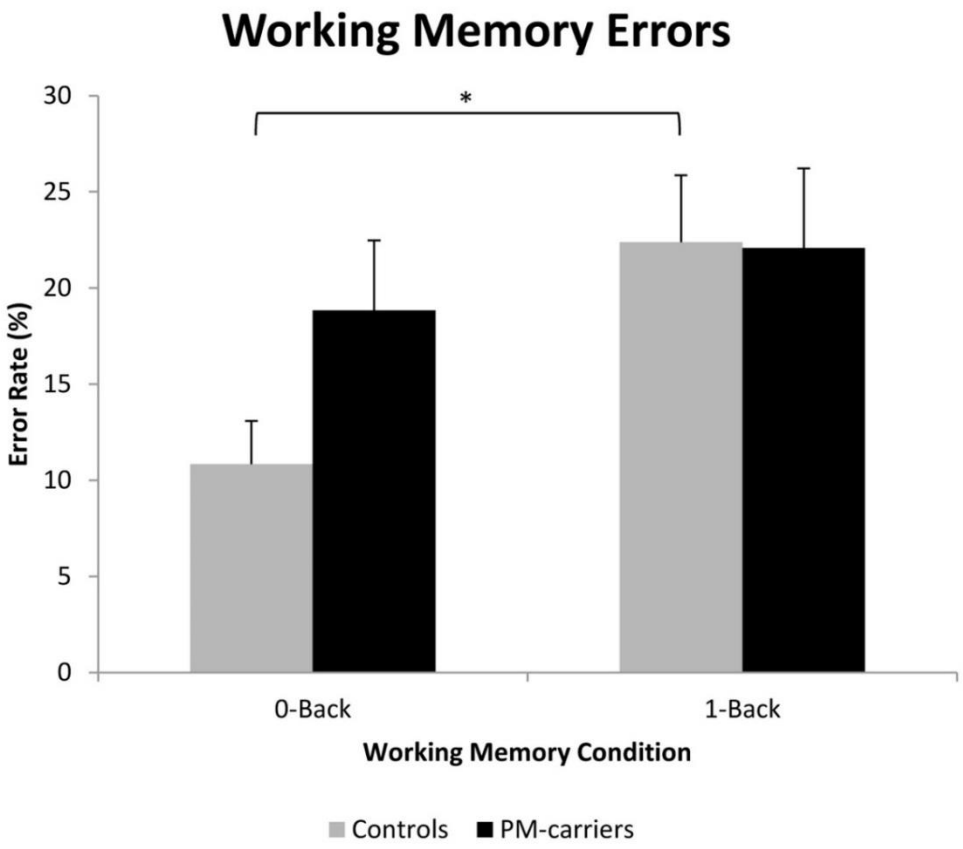

Figure 4.2: Mean working memory accuracy/error rates for *FMR1* PM-carriers and controls.

Error bars represent standard error of the mean and *p<0.05.

Response time

Working memory condition did not differentially affect response time for controls (0-back: Mean = 451.64ms, SD = 65.93, range = 216.24; 1-back: Mean = 450.24, SD = 64.95, range = 184.46; p = 0.957) or PM-carriers (0-back: Mean = 571.75, SD = 174.06, range = 559.47; 1-back: Mean = 563.67, SD = 176.54, range = 604.85; p = 0.904). Accordingly, WMeffect (RT)

scores were comparable between PM-carriers (Mean = -8.09, SD = 80.20, range = 302.47) and controls (Mean = -1.40, SD = 59.61, range = 196.44) (p = 0.809).

However, PM-carriers were found to have significantly longer response times than controls for both the 0-back [$t(25)$ = -2.403, p = 0.028] and 1-back conditions [$t(25)$ = -2.246, p = 0.039], suggesting that PM-carriers took longer to respond on the task than control participants, regardless of the cognitive load involved (Figure 4.3).

Working memory speed-accuracy trade off

There was no significant speed accuracy trade-off for either group, across the two working memory conditions [PM-carriers: 0-back (Spearman's rho r = -0.121, p = 0.68) 1-back (Pearson's r = 0.125 p = 0.67); Controls: 0-back (Pearson's r = 0.208, p = 0.495) 1-back (Pearson's r = 0.474, p = 0.102)].

Genetic and molecular correlations

Female PM-carriers were found to have *FMR1* mRNA expression ranging from 0.93-2.04 (Mean = 1.28, SD = 0.32). *FMR1* mRNA levels were significantly associated with WMeffect (RT) scores in PM-carriers (Table 4.1 and Figure 4.4). However, neither *FMR1* mRNA levels nor CGG repeat size were significantly correlated with WMeffect (accuracy).

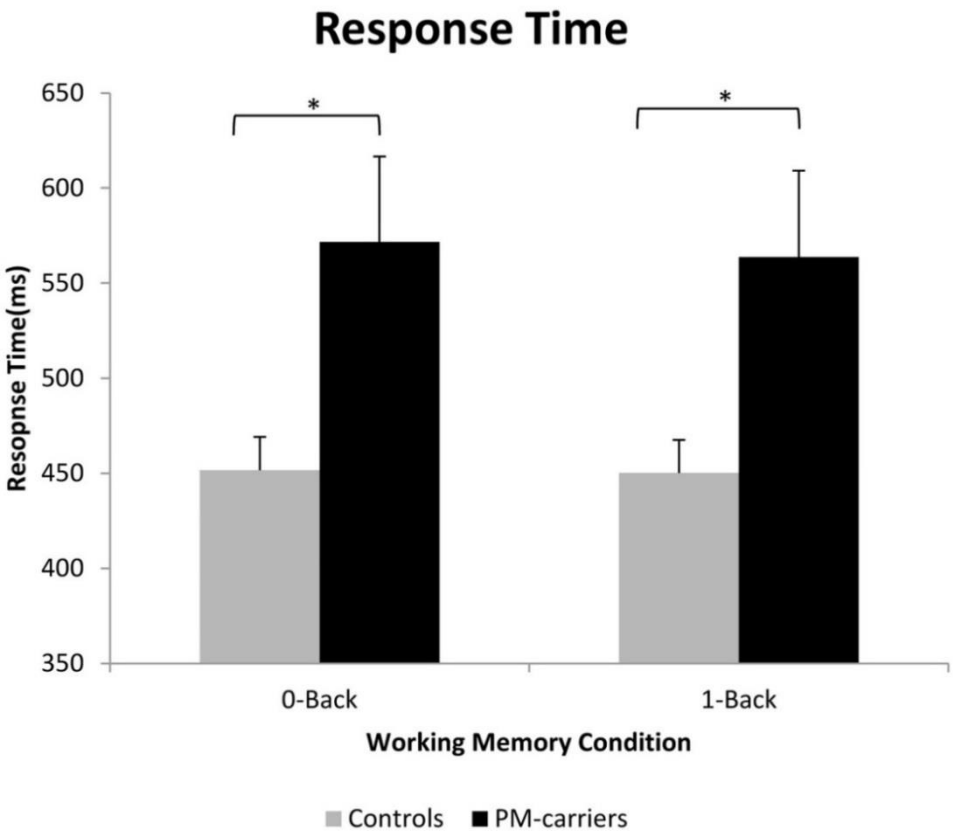

Figure 4.3: Mean working memory response time for *FMR1* PM-carriers and controls. Error bars represent standard error of the mean and *p<0.05.

Table 4.1: Assessing the relationship between each working memory effect (outcome) and CGG (predictor), and *FMR1* mRNA (predictor) in female PM-carriers, using univariate robust regression method.

	CGG			***FMR1* mRNA**		
	β	s.e	*p*	β	s.e	*p*
WMeffect (accuracy)	0.037	0.341	0.915	-0.009	0.341	0.980
WMeffect (RT)	-0.354	0.353	0.336	-0.995	0.440	**0.045**

Note: Figures in bold indicate that $p<0.05$; β = standardised regression coefficient; s.e = standard error, * $p<.05$

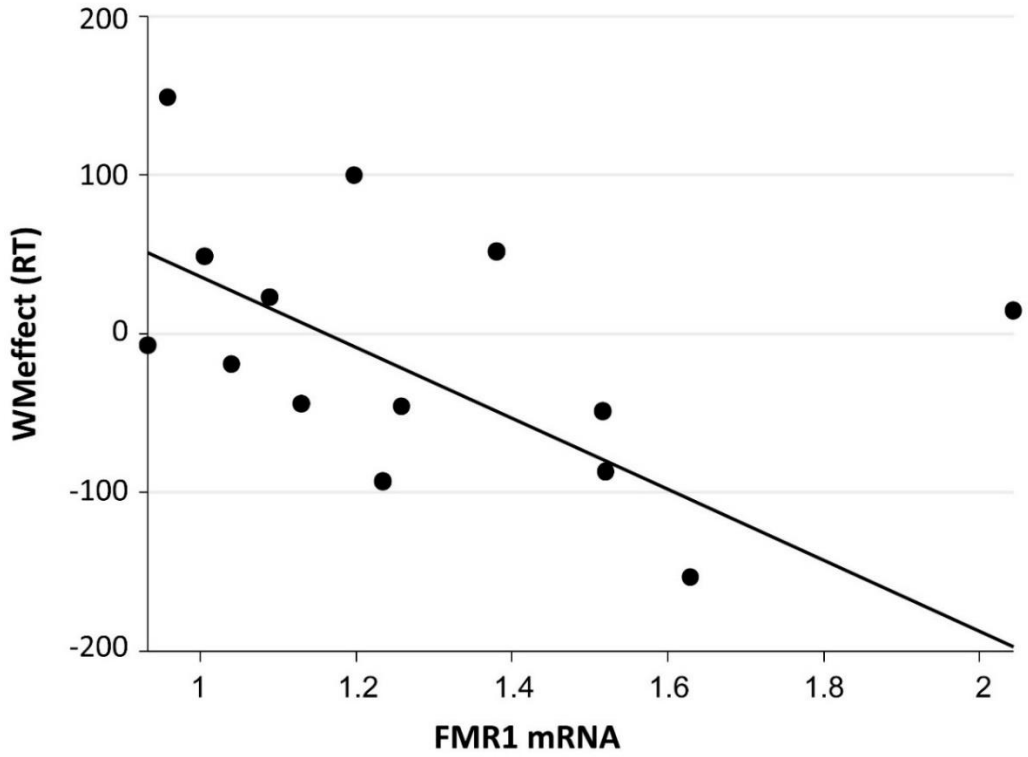

Figure 4.4: Correlation between *FMR1* mRNA and WMeffect (RT) for female PM-carriers
Plot of WMeffect (RT) versus *FMR1* mRNA with fitted line resulting from fitting robust regression to the data for female PM-carriers.

4.5 DISCUSSION

FMR1 CGG expansions are associated with subtle to severe cognitive dysfunction. This study revealed female PM-carriers to have attenuated working memory processes, characterised by prolonged RT and significantly, little effect of increasing cognitive load on error rate. Furthermore, *FMR1* mRNA levels in PM-carrier females were significantly correlated with differences in RT as a function of cognitive load for correctly executed responses, suggesting a molecular basis for these alterations. These results add to our previous study reporting inhibitory control deficits in a cohort of female PM-carriers using multiple ocular motor paradigms (Shelton *et al.*, 2014).

Although the female PM-carriers in the present study responded more slowly and they tended to record higher error rates than the control group of participants, increasing cognitive load did not elicit increases in error rate. This is in contrast to the control women in the present study, as well as other documented cohorts of neurologically healthy participants (Nagel, 2007; Jeter *et al.*, 2011). Our n-back task provided participants with minimal rehearsal time prior to responding, requiring efficient visuospatial attentional processes to allow effective encoding of the sequence prior to retrieval/responding. Spatial attention processes as well as increases in cognitive load during visuospatial working memory tasks both rely on strong IPS activation (Silk *et al.*, 2010; Vandenberghe *et al.*, 2012). Interestingly, young PM-carriers have been found to have reduced activation in the IPS and left inferior frontal gyrus during a magnitude comparison task compared to controls (Kim *et al.*, 2013). We propose that working memory deficits reflect inefficient encoding of the n-back sequence due to poor visuospatial attention primarily, rather than PM-carriers being resistant to increases in cognitive load, given the large proportion of errors recorded during the 0-back (minimal cognitive load) condition. We attribute this to difficulty engaging the IPS and visual attention mechanisms more broadly. This is consistent with previous reports of attentional control difficulties (Hunter *et al.*, 2012a) as well as inefficient encoding of verbal information (Gunning-Dixon and Raz, 2000) in female PM-carriers.

We further propose that the large amount of variability (given the range measure compared to mean score of each distribution) in WMeffect (accuracy) and WMeffect (RT) scores, for both groups, prevented any significant difference to be detected between PM-carriers and controls in this study.

Irrespective of the cognitive load, the current study found that female PM-carriers respond more slowly than controls. This parallels previous research, which has reported slower cognitive response times for a mixed gender cohort of PM-carriers during a temporal visuospatial working memory task (Kim *et al.*, 2014), and slower reaction times on a

cognitive visuospatial magnitude comparison task (Wong *et al.*, 2012). Widespread alterations in white matter integrity have been found in both male and female PM-carriers without FXTAS, particularly in frontal, parietal and cerebellar (middle cerebellar peduncles) connections (Jacquemont *et al.*, 2010; Hashimoto *et al.*, 2011c; Apartis *et al.*, 2012; Battistella *et al.*, 2012; Leow *et al.*, 2014). Interestingly, frontoparietal connections are critically important during visually based working memory tasks (Owen *et al.*, 2005). Significantly, a meta-analysis found that abnormalities in white matter structure are associated with increased response times, as well as difficulty with immediate and delayed recall, among other executive functions (Gunning-Dixon and Raz, 2000). Therefore, we propose that female PM-carriers take longer to respond correctly, irrespective of the cognitive load, and that this could be due to a reduction in white matter integrity of pathways fundamentally supporting both saccadic and visuospatial working memory networks (particularly the frontoparietal connections).

Contrary to previous research with male PM-carriers (with CGG >100 repeats), we found no relationship between CGG repeat levels and working memory measures (Cornish *et al.*, 2011; Hocking *et al.*, 2012). Our cohort, however, featured a limited CGG repeat range of between 61-102 repeats. Thus CGG lengths greater than 100 repeats were not well represented in this study. However, *FMR1* mRNA levels and WMeffect (RT) scores were significantly correlated, an effect similar to that demonstrated in a previous study investigating working memory scores in a normal *FMR1* CGG allele male population (CGG<45 repeats) (Wang *et al.*, 2013a). Increased levels of *FMR1* mRNA have also been associated with reduced activity of specific cortical regions and reduced integrity of white matter tracts during working memory tasks in PM-carriers (Hashimoto *et al.*, 2011a; Wang *et al.*, 2013b; Kim *et al.*, 2014). Increased *FMR1* mRNA levels are thought to be associated with a 'toxic gain-of-function' mechanism, as demonstrated by presence of *FMR1* mRNA within ubiquitin intracellular inclusions in neural and astrocyte cells within the cortex (Tassone *et al.*, 2000; Hagerman *et al.*, 2001; Greco *et al.*, 2002; Jacquemont *et al.*, 2003). This is consistent with our results showing the WMeffect

(RT) scores of female PM-carriers to be correlated with increasing *FMR1* mRNA levels. This may be explained by *FMR1* mRNA toxicity affecting white matter structure and neural functionality. Moreover, given that mRNA toxicity is the purported cause of FXTAS, the WMeffect (RT) scores may prove to be a behavioural biomarker for female PM-carriers most at risk of future neurodegeneration.

Although deficits in working memory are not a novel finding for PM-carriers, this is the first study to employ ocular motor tracking to describe working memory disruption in a young (<55 years old) asymptomatic female PM-carrier cohort. These findings should be viewed as preliminary, however, given the relatively small sample used. We have speculated neuronal changes as the foundation for slower response time, and lack of cognitive load effects, yet we have no direct measure of this. Moreover, investigating the influence of *FMR1* allele epigenetic markers and downstream molecular events, such as methylation patterns, X-inactivation and FMRP expression, on the cognitive measures of WMeffect are warranted. Further, we cannot exclude ascertainment bias in our sample, and that our sample may represent a group of premutation females that Steyaert and colleagues Steyaert *et al.* (2003a) identifies as having slower processing speed on tasks requiring high cognitive load.

Characterising the female PM-carrier cognitive profile is critically important to aid the development of useful markers critical for the clinical assessment of PM-carriers at-risk for FXS-associated disorders. In this study, we have added to the emerging profile by showing that female PM-carriers have an atypical working memory profile at a behavioural level, that was not seen at a basic cognitive level (comparable letter-number sequencing results with controls) (Kraan *et al.*, 2014c). We propose that this is due to difficulty in the acquisition/encoding of information (likely due to limited activation of the IPS and poor attentional control), as cognitive load was not seen to influence the accuracy of responses or response time as would be expected. Moreover, we also found strong evidence that female PM-carriers take longer to respond than control participants, which may indicate disruption

to neural pathways, predominantly in frontoparietal pathways, due to increased levels of *FMR1* mRNA and resulting molecular toxicity. This adds to our previous ocular motor findings (Shelton *et al.*, 2014), thus providing sensitive cognitive-behavioural assessment tools which add to the developing cognitive phenotype of asymptomatic female PM-carriers. Such tools may be able to identify those most at risk for future neurodegeneration associated with FXTAS. Together, these results indicate that female PM-carriers have similar working memory dysfunction as male PM-carriers, all of which are likely to stem from neurological alterations due to increasing *FMR1* mRNA levels, and may prove to be useful in the development of early predictors of PM-associated disorders.

CHAPTER 5: NEURAL CORRELATES OF EXECUTIVE DYSFUNCTION

The findings from Chapters 3 and 4 provide compelling evidence for the utility of saccade paradigms in characterising the executive function phenotype for PM females without FXTAS. A secondary aim of this thesis was, however, to examine the (neuro)biological correlates of executive dysfunction in PM females without FXTAS. Chapter 5 therefore examines the functional neural activation patterns with concurrent saccade performance, thereby exploring brain – behaviour relationships. This task, which assesses attention, response inhibition and working memory processes, has been validated in a healthy control population, in which frontal and parietal neural activation was prominent (Jamadar *et al.*, 2015).

This Chapter is written as a manuscript for publication: *Disassociation between brain activation and executive function in fragile X carriers*. It has accepted for publication in *Human Brain Mapping*, and appeared online on the 14th of October 2016. To maintain consistency throughout this thesis, changes have been made to formatting.

Declaration by candidate

In the case of Chapter 5, the nature and extent of my contribution to the work was the following:

Nature of contribution	Extent of contribution (%)
Conceptualisation, project design and programming of paradigms, data collection, data analysis and interpretation, and manuscript preparation	75%

The following co-authors contributed to the work. If co-authors are students at Monash University, the extent of their contribution in percentage terms must be stated:

Name	Nature of contribution	Extent of contribution (%) for student co-authors only
Kim Cornish	Conceptualisation, project design and manuscript preparation	
Meaghan Clough	Project design and manuscript preparation	
Sanuji Gajamange	Data analysis	
Scott Kolbe	Data analysis and manuscript preparation	
Joanne Fielding	Conceptualisation, project design, data interpretation, and manuscript preparation	

The undersigned hereby certify that the above declaration correctly reflects the nature and extent of the candidate's and co-authors' contributions to this work*.

Candidate's Signature		Date
Main Supervisor's Signature		Date

DISASSOCIATION BETWEEN BRAIN ACTIVATION AND EXECUTIVE FUNCTION IN FRAGILE X PREMUTATION FEMALES

Annie L. Shelton., Kim Cornish., Meaghan Clough., Sanuji Gajamange., Scott Kolbe, & Joanne Fielding

5.1 ABSTRACT

Executive dysfunction has been demonstrated among premutation (PM) carriers (55-199 CGG repeats) of the Fragile X mental retardation 1 (*FMR1*) gene. Further, alterations to neural activation patterns have been reported during memory and comparison based functional magnetic resonance imaging (fMRI) tasks in these carriers. For the *first* time, we examine the relationships between fMRI neural activation during an interleaved ocular motor prosaccade/antisaccade paradigm, and concurrent task performance (saccade measures of latency, accuracy and error rate) in PM females. Although no differences were found in whole brain activation patterns, regions of interest (ROI) analyses revealed reduced activation in the right ventrolateral prefrontal cortex (VLPFC) during antisaccade trials for PM females. Further, a series of divergent and group specific relationships were found between ROI activation and saccade measures. Specifically, for control females, activation within the right VLPFC and supramarginal gyrus correlated negatively with antisaccade latencies, while for PM females, activation within these regions was found to negatively correlate with antisaccade accuracy and error rate (right VLPFC only). For control females, activation within frontal and supplementary eye fields and bilateral intraparietal sulci correlated with prosaccade latency and accuracy, however no significant prosaccade correlations were found for PM females. This exploratory study extends previous reports of altered prefrontal neural engagement in PM carriers, and clearly demonstrates dissociation between control and PM females in the transformation of neural activation into overt measures of executive dysfunction.

5.2 INTRODUCTION

Large genetic expansions (>200 CGG repeats) of the of the Fragile X mental retardation 1 (*FMR1*) gene result in Fragile X syndrome, a neurodevelopmental disorder characterised by intellectual and behavioural impairments. Carriers of smaller genetic expansions (55-199 CGG repeats) are classified as having a premutation (PM) expansion which confers a risk of developing Fragile X-associated tremor/ataxia syndrome (FXTAS). FXTAS is a neurodegenerative disorder classified on the basis of clinical features (intention tremor, cerebellar ataxia, executive dysfunction) and radiological markers (white matter T2 hyperintensities in middle cerebellar peduncles and cerebrum, as well as generalised brain atrophy) (Jacquemont *et al.*, 2003). Characterising phenotype changes that predict the development of FXTAS is important for identifying those PM-carriers most at risk.

It is increasingly clear, that for some PM-carriers, alterations to both clinical and radiological markers are evident prior to the onset of FXTAS symptoms (Kraan *et al.*, 2013a; Brown and Stanfield, 2015). Firstly, executive dysfunction has been reported in young PM-carriers (Grigsby *et al.*, 2014), particularly involving tasks of response inhibition and working memory (Cornish *et al.*, 2008b; Cornish *et al.*, 2009; Shelton *et al.*, 2014; Shelton *et al.*, 2015). Secondly, overall reductions in cortical volumes have been reported for PM males (combined cohort with and without FXTAS) (Loesch *et al.*, 2005b), albeit not for PM males or females without FXTAS (Adams *et al.*, 2007; Hashimoto *et al.*, 2011b; Wang *et al.*, 2012a)/(Murphy *et al.*, 1999; Adams *et al.*, 2007). However, a number of studies have revealed reduced cerebellar volumes (Loesch *et al.*, 2005b; Battistella *et al.*, 2013), and white matter changes in cortico-cerebellar tracts and hippocampal connections (Jacquemont *et al.*, 2010; Hashimoto *et al.*, 2011c; Battistella *et al.*, 2013). Metabolic changes have also been found in the right inferior parietal gyrus and left cerebellum in PM females without FXTAS (Murphy *et al.*, 1999). Further, PM females without FXTAS were found to have reduced volumes throughout the neocortex and subcortical regions, and fewer local network connections compared to PM males without FXTAS (Leow *et al.*, 2014). Thus some gender effects are

likely to exist amongst PM-carriers. Thirdly, significant correlations have been found between structural MRI changes and measures of executive dysfunction in PM males. Specifically, volumetric measures of the inferior frontal and anterior cingulate cortices have been shown to correlate with working memory scores (Hashimoto *et al.*, 2011b), and measures of white matter integrity have been found to correlate with verbal fluency and processing speed, both aspects of executive function performance (Hippolyte *et al.*, 2014; Filley *et al.*, 2015).

While these studies support a relationship between executive function and structural MRI measures in PM-carriers, few studies have employed functional magnetic resonance imaging (fMRI) paradigms. With respect to performance on a temporal working memory task, PM males were found to have increased reaction times and decreased activation in the right temporoparietal junction, extending to the supramarginal gyrus, superior parietal lobule, insula, superior temporal gyrus and inferior parietal lobule, compared to controls (Kim *et al.*, 2014). Further, differences in the pattern of neural activation between PM and control individuals, in male or mixed gender cohorts, have also been revealed in the absence of differences in measures of executive function (Koldewyn *et al.*, 2008; Hashimoto *et al.*, 2011a; Kim *et al.*, 2013). However, only one of these studies, which used a memory recall task, examined the relationship between task performance and changes to neural activity concurrently (Koldewyn *et al.*, 2008). While significant relationships were revealed between task accuracy scores and bilateral parietal cortex activity (positive associations) for both PM and control groups, significant correlations between a measure of psychiatric symptoms and left hippocampal activity were revealed for PM males (Koldewyn *et al.*, 2008). Thus, Koldewyn *et al.* (2008) proposed that compensatory mechanisms may have altered the overall pattern of neural activity during the hippocampal-based memory task through recruitment of additional neuronal areas. This has not been explored for tasks of executive function in PM-carriers.

A clear executive phenotype has been identified in PM females (Wheeler *et al.*, 2014), yet we have no clear understanding of the functional neural correlates of the deficits reported. The aim of the present study was to identify the functional neural correlates of executive dysfunction in PM females without FXTAS using an ocular motor interleaved task. The ocular motor interleaved task requires executive control to alternate between the demands of the reflexive prosaccade and response inhibition antisaccade trials. This represents the *first* fMRI examination of relationships between neural activity and measures of executive function in PM females. This will provide preliminary evidence of the underlying, and potentially compensatory, neural mechanisms employed by PM females without FXTAS during executive function tasks.

5.3 METHODS

Participants

CGG repeat length was determined for 39 females aged between 22 and 54 years (20 with PM alleles between 55 and 199 CGGs; and 19 controls with CGG repeat length <44). CGG assessment was performed via DNA extracted from whole peripheral blood and analysed using the AmplideX *FMR1* PCR Kit according to manufacturer's instructions (Asuragen, Austin, TX). Participants were recruited from the Fragile X Alliance and the Fragile X Association Australia support groups, population-based Fragile X carrier screening studies (Metcalfe *et al.*, 2008), as well as local networks and via online advertisements. The study cohort included 5 families (four families with 2 PM females each, and one family with two PM females and one control female). The remaining 28 participants were unrelated.

All participants were English speaking with no history of any serious neurological damage/disease (including both clinical and radiological signs of FXTAS), and had normal (or corrected) vision and hearing. Exclusion criteria extended to those who thought they may be pregnant, as well as those with any MRI contraindications. Ethics approval for this study

was granted by Monash University and Southern Health Human Research Committees (Project Number 10147B); all participants gave their informed consent prior to inclusion in the study in accordance with the Declaration of Helsinki.

Executive function task: Ocular motor interleaved task

Participant's performed an ocular motor interleaved task during fMRI scanning (Figure 5.1). The task required participants to move their eyes either towards (prosaccade) or away from (antisaccade) a target as quickly and as accurately as possible depending on the colour of a central cue presented at the start of each trial. Each prosaccade and antisaccade trial began with a coloured cross (96 x 96 pixels) presented for 500, 1000, 1500 or 2000ms (randomized between trials) in the centre of a black screen. The coloured cross then disappeared and was replaced with a blank black screen for 200ms. A coloured target circle (circle filled diameter 96 pixels with 30 x 30 pixel cross hair in the centre) then appeared for 1500ms on either the left or right side of the screen at a visual angle of 7 degrees from centre. Upon extinction of the coloured target circle, a white fixation cross (96 x 96 pixel) was presented for the duration of the trial (3300, 2800, 2300, or 1800ms). Each prosaccade and antisaccade trial lasted for a total of 5500ms. The coloured cross and target circle were the same colour within each trial, with the colour cueing the participant to execute either a prosaccade or antisaccade (i.e. magenta = prosaccade, turquoise = antisaccade or vice versa, counterbalanced between participants) (Figure 5.1). Null trials consisted of the white fixation cross presented for 3500ms. The task was programmed using Experiment Builder v.10 (SR Research, Ontario Canada). Overall, participants completed a total of 96 prosaccade, 96 antisaccade, and 28 null trials (no target – remain looking at white fixation cross) randomised across 4 experimental blocks in an event-related fMRI design. The task stimuli were presented on a projection screen at the rear of the scanner by an LCD projector

(maximum flux = 1500 lumens; resolution = 1024 × 768; 60 Hz) viewed at a distance of 155cm.

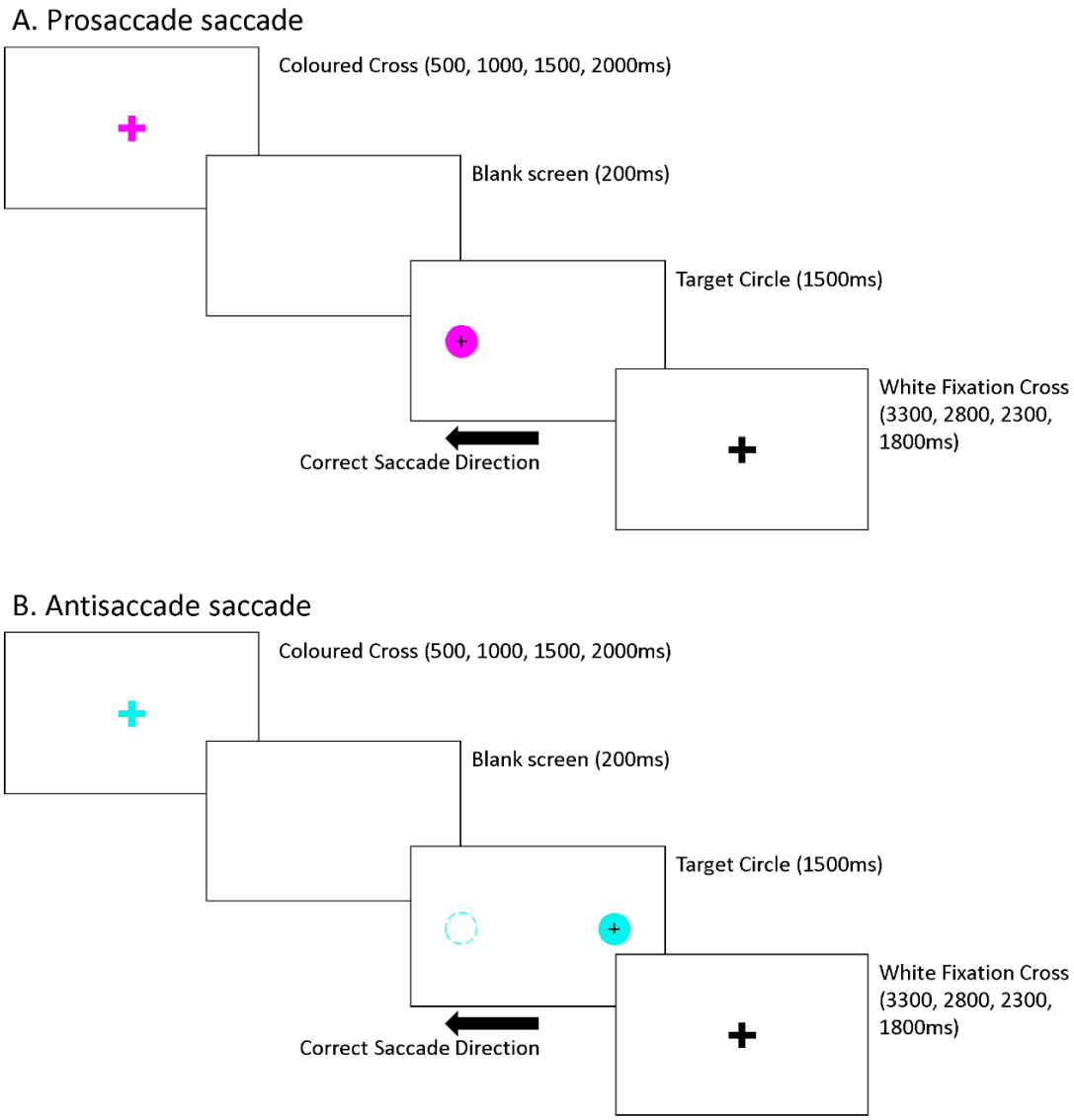

Figure 5.1: A schematic diagram of the ocular motor interleaved task

A) A prosaccade trial and **B)** An antisaccade trial – the dotted circle indicates the correct response location for an antisaccade trial and does not appear on the screen. Note that each trial lasted a total of 5500ms and target circles appeared at a distance of 7° from the central fixation cross. The colour indicating the trial type (prosaccade or antisaccade) was counterbalanced between participants.

Horizontal displacement of each participant's right eye was recorded using a MR-compatible video-based SR Research Eyelink 1000 system, with a spatial resolution of 0.01 degrees and a sampling rate of 500 Hz. Customized software written in Matlab was used to examine the eye trace, marking the time of target onset and offset, as well as time and direction of saccade onset. A criterion of $>30^0$/s was used to define saccade onset. Trials featuring blinks (at trial onset), or an unstable baseline (a failure to maintain fixation with 2.5° of central fixation) were removed from further analysis. Each trial was then examined for errors in saccade direction, defined as either looking toward the target circle on antisaccade trials, or looking away from the target circle on prosaccade trials. Anticipatory errors/eye movements, defined as saccades occurring within +/- 100ms of the target circle appearing were also identified and counted as anticipatory errors. All trials classified as *erroneous* were included in the fMRI prosaccade/antisaccade contrasts as covariates.

Variables of interest were error rate, saccade latency, and accuracy for both antisaccade and prosaccade trials. Error rate was calculated as a percentage of antisaccade/prosaccade error trials (anticipatory and directional combined) compared to total number of antisaccade/prosaccade trials. Saccade latency (measured in ms) for each correct prosaccade and antisaccade trial was calculated as the difference between target onset and saccade onset. The accuracy of correct prosaccade and antisaccade trials was calculated as the mean absolute position error as a percentage of the initial saccade, [absolute(final eye position of saccade – stimulus position)/stimulus position].

fMRI data acquisition

All MRI data were acquired on a 3T Siemens Magneto Skyra scanner using a 20-channel head coil. A T2*-weighted GRAPPA echo-planar imaging (EPI) sequence (TR = 2500ms, TE = 30ms, FOV = 192mm, acquisition matrix = 64 x 64 x 64, yielding a standard voxel size = $3x3x3mm^3$) was used to acquire the functional images. A total of 44 axial slices covered the entire brain

and a total of 133 volumes were collected during each of the four runs (5 minutes and 42 seconds per run). Additionally, a high resolution T1-weighted 3D MPRAGE scan (208 sagittal slices of 1mm thickness (no gap), TR = 1540ms, TE = 2.55ms, TI = 900ms, a flip angle of 9°, FOV=256 x 256 mm^2, yielding a standard voxel size = 1x1x1mm^3) was collected for use as an anatomical reference.

fMRI data preprocessing and analysis

Preprocessing and analysis of fMRI event-related task data was performed using FEAT (fMRI Expert Analysis Tool), part of the FSL version 5.0.4 software (FMRIB's software library, www.fmrib.ox.ac.uk) (Smith *et al.*, 2004). Preprocessing of the fMRI images from each run involved: 1) slice-time correction, 2) motion correction using rigid body transformations (MCFLIRT), 3) removal of non-brain tissue, 4) spatially smoothing with a 6x6x6m^3 FSHM Gaussian kernel, and 5) temporally filtering with a Gaussian high-pass cut-off of 50s. FMRIB's Linear Registration Tool (FLIRT) was then used to register the functional data to the T1-weighted image and then to the standard MNI atlas with a 12 degrees-of freedom affine transformation.

After preprocessing and registration, fMRI data for each run were analysed for the contrasts 1) prosaccade>fixation and 2) antisaccade>fixation. A second level analysis using FSL fixed effects statistical modelling was conducted to create subject level contrast maps for both contrasts across all four experimental runs. Finally, a third level analysis using FSL FLAME (FMRIB's Local Analysis of Mixed Effects) was conducted to create group mean and difference (controls > PMs) maps for the two contrasts. Images were thresholded using the default FDR setting of z>2.3 and a cluster significance threshold of p=0.05.

To investigate specific neural regions associated with performance of prosaccade and antisaccade tasks, *a priori* regions of interest (ROI) were extracted from a quantitative meta-

analysis examining prosaccade and antisaccade neural activation (Jamadar *et al.*, 2013). Further, cerebellar ROI were derived from both the prosaccade and antisaccade main effect at a threshold of z=6, clusters greater than 200mm. A total of eleven ROIs were assessed for the prosaccade>fixation contrast and nineteen for the antisaccade>fixation contrast (Table 5.1). The maximum percentage signal change (referred to as *activation* from this point forward) within each ROI for each participant was extracted using FSL Featquery (www.fmrib.ox.ac.uk/fsl/feat5/featquery.html).

Statistical analysis

Stata Statistical Software, Release 14 2015, was used for all statistical analyses. Each of the prosaccade and antisaccade behavioural measures, as well as activation within each ROI were assessed for normality of each group (using skewness and kurtosis), and equal variances (Levene's test). Comparison of demographic information, ocular motor measures, and ROI activation between PM and control females were conducted using independent samples *t*-tests (for equal or unequal variances) or Mann-Whitney U (when violations of the assumption of normality occurred). The generalized estimating equation was not employed, as correlations within a family were not seen to be significant.

To assess the relationships between activation for each ROI and ocular motor measures, we performed least squares or robust regression analyses (which down weighs the effect of outliers – through assigning a weight to each observation, with higher weights given to better behaving points). The goodness of fit was assessed for each analysis using the coefficient of determination (r^2). Further, the interaction effect of group*ROI was assessed using a general linear model in IBM SPSS Statistics 21.0. A significance level of $p<0.05$ was set for all analyses.

Table 5.1: ROI abbreviated labels for prosaccade>fixation and antisaccade>fixation contrasts.

	Cluster Number	Anatomical Label	Abbreviated Label
Prosaccade	1	Supplementary Eye Fields	SEF
	2	Right frontal eye fields	Right FEF
	3	Left frontal eye fields	Left FEF
	4	Right anterior intraparietal sulcus	Right aIPS
	5	Left posterior intraparietal sulcus	Left pIPS
	6	Left lingual gyrus	Left lingual gyrus
	7	Left anterior intraparietal sulcus	Left aIPS
	8	Right posterior intraparietal sulcus	Right pIPS
	9	Right cerebellar lateral VI	Right cerebellar lateral VI
	10	Right cerebellar medial VI	Right cerebellar medial VI
	11	Left cerebellar VI	Left cerebellar VI
Antisaccade	1	Supplementary Eye Fields	SEF
	2	Left intraparietal sulcus	Left IPS
	3	Right intraparietal sulcus	Right IPS
	4	Right thalamus/caudate	Right thalamus/caudate
	5	Right lateral frontal eye fields	Right lateral FEF
	6	Left frontal eye fields	Left FEF
	7	Left putamen	Left putamen
	8	Right supramarginal gyrus	Right SMG
	9	Left lingual gyrus	Left lingual gyrus
	10	Left thalamus	Left thalamus
	11	Right inferior frontal gyrus (ventrolateral prefrontal cortex)	Right VLPFC
	12	Right medial frontal eye fields	Right medial FEF
	13	Left supramarginal gyrus	Left SMG
	14	Left rostral frontal gyrus	Left rostral frontal gyrus
	15	Right cuneus	Right cuneus
	16	Right insula	Right insula
	17	Left cerebellar VI	Left cerebellar VI
	18	Right cerebellar VII	Right cerebellar VII
	19	Left cerebellar VII	Left cerebellar VII

Note: ROIs were taken from Jamadar *et al.* (2013), with additional cerebellar ROI created from functional mean contrast maps. The abbreviated label refers to the term that will be used to describe each ROI hereafter.

5.4 RESULTS

The control and PM groups were well matched for age, education and full scale IQ (assessed via the Wechsler Abbreviated Scale of Intelligence) (Wechsler, 1999) (Table 5.2).

Table 5.2: Statistics on participant demographic and molecular data

	Controls (n=19)		**PM (n=20)**		***p***
	Mean (SD)	Range	Mean (SD)	Range	
Age (years)	39.26 (9.34)	24-54	40.10 (9.77)	22-54	0.786
Education (years)	15.58 (2.91)	11-21	14.95 (3.05)	9-19	0.515
Full Scale IQ	114.26 (8.77)	97-130	110.85 (9.56)	88-127	0.254
CGG repeat	30.11 (3.05)	20-36	86.85 (16.59)	59-123	**0.000**

Note: Figures in red bold indicate that $p<0.05$.

Ocular motor behavioural results

PM females were found to have a higher prosaccade error rate than the control group (PM: Mean (M)=7.24, SD=5.57; Control: M=3.45, SD=3.98; p=0.01). However, no significant differences were found between control and PM groups for prosaccade latency (p=0.40), prosaccade accuracy (p=0.33), antisaccade latency (p=0.89), antisaccade accuracy (p=0.65) and antisaccade error rate (p = 0.09).

Whole brain analyses within and between groups

There were no significant group differences in the patterns of activation for either prosaccade>fixation or antisaccade>fixation contrasts (Figure 5.2). Importantly, activation cluster peaks of both groups closely matched the *a priori* ROIs derived from (Jamadar *et al.*, 2013) (Figure 5.2), validating their use for subsequent analyses.

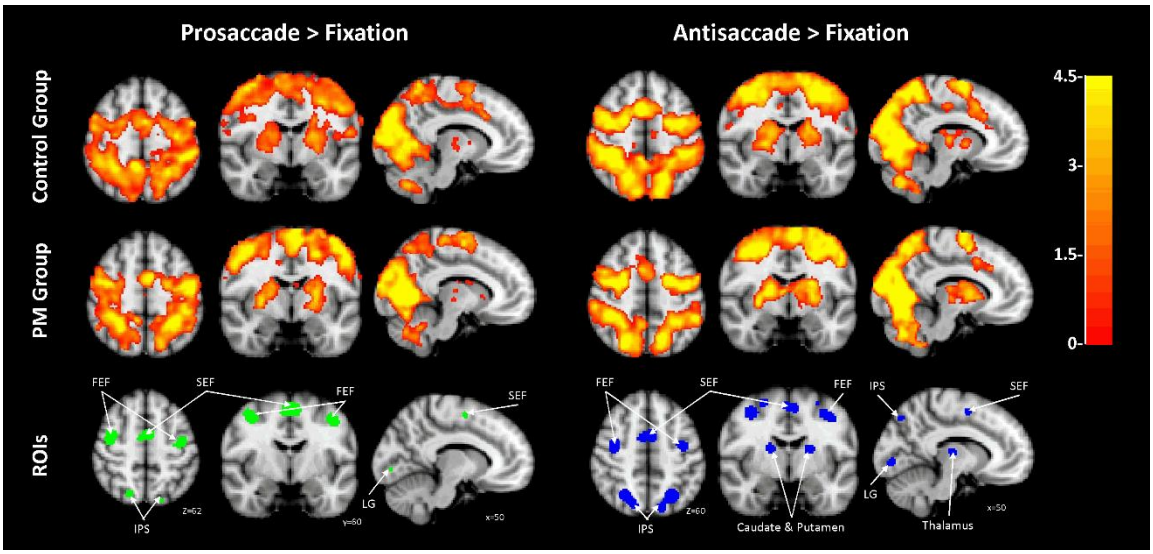

Figure 5.2: Whole brain within-group analysis for Prosaccade>Fixation and Antisaccade>Fixation contrasts for the control and premutation groups.

Images were thresholded using an FDR setting of z>2.3 and a cluster significance threshold of p=0.05. Both groups showed very similar activation patterns for both the prosaccade>fixation and antisaccade>fixation contrasts. Overall, both groups showed significant activation in regions associated with ocular motor control, which were seen to overlap with the ROIs derived from Jamadar *et al.* (2013). The colour bar on the right represents the z-statistic level of activation.

ROI analysis

No significant group differences in prosaccade ROI activation were found between the PM and control groups. For antisaccades, the control group activated the right VLPFC more strongly than the PM group (Control: M=0.34, SD = 0.14; PM: M=0.24, SD=0.11; p=0.018) (Table 5.3).

Table 5.3: Comparison of activation between healthy controls and premutation carriers for prosaccade>fixation and antisaccade>fixation contrasts.

		PM	Control	*p*-value
		Mean (SD)	Mean (SD)	
Prosaccade>fixation	Left FEF	0.346 (0.112)	0.369 (0.209)	0.673
	Left posterior IPS	0.400 (0.308)	0.450 (0.248)	0.585
	Left anterior IPS	0.197 (0.157)	0.241 (0.238)	0.866
	Left lingual gyrus	0.377 (0.210)	0.337 (0.175)	0.515
	Right FEF	0.380 (0.248)	0.353 (0.140)	0.888
	Right anterior IPS	0.312 (0.299)	0.433 (0.390)	0.227
	Right posterior IPS	0.227 (0.148)	0.290 (0.213)	0.369
	SEF	0.423 (0.187)	0.457 (0.223)	0.610
	Right cerebellar lateral VI	0.443 (0.189)	0.500 (0.269)	0.449
	Right cerebellar medial VI	0.265 (0.149)	0.338 (0.182)	0.181
	Left cerebellar VI	0.331 (0.152)	0.461 (0.306)	0.107
Antisaccade>fixation	SEF	0.523 (0.523)	0.573 (0.523)	0.556
	Right thalamus/caudate	0.445 (0.192)	0.416 (0.202)	0.800
	Left thalamus	0.188 (0.114)	0.238 (0.145)	0.236
	Right cuneus	0.684 (0.301)	0.782 (0.352)	0.357
	Left lingual gyrus	0.696 (0.345)	0.716 (0.430)	0.978
	Left putamen	0.308 (0.170)	0.323 (0.170)	0.789
	Left IPS	0.741 (0.331)	0.939 (0.506)	0.249
	Right IPS	0.809 (0.350)	0.978 (0.548)	0.431
	Right medial FEF	0.379 (0.224)	0.399 (0.198)	0.633
	Right lateral FEF	0.510 (0.262)	0.412 (0.160)	0.169
	Left FEF	0.490 (0.222)	0.498 (0.188)	0.653
	Left rostal frontal gyrus	0.112 (0.182)	0.168 (0.199)	0.238
	Right insula	0.305 (0.131)	0.397 (0.164)	0.060
	Right VLPFC	0.236 (0.113)	0.335 (0.138)	**0.018**
	Left cerebellar VI	0.741 (0.289)	0.971 (0.503)	0.092
	Right cerebellar VII	0.388 (0.183)	0.454 (0.270)	0.911
	Left cerebellar VII	0.260 (0.118)	0.282 (0.146)	0.608

Note: Figures in red bold indicate that $p<0.05$.

Prosaccade regression analysis

For the control group, longer prosaccade latencies were associated with greater activation in the left FEF (β=0.645, standard error (SE)=0.168, *p*=0.002), left aIPS (β=0.486, SE=0.179, *p*=0.015), right aIPS (β=0.600, SE =0.194, *p*=0.007), and SEF (β=0.461, SE =0.215, *p*=0.047). No significant relationships were detected between prosaccade latency and activation in any ROIs for the PM group. However, a significant differences in the relationships between prosaccade latency and i) left FEF and ii) right anterior IPS activation were found between the PM and control groups (Table 5.4).

For the control group, poorer prosaccade accuracy was associated with greater activation in left FEF (β=0.283, SE =0.0.91, *p*=0.006), right pIPS (β=0.391, SE =0.156, *p*=0.023), and SEF (β=0.492, SE =0.211, *p*=0.032). Again, no significant relationships were detected between prosaccade accuracy and activation in any ROIs for the PM group (Table 5.4). A significant difference in the relationship between prosaccade accuracy and cerebellar right lateral VI activation was found between the PM and control groups (Table 5.4).

No significant associations or interactions were found between prosaccade error rate and activation in prosaccade ROIs for either group (Table 5.4).

Table 5.4: Prosaccade ROI activation associations with prosaccade measures (Latency, Accuracy, Error Rate) in PM and control groups.

		Premutation Carriers			Controls			Interaction		
		β	*p*	r^2	β	*p*	r^2	*F*-stat	*p*	η_p^2
Latency	Left FEF	-0.039	0.871	0.002	0.645	**0.002**	0.496	4.982	**0.012**	0.217
	Left posterior IPS	0.175	0.460	0.031	0.044	0.858	0.002	0.256	0.776	0.014
	Left anterior IPS	0.194	0.413	0.038	0.486	**0.015**	0.303	1.874	0.168	0.094
	Left lingual gyrus	0.055	0.818	0.003	0.312	0.193	0.098	1.084	0.349	0.057
	Right FEF	-0.081	0.705	0.009	0.071	0.773	0.005	0.808	0.454	0.043
	Right anterior IPS	0.398	0.082	0.204	0.600	**0.007**	0.360	7.781	**0.002**	0.302
	Right posterior IPS	0.356	0.124	0.126	0.312	0.078	0.171	1.784	0.183	0.090
	SEF	0.136	0.569	0.018	0.461	**0.047**	0.213	3.167	0.054	0.150
	Right cerebellar lateral VI	-0.123	0.605	0.015	0.234	0.335	0.055	0.803	0.456	0.043
	Right cerebellar medial VI	0.005	0.982	0.000	-0.272	0.275	0.074	0.084	0.920	0.005
	Left cerebellar VI	0.330	0.155	0.109	0.176	0.470	0.031	1.416	0.256	0.073
Accuracy	Left FEF	0.077	0.747	0.006	0.283	**0.006**	0.364	0.673	0.517	0.036
	Left posterior IPS	0.045	0.851	0.002	0.172	0.481	0.030	0.107	0.899	0.006
	Left anterior IPS	-0.188	0.428	0.035	0.422	0.072	0.178	1.126	0.336	0.059
	Left lingual gyrus	-0.068	0.776	0.005	0.066	0.789	0.004	0.080	0.923	0.004
	Right FEF	0.085	0.652	0.012	0.443	0.057	0.196	1.639	0.208	0.083
	Right anterior IPS	0.048	0.840	0.002	0.240	0.322	0.058	0.178	0.838	0.010
	Right posterior IPS	-0.012	0.959	0.000	0.391	**0.023**	0.270	0.642	0.532	0.034
	SEF	-0.096	0.686	0.009	0.492	**0.032**	0.242	0.885	0.422	0.047
	Right cerebellar lateral VI	-0.424	0.063	0.180	0.164	0.503	0.027	3.325	**0.047**	0.156
	Right cerebellar medial VI	-0.170	0.473	0.029	0.267	0.268	0.072	0.684	0.511	0.037
	Left cerebellar VI	-0.376	0.102	0.142	0.261	0.319	0.058	2.499	0.096	0.122
Error Rate (%)	Left FEF	-0.316	0.175	0.100	-0.030	0.787	0.004	1.643	0.208	0.084
	Left posterior IPS	-0.251	0.285	0.063	0.308	0.199	0.095	1.219	0.307	0.063
	Left anterior IPS	-0.076	0.750	0.006	-0.229	0.345	0.053	0.562	0.575	0.030
	Left lingual gyrus	0.044	0.854	0.002	-0.088	0.721	0.008	0.066	0.937	0.004
	Right FEF	0.010	0.967	0.000	-0.143	0.560	0.020	0.050	0.951	0.003
	Right anterior IPS	-0.237	0.315	0.056	0.045	0.764	0.022	1.041	0.363	0.055
	Right posterior IPS	0.102	0.670	0.010	-0.042	0.863	0.002	0.082	0.921	0.005
	SEF	-0.592	0.076	0.174	-0.597	0.073	0.187	1.193	0.315	0.062
	Right cerebellar lateral VI	-0.555	0.069	0.181	-0.077	0.753	0.006	0.996	0.379	0.052
	Right cerebellar medial VI	-0.452	0.104	0.148	-0.132	0.591	0.017	0.295	0.746	0.016
	Left cerebellar VI	-0.411	0.222	0.086	0.192	0.431	0.037	0.481	0.622	0.026

Note: Figures in red bold indicate that p<0.05; β=standardized regression coefficients; *p*=p-value, r^2=coefficient of determination; F=F-test statistic with df=(2,36); and η_p^2=partial eta squared.

Antisaccade regression analysis

Significant negative relationships were found between antisaccade latency and activation in a number of antisaccade ROIs in the control group (Right thalamus/caudate: β=-0.670, SE=0.180, *p*=0.002; right cuneus: β=-0.457, SE=0.216, *p*=0.049; right insula: β=-0.595, SE=0.195, *p*=0.007; right VLPFC: β=-0.520, SE =0.207, *p*=0.022; and right SMG: β=-0.400, SE=0.121, *p*=0.004). These were absent in the PM group. Significant differences in the

relationships between antisaccade latency and i) right thalamus/caudate, ii) left thalamus, iii) right cuneus, iv) right insular, v) right VLPFC and vi) right SMG activation were found between the PM and control groups (Table 5.5).

No significant relationships were found between antisaccade accuracy and antisaccade ROI activation in the control group. However, significant *negative* relationships were found between antisaccade accuracy and bilateral SMG activation in the PM group (right: β=-0.894, SE=0.330, p=0.015; left: β=-0.557, SE=0.196, p=0.011). Significant differences in the relationships between antisaccade accuracy and i) SEF, ii) right VLPFC, and iii) bilateral SMG activation were found between the PM and control groups (Table 5.5).

Finally, while there were no significant relationships between antisaccade error rate and activation in antisaccade ROIs for the control group, two significant relationship was found between antisaccade error rate and antisaccade activation in the PM group (Right VLPFC: β=-0.510, s.e=0.203, p=0.022; cerebellar left VII: β=-0.467, SE =0.208, p=0.038). Further, a significant difference in the relationship between antisaccade error rate and right VLPFC activation was found between the PM and control groups (Table 5.5).

Table 5.5: Antisaccade ROI activation associations with antisaccade measures (Latency, Accuracy, Error Rate) in PM and control groups.

		Premutation Carriers			Controls			Interaction		
		β	*p*	r^2	*β*	*p*	r^2	*F*-stat	*p*	η_p^2
Latency	SEF	-0.157	0.509	0.025	0.435	0.166	0.116	0.404	0.670	0.022
	Right thalamus/caudate	0.244	0.301	0.059	-0.670	**0.002**	0.449	7.047	**0.003**	0.281
	Left thalamus	0.297	0.204	0.088	-0.270	0.399	0.045	5.551	**0.008**	0.236
	Right cuneus	0.296	0.206	0.087	-0.457	**0.049**	0.209	3.354	**0.046**	0.157
	Left lingual gyrus	0.434	0.056	0.188	-0.324	0.176	0.105	2.941	0.066	0.140
	Left putamen	0.172	0.468	0.030	-0.386	0.103	0.149	1.960	0.156	0.098
	Left IPS	0.333	0.152	0.111	-0.274	0.257	0.075	1.769	0.185	0.089
	Right IPS	0.254	0.280	0.064	-0.156	0.525	0.024	0.764	0.473	0.041
	Right medial FEF	-0.027	0.903	0.001	-0.440	0.059	0.194	2.414	0.104	0.118
	Right lateral FEF	-0.110	0.644	0.012	-0.489	0.056	0.198	1.057	0.358	0.055
	Left FEF	-0.026	0.912	0.001	0.458	0.213	0.095	0.006	0.994	0.000
	Left rostral frontal gyrus	-0.094	0.565	0.019	-0.404	0.086	0.163	2.536	0.093	0.123
	Right insula	-0.184	0.437	0.034	-0.595	**0.007**	0.355	4.708	**0.015**	0.207
	Right VLPFC	-0.316	0.142	0.116	-0.520	**0.022**	0.271	3.312	**0.048**	0.155
	Right SMG	-0.258	0.272	0.067	-0.400	**0.004**	0.392	4.269	**0.022**	0.192
	Left SMG	-0.307	0.188	0.094	-0.370	0.119	0.137	2.427	0.103	0.119
	Left cerebellar VI	-0.140	0.557	0.020	-0.464	**0.045**	0.215	2.633	0.086	0.128
	Right cerebellar VII	-0.156	0.512	0.024	-0.469	**0.043**	0.220	2.832	0.072	0.136
	Left cerebellar VII	0.083	0.729	0.007	0.063	0.856	0.002	1.464	0.245	0.075
Accuracy	SEF	-0.428	0.060	0.184	-0.178	0.466	0.032	3.389	**0.045**	0.158
	Right thalamus/caudate	0.367	0.112	0.135	-0.132	0.591	0.017	2.316	0.113	0.114
	Left thalamus	0.088	0.711	0.008	0.030	0.903	0.001	0.075	0.928	0.004
	Right cuneus	0.052	0.829	0.003	-0.032	0.897	0.001	0.033	0.967	0.002
	Left lingual gyrus	-0.301	0.260	0.074	-0.122	0.640	0.032	2.285	0.116	0.113
	Left putamen	0.024	0.923	0.001	-0.267	0.270	0.071	0.264	0.769	0.014
	Left IPS	0.053	0.825	0.003	0.316	0.092	0.158	0.065	0.937	0.004
	Right IPS	0.405	0.056	0.188	0.204	0.392	0.043	1.251	0.298	0.065
	Right medial FEF	0.236	0.317	0.317	0.027	0.914	0.001	0.820	0.449	0.044
	Right lateral FEF	0.271	0.248	0.073	-0.187	0.443	0.035	1.317	0.281	0.068
	Left FEF	-0.213	0.368	0.045	0.049	0.842	0.002	0.696	0.505	0.037
	Left rostral frontal gyrus	0.091	0.584	0.017	-0.062	0.801	0.004	0.024	0.977	0.001
	Right insula	-0.271	0.247	0.074	0.113	0.644	0.013	1.318	0.280	0.068
	Right VLPFC	-0.399	0.081	0.159	0.412	0.079	0.170	3.619	**0.037**	0.167
	Right SMG	-0.894	**0.015**	0.302	0.205	0.162	0.112	5.234	**0.010**	0.225
	Left SMG	-0.557	**0.011**	0.310	0.205	0.401	0.042	6.258	**0.005**	0.258
	Left cerebellar VI	-0.039	0.872	0.002	-0.221	0.362	0.049	0.271	0.764	0.015
	Right cerebellar VII	-0.146	0.540	0.021	-0.044	0.816	0.003	0.560	0.576	0.030
	Left cerebellar VII	0.052	0.828	0.003	0.117	0.634	0.014	0.067	0.936	0.004
Error Rate (%)	SEF	-0.439	0.053	0.193	0.004	0.988	0.000	2.496	0.097	0.122
	Right thalamus/caudate	-0.005	0.982	0.000	0.073	0.767	0.005	0.064	0.938	0.004
	Left thalamus	0.292	0.109	0.137	0.064	0.793	0.004	0.082	0.922	0.005
	Right cuneus	-0.379	0.099	0.144	0.184	0.450	0.034	2.132	0.133	0.106
	Left lingual gyrus	-0.148	0.534	0.022	0.051	0.835	0.003	0.260	0.773	0.014
	Left putamen	-0.411	0.072	0.169	0.099	0.688	0.010	2.068	0.141	0.103
	Left IPS	-0.433	0.057	0.188	-0.093	0.705	0.009	3.127	0.056	0.148
	Right IPS	-0.255	0.278	0.065	-0.217	0.373	0.047	1.560	0.224	0.080
	Right medial FEF	-0.057	0.811	0.003	-0.282	0.242	0.080	0.650	0.528	0.035
	Right lateral FEF	-0.015	0.951	0.000	-0.261	0.280	0.068	0.161	0.852	0.009
	Left FEF	-0.321	0.167	0.103	-0.104	0.672	0.011	1.235	0.303	0.064
	Left rostral frontal gyrus	0.248	0.119	0.130	0.197	0.419	0.039	0.399	0.674	0.022
	Right insula	-0.297	0.203	0.088	0.255	0.293	0.065	1.806	0.179	0.091
	Right VLPFC	-0.510	**0.022**	0.260	-0.286	0.236	0.082	5.757	**0.007**	0.242
	Right SMG	-0.335	0.148	0.112	0.101	0.509	0.026	1.611	0.214	0.082
	Left SMG	-0.203	0.391	0.041	-0.208	0.392	0.043	0.765	0.473	0.041
	Left cerebellar VI	-0.290	0.215	0.084	-0.273	0.259	0.074	2.430	0.102	0.119
	Right cerebellar VII	-0.288	0.218	0.083	0.029	0.876	0.001	1.340	0.275	0.069
	Left cerebellar VII	-0.467	**0.038**	0.218	0.000	0.999	0.000	2.826	0.072	0.136

Note: Figures in red bold indicate that p<0.05; β=standardized regression coefficients; *p*=p-value, r^2=coefficient of determination; F=F-test statistic with df=(2,36); and η_p^2=partial eta squared.

5.5 DISCUSSION

Using an ocular motor interleaved task, our study provides preliminary evidence of neural activation changes in the absence of corresponding behavioural changes, with the exception of prosaccade error rate, in PM females. While the task similarly activated key ocular motor regions for both PM and control females, reduced neural activation was evident in the right VLPFC during antisaccade trials of PM females compared to controls. Further, we reveal strong evidence for diverging, and group specific, relationships between functional neural activation, particularly in frontal regions, and executive function measures in PM and control females. We propose that these dissociations may represent both aberrance as well as compensatory changes supporting conserved or minimally disturbed functional changes associated with *FMR1* PM status.

The ocular motor neural network is well defined and encompasses prefrontal, parietal, subcortical and cerebellar regions (Leigh and Zee, 2006; McDowell *et al.*, 2008). While prosaccades are regarded as direct sensorimotor behaviours, a correct antisaccade requires the inhibition of the reflexive prosaccade generated in response to the target, and the initiation of a volitional response to the mirror opposite location. Consequently, antisaccades confer additional cognitive demands resulting in a greater reliance on prefrontal areas (specifically DLPFC and medial regions of the FEF and anterior mid cingulate cortex) (McDowell *et al.*, 2008; Jamadar *et al.*, 2013; Cieslik *et al.*, 2016). This pattern of cortical recruitment was evident for both PM and control groups (Figure 5.2), and was reflected in similar performance between the two groups, with the exception of PM females recording a greater incidence of prosaccade errors.

Interestingly, while PM females generated a higher proportion of prosaccade errors than control females, these did not correlate with activation within any of the prosaccade ROIs. It is also likely to be influenced by the paradoxical cost/benefit for prosaccades/antisaccades during an ocular motor interleaved task (Barton *et al.*, 2006a; Chan and DeSouza, 2013;

DeSimone *et al.*, 2014), given that PM females are seen to be adversely affected by increasing task demands compared to controls (Shelton *et al.*, 2015).

Both lesion and imaging studies support the influence of the FEF, parietal lobe (specifically the IPS) and middle temporal gyrus on saccade latencies for more reflexive saccades such as the prosaccades in our interleaved paradigm (Leigh and Zee, 2006; Sestieri *et al.*, 2008). Conversely, saccade accuracy depends on the integrity of posterior parietal cortical regions (Blohm *et al.*, 2005; Leigh and Zee, 2006). Significant positive relationships between FEF and IPS activation and prosaccade latency and accuracy measures were found for controls. Yet, a complete absence of significant prosaccade relationships were revealed for PM females. Further, divergent relationships were found between groups in the direction of a number of neural-behavioural associations: i) FEF activation and prosaccade latency, ii) right anterior IPS activation and prosaccade latency, and iii) right cerebellar lateral VI and prosaccade accuracy. Thus, the divergent relationships seen for prosaccade latency and accuracy relationships within these ROIs reinforces the hypothesis that PM females use compensatory (fronto-parietal) neural mechanisms to execute cognitively driven tasks.

This study also revealed a number of significant relationships between ROIs within the fronto-parietal network and antisaccade latency for controls, and accuracy and error rate for PM females. Group specific differences were found predominantly in the relationships between right VLPFC and bilateral SMG activation and antisaccade latency, accuracy and error rate. Firstly, the prefrontal cortex plays a critical role in the attention, planning, spatial orientation and inhibition of cognitively driven saccades (Leigh and Zee, 2006; McDowell *et al.*, 2008), as required during antisaccade trials. Reduced prefrontal cortical activation, specifically in the inferior frontal gyrus, has previously been identified in PM cohorts (Hashimoto *et al.*, 2011a; Kim *et al.*, 2013). Similarly, we found reduced activation within the right VLPFC for PM females. Interestingly, relationships between saccade performance and activation within the right VLPFC differed between our two groups; with a negative relationship seen with antisaccade latency for control participants, and a significant negative

relationship with antisaccade error rate for PM females. Thus greater activation in this region corresponded to faster generation of antisaccades in controls, yet for PM females, to lower error rates.

Further, PM females had significant negative relationships, while controls did not have any significant relationship between SMG activation and antisaccade accuracy. The posterior parietal cortex is primarily responsible for shifts of attention, planning of saccades as well as sensorimotor transformations (Goldberg *et al.*, 2006; Ptak and Müri, 2013). Therefore, the relationship between SMG activation and antisaccade accuracy for PM females may reflect an increase in the spatial attentional demand required to plan the appropriate volitional saccade (Steyaert *et al.*, 2003b; Hunter *et al.*, 2008).

Moreover, greater activation in the left cerebellar VII was associated with fewer errors for PM females; while for controls, greater cerebellar activity correlated with quicker antisaccade responses. Structural cerebellar and prosaccade/antisaccade performance has previously been revealed for controls, in which cerebellar lobules I-V and IX-X volumes were found to correlate with antisaccade speed; and PM males, in which cerebellar lobule VI-VII volume was found to correlate with the difference in antisaccade-prosaccade latency (Wong *et al.*, 2014). Together, these studies both highlight the pivotal role that cerebellar lobules V-VII play in the control of saccades. This is completed through internal feedback mechanisms (via projections to and from brainstem within the middle and superior cerebellar peduncles) allowing for adaptation and motor learning (Scudder *et al.*, 1996; Zee and Walker, 2009; Schubert and Zee, 2010). However differences in the associations are likely due to i) the interleaved presentation of prosaccade and antisaccade trials and functional neural activation of the cerebellum in the current study, rather than block presentation of similar trials and volumetric measures as presented by Wong *et al.* (2014). Thus, we propose that the current and previous associations between the cerebellar lobules and executive function indicate differential cerebellar learning outcomes. This may be due to altered MCP projections to the cerebellum, as this region is associated with FXTAS neuropathology.

The proposed compensatory mechanisms first proposed by Koldewyn *et al.* (2008), as well as those described herein, may be influenced by a number of factors. The Fragile X mental retardation protein (FMRP) is critical for neural synapse maturation (Willemsen *et al.*, 2011) and seen to correlate with amygdala, prefrontal and hippocampal activation (during a task) in PM males (Hessl *et al.*, 2011; Wang *et al.*, 2012a) and control males (Wang *et al.*, 2013a). Further, *FMR1* mRNA levels have been found to negatively relate with right prefrontal activation (Hashimoto *et al.*, 2011a; Wang *et al.*, 2012a), and positively with IPS activation (Koldewyn *et al.*, 2008) in PM cohorts. Thus, the attenuated pattern of activation, as well as the diverging neural activation and saccade measure relationships, may be a consequence of altered molecular outcomes associated with PM expansions.

At this point it must be acknowledged that there are innate limitations concerning the interpretation of our fMRI analyses. Firstly, inferences regarding neural activation were indirectly measured through fMRI blood-oxygen-level dependent (BOLD) response analysis techniques. Secondly, due to the nature of the BOLD response and the EPI sequence used, we cannot determine whether activation within specific ocular motor ROIs represents the planning/intention phase or motor execution of the desired response. This is important, as subregions (medial and lateral) within the FEF and SEF (as well as other ocular motor nodes) are suggested to have differing roles and activation levels with respect to the control of pro- and antisaccades during the planning and performance stages of the saccade (McDowell *et al.*, 2008; Cieslik *et al.*, 2016). However, this effect is minimised through the use of validated ROIs derived from a meta-analysis by Jamadar *et al.* (2013). We also conducted a number of multiple comparisons without statistical correction. Further, this study has not examined how the functional connectivity between ocular motor foci relate within and between groups, which is an important consideration when evaluating how neural activity relates to executive functioning in PM females. Additionally, we have not investigated the *prior-antisaccade effect* in this study (Cherkasova *et al.*, 2002; Barton *et al.*, 2006b), as this would

have created large variances in the number of prosaccades trials preceded by an antisaccade or a prosaccade for fMRI analysis.

This is the *first* fMRI study that has concurrently linked executive function performance with neural activation in a cohort of PM females. Although performance on the task and within group whole brain activation maps were similar, diverging and group specific neural – behavioural performance relationships were found between controls and PM females. This exploratory analysis suggests that activation within prefrontal, parietal and cerebellar regions differentially translate into measurable executive function performance in PM females. We also reinforce the notion of altered prefrontal activation within the PM population. Finally, we suggest that investigating the influence of FMRP and *FMR1* mRNA, as well as white matter connectivity when evaluating the translation of neural activation to behaviour, will further aid in our understanding of the biological mechanisms that underlie executive dysfunction within the PM population.

CHAPTER 6: NEURAL CORRELATES OF EXECUTIVE DYSFUNCTION - GREY MATTER

Chapter 5 provided insights into the functional neuronal correlates of saccade behaviour in PM females without FXTAS, acknowledging that the genetic and neuronal structure measures may influence the diverging and group specific brain – behaviour relationships revealed. To further delineate the biological correlates, the following two chapters will provide a comprehensive and integrated assessment of genetic markers, brain structure, and executive dysfunction. The genetic analysis will include novel epigenetic markers which have been shown to be predictive of dysexecutive processing, particularly for Haylings sentence completion tasks, for PM females without FXTAS (Cornish *et al.*, 2015), as well as measures of CGG, AR and *FMR1* mRNA. Further, this chapter will specifically examine relationships between cortical thickness of frontal and parietal regions, genetic markers, and executive dysfunction based on a combined score derived from performance on the saccade task from Chapter 5 and the Haylings sentence completion task.

This Chapter is written as a manuscript for publication: *Brain structure and intragenic DNA methylation are correlated, and predict executive dysfunction in Fragile X premutation females*. It was published in *Translational Psychiatry*, Volume 6, Issue 12 2016. To maintain consistency throughout this thesis, changes have been made to formatting.

Declaration by candidate

In the case of Chapter 6, the nature and extent of my contribution to the work was the following:

Nature of contribution	Extent of contribution (%)
Conceptualisation, project design and programming of paradigms, data collection, data analysis and interpretation, and manuscript preparation	70%

The following co-authors contributed to the work. If co-authors are students at Monash University, the extent of their contribution in percentage terms must be stated:

Name	Nature of contribution	Extent of contribution (%) for student co-authors only
Kim Cornish	Conceptualisation, project design and manuscript preparation	
Scott Kolbe	Data analysis and manuscript preparation	
Meaghan Clough	Manuscript analysis	
Howard R. Slater	Manuscript preparation	
Xin Li	Genetic analysis and manuscript preparation	
Claudine Kraan	Manuscript preparation	
Minh Bui	Statistical analysis and manuscript preparation	
David E. Godler	Genetic analysis and manuscript preparation	
Joanne Fielding	Conceptualisation, project design, data interpretation, and manuscript preparation	

The undersigned hereby certify that the above declaration correctly reflects the nature and extent of the candidate's and co-authors' contributions to this work*.

Candidate's Signature		Date
Main Supervisor's Signature		Date

BRAIN STRUCTURE AND INTRAGENIC DNA METHYLATION ARE CORRELATED, AND PREDICT EXECUTIVE DYSFUNCTION IN FRAGILE X PREMUTATION FEMALES

Annie L Shelton, Kim M. Cornish, Scott Kolbe, Meaghan Clough, Howard R. Slater, Xin Li, Claudine Kraan, Minh Bui, David E. Godler, & Joanne Fielding

6.1 ABSTRACT

DNA methylation of the Fragile X mental retardation 1 (*FMR1*) exon 1/intron 1 boundary has been associated with executive dysfunction in female carriers of a *FMR1* premutation (PM: 55-199 CGG repeats), while neuroanatomical changes have been associated with executive dysfunction in PM males. This study, for the first time, examined the inter-relationships between executive function, neuroanatomical structure, and molecular measures (DNA methylation, and *FMR1* mRNA levels in blood) in PM and control (<44 CGG repeats) females. In the PM group, *FMR1* intron 1 methylation was positively associated with i) executive function, and ii) cortical thickness in middle and superior frontal gyri, and left inferior parietal gyrus. By contrast, in the control group, *FMR1* intron 1 methylation was *negatively* associated with cortical thickness of the left middle frontal gyrus and superior frontal gyri. No significant associations were revealed for either group between *FMR1* mRNA and neuroanatomical structure or executive function. In the PM group, the lack of any significant association between *FMR1* mRNA levels and phenotypic measures found in this study, suggests that either *FMR1* expression is not well conserved between tissues, or that *FMR1* intron 1 methylation is linked to neuroanatomical and cognitive phenotype in PM females via a different mechanism.

6.2 INTRODUCTION

Trinucleotide CGG repeat expansions of the *Fragile X mental retardation 1 (FMR1)* gene are related to a number of Fragile X-associated disorders. Full mutations alleles (FM: greater than 200 CGG repeats) are associated with silencing of *FMR1* through methylation of the promoter region located in the 5' untranslated region (Godler *et al.*, 2010b), resulting in a neurodevelopmental disorder known as Fragile X syndrome (FXS). The prevalence of FXS in the general population is approximately 1 in 4000 (Coffee *et al.*, 2009). The more common *FMR1* premutation (PM) expansion (55-199 CGG repeats), which is found in approximately 1 in 209 females and 1 in 430 males (Tassone *et al.*, 2012), confers the risk of developing Fragile X-associated tremor/ataxia syndrome (FXTAS). FXTAS is a progressive neurodegenerative disorder, thought to result, in part, from elevated levels of *FMR1* mRNA, leading to protein aggregation (ubiquitin-positive intracellular inclusion bodies likely due to repeat associated non-AUG initiated translation) and reduced neuronal cell function (Willemsen *et al.*, 2003; Arocena *et al.*, 2005; Todd *et al.*, 2013). FXTAS manifests in a range of neurological and clinical symptoms as well as executive dysfunction (Hagerman *et al.*, 2001). Executive dysfunction, specifically pertaining to working memory and response inhibition processes, has been reported in both PM males (Cornish *et al.*, 2008b; Cornish *et al.*, 2009; Cornish *et al.*, 2011) and females *without* FXTAS (Goodrich-Hunsaker *et al.*, 2011a; Semenza *et al.*, 2012; Kraan *et al.*, 2013b, 2014c; Shelton *et al.*, 2014), and may represent either an independent PM phenotype or a precursor to FXTAS.

Significant associations between neuroanatomical structure (white and grey matter) and measures of cognition, including executive function, have been reported in PM males and females (Jäkälä *et al.*, 1997; Cohen *et al.*, 2006; Hashimoto *et al.*, 2011b; Wang *et al.*, 2013b; Hippolyte *et al.*, 2014; Filley *et al.*, 2015). More recently, a link has also been demonstrated between molecular changes and the risk of developing executive dysfunction in PM females; specifically, methylation changes at the exon 1/intron 1 boundary measured in blood DNA - a region also known as Fragile X related epigenetic element 2 (FREE2) (Cornish *et al.*, 2015).

This study for the *first* time examined whether CGG repeat length, *FMR1* mRNA levels, and methylation levels of the CpG island (or the activation ratio, AR) and FREE2 region correlate significantly with altered neuroanatomy in PM females without FXTAS. It also examined the relationships between these molecular and neural measures and cognitive performance; specifically changes in executive function based on an ocular motor switch task.

6.3 METHODS

Participants

CGG repeat lengths were determined for 36 females aged between 22 and 54 years. Of these, 19 exhibited PM alleles with a CGG repeat length between 55-199, and 17 exhibited normal alleles with CGG repeat length <44 (thus providing control data). All were recruited from support groups and population-based Fragile X carrier screening studies (Metcalfe *et al.*, 2008), as well as local networks and via online advertisements.

All participants were English speaking, had normal (or corrected) vision and hearing, and had no history of any serious neurological damage/disease (including FXTAS). Exclusion criteria extended to those who thought they may be pregnant, as well as those with any MRI contraindication. Ethics approval for this study was granted by Monash University and Southern Health Human Research Committees (Project Number 10147B); all participants gave their informed consent prior to inclusion in the study in accordance with the declaration of Helsinki.

Molecular analyses

DNA was extracted from whole blood for CGG sizing and methylation analysis. AmplideX *FMR1* PCR Kit was used for CGG sizing, as per the manufacturer's instructions (Asuragen, Austin, TX). RNA was extracted from peripheral blood mononuclear cells, followed by cDNA

synthesis and real-time PCR gene expression analysis performed on a ViiA 7 Real-Time PCR System (Life Technologies, Global). The relative standard curve method was utilized for *FMR1* 5' and 3' mRNA quantification normalized to mRNA levels of 2 internal control genes (SDHA and EIF4A2), as previously described (Loesch *et al.*, 2011). Activation ratio (AR) was determined using methylation sensitive Southern Blot targeting a NruI restriction site within the *FMR1* CpG island, as previously described (Cornish *et al.*, 2015). The EpiTYPER system was used to analyse FREE2 methylation in blood, consisting of 5 CpG unit outputs (targeting 9 CpG sites) per sample tested (Godler *et al.*, 2011). Blood DNA from each participant was bisulfite converted in duplicate, with each conversion analysed twice using the EpiTYPER system. A summary measure for each CpG unit was determined as the mean of the 4 methylation output ratio measurements per sample. These procedures resulted in a total of eight molecular measures: CGG, activation ratio (AR), *FMR1* mRNA, *FMR1* exon 1 (CpG 1 and CpG 2) and intron 1 (CpG 6/7, CpG 8/9 and CpG 10-12) methylation markers.

Assessment and analysis of executive function

Haylings sentence completion test

The Haylings sentence completion test (Burgess and Shallice, 1997), a test of response inhibition, required participants to respond to 15 sentences with the last word omitted, by providing a word that was unconnected to the sentence. Responses were classified as either correct, a Category A error (word plausibly finished the sentence) or Category B error (word was somewhat connected to the sentence) – both of which measure inhibitory processing. The total number of Category A and Category B errors were recorded, with larger error numbers indicates impaired response inhibition processes.

Ocular motor switch task

The ocular motor switch task (Jamadar *et al.*, 2015) assesses attention, response inhibition and working memory processes. It required participants to move their eye either towards (prosaccade trial) or away (antisaccade) from a target as quickly and as accurately as possible depending on a central colour cue given at the start of each trial (Supplementary Note 6.S1 for more details). As this study was interested in executive dysfunction, antisaccade data were removed from this analysis to avoid any contamination of the paradoxical 'benefit' that is commonly seen for antisaccade trials following a prosaccade trial (antisaccade switch trials) (Barton *et al.*, 2006a; Chan and DeSouza, 2013; DeSimone *et al.*, 2014). This yielded a total of seven prosaccade variables: correct latency (ms), error latency (ms), time to correct (ms), switch/non-switch directional error percentage and switch/non-switch anticipatory error percentage.

MRI acquisition and analysis

Structural MRIs were acquired on a 3T Siemens Magneto Skyra scanner using a 20-channel head coil using a T1-weighted 3D MPRAGE scan (208 sagittal slices of 1 mm thickness (no gap), repetition time=1540 ms, echo time=2.55 ms, inversion time=900 ms, a flip angle of 9°, field of view=256×256 mm^2, yielding a standard voxel size=1×1×1 mm^3).

T1-weighted 3D MPRAGE data were analysed using FreeSurfer version 5.1.0 (http://surfer.nmr.mgh.harvard.edu) with technical details previously described (Fischl and Dale, 2000; Fischl *et al.*, 2002; Fischl *et al.*, 2004). Automated anatomic segmentation procedure was used to measure volume of T1 white matter hypointensities (Fischl *et al.*, 2002; Fischl, 2012), while regional cortical thickness measures were obtained from the automated anatomic parcellation procedure (Fischl, 2012) for each participant.

Regional cortical thickness from the middle and superior frontal gyri (representing the dorsolateral prefrontal cortex) and inferior parietal gyrus from both left and right hemispheres were selected as they are pivotally involved in the control of saccades (Munoz and Everling, 2004; McDowell *et al.*, 2008; Jamadar *et al.*, 2013).

Statistical Analysis

Composite cognitive scores

To reduce the number of executive function variables, separate principal component analyses, using oblique direct rotation with 1 fixed factor, were hypothesised and tested using IBM SPSS Statistics software (version 21, IBM, Armonk, NY, USA). This resulted in the creation of three composite cognitive scores: 1) prosaccade response time, 2) prosaccade error score, and 3) executive function score (Supplementary Note 6.S2 for more details).

Between-group differences

The Stata statistical software (version 14, StataCorp, College Station, Texas, USA), was used for all further statistical analyses. Comparisons of demographic information, molecular, composite cognitive scores, and neuroanatomical measures between PM and control females were conducted using independent samples *t*-tests (for equal or unequal variances) or Mann-Whitney U (when violations of the assumption of normality occurred). The generalized estimating equation was not employed, as correlations within a family were not seen to be significant.

Regression models

To assess the inter-relationships between molecular variables, neuroanatomical measures and composite cognitive scores for both PM and control groups, we performed least squares

or robust regression analyses (which down weighs the effect of outliers when present). The following models were examined: I) molecular markers (predictor) and composite cognitive scores (outcome), II) molecular markers (predictor) and neuroanatomical measures (outcome), and III) neuroanatomical measures (predictor) and composite cognitive scores (outcome). The goodness of fit was assessed for each regression analysis using the coefficient of determination (r^2). Further, the interaction effect of group by i) composite cognitive score and ii) neuroanatomical measures was assessed using a general linear model in IBM SPSS Statistics 21.0. The relationships between *FMR1* mRNA levels and *FMR1* methylation (AR and FREE2 methylation) in both groups were examined using regression analyses.

6.4 RESULTS

Clinical and molecular inter-group comparisons

PM and control groups were well matched for age, education and full scale IQ (assessed via the Wechsler Abbreviated Scale of Intelligence) (Wechsler, 1999) (Supplementary Table S6.1).

Significant group differences were found for *FMR1* mRNA levels; PM females had a 1.31 mean fold increase in *FMR1* mRNA levels compared to controls (Supplementary Table S1). Mean methylation levels of exon 1 CpG sites 1 and 2; intron 1 CpG sites 6/7, 8/9 and 10-12, and of the CpG island (AR) (CpG locations indicated in Figure 6.1A) were not significantly different between PM and control groups. Further, *FMR1* mRNA levels were not found to be significantly correlate with any *FMR1* methylation measure for either the PM or control group (Supplementary Table S6.2).

Higher prosaccade error and executive function scores were found for PM females compared to controls, indicating executive dysfunction. No significant differences were found between PM and control groups for prosaccade response time, white matter hypointensities or any cortical thickness measure (Supplementary Table S6.3).

Epigenotype-phenotype relationships in PM and control groups

FREE2 methylation levels of *FMR1* intron 1 CpG sites showed the greatest number of significant relationships with composite cognitive scores in the PM group compared to CGG size, AR, exon 1 methylation or *FMR1* mRNA levels in blood (Table 6.1). Significant molecular – composite cognitive score relationships were completely absent from the control group (Table 6.2).

Again, *FMR1* intron 1 methylation levels showed the greatest number of significant relationships with neuroanatomical measures for both the PM and control groups compared to CGG size, AR, exon 1 methylation or *FMR1* mRNA levels in blood (Figure 6.1 and Table 6.1). Methylation of *FMR1* intron 1 CpG sites correlated positively with MRI measures in the PM group (Figure 6.1B, Figure 6.2 and Table 6.1). Conversely, for controls, increased methylation of *FMR1* CpG 2, 6/7, 10-12 was associated with decreased cortical thickness in frontal lobe regions. No significant CpG 8/9 – neuroanatomical relationships were found for the control group (Figure 6.1C, Figure 6.2 and Table 6.2). Interaction analysis revealed significant group differences in the relationships between *FMR1* intron 1 methylation and middle frontal, superior frontal and inferior parietal thickness were evident (Table 6.3).

Neuroanatomical measures related to executive function measures for both PM and control groups. The three significant relationships for the PM group suggest that executive function deficits, denoted by composite cognitive scores, were related to increased white matter hypointensities (prosaccade response time: coefficient (β)=0.491, standard error (s.e)=0.211, p=0.033, r^2=0.241) and decreased cortical volume in the left middle frontal gyrus (prosaccade error score: β=-0.495, s.e =0.211, p=0.031, r^2=0.245), and left inferior parietal gyrus (executive function score: β=-0.547, s.e=0.203, p=0.015, r^2=0.299). Conversely, increased bilateral inferior parietal gyri thickness was positively associated with greater prosaccade error scores in controls (left: β=0.439, s.e =0.166, p=0.018, r^2=.319: β=0.490, s.e = 0.225, p=0.046, r^2=0.240).

Table 6.1: Relationships between molecular parameters and composite cognitive scores and neuroanatomical measures outcome variables for the PM group

Outcome Variables	CGG	AR	*FMR1* mRNA	CpG 1	CpG 2	CpG 6/7	CpG 8/9	CpG 10-12
	β (r^2)	β (r^2)	β (r^2)	β (r^2)	β (r^2)	β (r^2)	β (r^2)	β (r^2)
Prosaccade response time	-0.142 (0.020)	0.450 (0.199)	0.288 (0.093)	-0.105 (0.011)	0.232 (0.054)	**0.791 (0.366)**	0.321 (0.103)	0.281 (0.064)
Prosaccade error score	0.217 (0.047)	**-0.469 (0.350)**	0.038 (0.001)	**0.364 (0.261)**	-0.253 (0.064)	**-0.760 (0.353)**	**-0.591 (0.344)**	**-0.670 (0.478)**
Executive function score	0.229 (0.053)	-0.196 (0.009)	0.132 (0.017)	0.010 (0.000)	0.213 (0.045)	-0.455 (0.198)	**-0.511 (0.261)**	-0.310 (0.086)
White matter hypointensities	-0.079 (0.006)	0.386 (0.158)	0.265 (0.100)	**-0.511 (0.261)**	0.113 (0.013)	**0.471 (0.222)**	0.076 (0.005)	0.405 (0.079)
Left middle frontal gyrus	-0.146 (0.021)	0.215 (0.051)	-0.254 (0.066)	0.106 (0.011)	0.331 (0.109)	0.427 (0.179)	**0.564 (0.319)**	**0.504 (0.220)**
Right middle frontal gyrus	0.035 (0.001)	0.039 (0.002)	-0.346 (0.116)	0.065 (0.004)	0.055 (0.003)	0.250 (0.062)	**0.655 (0.430)**	0.375 (0.117)
Left superior frontal gyrus	-0.024 (0.001)	-0.051 (0.003)	-0.324 (0.104)	0.252 (0.064)	0.292 (0.085)	0.426 (0.176)	**0.541 (0.293)**	0.455 (0.183)
Right superior frontal gyrus	0.030 (0.001)	0.065 (0.005)	-0.186 (0.033)	0.305 (0.093)	0.276 (0.076)	0.293 (0.086)	**0.612 (0.374)**	0.415 (0.168)
Left inferior parietal gyrus	-0.081 (0.007)	-0.200 (0.040)	-0.294 (0.084)	0.058 (0.003)	0.104 (0.011)	**0.558 (0.312)**	**0.494 (0.241)**	0.317 (0.077)
Right inferior parietal gyrus	-0.020 (0.000)	-0.242 (0.056)	-0.350 (0.119)	-0.039 (0.002)	0.052 (0.003)	0.242 (0.045)	0.089 (0.008)	-0.023 (0.000)

Note: Figures in red bold indicate that $p<0.05$; β=standardized regression coefficients; and r^2=coefficient of determination

Table 6.2: Relationships between molecular parameters and composite cognitive scores and neuroanatomical measures outcome variables for the healthy control group

Outcome Variables	CGG	AR	*FMR1* mRNA	CpG 1	CpG 2	CpG 6/7	CpG 8/9	CpG 10-12
	β (r^2)	β (r^2)	β (r^2)	β (r^2)	β (r^2)	β (r^2)	β (r^2)	β (r^2)
Prosaccade response time	-0.249 (0.062)	-0.353 (0.125)	0.475 (0.225)	0.148 (0.020)	-0.267 (0.067)	0.087 (0.008)	0.075 (0.006)	-0.054 (0.003)
Prosaccade error score	0.109 (0.018)	-0.011 (0.000)	-0.282 (0.190)	0.032 (0.002)	0.296 (0.159)	0.314 (0.099)	0.153 (0.023)	0.205 (0.042)
Executive function score	0.201 (0.040)	0.248 (0.061)	-0.402 (0.162)	0.152 (0.023)	0.089 (0.009)	0.016 (0.000)	-0.330 (0.109)	-0.164 (0.027)
White matter hypointensities	-0.426 (0.206)	-0.254 (0.074)	0.360 (0.130)	0.105 (0.011)	0.271 (0.071)	0.418 (0.174)	0.429 (0.184)	0.206 (0.042)
Left middle frontal gyrus	0.117 (0.010)	-0.271 (0.074)	-0.158 (0.025)	-0.015 (0.000)	**-0.588 (0.334)**	**-0.651 (0.424)**	-0.466 (0.217)	**-0.621 (0.386)**
Right middle frontal gyrus	0.133 (0.014)	-0.280 (0.078)	-0.084 (0.006)	-0.124 (0.015)	-0.151 (0.021)	-0.293 (0.086)	-0.045 (0.002)	-0.261 (0.068)
Left superior frontal gyrus	-0.454 (0.063)	-0.212 (0.045)	-0.306 (0.093)	0.253 (0.030)	-0.022 (0.000)	-0.378 (0.143)	-0.119 (0.014)	-0.728 (0.302)
Right superior frontal gyrus	0.164 (0.021)	-0.297 (0.088)	-0.259 (0.067)	-0.076 (0.005)	-0.085 (0.007)	**-0.507 (0.257)**	-0.175 (0.031)	-0.521 (0.166)
Left inferior parietal gyrus	0.098 (0.008)	-0.269 (0.072)	-0.293 (0.086)	-0.349 (0.132)	-0.006 (0.000)	-0.426 (0.182)	-0.076 (0.006)	-0.302 (0.079)
Right inferior parietal gyrus	-0.433 (0.056)	-0.052 (0.002)	-0.340 (0.115)	-0.081 (0.005)	0.060 (0.004)	-0.043 (0.002)	-0.310 (0.087)	-0.301 (0.078)

Note: Figures in red bold indicate that $p<0.05$; β=standardized regression coefficients; and r^2=coefficient of determination

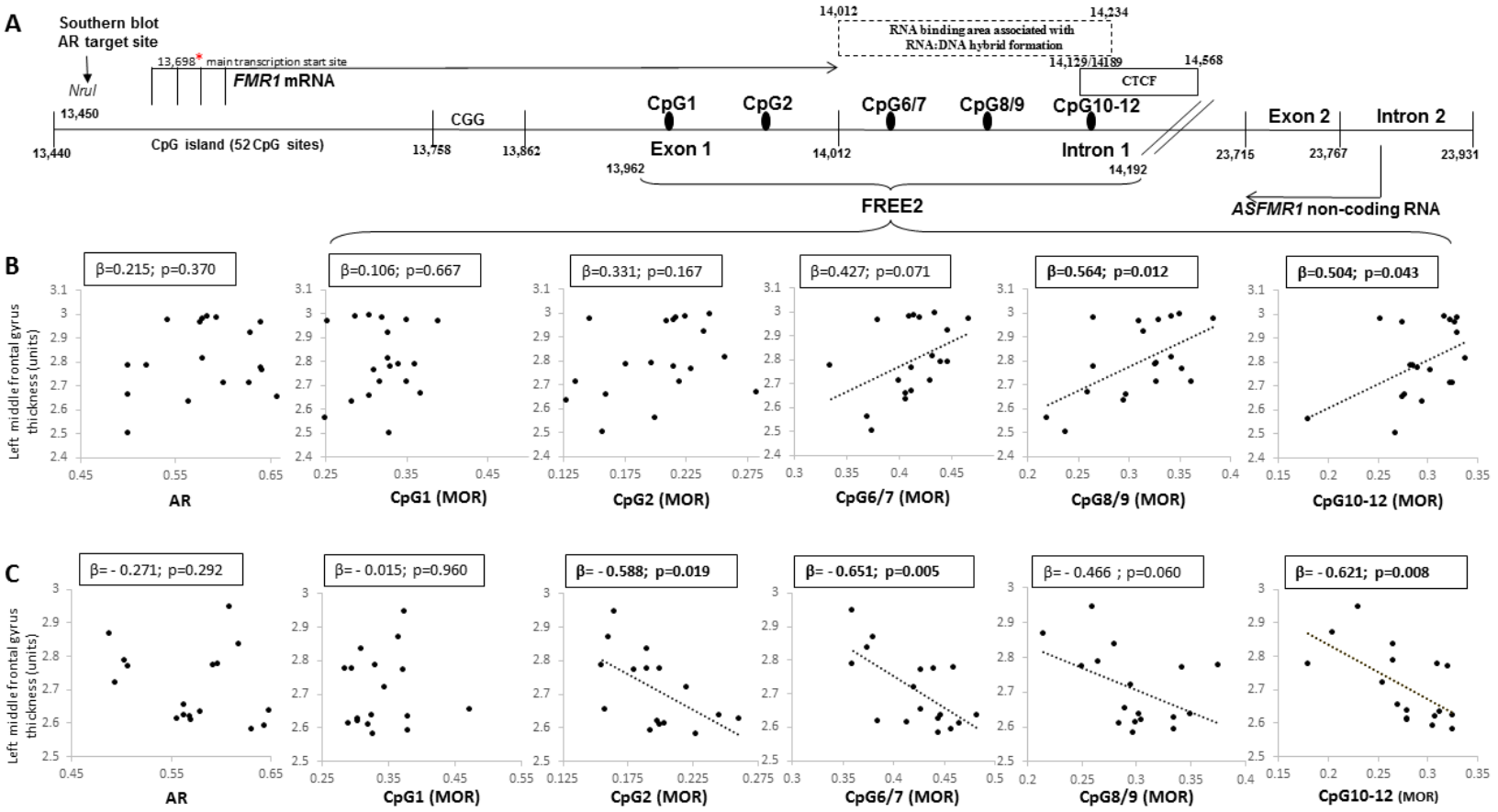

Figure 6.1: *FMR1* methylation sites and associations with left middle frontal gyrus in PM and control groups

A) Organization of the Xq27.3 sequence encompassing specific FREE2 CpG sites (GenBank L29074 L38501) targeted by FREE2 EpiTYPER system. The CTCF box indicates 5' CTCF binding sites from UCSF Chip-Seq which overlap with FREE2 CpG10-12; the RNA:DNA hybrid box indicates locations of forward and reverse primers used in ChiRP to show formation of RNA:DNA hybrids denoted as fP(200-400) (Colak et al 2014; Figure 4 and Figure S16 and Table S1). Associations between biomarker methylation within *FMR1* CpG island (represented by AR), exon 1 and intron 1 and left middle frontal gyrus thickness (assessed using structural MRI Model II) (unstandardized values) in PM **B)** and control **C)** groups. β represents standardized coefficients from least or robust (down weighs outliers) regression analysis.

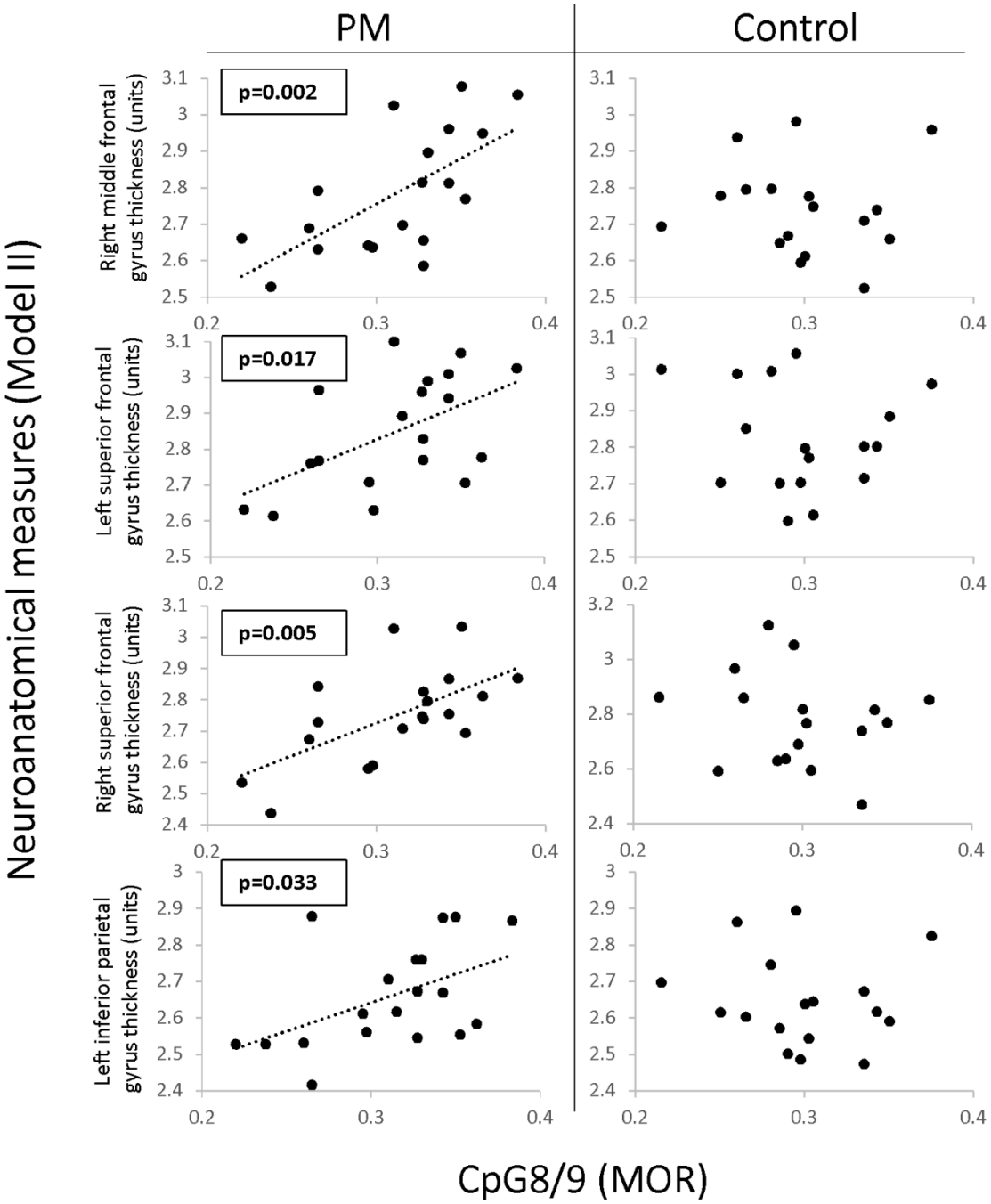

Figure 6.2: Associations between neuroanatomical cortical thickness and CpG8/9 methylation in PM and control groups.

P values represent results from individual least squares regression analyses assessing the relationship between CpG 8/9 and cortical thickness (unstandardized values), and are presented only for values reaching significance of $p<0.05$.

Table 6.3: The interaction effect of group by i) composite cognitive score and ii) neuroanatomical measures for each molecular parameter

Outcome Variables	CGG	AR	*FMR1* mRNA	CpG 1	CpG 2	CpG 6/7	CpG 8/9	CpG 10-12
	F (η_p^2)	F (η_p^2)	F (η_p^2)	F (η_p^2)	F (η_p^2)	F (η_p^2)	F (η_p^2)	F (η_p^2)
Prosaccade response time	0.235 (0.014)	3.038 (0.160)	1.418 (0.081)	0.416 (0.025)	0.983 (0.058)	2.535 (0.133)	0.923 (0.053)	0.556 (0.033)
Prosaccade error score	**15.533 (0.485)**	0.218 (0.013)	1.803 (0.101)	0.185 (0.011)	0.691 (0.041)	1.703 (0.094)	2.108 (0.113)	0.855 (0.049)
Executive function score	**6.620 (0.286)**	1.914 (0.107)	1.077 (0.063)	0.017 (0.001)	1.168 (0.068)	1.905 (0.104)	1.309 (0.074)	2.394 (0.127)
White matter hypointensities	0.421 (0.025)	1.905 (0.104)	2.224 (0.122)	2.125 (0.114)	0.595 (0.036)	3.080 (0.157)	1.664 (0.092)	0.580 (0.034)
Left middle frontal gyrus	1.692 (0.093)	1.012 (0.059)	0.386 (0.024)	0.032 (0.002)	3.241 (0.168)	**8.131 (0.330)**	**6.061 (0.269)**	**6.088 (0.270)**
Right middle frontal gyrus	0.374 (0.022)	0.549 (0.033)	1.069 (0.063)	0.253 (0.015)	0.118 (0.007)	1.405 (0.078)	**5.600 (0.253)**	1.803 (0.099)
Left superior frontal gyrus	0.101 (0.006)	0.319 (0.020)	1.294 (0.075)	0.701 (0.041)	1.050 (0.062)	3.033 (0.155)	**3.532 (0.176)**	2.678 (0.140)
Right superior frontal gyrus	0.072 (0.004)	0.767 (0.046)	0.853 (0.051)	0.797 (0.046)	0.896 (0.053)	**3.497 (0.175)**	**4.596 (0.218)**	1.790 (0.098)
Left inferior parietal gyrus	0.035 (0.002)	0.855 (0.051)	1.134 (0.066)	0.835 (0.048)	0.129 (0.008)	**5.031 (0.234)**	2.717 (0.141)	1.604 (0.089)
Right inferior parietal gyrus	0.045 (0.003)	0.477 (0.029)	1.614 (0.092)	0.177 (0.011)	0.059 (0.004)	0.372 (0.022)	0.120 (0.007)	0.303 (0.018)

Note: Figures in red bold indicate that $p<0.05$; F =F-test statistic; and η_p^2=partial eta squared

6.5 DISCUSSION

Understanding the disorder specific role of intragenic DNA methylation is critically important (Robertson, 2005; Neidhart, 2016), providing a unique opportunity to investigate gene/environment interactions of clinical significance (Zannas and West, 2014). In this study, highly significant relationships were found between the intragenic methylation within the 5'end of the *FMR1* intron 1 and phenotype measures of executive function, volume of white matter hypointensities and regional cortical thickness in the frontal and parietal cortices of PM females without FXTAS. The differences in the relationships between methylation markers CpG 6/7 and CpG 8/9 and cortical thickness between PM and control females suggest that in *normal* neurobiology, *FMR1* methylation (potentially X chromosome inactivation (XCI)) is related to thickness of specific cortical regions and volume of white matter hypointensities, which are disrupted in PM females without FXTAS through a currently unknown mechanism that modifies the observed associations.

FMR1 intron 1 methylation, but not *FMR1* mRNA, predicts executive dysfunction in PM Females

In PM females without FXTAS, decreased methylation of both *FMR1* promotor (AR) and *FMR1* intron 1 regions was found to relate to executive dysfunction. This relationship was absent in controls entirely. Further, the strongest relationships for each composite cognitive score were seen within the 5'end of *FMR1* intron 1, as compared to methylation of exon 1 or AR. This is consistent with the study by Cornish and colleagues (Cornish *et al.*, 2015), supporting the prior hypothesis that methylation of *FMR1* intron 1 CpG sites is a good predictor of deficits within the executive function phenotype of PM and FM females (Godler *et al.*, 2010a; Godler *et al.*, 2012; Godler *et al.*, 2013; Inaba *et al.*, 2013; Pastori *et al.*, 2014; Cornish *et al.*, 2015).

Unlike previous ocular motor studies, *FMR1* mRNA levels were not correlated with executive function scores in this cohort of PM females without FXTAS (Shelton *et al.*, 2015). Conversely, *FMR1* intron 1 methylation correlated with both executive function and neuroanatomical structure in the PM group. We also found no significant relationships between any methylation measure (AR and FREE2 methylation) and *FMR1* mRNA for PM or control groups. This suggests that, in PM females without FXTAS, *FMR1* intron 1 methylation has clinical significance involving a different mode or pathway of action which does not directly involve over-expression of *FMR1* mRNA.

It is important to note that in this study, *FMR1* mRNA was normalised to two control genes (*SDHA* and *EIF4A2*) and not beta-glucuronidase (*GUS*), as in previous observations assessing differing aspects of executive function (Cornish *et al.*, 2015; Hocking *et al.*, 2015; Shelton *et al.*, 2015). *GUS* is a commonly used reference gene or internal control for transcript quantification by PCR. In a study of FM males where *FMR1* mRNA was normalised to actin B and *GUS*, a positive linear relationships between *FMR1* mRNA and methylation of the *FMR1* promotor region was found (Brasa *et al.*, 2016), which was not evident in this study. This difference could have several explanations including that: (a) the Brasa and colleagues study(Brasa *et al.*, 2016) performed correlation analyses for different CpG sites, (b) used FM males as opposed to PM females without FXTAS, (c) had a much smaller sample size of only 7 individuals (susceptible to the effects of outliers), or most likely (d) used a different normalization strategy of *FMR1* mRNA. In relation to the last potential explanation, it is important to note that variability in gene expression of internal control genes has been well documented to impact target gene real-time PCR outputs(Hellemans *et al.*, 2007), which we have recently shown to apply in PM females without FXTAS (Kraan *et al.*, 2016).

FMR1 intron 1 differently predicts neuroanatomical structure between PM and control groups

Juxtaposing associations were found between increased FREE2 methylation and cortical thickness in our PM and control groups: increased cortical thickness for the PM group, decreased cortical thickness for the control group. This was most evidenced when assessing the FREE2 methylation relationships with cortical thickness of the left middle frontal gyrus, where there was a trend toward increased cortical thickness for the PM group compared to controls (p=0.058). The clear dissociation between *FMR1* intron 1 methylation and cortical thickness of the left middle frontal gyrus, as well as other *FMR1* intron 1 methylation – frontal and inferior parietal relationships, between groups, suggests a possible involvement for XCI skewing in regulating the thickness of this region as part of normal biology. This also suggests that *FMR1* intron 1 methylation in peripheral blood is important when considering XCI in neurological disorders without a PM expansion. This is reinforced by the absence of significant associations between methylation of FREE2 CpG 8/9 and cortical thickness in the control group, compared to the highly significant relationships seen for the PM group. Not only does this study show that methylation of *FMR1* intron 1 CpG sites is a useful biomarker of cortical thickness in PM females without FXTAS, but it also opens up the broader possibility that this may be the case for other disorders involving cortical thickness disruption, such as Alzheimer's (PSEN1 mutations) (Fortea *et al.*, 2010), Parkinson's (Jubault *et al.*, 2011; Madhyastha *et al.*, 2015), major depressive disorder (Qiu *et al.*, 2014), and social anxiety disorder (Brüuhl *et al.*, 2013).

Multiple neuroanatomical correlates of executive function found in the PM group

Each of the composite cognitive scores was found to be associated with either regional cortical thickness, or volume of white matter hypointensities within the fronto-parietal executive processing network (Model III) for PM females without FXTAS, while only inferior parietal thickness related to prosaccade error score in the control group. Specifically, a

positive relationship was found between white matter hypointensities and prosaccade reaction time in PM females without FXTAS, which is consistent with the hypothesis that reduced white matter integrity results in increased response times in cognitive tasks generally (Gunning-Dixon and Raz, 2000).

Similarly to our findings of an association between left middle frontal gyrus thickness and prosaccade error scores, decreased cortical thickness in the middle frontal cortex has been linked to executive dysfunction (Alahyane *et al.*, 2007). Equally, we also reveal that decreased cortical thickness of the left inferior parietal gyrus related to impaired executive function scores in PM females without FXTAS. Collectively, these findings are in direct contrast to a previous FXS study, where increased cortical thickness was associated with poorer performance on multiple domains of the Stanford-Binet Intelligence Scale (Meguid *et al.*, 2012). In that study, the FXS findings were hypothesised to reflect inefficient synaptic pruning due to FMRP deficiencies (Meguid *et al.*, 2012). As such, other mechanism(s) and pathways discussed below are likely to underlie these neuroanatomical – executive function relationships in PM females without FXTAS.

Alternative explanations to the observed relationships

The process of XCI, where only one of the two X chromosomes becomes inactivated in females, is complex and relies on a number of factors including DNA methylation, non-coding RNAs, and nuclear protein. DNA methylation is an important process in the regulation of XCI and gene expression. DNA hydroxymethylation (5-hydroxymethylcytosine (5hmC)), is thought to be an epigenetic modifier and a possible intermediate product within an active DNA demethylation pathway, potentially playing a role in both neurodevelopmental and neurodegenerative diseases/disorders (Branco *et al.*, 2012; Al-Mahdawi *et al.*, 2014; Cheng *et al.*, 2015). In a FXTAS mouse model, 5hmC levels were found to be reduced compared to wild-type littermates, suggesting that for PM individuals, 5hmC may have a

neurodegenerative role (Yao *et al.*, 2014). Moreover, non-coding RNA are most commonly derived from intragenic DNA regions (St Laurent *et al.*, 2012). Specifically, RNA:DNA hybrids are thought to form at the location of *FMR1* intron 1 CpG sites (Colak *et al.*, 2014) and may also play a role in XCI. Further, over-expression of *ASFMR1* and long non-coding RNA have previously been reported in PM individuals (Ladd *et al.*, 2007), and have also been associated with parkinsonism and mitochondrial dysfunction (Loesch *et al.*, 2011). Future studies should explore the contribution of the aforementioned pathways as alternative explanations for the relationships observed in this study between *FMR1* intron 1 methylation, and phenotype measures.

Conclusion

Overall, understanding how epigenetic changes influence neuroanatomy, executive function and clinical outcomes is highly important for both *FMR1* PM and FM related disorders, and broader neurological disorders impacted by abnormal XCI. Although preliminary, this is the *first study* to link *FMR1* intron 1 methylation and neuroanatomical structure in PM and control females. Secondly, *FMR1* intron 1 methylation produced the greatest number of associations (for both phenotype measures), compared to *FMR1* exon 1 methylation, AR, CGG repeat size and *FMR1* mRNA levels in blood, confirming our previous observation (Cornish *et al.*, 2015). Frontal and parietal cortical thickness, as well as white matter hypointensities, in brain regions that support executive function, also negatively related to composite cognitive scores. Importantly, differences in the relationships between *FMR1* intron 1 methylation and left middle frontal gyrus thickness, and between CpG site 8/9 and frontal and parietal cortical thickness, suggest that XCI skewing in controls may be critical when assessing changes in cortical thickness in females with other neurological diseases. While we provide specific hypotheses regarding the mechanisms underlying such relationships, further confirmatory analysis of the molecular pathways that link *FMR1* intron 1 methylation to neuroanatomical structure and executive dysfunction are needed to support these

assertions for the PM neuro-cognitive phenotype and in normal neurobiology. Importantly, together with our previous studies (Cornish *et al.*, 2015), the utility of FREE2 methylation, particularly methylation of the 5' *FMR1* intron 1 region, as a sensitive measure that relates to both neuroanatomical structure and executive dysfunction in PM females without FXTAS, have been now confirmed.

SUPPLEMENTARY MATERIAL

Supplementary Note 6.S1: Ocular motor interleaved task

Participant's performed an ocular motor interleaved task within the MRI environment. The task required participants to move their eye either towards (prosaccade) or away (antisaccade) from a target as quickly and as accurately as possible depending on a central colour cue given at the start of each trial (Figure 6.3). Participants completed a total of 96 prosaccade, 96 antisaccade, and 28 null trials (no target – remain looking at white fixation cross) randomised across 4 experimental blocks. The task stimuli were presented on a projection screen at the rear of the scanner by an LCD projector (maximum flux = 1500 lumens; resolution = 1024 × 768; 60 Hz) viewed at a distance of 155cm.

Horizontal displacement of each participant's right eye was recorded using a MR-compatible video-based SR Research Eyelink 1000 system, with a spatial resolution of 0.01 degrees and a sampling rate of 500 Hz. Customized software written in Matlab was used to examine the eye trace, marking the time of target onset and offset, as well as time and direction of saccade onset. A criterion of $>30^0$/s was used to define saccade onset. Trials featuring blinks (at trial onset), or an unstable baseline (a failure to maintain fixation with 2.5° of central fixation) were removed from further analysis. Each trial was then examined for errors in saccade direction, defined as either looking toward the target circle on antisaccade trials, or looking away from the target circle on prosaccade trials. Anticipatory errors/eye movements, defined as saccades occurring within +/- 100ms of the target circle appearing were also identified and counted as anticipatory errors.

All trials were defined by their trial type (either prosaccade or antisaccade), and secondarily as either a switch (where the current trial was preceded by a dissimilar trial occurred; prosaccade preceded by a antisaccade or an antisaccade preceded by an prosaccade) or non-switch (where a repetition of trial type occurred; prosaccade preceded by a prosaccade or

an antisaccade preceded by an antisaccade) trial. Antisaccade trials were then removed from further analysis.

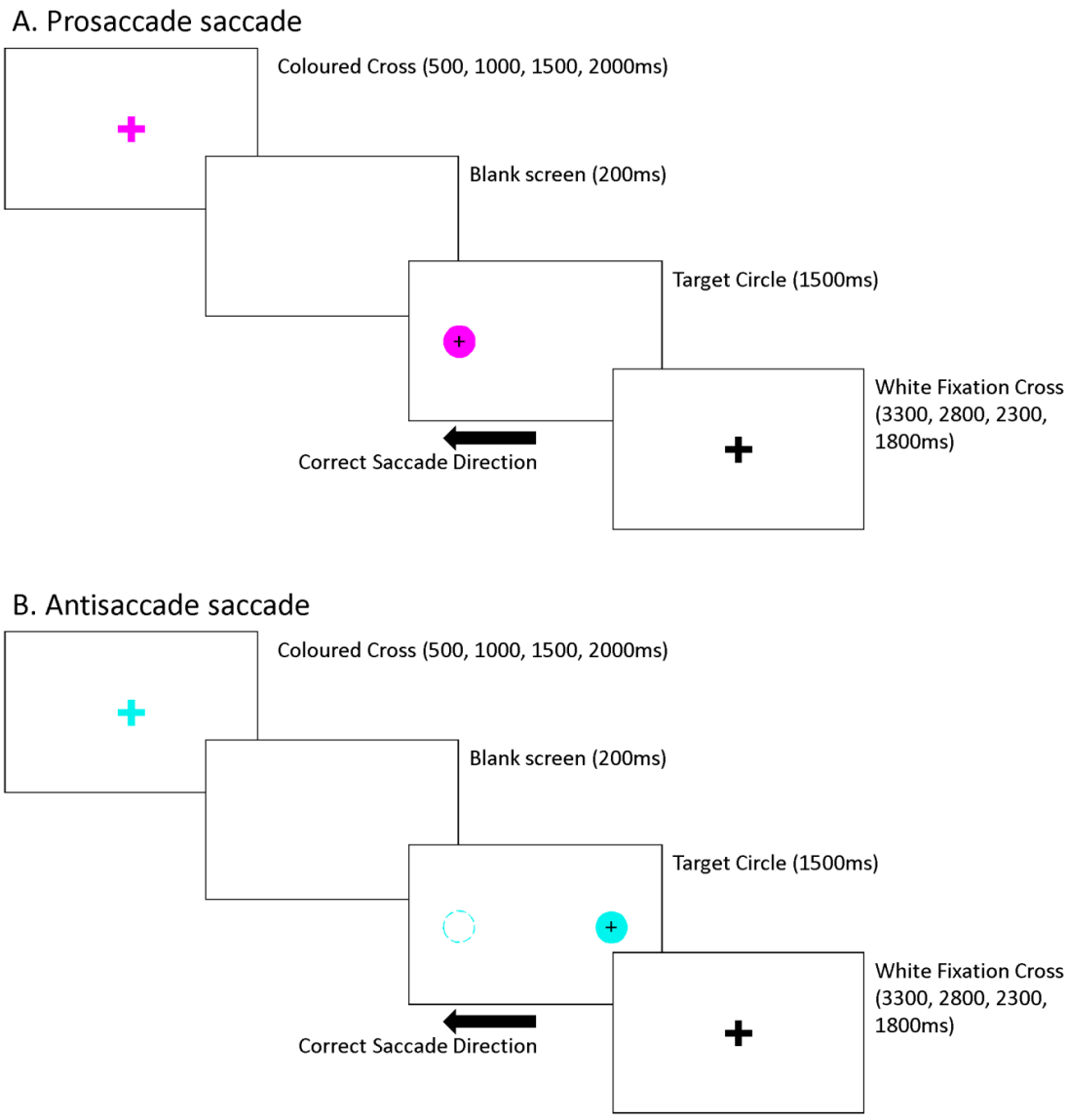

Figure 6.3: A schematic diagram of the ocular motor switch task.

A) A prosaccade trial and **B)** An antisaccade trial – the dotted circle indicates the correct response location for an antisaccade trial and does not appear on the screen. Note that each trial lasted a total of 5500ms. The colour indicating the trial type (prosaccade or antisaccade) was counterbalanced between participants.

This yielded a total of seven prosaccade variables: correct latency (ms) (calculated as the difference between target onset and correct saccade onset), error latency (ms) (calculated as the difference between target onset and erroneous saccade onset), time to correct (ms) (calculated as the difference in error saccade completion and corrective saccade onset) (ms), switch/non-switch directional error percentage and switch/non-switch anticipatory error percentage.

Supplementary Note 6.S2: Composite cognitive scores

Principle component analysis was used to derive three composite cognitive scores. Here we provide details regarding the variables included in each composite cognitive score and the inter-relationships between the three cognitive measures.

Prosaccade response time explained 69.79% of variance in the sample (81.79% of variance in the PM group and 62.68% in the control group), and included prosaccade correct latency, prosaccade error latency and prosaccade time to correct.

Prosaccade error score explained 55.77% of variance in the sample (56.72% of variance in the PM group and 38.16% in the control group), and included prosaccade switch/non-switch directional error percentage and prosaccade switch/non-switch anticipatory error percentage.

Finally, *executive function score* explained 50.63% of the variance in the sample (49.28% of variance in the PM group and 45.73% in the control group), and included prosaccade switch/non-switch directional error percentage and Haylings B error score. Inclusion of Haylings A error score in this analysis, explained less than 50% of the variance in the sample, and yielded a non-significant Barlett's Test of Sphericity ($p>0.05$), suggesting that its inclusion of Haylings A with the other three variables was inappropriate and unsuitable for principle component analysis.

The three composite scores showed some degree of correlation (*prosaccade response time* vs *executive function score* r=-0.557 p<0.01; and *prosaccade error score* vs *executive function score* r=0.683 p<0.01; *prosaccade response time* vs *prosaccade error score* r=-0.307 p<0.07).

Supplementary Table 6.S1: Statistics on participant demographic and molecular data

	Control (n=17)		PM (n=19)		p-value
	Mean (SD)	Range	Mean (SD)	Range	
Age (years)	39.76 (9.72)	24-54	39.37 (9.46)	22-53	0.902
Education (years)	15.41 (3.02)	11-26	14.84 (3.10)	9-19	0.581
Full Scale IQ	113.9 (9.22)	97-130	110.95 (9.81)	88-127	0.354
CGG repeat	30.12 (3.14)	20-36	84.05 (17.0)	59-123	**0.000**
FMR1 mRNA	1.37 (0.37)	0.90-2.24	1.80 (0.62)	1.03-3.25	**0.019**
Activation ratio	0.57 (0.05)	0.49-0.65	0.58 (0.05)	0.50–0.66	0.582
CpG 1	0.34 (0.50)	0.29-0.47	0.32 (0.04)	0.25-0.39	0.374
CpG 2	0.20 (0.03)	0.16-0.26	0.20 (0.04)	0.14-0.28	0.607
CpG 6/7	0.42 (0.04)	0.36-0.48	0.41 (0.03)	0.34-47.0	0.392
CpG 8/9	0.30 (0.04)	0.25-0.38	0.31 (0.04)	0.22-0.38	0.399
CpG 10-12	0.28 (0.04)	0.18-0.33	0.29 (0.04)	0.18-0.34	0.136

Note: Figures in bold indicate that $p<0.05$

Supplementary Table 6.S2: Relationships between *FMR1* Methylation (predictor) and *FMR1* mRNA (outcome) for female premutation carriers and controls.

	PM *FMR1* mRNA			Control *FMR1* mRNA		
	β	s.e	p-value	β	s.e	p-value
CpG island (AR)	-0.082	0.278	0.771	-0.207	0.253	0.425
CpG 1	-0.316	0.262	0.245	0.008	0.258	0.976
CpG 2	-0.014	0.243	0.955	0.002	0.252	0.992
CpG 6/7	-0.296	0.252	0.257	0.311	0.245	0.225
CpG 8/9	-0.213	0.238	0.386	0.071	0.258	0.786
CpG 10-12	-0.422	0.230	0.086	0.208	0.287	0.482

Note: β =standardized regression coefficients; s.e = standard error.

Supplementary Table 6.S3: Comparison of white matter hypointensities (volume) and cortical thickness between healthy controls and premutation carriers.

	Control (n=17)	PM (n=19)	*p*-value
	Mean (SD)	Mean (SD)	
White matter hypointensities	1306.06 (381.03)	1492.37 (572.86)	0.265
Left middle frontal gyrus	2.71 (0.11)	2.80 (0.16)	0.058
Right middle frontal gyrus	2.74 (0.13)	2.78 (0.17)	0.426
Left superior frontal gyrus	2.82 (0.15)	2.85 (0.16)	0.613
Right superior frontal gyrus	2.78 (0.17)	2.75 (0.15)	0.591
Left inferior parietal gyrus	2.65 (0.13)	2.66 (0.15)	0.757
Right inferior parietal gyrus	2.71 (0.12)	2.72 (0.13)	0.718

CHAPTER 7: NEURAL CORRELATES OF EXECUTIVE DYSFUNCTION – WHITE MATTER

Chapters 5 and 6 provide evidence of cortical grey matter disturbances relating to executive dysfunction in PM females without FXTAS. However, FXTAS is predominantly viewed as a white-matter disease, and correlations between white matter microstructure and executive dysfunction have been revealed for PM-carriers with and without FXTAS (Battistella *et al.*, 2013; Wang *et al.*, 2013b; Hippolyte *et al.*, 2014; Leow *et al.*, 2014; Filley *et al.*, 2015). It is critically important to assess white matter integrity, and its associations with genetic markers and executive dysfunction, to gain a full understanding of the biological correlates of executive dysfunction in young PM females without FXTAS. Chapter 7 will therefore adopt a similar integrative approach to Chapter 6, and will assess a range of genetic markers, white matter microstructure in the corpus callosum and cerebellar peduncles, and executive function performance on a range of tasks including the saccade tasks described in Chapter 5.

This Chapter is written as a manuscript for publication: *White matter microstructure relates to cognition and FMR1 mRNA in fragile X premutation females.* It is currently under review. To maintain consistency throughout this thesis, changes have been made to formatting.

Declaration by candidate

In the case of Chapter 7, the nature and extent of my contribution to the work was the following:

Nature of contribution	Extent of contribution (%)
Conceptualisation, project design and programming of paradigms, data collection, data analysis and interpretation, and manuscript preparation	80%

The following co-authors contributed to the work. If co-authors are students at Monash University, the extent of their contribution in percentage terms must be stated:

Name	Nature of contribution	Extent of contribution (%) for student co-authors only
Kim Cornish	Conceptualisation, project design and manuscript preparation	
David E. Godler	Genetic analysis and manuscript preparation	
Minh Bui	Statistical analysis and manuscript preparation	
Scott Kolbe	Data analysis and manuscript preparation	
Minh Bui	Statistical analysis support and manuscript preparation	
Joanne Fielding	Conceptualisation, project design, data interpretation, and manuscript preparation	

The undersigned hereby certify that the above declaration correctly reflects the nature and extent of the candidate's and co-authors' contributions to this work*.

Candidate's Signature		Date
Main Supervisor's Signature		Date

WHITE MATTER MICROSTRUCTURE RELATES TO COGNITION AND *FMR1* MRNA IN FRAGILE X PREMUTATION FEMALES

Annie L. Shelton., Kim M. Cornish., David Godler., Minh Bui., Scott Kolbe., & Joanne Fielding

7.1 ABSTRACT

Objective: To examine the inter-relationships between i) *FMR1* mRNA and the *FMR1* exon 1/intron 1 boundary methylation in blood, ii) white matter microstructure and iii) executive function, in *FMR1* premutation (PM: 55-199 CGG repeats) and control (CGG<44) females.

Methods: Twenty PM females without fragile X-associated tremor/ataxia syndrome (FXTAS) and 20 control females aged between 22 and 54 years completed this study. *FMR1* mRNA and methylation levels for 9 CpG sites within the *FMR1* exon 1/intron 1 boundary from peripheral blood samples were analysed. Diffusion-weighted imaging was used to extract fractional anisotropy (FA) and mean diffusivity (MD) values from anatomical regions within the corpus callosum and cerebellar peduncles. Executive function was assessed with a range of tasks.

Results: No differences were revealed in white matter microstructure between PM and control females. However, we reveal that for PM females (but not controls): (1) higher *FMR1* mRNA correlated with lower MD values within the middle cerebellar peduncle and PASAT scores; (2) higher methylation of the *FMR1* exon 1/intron 1 boundary correlated with lower MD within the inferior and middle cerebellar peduncles and longer prosaccade latencies; and (3) higher FA values within the corpus callosum and cerebellar peduncle regions corresponded with superior executive function.

Conclusion: We provide evidence linking white matter microstructure to executive dysfunction and elevated *FMR1* mRNA and *FMR1* exon 1/intron 1 boundary methylation in PM females without FXTAS. This suggests that the FXTAS phenotype may not be distinct, but form part of a spectrum of PM involvement.

7.2 INTRODUCTION

Premutation (PM) expansions (55-199 CGG repeats) in the 5' untranslated region of the *fragile X mental retardation 1* (*FMR1*) gene confer a risk of developing fragile X-associated tremor/ataxia syndrome (FXTAS). Featuring both motor and cognitive impairment (executive dysfunction and dementia), FXTAS is thought to arise as a consequence of a RNA toxic gain-of-function, leading to protein aggregation (Hagerman and Hagerman, 2016). The major radiological features of FXTAS are white matter lesions in the middle cerebellar peduncles (MCP), corpus callosum (CC) splenium and throughout the cerebrum, along with generalised brain atrophy (Hall *et al.*, 2016b).

Although not consistently reported, reductions to both executive function and white matter integrity, have been reported in PM carriers *without* FXTAS (Grigsby *et al.*, 2014; Brown and Stanfield, 2015). Studies have also reported correlations between executive dysfunction and white matter microstructure for PM carriers (Battistella *et al.*, 2013; Wang *et al.*, 2013b; Hippolyte *et al.*, 2014; Leow *et al.*, 2014; Filley *et al.*, 2015). Specifically, in a small cohort of PM males with (*n*=5) and without FXTAS (*n*=8), a relationship between executive dysfunction and microstructural white matter changes in the CC genu, CC splenium and MCP was revealed (Filley *et al.*, 2015). These regions are known to be involved in FXTAS pathology.

Our group has demonstrated associations between executive function and PM specific methylation changes at the *FMR1* exon 1/intron 1 boundary (Cornish *et al.*, 2015; Shelton *et al.*, 2016b). Here we aimed to characterise the associations between executive dysfunction, measures of white matter microstructure in tracts susceptible to FXTAS pathology, *FMR1* mRNA levels, and methylation within the *FMR1* exon 1/intron 1 boundary in PM females without FXTAS compared to age matched controls. This has the potential to provide insights into the relationships between molecular and white matter microstructural influences on executive dysfunction in PM females without FXTAS.

7.3 METHODS

Participants

Based on previous studies (Shelton *et al.*, 2016a; Shelton *et al.*, 2016b; Shelton *et al.*, 2016c), CGG repeat length was determined for 40 females aged between 22 and 54 years [20 with PM alleles (Mean=85, Range: 59-123); and 20 controls with CGG repeat length <44 (Mean=30.11, Range:20-36)]. Participants were recruited from the Fragile X Alliance and the Fragile X Association Australia support groups, population-based fragile X carrier screening studies (Metcalfe *et al.*, 2008), as well as local networks and via online advertisements.

All participants were English speaking with normal (or corrected) vision and hearing, no history of any serious neurological damage/disease, and were screened for FXTAS (Leehey, 2009). Exclusion criteria extended to those who thought they may be pregnant, as well as those with any MRI contraindications.

Standard protocol approvals, registrations, and patient consents'

Ethics approval for this study was granted by Monash University and Southern Health Human Research Committees (Project Number 10147B); all participants gave their informed consent prior to inclusion in the study in accordance with the Declaration of Helsinki.

Molecular analysis

CGG assessment was performed on DNA extracted from whole peripheral blood and analysed using the AmplideX *FMR1* PCR Kit according to manufacturer's instructions (Asuragen, Austin, TX). The relative standard curve method was utilized for *FMR1* 5' and 3' mRNA quantification normalized to mRNA levels of 2 internal control genes (*SDHA* and *EIF4A2*), in peripheral blood mononuclear cells as previously described (Kraan *et al.*, 2016). Blood DNA

from each participant was bisulfite converted in duplicate, with each conversion analysed twice using the EpiTYPER system. A summary measure for each CpG unit was determined as the mean of the 4 methylation output ratio measurements per sample (see gene map (Cornish *et al.*, 2015)). Methylation sensitive Southern blot targeting the *NruI* restriction site within the *FMR1* CpG island was used to determine activation ratio (AR), based on the band density of all unmethylated alleles as the proportion of the total density of all alleles: AR=[normal size active (NA)/(NA+normal size inactive (NI))] + [PM active (PM.A)/(PM.A+PM inactive (PM.I))]) as previously described (Kaufmann *et al.*, 1999). Therefore a total of eight molecular measures were included: CGG, AR, *FMR1* mRNA, *FMR1* exon 1 (CpG 1 and CpG 2) and intron 1 (CpG 6/7, CpG 8/9 and CpG 10-12) methylation sites, which were not highly correlated (except for intron 1 measures) (Supplementary Table 7.S1-3).

Executive function tasks

Executive function was assessed using the Behavioural Dyscontrol Scale (BDS) (Grigsby and Kaye, 1996), the Paced Auditory Serial Addition Test (PASAT) (Gronwall, 1977), the Symbol Digit Modality Test (SDMT) (Smith, 1973), the Controlled Oral Word Association test (COWAT) (Benton *et al.*, 1983), and an ocular motor prosaccade/antisaccade interleaved task (Shelton *et al.*, 2016a) (Supplementary Note 7.S1 and Supplementary Figure 7.S1 for details). Each task yielded a single score, except for the ocular motor task, where prosaccade and antisaccade latencies were calculated. Therefore a total of six executive function scores were calculated.

MRI acquisition and analysis

A 3 Tesla Siemens Magnetom Skyra scanner and 20-channel head coil were used to acquire a high-resolution diffusion weighted EPI sequence (TR=8800ms, TE=110ms, *b* 3000 s/mm^2, 64 directions, 60 axial 2.5 mm thick axial slices, and a FOV of 240*240mm, matrix 96*96).

Whole brain diffusion weighted images from each participant were preprocessed using FSL Eddy to correct for magnetic susceptibility and eddy current distortions (Andersson and Sotiropoulos, 2016), and reconstructed to create fractional anisotropy (FA) and mean diffusivity (MD) maps from normalised DTI data (Tournier *et al.*, 2012). Tract-based spatial statistics (TBSS), in FSL was then used to nonlinearly register FA and MD maps to standard space and skeletonise the white matter for voxel-wise analysis (Smith *et al.*, 2006). The mean FA and MD values were then extracted from six regions of interest (ROIs) (CC genu, CC splenium, CC body, MCP, inferior cerebellar peduncle (ICP) and superior cerebellar peduncle (SCP)) from the JHU ICBM-DTI 81 white matter labels atlas (Mori *et al.*, 2005) – yielding twelve diffusion measures which were somewhat inter-correlated (Supplementary Table 7.S4).

Statistical analysis

Between group differences

Stata Statistical Software, Release 14 2015, was used for all statistical analyses. Molecular measures, executive function scores, and FA and MD for each ROI were assessed for normality for each group (using skewness and kurtosis), and equal variances (Levene's test). Comparison of demographic information, molecular measures, executive functions scores and regional FA and MD between groups were conducted using independent samples t-tests (for equal or unequal variances) or Mann-Whitney U (when violations of the assumption of normality occurred).

Whole brain voxel-wise between group comparisons of FA and MD employed a general linear model with family-wise error corrected significance levels using a permutation based statistical testing method with 500 samples and threshold-free cluster enhancement (RANDOMISE, FSL) (Winkler *et al.*, 2014).

Correlation and regression analyses

Nonparametric Spearman's rank correlation was used to compute correlation among molecular measures and diffusivity measures. The relationships between each of the eight molecular measures (predictor) and each executive function score, and FA and MD for each ROI (outcome) were initially explored using scatter plot and nonparametric smoothing, using locally weighted regression, to determine whether the relationship was linear or non-linear and identify potential outliers. The outliers were then formally checked if they were influential data points that could distort the estimated regression coefficients (Chatterjee and Hadi, 1986). The variables were then standardised, and if outliers were not present, the least square estimation method, was used to conduct regression analysis, using the Hubert-White-Sandwich method where appropriate to account for heteroscedasticity. If outliers were present, robust regression using default settings was used to downweight their effect. Regression analysis was first conducted for all data combined (PM and control), and then examined for possible group differences by adding an interaction term between group and predictor. If the interaction term was significant, at $p \leq 0.15$ due to the small sample size, separate analyses for PM and controls were conducted. In these analyses, a $p<0.05$ was considered significant and adjusted for multiple comparisons, using the false discovery rate (FDR) method of Benjamini and Hochberg. The same procedure was carried out for the relationship between FA and MD for each ROI (predictor) and executive function scores (outcome).

7.4 RESULTS

The control and PM groups were well matched for age, education and full scale IQ (assessed via the Wechsler Abbreviated Scale of Intelligence) (Wechsler, 1999) (Table 7.1).

FMR1 mRNA levels were higher for PM females than controls, and correlated with CGG repeat length prior to FDR adjustment. Other *FMR1* molecular measures, TBSS whole brain voxel-wise analysis, as well as ROI FA and MD values were not significantly different between PM and control groups (Supplementary Table 7.S5).

PM females had lower BDS scores (indicating impairment) compared to controls, while PASAT and SDMT scores showed a similar trend prior to FDR adjustment (Table 7.1). Age was not significantly correlated with executive function measures (Supplementary Table 7.S6).

Table 7.1. Participant demographic and executive function data intergroup comparisons between PM and control females.

	PM (n=20) Mean ± SD	Controls (n=20) Mean ± SD	p-value
Demographics			
Age (years)	40.1 ± 9.77	39.1 ± 8.61	0.720
Education (years)	15.0 ± 3.05	16.3 ± 3.71	0.217
Full Scale IQ	111 ± 9.56	114 ± 9.04	0.235
Executive Function			
BDS	23.5 ± 2.40	25.7 ± 1.09	**0.001**
COWAT	37.9 ± 10.4	42.8 ± 7.01	0.092
PASAT	74.9 ± 21.0	87.0 ± 11.2	0.029
SDMT	57.1 ± 9.85	65.5 ± 11.6	0.019
Prosaccade Latency	232 ± 36.3	245 ± 53.0	0.397
Antisaccade Latency[+]	311 ± 64.4	329 ± 64.8	0.770

Note: [+]Median and interquartile were used instead of mean and standard deviation (SD); Figures in bold indicate $p<0.05$ after adjusting for multiple comparisons using FDR.

No significant relationships were revealed between *FMR1* molecular measures and diffusion or executive function measures for all participants combined (Supplementary Table 7.S7). However, significant interactions revealed, higher *FMR1* mRNA levels correlated with lower MD MCP, and higher CpG 1 methylation within *FMR1* exon 1 correlated with lower MD MCP and ICP, in the PM but not the control group (Table 7.2 and Figure 7.1 B, D-E). Surprisingly, CpG 1 methylation and *FMR1* mRNA levels were not significantly correlated in this study (Supplementary Table 7.S1). In contrast, higher *FMR1* intron 1 methylation for CpG 6/7 and to a lesser extent AR, significantly correlated with longer prosaccade latencies (indicating dysfunction), as well as higher *FMR1* mRNA and lower PASAT scores (indicating dysfunction) for the PM group (Table 7.2 and Figure 7.1 A, C, & F). While this relationship was not significant for *FMR1* intron 1 methylation in the control group; higher AR significantly correlated with shorter prosaccade latencies in the control group (Table 7.2 and Figure 7.1A). This suggests that *FMR1* intron 1 methylation for CpG 6/7 is the best predictor of all molecular measures included in this study for PM specific ocular motor measures of executive function in females; while *FMR1* exon 1 methylation for CpG 1 is the best PM specific predictor of diffusivity within the cerebellar peduncles.

A number of significant relationships were also found between diffusivity measures and executive function tasks for all participants combined (Supplementary Table 7.S10). When these relationships were split by group, relationships were revealed for the PM group, but not for the control group (Table 7.3 upper panel, Figure 7.2 A-C). Significant interactions for group were also found, whereby positive associations between some FA measures and executive function scores were present for the PM but not the control group (Table 7.3 lower panel, Figure 7.2 D-F). Overall, a number of PM group specific relationships were revealed between white matter microstructure (primarily FA in the MCP) and executive function measures.

Table 7.2: Relationship between each *FMR1* molecular measure (predictor) and each diffusivity and executive function measure (outcome), separated by group (PM and control) when a significant interaction was present for all participants combined.

		PM			Controls		
Predictor	Outcome	*β*	*s.e*	*p*	*β*	*s.e*	*p*
FMR1 molecular, diffusivity and executive measures							
AR	PL	0.41	0.15	**0.016**	-0.38+	0.14	**0.020**
FMR1 mRNA	MD MCP	-0.44+	0.18	**0.029**	0.70+	0.25	**0.013**
	PASAT	-0.61+	0.22	**0.013**	0.01+	0.20	0.972
CpG 1	MD ICP	-0.70	0.19	**0.002**	0.05	0.25	0.837
	MD MCP	-0.59	0.21	**0.013**	0.25	0.25	0.344
CpG 2	PASAT	0.37	0.19	0.066	-0.38	0.14	**0.018**
CpG 6/7	FA CC Body	0.27+	0.27	0.329	-0.33+	0.14	**0.029**
	PL	0.75+	0.20	**0.002**	0.09	0.29	0.775

Note: AR = Activation Ratio; PL = Prosaccade Latency; AL = Antisaccade Latency; Sp = Splenium; FA = Fractional Anisotropy; MD = Mean Diffusivity; β = standardised regression coefficient; +Robust regression; Figures in bold indicate p<0.05 after adjusting for multiple comparisons using FDR.

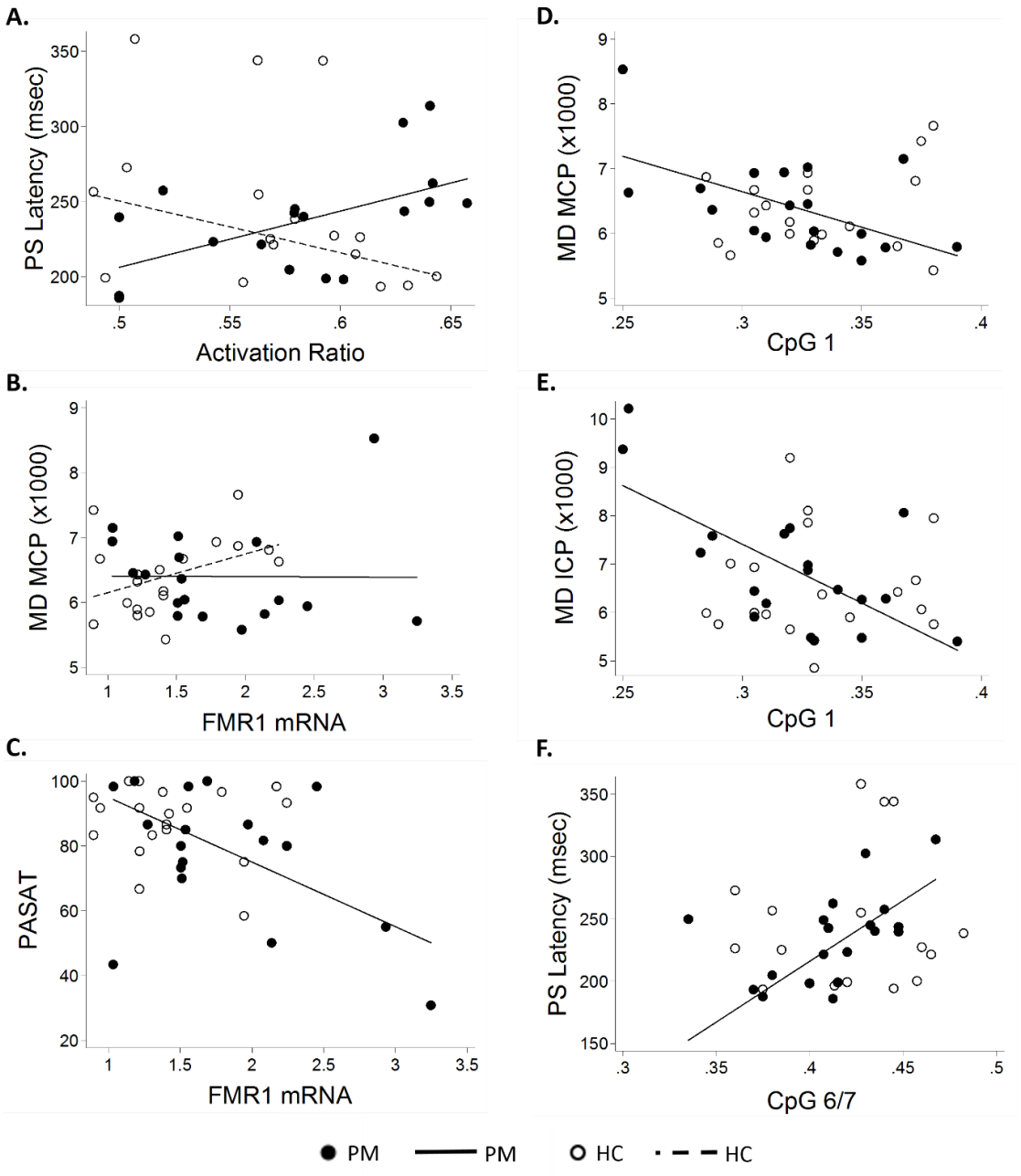

Figure 7.1: Significant relationships between *FMR1* molecular and mean diffusivity (B, D-F) and measures of executive function for PM and control groups.

Significant interactions between PM and controls show strong relationships for PM but only two significant correlations for controls (A and B). Higher mean diffusivity (MD) indicates greater movement of water molecules within the axons, while longer prosaccade (PS) latency times and lower PASAT scores indicate executive function weakness.

Table 7.3: Relationships between each diffusivity and each executive function measure for PM and control groups when the interaction term was not significant (upper panel) and significant (lower panel).

		PM			Controls		
Predictor	Outcome	*β*	*s.e*	*p*	*β*	*s.e*	*p*
No Significant Interaction							
FA CC Body	SDMT	0.75	0.27	0.013	0.15	0.18	0.423
FA CC Genu	PASAT	0.55	0.23	0.030	0.46	0.29	0.136
	SDMT	0.88+	0.29	**0.007**	0.08	0.11	0.483
FA CC Sp	PASAT	0.55+	0.15	**0.002**	0.41+	0.29	0.172
	SDMT	0.92+	0.27	**0.003**	0.17	0.10	0.108
FA MCP	BDS	0.43	0.16	0.018	0.22	0.48	0.661
	SDMT	0.71	0.25	**0.010**	0.20	0.16	0.231
	COWAT	0.44	0.20	0.038	0.59	0.25	0.027
MD CC Sp	SDMT	-0.55	0.23	0.029	-0.10	0.16	0.524
Significant Interaction							
FA CC Body	PASAT	0.63	0.19	**0.004**	0.32	0.26	0.243
FA CC Sp	AL	0.21+	0.31	0.516	-0.32+	0.16	0.055
FA ICP	COWAT	0.41+	0.20	0.056	-0.25	0.34	0.465
FA MCP	PASAT	0.56	0.14	**0.001**	0.41+	0.31	0.207
	AL	0.08	0.24	0.738	-0.68+	0.28	0.028
FA SCP	BDS	0.51+	0.14	**0.001**	-0.08+	0.44	0.858
	PASAT	0.49+	0.16	**0.008**	0.56+	0.32	0.093
	COWAT	0.42+	0.17	0.026	-0.19+	0.28	0.504
MD CC body	PL	-0.15+	0.33	0.657	0.36+	0.11	**0.004**
	AL	-0.24	0.21	0.274	0.64+	0.19	**0.004**
MD CC Genu	SDMT	-0.58	0.21	0.014	0.16	0.15	0.305
MD MCP	BDS	0.34+	0.17	0.068	0.30	0.15	0.059
MD SCP	BDS	0.33+	0.22	0.141	-0.20+	0.33	0.563

Note: PL = Prosaccade Latency; AL = Antisaccade Latency; Sp = Splenium; FA = Fractional Anisotropy; MD = Mean Diffusivity; *β* = standardised regression coefficient; +Robust regression; Figures in bold indicate p<0.05 after adjusting for multiple comparisons using FDR.

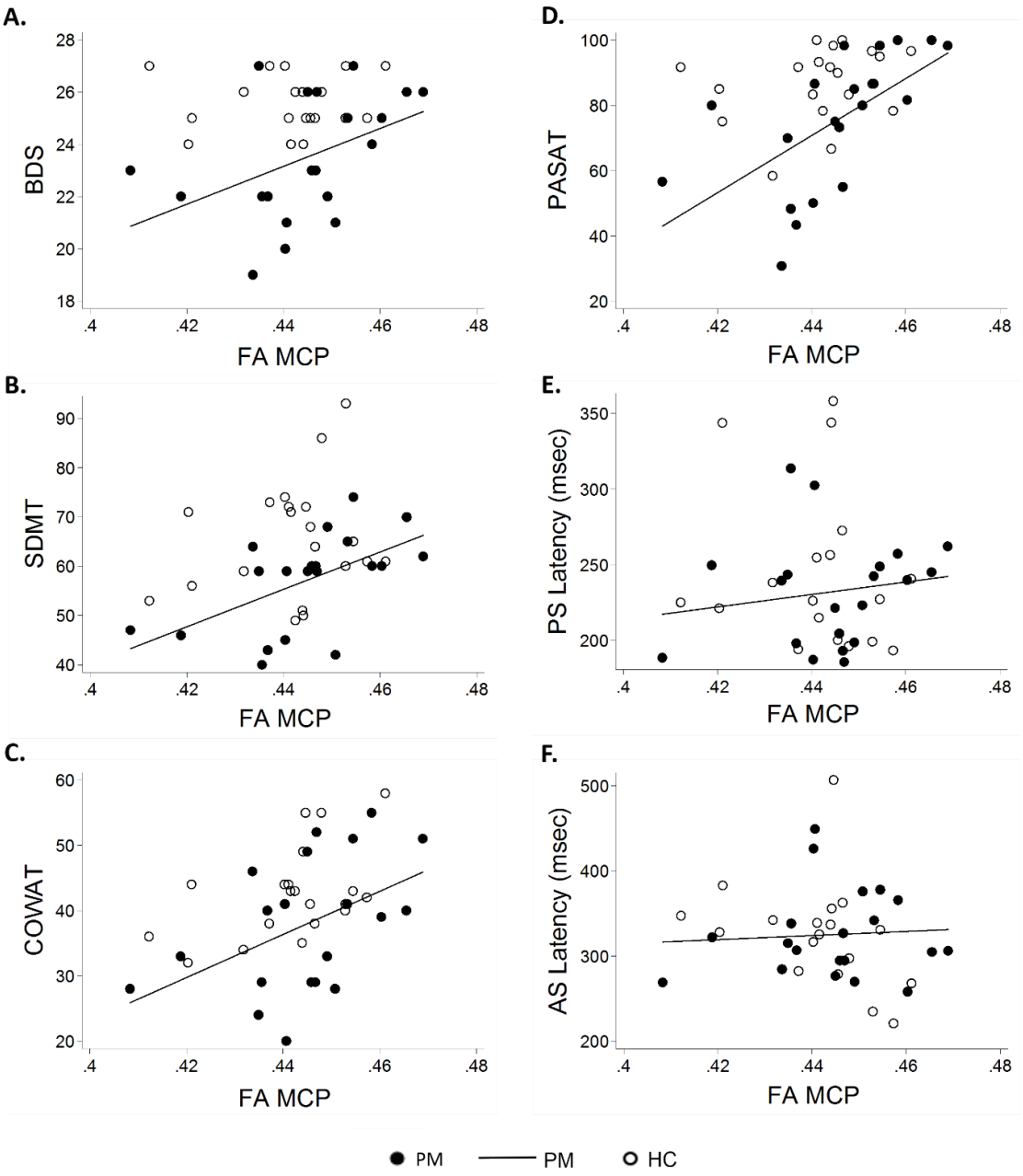

Figure 7.2: Relationships between FA MCP and executive function measures for PM and control groups.

Significant relationships, found only for the PM group, are indicated by a line of best fit. Plots A-C depict the relationships between fractional ansiotopy (FA) in the middle cerebellar peduncles (MCP) and executive function relationships when a significant relationship was found for all participants combined, but without a significant interaction effect for group. The panel on the right depicts relationships between FA MCP and executive function when a significant interaction effect for group was found. Impaired executive function is indicated by lower scores on the BDS, SDMT, COWAT and PASAT and longer antisaccade (AS) and prosaccade (PS) latencies.

7.5 DISCUSSION

This study provides converging evidence that PM specific relationships exist when assessing the relationships between *FMR1* exon 1/intron 1 boundary methylation and *FMR1* mRNA levels, white matter microstructure, and executive function in PM females without FXTAS. We demonstrated PM specific relationships between: (a) increased *FMR1* mRNA levels and *FMR1* exon 1 (CpG 1) methylation with decreased cerebellar peduncle microstructure (MD ICP and MD MCP); and (b) increased *FMR1* intron 1 (CpG 6/7) methylation and AR with prosaccade latency. These relationships are consistent with our previous findings for the significant correlations between *FMR1* exon 1/ intron 1 boundary methylation and executive dysfunction (Cornish *et al.*, 2015; Shelton *et al.*, 2016b).

This work also confirms and extends a previous finding in PM males with and without FXTAS (Filley *et al.*, 2015), given the significant associations between white matter microstructure (FA) in both CC and cerebellar peduncle tracts and a range of executive function measures revealed herein. Focusing specifically on PM females without FXTAS in this study, allows for characterisation of early changes in white matter microstructure that might underlie executive dysfunction prior to FXTAS onset.

FMR1 molecular measures, white matter microstructure and executive function

One of the mechanisms postulated to contribute to FXTAS has been RNA toxic gain-of-function associated with over-expression of *FMR1* mRNA in PM individuals (Botta-Orfila *et al.*, 2016; Hagerman and Hagerman, 2016). Specifically, in PM males with FXTAS, higher levels of *FMR1* mRNA have been shown to correlate with altered white matter microstructure (FA and MD) within the CC, MCP and SCP (Hashimoto *et al.*, 2011c; Wang *et al.*, 2013b). Similarly, we found that higher *FMR1* mRNA levels were associated with reduced MD MCP for PM females. Although reductions in MD are difficult to interpret pathologically, they could represent a reduction in fast diffusing extra-cellular fluid due to axonal swelling

observed post-mortem in two FXTAS males (Greco *et al.*, 2002). Further, a previous study found differences in magnetization transfer ratio and higher radial diffusivity in the MCP between controls and PM males without FXTAS, suggesting that myelination might also be affected (Battistella *et al.*, 2013). Given that *FMR1* mRNA levels, and radiological lesions in the MCP, are often implicated in FXTAS pathology, our findings suggest that the relationships between *FMR1* mRNA and MCP microstructure could i) be common amongst PM with and without FXTAS, and/or ii) provide early evidence of presymptomic FXTAS related changes amongst young PM females at risk.

For PM females, the only *FMR1* exon 1/intron 1 methylation site found to correlate with diffusivity measures (lower MD ICP and MCP) was CpG 1. This compliments the recent PM female finding where increased CpG 1 methylation associated with fewer cortical white matter hypointensities (T1-weighted scan) (Shelton *et al.*, 2016b). This CpG 1 site is located within *FMR1* exon 1, proximal to the ATG start site for fragile X mental retardation protein (FMRP) translation (Godler et al., 2010b), which is critical for protein synthesis-dependent synaptic plasticity.(Callan and Zarnescu, 2011). Increased methylation of this site may be related to increased transcription of *FMR1* mRNA and decreased FMRP levels previously reported in PM, which is consistent with associations previously found between increased exon methylation and gene expression in other settings and for other genes (Singer *et al.*, 2015).

In this study *FMR1* methylation at the CpG island (AR) and intron 1 (CpG 6/7) were found to significantly correlate with prosaccade latency. This compliments our previous findings between *FMR1* intron 1 methylation (CpG 6/7) and prosaccade response time (a composite score including prosaccade latency) (Shelton *et al.*, 2016b). Further correlations between methylation of *FMR1* intron 1 site CpG 10-12 and both prosaccade latency and COWAT were also observed in this study for PM females, although did not survive FDR (Supplementary Table 7.S8 and Supplementary Figure 7.S2). This suggests that *FMR1* intron 1 methylation (at the exon 1/intron 1 boundary) in PM females relates to cortical grey matter thickness

(Shelton *et al.*, 2016b) and executive dysfunction (Cornish *et al.*, 2015; Shelton *et al.*, 2016b), which is different for controls. In contrast *FMR1* mRNA levels and *FMR1* exon 1 (CpG 1) methylation uniquely relates to cerebellar peduncle microstructure in PM females.

The distinction between the epigenotype-phenotype relationships described here and our previous reports (Godler *et al.*, 2012; Inaba *et al.*, 2014; Cornish *et al.*, 2015; Shelton *et al.*, 2016b), is likely due to the EpiTYPER assay used. Our assay is able to quantitatively examine the methylation of 9 CpG sites within the *FMR1* regulatory region for both PM and *FMR1* full expansions (>200 CGG repeats). A recent report found no statistically significant epigenotype-phenotype relationships for 39 PM females, where *FMR1* methylation was examined using another commercially available PCR based assay (Hadd *et al.*, 2016). This commercial assay examines methylation of other sites, however it is unable to differentiate between two CpG sites – with one site within the CpG island and another within exon 1. Our method allows for this differentiation, which we have shown to be associated with neural and cognitive measures for PM females (Cornish *et al.*, 2015; Shelton *et al.*, 2016b).

Specific relationships between white matter microstructure and executive dysfunction in PM females

Associations between white matter microstructure and cognitive deficits, specifically of executive dysfunction, have been found in studies of aging (Madden *et al.*, 2009b), as well as numerous clinical cohorts. Further, the three cerebellar peduncles are critical for cerebellar mediated executive processing, through its contralateral input via the cortico-ponto-cerebellar fibres (Ramnani, 2012). Indeed, associations have been revealed between executive dysfunction and cerebral white matter diffusivity in FXTAS males (Battistella *et al.*, 2013; Wang *et al.*, 2013b; Hippolyte *et al.*, 2014; Filley *et al.*, 2015), although associations between executive function and cerebellar peduncle diffusivity are rare. However, we found PM specific correlations between FA within the cerebellar peduncle tracts (MCP and SCP)

and BDS, PASAT, SDMT and COWAT (although this later association did not survive FDR). Therefore, we provide preliminary evidence for disruption of the relationship between white matter microstructure and executive dysfunction prior to FXTAS onset, which may affect those with PM expansions more generally.

T2 hyperintensity lesions or changes in CC microstructure are now recognised within the radiological phenotype of FXTAS (Hall *et al.*, 2016b). The tracts within the CC provide critical inter-hemispheric integration, allowing for quick and efficient processing speed by connecting cognitive processing areas (van der Knaap and van der Ham, 2011). We report relationships between increased FA within the CC genu and splenium and measures of executive function, particularly processing speed, for PM females without FXTAS, similar to those previously reported for PM males with and without FXTAS (Filley *et al.*, 2015). Although more research concerning the involvement of white matter changes within CC fibres is warranted, we provide evidence linking these changes with executive dysfunction in PM females without FXTAS.

However, unlike the previous report (Filley *et al.*, 2015), we did not find correlations between white matter microstructure and executive function in our control group. Key differences between the controls involved in the previous (Filley *et al.*, 2015) and current study are the number of participants (n=7 compared to n=20), age (mean age 67.3 years compared to 39.05 years) and gender (male v female). Thus, it is possible that the control group associations previously reported (Filley *et al.*, 2015) could be age-related, which is consistent with previous reports of age-related changes (Madden *et al.*, 2009b).

Although our results show significant relationships between *FMR1* mRNA levels and exon1/intron 1 boundary methylation, white matter microstructure and executive dysfunction in PM females without FXTAS, interpretation is limited by the cross-sectional nature of the study and a relatively small sample size. Future longitudinal analysis of the inter-relationships between biological markers and executive dysfunction, in a larger sample

of PM males and females, will be critical when determining whether relationships between white matter microstructure and executive dysfunction are precursors to FXTAS or simply common amongst PM individuals. Although FA and MD measures are sensitive to changes in white matter microstructure, they are not pathologically specific. Further, the strong molecular-clinical correlations presented in this study suggest a degree of consistency between blood and CNS for these molecular measures. However, *FMR1* mRNA levels and *FMR1* exon 1/intron 1 boundary methylation were determined in peripheral blood and may be different from the brain specific changes. This may explain why we did not observe significant correlation between CpG 1 methylation and *FMR1* mRNA levels in blood (Supplementary Table 7.S1), while both were significantly correlated with the same diffusivity measures.

This study integrates *FMR1* molecular, white matter microstructure and executive function measures in PM females without FXTAS. Strong and PM specific relationships between *FMR1* mRNA levels and *FMR1* exon 1/intron 1 methylation with MD ICP and MCP, along with relationships between FA CC and cerebellar peduncles and executive dysfunction suggest a spectrum of possible preclinical PM involvement, rather than distinct FXTAS and non-FXTAS PM phenotypes.

SUPPLEMENTARY MATERIAL

Supplementary Table 7.S1: Spearman rank's correlations among molecular measures for all data.

	CGG	AR	*FMR1* mRNA	CpG 1	CpG 2	CpG 6/7	CpG 8/9	CpG 10-12
CGG		-0.008	0.348	-0.014	0.123	-0.303	0.121	0.132
AR	0.963		-0.047	0.285	-0.203	-0.161	-0.230	-0.369
FMR1 mRNA	0.038	0.789		-0.054	0.035	-0.015	0.072	-0.018
CpG 1	0.936	0.092	0.757		-0.061	-0.013	-0.051	-0.067
CpG 2	0.474	0.243	0.844	0.726		0.353	0.222	0.372
CpG 6/7	0.068	0.348	0.930	0.938	0.035		**0.449**	**0.542**
CpG 8/9	0.476	0.178	0.682	0.765	0.193	0.005		**0.728**
CpG 10-12	0.435	0.027	0.920	0.692	0.026	<0.001	<0.001	

Note: Upper triangle represents estimated correlation coefficients, while their corresponding unadjusted p-values are in the lower triangle; Figures in bold indicate $p<0.05$ after adjusting for multiple comparisons using FDR.

Supplementary Table 7.S2: Spearman rank's correlations among molecular measures for the PM group

	CGG	AR	*FMR1* mRNA	CpG 1	CpG 2	CpG 6/7	CpG 8/9	CpG 10-12
CGG		0.299	0.190	0.364	0.178	-0.018	-0.078	-0.285
AR	0.228		-0.128	0.530	-0.188	-0.006	-0.275	-0.378
FMR1 mRNA	0.450	0.625		-0.207	-0.073	-0.031	-0.163	-0.248
CpG 1	0.126	0.024	0.409		0.071	0.055	-0.049	-0.118
CpG 2	0.466	0.454	0.773	0.772		0.363	0.073	0.335
CpG 6/7	0.940	0.981	0.903	0.822	0.127		0.511	0.595
CpG 8/9	0.750	0.270	0.517	0.841	0.765	0.025		0.721
CpG 10-12	0.238	0.122	0.322	0.631	0.161	0.007	<0.001	

Note: Upper triangle represents estimated correlation coefficients, while their corresponding unadjusted p-values are in the lower triangle.

Supplementary Table 7.S3: Spearman rank's correlations among molecular measures for the control group

	CGG	AR	*FMR1* mRNA	CpG 1	CpG 2	CpG 6/7	CpG 8/9	CpG 10-12
CGG		0.219	0.045	-0.079	-0.235	**-0.689**	-0.073	-0.081
AR	0.369		0.093	0.032	-0.135	-0.375	-0.062	-0.267
FMR1 mRNA	0.858	0.713		0.115	0.109	0.220	0.248	-0.025
CpG 1	0.756	0.900	0.660		-0.239	-0.015	0.006	0.026
CpG 2	0.364	0.606	0.687	0.355		0.504	0.524	0.438
CpG 6/7	0.002	0.125	0.396	0.953	0.039		0.452	0.585
CpG 8/9	0.773	0.807	0.338	0.981	0.031	0.060		**0.660**
CpG 10-12	0.750	0.285	0.925	0.917	0.079	0.011	0.003	

Note: Upper triangle represents estimated correlation coefficients, while their corresponding unadjusted p-values are in the lower triangle; Figures in bold indicate $p<0.05$ after adjusting for multiple comparisons using FDR.

Supplementary Note 7.S1: Ocular Motor Interleaved Task

Participant's performed an ocular motor interleaved task within the MRI environment. The task required participants to move their eye either towards (prosaccade) or away (antisaccade) from a target as quickly and as accurately as possible depending on a central colour cue given at the start of each trial (Supplementary Figure 7.S1). Participants completed a total of 96 prosaccade, 96 antisaccade, and 28 null trials (no target – remain looking at the white fixation cross) randomised across 4 experimental blocks. The task stimuli were presented on a projection screen at the rear of the scanner by an LCD projector (maximum flux = 1500 lumens; resolution = 1024 × 768; 60 Hz) viewed at a distance of 155cm.

Horizontal displacement of each participant's right eye was recorded using a MR-compatible video-based SR Research Eyelink 1000 system, with a spatial resolution of 0.01 degrees and a sampling rate of 500 Hz. Customized software written in Matlab was used to examine the eye trace, marking the time of target onset and offset, as well as time and direction of saccade onset. A criterion of $>30^0/s$ was used to define saccade onset. Trials featuring blinks (at trial onset), or an unstable baseline (a failure to maintain fixation with 2.5° of central fixation) were removed from further analysis. Each trial was then examined for errors in saccade direction, defined as either looking toward the target circle on antisaccade trials, or looking away from the target circle on prosaccade trials. Saccade latency (measured in ms) for each correct prosaccade and antisaccade trial was calculated as the difference between target onset and saccade onset.

Two controls participants were unable to complete this task due to system faults, and therefore were not included in the analyses related to saccade latency.

Supplementary Figure 7.S1

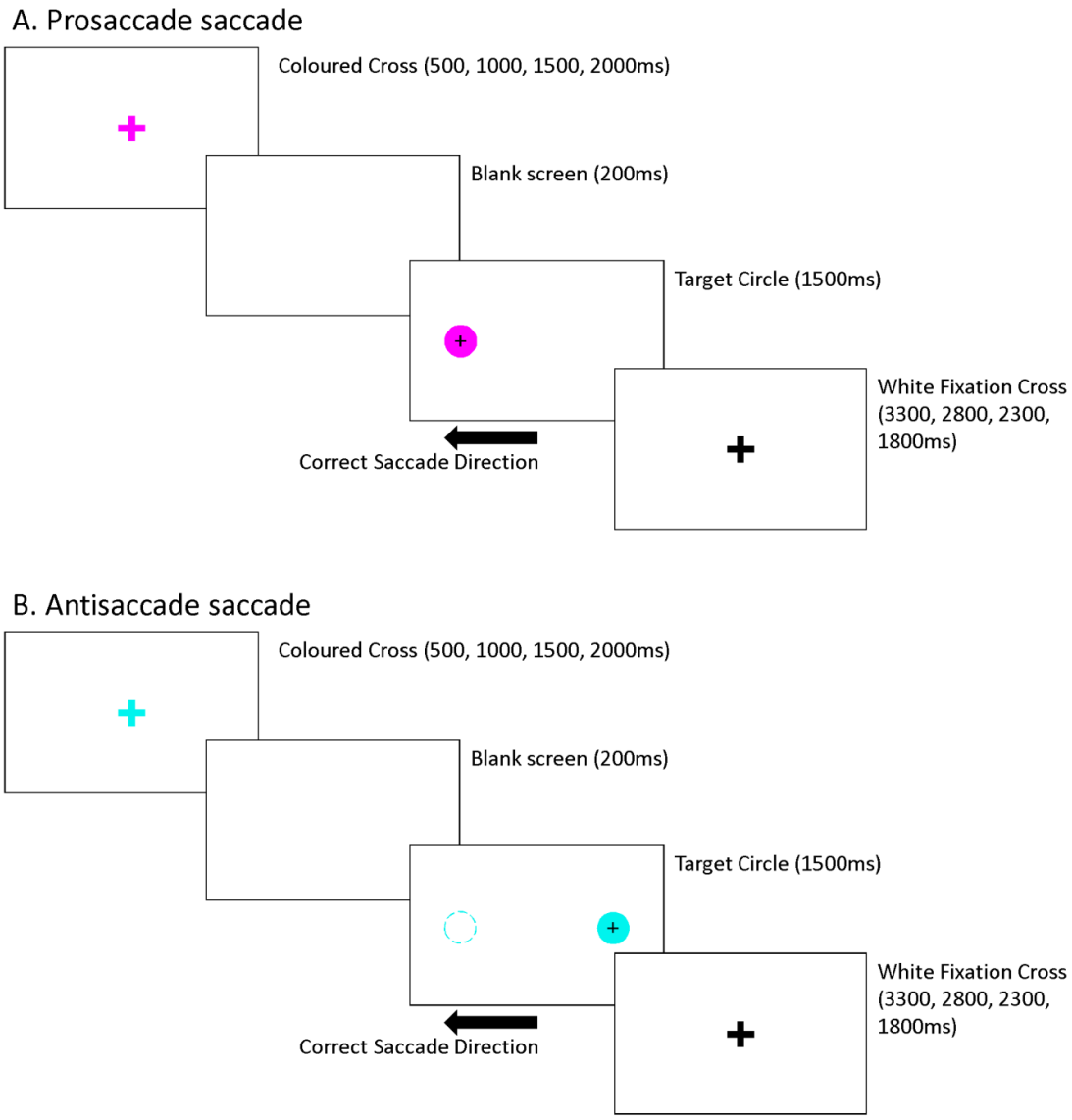

A schematic diagram of the ocular motor interleaved task.

A) a prosaccade trial and **B)** an antisaccade trial – the dotted circle indicates the correct response location for an antisaccade trial and does not appear on the screen. Note that each trial lasted a total of 5500ms. The colour indicating the trial type (prosaccade or antisaccade) was counterbalanced between participants.

Supplementary Table 7.S4: Spearman rank's correlations among diffusivity measures for all participants combined.

		FA						MD					
		CC Body	CC Genu	CC Sp	ICP	MCP	SCP	CC Body	CC Genu	CC Sp	ICP	MCP	SCP
	CC Body		**0.762**	**0.758**	0.220	**0.704**	**0.455**	-0.235	-0.169	-0.121	-0.253	-0.160	0.033
	CC Genu	<0.001		**0.773**	0.204	**0.559**	**0.381**	-0.364	**-0.387**	-0.358	-0.220	-0.304	-0.109
FA	CC Sp	<0.001	<0.001		0.247	**0.702**	**0.435**	**-0.418**	**-0.442**	**-0.393**	-0.306	-0.299	-0.086
	ICP	0.173	0.207	0.125		0.321	0.333	-0.129	-0.351	-0.092	0.024	0.056	-0.073
	MCP	<0.001	<0.001	<0.001	0.044		**0.634**	-0.161	-0.275	-0.180	0.002	-0.201	0.114
	SCP	0.003	0.015	0.005	0.036	<0.001		0.040	0.015	0.060	0.160	-0.077	0.126
	CC Body	0.144	0.021	0.007	0.426	0.322	0.809		**0.416**	**0.480**	**0.459**	0.310	0.295
	CC Genu	0.298	0.014	0.004	0.026	0.087	0.925	0.008		**0.655**	0.163	0.256	0.227
MD	CC Sp	0.459	0.023	0.012	0.574	0.267	0.715	0.002	<0.001		0.375	0.325	0.244
	ICP	0.116	0.173	0.055	0.886	0.990	0.325	0.003	0.315	0.017		**0.484**	**0.475**
	MCP	0.325	0.056	0.061	0.734	0.214	0.639	0.052	0.111	0.041	0.002		**0.470**
	SCP	0.842	0.503	0.599	0.657	0.485	0.437	0.064	0.160	0.130	0.002	0.002	

Note: Upper triangle represents estimated correlation coefficients, while their corresponding unadjusted p-values are in the lower triangle; Figures in bold indicate p<0.05 after adjusting for multiple comparisons using FDR.

Supplementary Table 7.S5: Statistics on participant molecular and diffusivity data

	PM (n=20)	**Controls (n=20)**	***p*-value**
	Mean ± SD	Mean ± SD	
***FMR1* molecular measures**			
FMR1 mRNA	1.80 ± 0.62	1.44 ± 0.41*	0.041
AR	0.58 ± 0.05	0.57 ± 0.05^	0.416
CpG 1	0.32 ± 0.04	0.33 ± 0.03*	0.364
CpG 2	0.20 ± 0.04	0.20 ± 0.03*	0.604
CpG 6/7	0.41 ± 0.03	0.42 ± 0.04*	0.480
CpG 8/9	0.31 ± 0.04	0.30 ± 0.04*	0.391
CpG 10-12+	0.30 ± 0.05	0.28 ± 0.06*	0.117
FA*			
CC Genu	51.1 ± 2.78	51.7 ± 1.70	0.392
CC Splenium	56.6 ± 3.06	57.2 ± 1.96	0.485
CC Body	66.8 ± 2.27	67.3 ± 1.52	0.486
ICP	41.5 ± 1.99	41.4 ± 2.02	0.939
MCP	44.5 ± 1.47	44.2 ± 1.26	0.530
SCP	51.0 ± 2.16	51.0 ± 2.03	0.980
MD**			
CC Genu	0.93 ± 0.15	1.01 ± 0.13	0.104
CC Splenium	1.09 ± 0.20	1.13 ± 0.18	0.481
CC Body	1.04 ± 0.08	1.00 ± 0.06	0.114
ICP+	0.65 ± 0.16	0.61 ± 0.11	0.344
MCP+	0.64 ± 0.10	0.64 ± 0.01	0.978
SCP+	0.73 ± 0.14	0.70 ± 0.08	0.194

Note: Mean (median) and SD (inter-quartile) were multiple by *100 and **1000.
+Median and inter-quartile were used instead of mean and standard deviation (SD);
^n=19, & *n=18 indicates missing data due to failure of quality control during molecular analysis.

Supplementary Table 7.S6: Relationship between each executive measure (outcome) and age (predictor) using regression analysis, for all participants combined and separately for PM and control groups.

	All			PM			Controls			
Executive measure	β	s.e	p-value	β	s.e	p-value	β	s.e	p-value	p-value**
BDS*	-0.34	3.80	0.928	0.17	5.78	0.977	0.59	2.98	0.844	0.950
PASAT	-0.29	0.27	0.282	-0.53	0.39	0.186	0.11	0.35	0.763	0.295
SDMT^{+}	-0.39	0.20	0.059	-0.40	0.24	0.110	-0.45	0.32	0.170	0.892
COWAT*	-7.50	16.10	0.645	-1.15	25.00	0.964	-12.10	19.00	0.531	0.735
Prosaccade Latency	0.36	0.80	0.660	-0.69	0.86	0.453	1.92	1.41	0.193	0.112
Antisaccade Latency	0.57	0.90	0.543	-0.49	1.27	0.700	1.52	1.43	0.304	0.147

Note: β = unstandardized estimated regression coefficient, *β and standard error (s.e) were multiple by 100. **p-value for testing the significance of the interaction term. $^{+}$Robust regression was used for analysis.

Supplementary Table 7.S7: Relationship between each *FMR1* molecular (predictor) and each diffusivity and executive measures (outcome) for all participants combined.

Outcome variable	Predictor															
	CGG		AR		*FMR1* mRNA		CpG 1		CpG 2		CpG 6/7		CpG 8/9		CpG 10/12	
	β	*p*	*β*	*p*	*β*	*p*	*β*	*p*	*β*	*p*	*β*	*p*	*β*	*p*	*β*	*p*
FA																
CC Body	0.03+	0.862	-0.11	0.478	-0.12	0.413	0.20	0.167	0.15	0.200	-0.11+	0.476	0.10	0.491	-0.10	0.440
CC Genu	0.00+	0.997	-0.09+	0.552	-0.08	0.462	-0.02+	0.901	0.03+	0.830	0.03+	0.836	0.01+	0.951	-0.07+	0.609
CC Splenium	0.11+	0.450	0.10+	0.473	-0.20	0.078	-0.01+	0.954	0.04+	0.777	-0.02+	0.897	0.00+	0.993	-0.12+	0.419
ICP	0.11	0.511	-0.19+	0.239	-0.09	0.547	0.11	0.519	-0.05	0.792	-0.05	0.738	0.00	0.974	-0.06	0.712
MCP	0.14	0.434	-0.06	0.709	-0.12	0.470	0.02	0.901	0.13	0.263	-0.01	0.976	0.29	0.035	0.06	0.691
SCP	0.05	0.766	0.00+	0.995	-0.09+	0.546	-0.07+	0.660	-0.05+	0.775	-0.11+	0.526	0.21+	0.198	0.06+	0.732
MD																
CC Body	0.14+	0.352	-0.15+	0.265	0.19	0.057	-0.26+	0.079	-0.04+	0.780	-0.02+	0.912	0.12+	0.401	-0.02+	0.898
CC Genu	-0.34	0.030	-0.01+	0.940	-0.01	0.938	0.08+	0.676	-0.17	0.290	-0.18+	0.345	-0.16+	0.413	-0.24	0.054
CC Splenium	-0.20	0.196	-0.12	0.471	0.12	0.443	-0.18+	0.327	-0.05	0.756	0.01	0.965	-0.12	0.437	-0.21	0.105
ICP	0.00+	0.982	-0.02+	0.897	-0.02	0.933	-0.37+	0.032	0.15	0.374	0.30+	0.045	0.05	0.786	0.02	0.939
MCP	-0.01+	0.955	0.08	0.566	-0.13+	0.439	-0.22+	0.181	0.17+	0.285	0.01+	0.961	-0.25	0.278	-0.25	0.151
SCP	0.18+	0.237	0.02+	0.918	-0.03+	0.843	-0.30+	0.043	0.17+	0.322	0.01+	0.969	0.05+	0.755	-0.08+	0.621
Executive Function																
BDS	-0.40	0.018	-0.04+	0.842	-0.53	0.001	0.09+	0.600	0.16	0.298	0.09	0.599	-0.11	0.565	-0.10	0.494
PASAT	-0.27	0.137	-0.12+	0.424	-0.45+	0.003	0.27+	0.080	0.12	0.463	-0.09	0.614	0.05	0.785	-0.02	0.923
SDMT	-0.29+	0.087	-0.06	0.778	-0.13+	0.411	0.10+	0.543	0.07+	0.681	0.14+	0.404	-0.01+	0.936	-0.08+	0.654
COWAT	-0.09+	0.607	-0.26	0.139	-0.08	0.579	0.02	0.891	-0.08	0.642	0.03	0.815	0.03	0.835	-0.09	0.571
PS Latency	-0.20	0.230	0.01	0.935	0.16	0.339	-0.06	0.716	0.06	0.736	0.26	0.097	0.14	0.442	0.06	0.809
AS Latency	-0.11	0.490	-0.16	0.439	0.07+	0.660	0.02+	0.896	-0.26	0.088	-0.01+	0.970	-0.13+	0.394	-0.13+	0.410

Note: *β* = standardised regression coefficient; +Robust regression; PS= prosaccade; AS = antisaccade.

Supplementary Table 7.S8: Relationship between each *FMR1* molecular (predictor) and each diffusivity and executive measures (outcome) for the PM group

Outcome variable	Predictor															
	CGG		AR		*FMR1* mRNA		CpG 1		CpG 2		CpG 6/7		CpG 8/9		CpG 10/12	
	β	*p*	*β*	*p*	*β*	*p*	*β*	*p*	*β*	*p*	*β*	*p*	*β*	*p*	*β*	*p*
FA																
CC Body	0.11	0.807	-0.32^{+}	0.257	-0.16	0.429	0.31	0.104	0.31^{+}	0.155	-0.27^{+}	0.329	0.13^{+}	0.630	0.07	0.795
CC Genu	-0.05	0.893	-0.37^{+}	0.166	-0.08	0.688	-0.05^{+}	0.828	0.14^{+}	0.511	0.07^{+}	0.836	0.03^{+}	0.891	-0.07	0.793
CC Splenium	0.21	0.567	0.08^{+}	0.551	-0.26	0.147	0.17^{+}	0.507	0.15^{+}	0.496	-0.17^{+}	0.602	0.05^{+}	0.859	-0.14	0.647
ICP	0.38	0.316	-0.27^{+}	0.224	-0.28	0.143	-0.06	0.794	-0.02	0.905	0.19	0.390	0.09	0.661	0.21	0.390
MCP	0.05	0.920	-0.04^{+}	0.868	-0.15	0.447	0.01	0.973	0.13	0.343	-0.07^{+}	0.808	0.22^{+}	0.295	0.02	0.946
SCP	0.25	0.438	-0.13^{+}	0.584	-0.21^{+}	0.281	-0.21^{+}	0.325	-0.03^{+}	0.869	-0.22^{+}	0.431	0.05^{+}	0.838	-0.11	0.632
MD																
CC Body	0.02	0.969	-0.08^{+}	0.688	0.18	0.188	-0.40^{+}	0.062	-0.01^{+}	0.968	0.04^{+}	0.886	0.13^{+}	0.514	0.10	0.725
CC Genu	-0.46^{+}	0.351	0.27^{+}	0.292	0.07^{+}	0.788	-0.21^{+}	0.432	-0.06	0.780	-0.24^{+}	0.436	-0.13	0.605	-0.15	0.602
CC Splenium	-0.23^{+}	0.645	0.07^{+}	0.807	0.11^{+}	0.682	-0.49^{+}	0.088	-0.04	0.866	0.08^{+}	0.812	-0.07^{+}	0.797	-0.17	0.546
ICP	-0.67^{+}	0.107	-0.05^{+}	0.825	-0.22	0.292	-0.70	0.005	0.14	0.341	0.33^{+}	0.203	-0.17^{+}	0.490	-0.21	0.474
MCP	-0.08^{+}	0.849	0.09^{+}	0.684	-0.44^{+}	0.029	-0.59	0.013	0.17	0.320	0.15^{+}	0.567	0.02^{+}	0.935	0.43^{+}	0.213
SCP	-0.42^{+}	0.380	-0.08	0.705	-0.27	0.303	-0.28^{+}	0.250	0.19	0.323	0.20^{+}	0.487	-0.17	0.510	-0.18	0.544
Executive Function																
BDS	0.27	0.491	0.35^{+}	0.235	-0.46	0.064	-0.10	0.781	0.30	0.208	0.16	0.539	-0.06^{+}	0.833	0.02	0.927
PASAT	0.20	0.641	0.18^{+}	0.558	-0.61^{+}	0.013	0.36^{+}	0.210	0.37	0.066	0.05^{+}	0.873	0.12	0.668	0.19	0.432
SDMT	0.02	0.930	0.06^{+}	0.811	0.01	0.967	0.03	0.875	0.25	0.135	0.15	0.563	0.14^{+}	0.526	-0.14	0.444
COWAT	0.76^{+}	0.133	-0.50^{+}	0.097	-0.06	0.816	0.09	0.739	-0.13	0.583	0.05	0.882	-0.08	0.716	-0.94^{+}	0.045
PS Latency	-0.39^{+}	0.280	0.41	0.016	0.10^{+}	0.533	-0.10	0.589	0.11	0.499	0.75^{+}	0.002	0.25	0.109	0.34	0.037
AS Latency	-0.37^{+}	0.336	0.05^{+}	0.832	0.02	0.914	0.10	0.655	-0.28^{+}	0.126	-0.05^{+}	0.836	-0.15^{+}	0.472	-0.10	0.602

Note: β = standardised regression coefficient; $^{+}$Robust regression; PS= prosaccade; AS = antisaccade.

Supplementary Table 7.*S*9: Relationship between each *FMR1* molecular (predictor) and each diffusivity and executive measures (outcome) for the control group

Outcome variable	Predictor															
	CGG		AR		*FMR1* mRNA		CpG 1		CpG 2		CpG 6/7		CpG 8/9		CpG 10/12	
	β	*p*	*β*	*p*	*β*	*p*	*β*	*p*	*β*	*p*	*β*	*p*	*β*	*p*	*β*	*p*
FA																
CC Body	-0.07	0.977	0.07^{+}	0.714	-0.07	0.806	0.06	0.764	-0.13^{+}	0.552	-0.33^{+}	0.029	0.04^{+}	0.837	-0.25	0.125
CC Genu	0.68	0.264	0.10^{+}	0.591	-0.12	0.634	0.05^{+}	0.775	0.31^{+}	0.154	-0.14^{+}	0.426	-0.04^{+}	0.850	-0.21	0.117
CC Splenium	0.67	0.623	0.21^{+}	0.218	-0.17	0.490	-0.17^{+}	0.352	0.19	0.291	-0.11^{+}	0.537	-0.07^{+}	0.733	-0.25	0.096
ICP	2.21^{+}	0.402	-0.11^{+}	0.697	0.19^{+}	0.603	0.39	0.089	0.14^{+}	0.746	-0.21^{+}	0.401	-0.15^{+}	0.634	-0.33	0.112
MCP	5.01^{+}	0.198	-0.12^{+}	0.516	-0.27^{+}	0.390	-0.13^{+}	0.541	0.05^{+}	0.780	-0.27^{+}	0.162	0.27^{+}	0.266	-0.04+	0.856
SCP	-4.62^{+}	0.220	0.11^{+}	0.662	-0.03^{+}	0.916	0.05^{+}	0.852	-0.12^{+}	0.743	0.01^{+}	0.979	0.40^{+}	0.128	0.01	0.951
MD																
CC Body	1.02	0.424	-0.25^{+}	0.196	0.18	0.373	-0.04^{+}	0.834	-0.10	0.687	-0.03	0.852	0.08	0.683	-0.11	0.539
CC Genu	-1.36^{+}	0.733	-0.25^{+}	0.197	0.10	0.732	0.15^{+}	0.521	-0.32^{+}	0.261	-0.19^{+}	0.328	-0.11	0.644	-0.20	0.331
CC Splenium	-1.48^{+}	0.703	-0.21^{+}	0.342	0.30	0.330	0.14^{+}	0.502	-0.02^{+}	0.936	-0.10^{+}	0.612	-0.16	0.497	-0.20	0.320
ICP	0.58	0.696	0.04^{+}	0.839	0.06^{+}	0.836	0.05	0.779	0.14	0.684	0.29^{+}	0.153	0.28	0.249	0.14	0.521
MCP	2.16^{+}	0.381	0.19^{+}	0.478	0.70^{+}	0.013	0.26^{+}	0.363	0.10^{+}	0.743	-0.08^{+}	0.745	-0.11	0.670	-0.10	0.664
SCP	1.06	0.252	-0.02	0.914	-0.05^{+}	0.805	-0.22^{+}	0.190	0.17	0.509	-0.15	0.330	0.09	0.713	-0.23	0.269
Executive Function																
BDS	1.68	0.170	-0.01^{+}	0.994	-0.30	0.067	0.06	0.662	-0.01	0.937	-0.07	0.522	-0.02^{+}	0.927	0.03	0.808
PASAT	0.24	0.692	-0.17	0.137	0.01^{+}	0.972	0.06^{+}	0.727	-0.38	0.018	-0.19^{+}	0.236	0.06	0.735	-0.05	0.760
SDMT	-2.35^{+}	0.373	0.05^{+}	0.860	-0.13	0.697	0.11	0.715	-0.14	0.706	0.01	0.941	0.07	0.761	0.04	0.872
COWAT	-1.82^{+}	0.422	0.11^{+}	0.531	0.06	0.836	-0.14	0.459	0.12	0.590	-0.02	0.903	0.26	0.073	0.09	0.532
PS Latency	0.83	0.587	-0.38^{+}	0.020	0.54^{+}	0.187	-0.07	0.845	-0.01	0.988	0.09	0.775	0.04	0.922	0.06	0.809
AS Latency	-0.12	0.965	-0.36^{+}	0.091	0.25^{+}	0.445	-0.18	0.459	-0.23^{+}	0.502	0.01^{+}	0.968	-0.18	0.587	-0.13^{+}	0.410

Note: *β* = standardised regression coefficient; $^{+}$Robust regression; PS= prosaccade; AS = antisaccade.

Supplementary Figure 7.S2

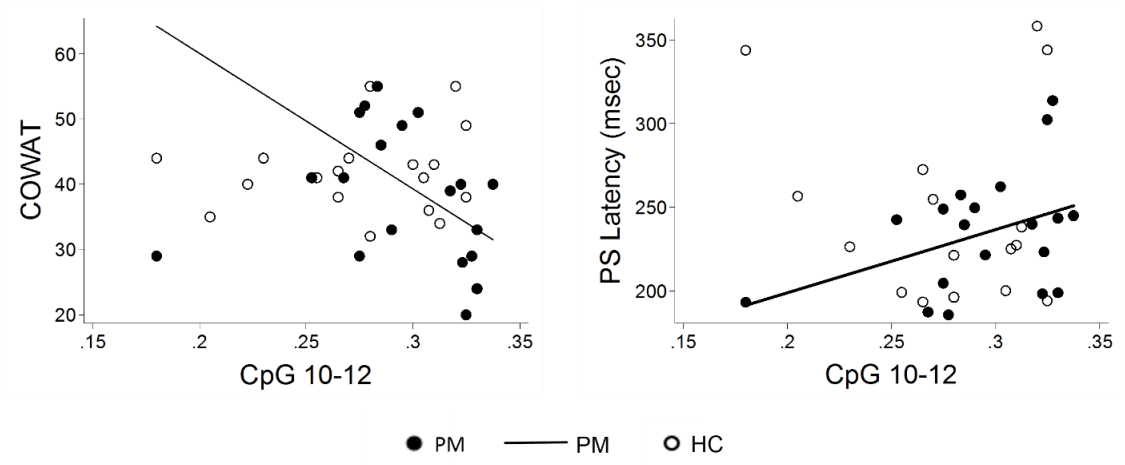

Relationships between CpG 10-12 and executive function measures for PM and control groups.

Significant correlations prior to FDR were found for the PM group for the relationships between i) CpG 10-12 and COWAT, and ii) CpG 10-12 and Prosaccade latency (PS latency). Both of these plots indicate that increased methylation of CpG 10-12 site correlates with increased executive dysfunction for the PM group only.

Supplementary Table 7.S10: Relationship between each diffusivity measures (predictor) and executive function measures (outcome) for all participants combined.

	Outcome											
	BDS		PASAT		SDMT		COWAT		Prosaccade Latency		Antisaccade Latency	
Predictor	*β*	*p*	*β*	*p*	*β*	*p*	*β*	*p*	*β*	*p*	*β*	*p*
FA												
CC Body	0.26	0.059	0.53	**<0.001**	0.39	**0.001**	0.53^{+}	**0.001**	0.07	0.624	-0.02	0.891
CC Genu	0.22	0.125	0.51	**0.001**	0.39^{+}	0.011	0.45^{+}	**0.006**	-0.10	0.534	-0.03	0.833
CC Splenium	0.32	0.012	0.61	**<0.001**	0.44^{+}	**0.004**	0.49^{+}	**0.002**	-0.14	0.380	-0.09^{+}	0.533
ICP	0.17	0.289	0.07	0.656	-0.07	0.656	0.17	0.281	-0.19	0.340	-0.21	0.211
MCP	0.24	0.099	0.42	**0.004**	0.32	**0.007**	0.43	**<0.001**	-0.03	0.834	-0.14^{+}	0.347
SCP	0.24	0.085	0.49	**0.001**	0.18	0.281	0.31	0.015	-0.24	0.119	-0.04	0.643
MD												
CC Body	-0.41	**<0.001**	-0.33	0.023	-0.35	0.015	-0.27	0.130	0.25^{+}	0.113	0.10^{+}	0.487
CC Genu	0.09	0.589	0.03	0.886	-0.07^{+}	0.688	-0.07	0.655	0.18	0.189	0.13^{+}	0.376
CC Splenium	-0.01	0.949	-0.11	0.516	-0.21^{+}	0.193	-0.03	0.861	0.27	0.078	0.13^{+}	0.352
ICP	-0.02	0.887	-0.23	0.200	-0.10^{+}	0.552	-0.12	0.440	0.03	0.857	0.03	0.857
MCP	0.19	0.305	-0.25	0.115	-0.05^{+}	0.778	-0.11	0.481	-0.08	0.577	-0.10^{+}	0.521
SCP	0.05	0.687	0.02	0.904	-0.17	0.248	0.02	0.861	-0.07	0.575	-0.15	0.325

Note: *β* = standard regression coefficient, $^{+}$Robust regression; Figures in bold indicate p<0.05 after adjusting for multiple comparisons using FDR.

Supplementary Table 7.S11: Relationship between each diffusivity measures (predictor) and executive function measures (outcome) for PM.

	Outcome											
	BDS		PASAT		SDMT		COWAT		Prosaccade Latency		Antisaccade Latency	
Predictor	*β*	*p*	*β*	*p*	*β*	*p*	*β*	*p*	*β*	*p*	*β*	*p*
FA												
CC Body	0.31	0.159	0.63	0.004	0.75	0.013	0.42	0.054	0.16^{+}	0.340	0.13	0.484
CC Genu	0.17	0.451	0.55	0.03	0.88^{+}	0.007	0.38	0.079	0.16^{+}	0.386	0.05^{+}	0.801
CC Splenium	0.34	0.115	0.55^{+}	**0.002**	0.92^{+}	0.003	0.42	0.050	0.20^{+}	0.291	0.21^{+}	0.516
ICP	0.16	0.545	0.17	0.546	0.19^{+}	0.468	0.41^{+}	0.056	0.02^{+}	0.926	-0.01^{+}	0.955
MCP	0.43	0.018	0.56	**0.001**	0.71	0.010	0.44	0.038	0.12	0.485	0.08	0.738
SCP	0.51^{+}	**0.001**	0.49^{+}	0.008	0.35	0.066	0.42^{+}	0.026	0.03^{+}	0.888	-0.01	0.962
MD												
CC Body	-0.35	0.135	-0.37	0.136	-0.38	0.029	-0.28^{+}	0.285	-0.15^{+}	0.657	-0.24	0.274
CC Genu	-0.01	0.958	-0.14	0.597	-0.58	0.014	-0.31^{+}	0.271	0.01	0.943	0.07	0.728
CC Splenium	-0.03^{+}	0.913	-0.23^{+}	0.419	-0.55	0.029	-0.07^{+}	0.807	0.04^{+}	0.850	-0.05^{+}	0.801
ICP	0.11	0.667	-0.28	0.276	0.21^{+}	0.444	-0.05	0.831	-0.35^{+}	0.080	-0.21	0.293
MCP	0.34^{+}	0.068	-0.22	0.397	-0.03	0.870	-0.15	0.534	-0.28	0.098	-0.65^{+}	0.025
SCP	0.33^{+}	0.141	0.08	0.764	0.05	0.772	0.04	0.854	-0.17	0.308	-0.19^{+}	0.357

Note: *β* = standard regression coefficient, $^{+}$Robust regression; Figures in bold indicate p<0.05 after adjusting for multiple comparisons using FDR.

Supplementary Table 7.S12: Relationship between each diffusivity measures (predictor) and executive function measures (outcome) for controls.

	Outcome											
	BDS		PASAT		SDMT		COWAT		Prosaccade Latency		Antisaccade Latency	
Predictor	*β*	*p*	*β*	*p*	*β*	*p*	*β*	*p*	*β*	*p*	*β*	*p*
FA												
CC Body	-0.11^{+}	0.608	0.32	0.243	0.15	0.423	0.52	0.015	0.01	0.986	-0.35	0.292
CC Genu	0.10	0.531	0.46	0.136	0.08	0.483	0.31^{+}	0.127	-0.18	0.643	-0.42	0.242
CC Splenium	0.09	0.588	0.41^{+}	0.172	0.17	0.108	0.47	0.038	-0.36	0.338	-0.32^{+}	0.055
ICP	0.20	0.088	0.00^{+}	0.975	-0.45^{+}	0.021	-0.25	0.465	-0.18^{+}	0.497	-0.37	0.170
MCP	0.22	0.661	0.41^{+}	0.207	0.20	0.231	0.59	0.027	-0.15^{+}	0.587	-0.68^{+}	0.028
SCP	-0.08^{+}	0.858	0.56^{+}	0.093	0.00	0.991	-0.19^{+}	0.504	-0.18	0.569	-0.09	0.765
MD												
CC Body	-0.20	0.161	-0.06	0.737	-0.07	0.808	0.11^{+}	0.637	0.36^{+}	0.004	0.64^{+}	0.004
CC Genu	-0.11^{+}	0.466	0.03	0.840	0.16	0.305	0.23^{+}	0.225	0.37	0.254	0.27^{+}	0.315
CC Splenium	-0.14	0.277	-0.11	0.475	-0.10	0.524	0.14^{+}	0.494	0.48	0.108	0.33^{+}	0.113
ICP	-0.01	0.955	0.18^{+}	0.218	-0.08	0.776	-0.12	0.545	0.12	0.731	0.20	0.522
MCP	0.30	0.059	-0.06^{+}	0.725	-0.11	0.681	-0.04	0.853	0.10^{+}	0.720	0.12^{+}	0.624
SCP	-0.20^{+}	0.563	0.16	0.372	-0.33	0.246	0.18	0.422	0.62	0.214	0.27^{+}	0.480

Note: *β* = standard regression coefficient, $^{+}$Robust regression.

CHAPTER 8: GENERAL DISCUSSION

Genetic and neural correlates of executive dysfunction are apparent in a range of neurodevelopmental and neurodegenerative disorders, including Fragile X syndrome (FXS) and Fragile X-associated tremor/ataxia syndrome (FXTAS). There is now compelling evidence to suggest that a subset of PM-carriers without FXTAS have impaired executive functions, although the nature and extent of these deficits is less clear for PM females (Grigsby *et al.*, 2014). The overarching aim of this thesis was to examine executive function in PM females without FXTAS. This was completed through a battery of ocular motor and neuropsychological tasks, primarily assessing response inhibition and working memory processes. Saccadic ocular motor paradigms provide an elegant means by which to examine these functions, given that they generate stereotypical and reproducible outcome measures (Hutton, 2008). The neural circuits involved in the production of saccades are well defined, traversing widely through cortico-cerebellar pathways, and are sensitive to subtle and overt neural changes.

A second aim of this thesis was to investigate how genetic and neural markers may influence executive dysfunction in PM females without FXTAS, through assessing the inter-relationships between these variables. The central finding of this thesis is that executive dysfunction is consistently found across a range of tasks for PM females without FXTAS, especially evident in tasks requiring the rapid generation of a response. Collectively, the nature of deficits revealed, suggest cortico-cerebellar processing deficits may have a genetic origin (Figure 8.1). This discussion will i) provide an overview of the main findings contained within Chapters 2-7, ii) propose molecular mechanisms that may influence grey and white matter structure within the cortico-cerebellar pathways, and iii) evaluate the limitations and future directions arising from this study.

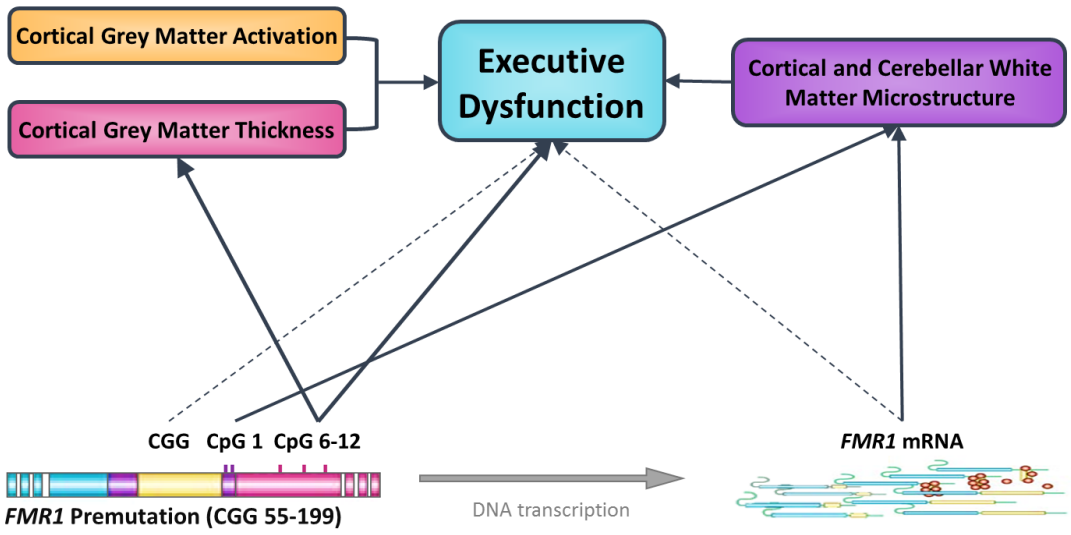

Figure 8.1: Summary diagram depicting the significant genetic – brain – behaviour relationships revealed in PM females without FXTAS.

PM females without FXTAS were found to exhibit executive dysfunction in all experimental chapters (Chapters 2-7). These deficits where found to correlate with genetic and molecular markers (CGG, *FMR1* exon 1 methylation marker CpG 1, *FMR1* intron 1 methylation markers CpG 6/7, 8/9, and 10-12, as well as *FMR1* mRNA) (Chapters 3-4 and 6-7), as well as neural measures (Chapters 5-7). Dotted lines represented significant, although unanticipated, correlations.

8.1 EXECUTIVE SUMMARY

Chapter 2 employed neuropsychological assessment, to explore the executive function profile in PM females without FXTAS, correlating performance with the age of participants. Consistent with previous reports (Yang *et al.*, 2013; Kraan *et al.*, 2014b; Kraan *et al.*, 2014c; Cornish *et al.*, 2015), impaired executive functioning was found for PM females across a range of tasks requiring the rapid generation of a response. However, unlike studies in PM males (Cornish *et al.*, 2008b; Cornish *et al.*, 2009; Cornish *et al.*, 2011; Kraan *et al.*, 2014c), the deficits revealed were not age-related. Results from this chapter provide evidence for the hypothesis that PM females without FXTAS have a similar, yet *subtly different cognitive signature* then PM males.

Chapter 3 provides a comprehensive assessment of executive dysfunction through the use of both ocular motor and neuropsychological assessments. In PM females without FXTAS results firstly reflected response inhibition deficits, which were best delineated using saccadic paradigms. Although saccade latency and accuracy were preserved in PM females without FXTAS across all paradigms, a greater proportion of errors were recorded during the antisaccade and memory-guided tasks for PM females without FXTAS compared to controls. Secondly, BDS test item analysis demonstrated that procedural motor learning was impaired in PM females without FXTAS. Together, these results parallel those previously reported in PM males (Cornish *et al.*, 2008b; Cornish *et al.*, 2011), and suggest disruption to cortico-cerebellar pathways, in particular, prefrontal and cerebellar nodes (Georgopoulos, 2000; Ramnani, 2006).

Chapter 4 employs a saccadic n-back task to ascertain the impact of increasing cognitive load on working memory performance. Results from this chapter indicate a working memory profile in PM females without FXTAS that is characterised by increased response time (saccade latency), and unaffected by increasing cognitive load. Although this is the *first* study to examine the impact of increased cognitive load using a single paradigm, similar deficits related to increased task complexity have been found in PM females without FXTAS during dual task paradigms. Specifically, balance and gait deficits were exacerbated when performing a concurrent executive function task for PM females without FXTAS (Kraan *et al.*, 2013b; Hocking *et al.*, 2015).

Chapters 3 and 4 also provide evidence of genetic links with saccade outcomes. Specifically, higher CGG repeat length, as well as higher *FMR1* mRNA levels were found to correlate with superior executive function (lower antisaccade error rate and higher working memory capacity). These findings are somewhat counter-intuitive given the given that i) executive dysfunction is a clinical hallmark of FXTAS, ii) higher CGG repeats are associated with earlier onset and greater severity of FXTAS symptoms, and iii) increased levels of *FMR1* mRNA are associated with the formation of intranuclear inclusions, a pathological hallmark FXTAS

(Willemsen *et al.*, 2003; Arocena *et al.*, 2005; Tassone *et al.*, 2007a; Leehey *et al.*, 2008; Todd *et al.*, 2013; Botta-Orfila *et al.*, 2016). However, these results may be impacted by the restricted CGG repeat range of PM females without FXTAS investigated (highest CGG repeat length was 102).

Chapter 5 investigates the associations between the neural activation during an ocular motor interleaved task and saccadic measures of executive function. Dissociations were evident between PM females without FXTAS and controls for brain - behaviour relationships, specifically involving frontal, parietal and cerebellar regions. Further, compared to controls, PM females without FXTAS were found to have reduced activity within the right ventrolateral prefrontal cortex during antisaccade trials. Not only does this align with previously reported alterations to prefrontal networks in PM-carriers without FXTAS (Hashimoto *et al.*, 2011a; Wang *et al.*, 2012a; Kim *et al.*, 2013), but further implicates disruption within the cortico-cerebellar pathway in executive dysfunction.

Chapter 6 provides an integrative analytical approach in the examination of the associations between i) *FMR1* molecular measures, ii) cortical thickness within frontal and parietal regions, and iii) executive function assessed using an ocular motor interleaved task. Specific inter-relationships were found between all three measures in PM females without FXTAS; with divergent associations revealed PM-carriers without FXTAS and controls for relationships between *FMR1* intron 1 methylation and cortical thickness. These results not only endorse a previous report regarding the influence of *FMR1* intron 1 methylation on executive function in PM females without FXTAS (Cornish *et al.*, 2015), but imply that both *FMR1* intron 1 methylation markers and cortical structure are related and may individually influence executive dysfunction in PM females without FXTAS.

Chapter 7 uses a similar analytical approach to investigate the relationships between i) white matter microstructure, ii) *FMR1* molecular measures, and iii) executive function using an ocular motor interleaved task (**Chapters 5 and 6**). Analysis of white matter

microstructure was restricted to the corpus callosum and cerebellar peduncles, both of which have been implicated in FXTAS pathology (Hall *et al.*, 2014; Renaud *et al.*, 2015a; Renaud *et al.*, 2015b; Hall *et al.*, 2016b). Results align with previous reports of MCP and corpus callosum white matter microstructure associations with executive dysfunction in PM males with and without FXTAS (Filley *et al.*, 2015). However, they also reveal that *FMR1* mRNA and *FMR1* exon 1 methylation marker CpG 1 correlate with white matter microstructure within the ICP and MCP tracts. This highlights the importance of ascertaining the integrity of white matter connections within the cortico-cerebellar pathway, as well as inter-hemispheric neural connections in PM-carriers without FXTAS. Finally, this chapter furthers the notion that *FMR1* intron 1, but not exon 1 methylation markers significantly relate to executive dysfunction in PM females, as suggested in **Chapter 6** and previously (Cornish *et al.*, 2015).

8.2 POTENTIAL MOLECULAR MECHANISMS INVOLVED IN CORTICO-CEREBELLAR NETWORK DISRUPTION

Ultimately, the deficits in executive function, and their relationship with neural structure and function, reported herein, converge to indicate disrupted cortico-cerebellar processing in PM females without FXTAS, specifically originating from processing in the prefrontal cortex. This hypothesis is consistent with previous findings from neuromotor (balance and gait) (Chonchaiya *et al.*, 2010; Kraan *et al.*, 2013b; Hocking *et al.*, 2015; O'Keefe *et al.*, 2015a) and neuroimaging investigations amongst PM carriers without FXTAS (Jacquemont *et al.*, 2010; Hashimoto *et al.*, 2011a; Hashimoto *et al.*, 2011b; Hashimoto *et al.*, 2011c; Wang *et al.*, 2012a; Battistella *et al.*, 2013; Conde *et al.*, 2013; Kim *et al.*, 2013; Kim *et al.*, 2014; Leow *et al.*, 2014).

The cortico-cerebellar network forms a closed loop cognitive and motor control system. Reciprocal cognitive projections from the prefrontal cortex, specifically the DLPFC (Middleton and Strick, 2001; Kelly and Strick, 2003), reach the posterior cerebellum (lobules

VI-VII and crus I-II) via the pontine nuclei, and return to the cortex via cerebellar nuclei and thalamic projections (Ramnani, 2006; Kamali *et al.*, 2010; Stoodley and Schmahmann, 2010; Stoodley, 2012). Alterations to this circuit in PM females without FXTAS, particularly in prefrontal or cerebellar regions, may arise for several reasons.

Results from **Chapters 6 and 7** in particular, provide the possibility of two divergent molecular mechanisms that disrupt neural *structure* within cortico-cerebellar pathways. While relationships were revealed between *FMR1* intron 1 methylation and cortical grey matter (**Chapter 6**), *FMR1* mRNA and exon 1 methylation were related to white matter microstructure (**Chapter 7**) (Figure 8.1). These discrepant *FMR1* molecular – brain associations suggest that grey and white matter may be impacted differently in PM females without FXTAS. The following discussion considers the pathways that may mediate these associations.

Associations between cortical grey matter and *FMR1* intron 1 methylation

FMR1 intron 1 methylation was correlated with both executive dysfunction and cortical grey matter thickness (**Chapter 6**). Epigenetic methylation markers have been previously implicated in executive dysfunction for both PM and FXS females (Godler *et al.*, 2011; Godler *et al.*, 2012; Inaba *et al.*, 2014; Cornish *et al.*, 2015).

Epigenetic modification within the Fragile X related epigenetic element 2 (which contain *FMR1* exon 1 and intron 1), is thought to be well conserved between peripheral tissues, and thus appropriate for correlations with neural measures (Godler *et al.*, 2011; Godler *et al.*, 2012; Inaba *et al.*, 2014; Cornish *et al.*, 2015). In particular, *FMR1* intron 1 methylation is thought to play a regulatory role in the formation of a RNA:DNA complex, and thus long non-coding RNAs in FXS (Colak *et al.*, 2014). Moreover, *FMR1* intragenic regions are known to produce long non-coding RNAs, such as *FMR4* and *FMR5* (St Laurent *et al.*, 2012). The relative abundance of a *FMR1* long non-coding RNAs is seen to differ i) according to CGG repeat length

(*FMR4* is up regulated in PM carriers) (Khalil *et al.*, 2008), and ii) between brain regions (*FMR5* levels are highest in the cerebellum) (Pastori *et al.*, 2014). Further, over-expression of antisense *FMR1* (*ASFMR1*) and long non-coding RNA have previously been reported in PM individuals (Ladd *et al.*, 2007), and have also been associated with parkinsonism and mitochondrial dysfunction (Loesch *et al.*, 2011). Therefore, the presence or absence of long non-coding RNAs derived from *FMR1* intron 1 methylation sites, and *ASFMR1* may alter the density and thickness of cortical grey matter, through as yet unknown pathways, in PM females without FXTAS.

FMR1 intron 1 methylation is also seen to inversely correlate with FMRP levels in both PM and FM females and FM males (Godler *et al.*, 2010b; Godler *et al.*, 2011). Increased FMRP levels have been found to correlate with increased neural activation within the right ventrolateral prefrontal cortex and insular regions of PM males (Hessl *et al.*, 2011; Wang *et al.*, 2012a), as well as grey matter voxel density in amygdalo-hipppocampal complex, thalamus, and brainstem (Moore *et al.*, 2004b). Although speculative, *FMR1* intron 1 methylation may influence FMRP production through long non-coding RNAs pathways – given that FMRP binds to RNA species (Ashley, Wilkinson, Reines, & Warren 1993). Thus, epigenetic methylation modification within *FMR1* intron 1 may affect grey matter structure though pathways associated with long non-coding RNAs, leading to attenuated cortical thickness.

Associations between white matter structure and *FMR1* mRNA

Associations were also revealed between *FMR1* mRNA levels, and *FMR1* exon1 methylation (CpG 1) and white matter structure (**Chapter 6 and 7**). These results compliment previous associations revealed in FXTAS males (albeit using different analytical procedures including the normalisation of *FMR1* mRNA) (Hashimoto *et al.*, 2011c; Wang *et al.*, 2013b), reinforcing

the proposal that the *FMR1* mRNA pathway is particularly pertinent for PM-carriers with and without FXTAS.

Levels of *FMR1* mRNA are greater in PM carriers than controls (<45 CGG repeats), due to increased *FMR1* transcription (Tassone *et al.*, 2007b), indeed a 1.3-fold mean increase was found in our PM female sample compared to controls. It is thought that excess RNA binds to proteins within the nucleus, and ultimately forms aggregates. Not only are these protein aggregates thought to be toxic (given that they form inclusion bodies – a pathological hallmark of FXTAS), but the sequestration of proteins to these aggregates means that these proteins are unavailable for *normal* cellular processes (Willemsen *et al.*, 2003; Tassone *et al.*, 2004b; Arocena *et al.*, 2005; Greco *et al.*, 2006; Todd *et al.*, 2013).

A number of processes may be affected by these *FMR1* mRNA mediated changes in the intracellular environment, leading to attenuated diffusivity measures. Firstly, changes in myelin structure may result from limited intracellular protein availability. Secondly, axonal swelling has been reported in Purkinje cells of two FXTAS males, via post-mortem analysis (Greco *et al.*, 2002). Given that diffusion is based on the movement of water molecules to infer microstructure, axonal swelling will lead to changes in these measures. Thirdly, post-mortem analysis has also revealed that for at least a subset of FXTAS patients, shifts toward intracellular iron accumulation within the cerebellum and choroid plexus exist (Ariza *et al.*, 2015; Rogers *et al.*, 2016). Changes in iron chelation may be the result of an attenuated intracellular environment associated with increased *FMR1* mRNA levels, and aligns with the iron homeostasis hypothesis of neurodegeneration. Further, these later two processes may be the result of oxidative stress and neurodegenerative processes. Whether or not these processes listed are facilitated by increased *FMR1* mRNA levels remains unknown. Therefore, systematic evaluation of these processes, their association with *FMR1* mRNA levels in PM-carriers with and without FXTAS is warranted.

Increased *FMR1* exon 1 CpG 1 methylation, was found to correlate with both the volume of white matter hypointensities in the cortex (**Chapter 6**) and MD within the ICP and MCP (**Chapter 7**). *FMR1* exon 1 methylation has been associated with modified histones (repressive chromatin marks) in FXS patients (Kumari and Usdin, 2010), thus affecting *FMR1* transcription. Therefore, CpG 1 methylation may represent a transcript control mechanism, in which methylation levels may alter *FMR1* mRNA transcription, and therefore affect white matter structure through the *FMR1* mRNA pathway suggested.

Overall, in the absence of overt neuroanatomical changes, two molecular mechanisms are proposed here. Although speculative, it appears that grey matter structure may be influenced by *FMR1* intron 1 methylation and long non-coding RNAs, while white matter structure is predominantly affected by changes to *FMR1* mRNA levels and the intracellular environment. It is therefore imperative that future studies utilise use similar integrative analyses, and investigate these pathways in the presence of neuroanatomical change, as the second mechanism (*FMR1* mRNA) is thought to be neurodegenerative in nature and may represent early FXTAS-related neuropathological change.

8.3 LIMITATIONS

Throughout this evaluation of executive dysfunction and its biological correlates in PM females without FXTAS, there are a number of inherent limitations. Firstly, the small sample size, which may be affected by ascertainment bias, and restricted CGG repeat (highest CGG repeat was 123) range of the PM females without FXTAS must be acknowledged. In particular, a small sample size carries the risk of reduced statistical power, and replication of this study with a larger cohort is required. Further, all but one PM female was identified as being a carrier through their proband child or family member, and therefore awareness of the consequences associated with FM and PM expansions may have biased these studies. It must also be acknowledged that these analyses are overly vulnerable to type 1 error, due

to multiple comparisons. However, the preliminary and exploratory nature of the studies herein has been stressed throughout. Additionally, all studies employed a cross-sectional design, which limits the interpretability of the causal nature (developmental or degenerative) of the deficits, and genetic – brain - behavioural relationships revealed. Due to technical difficulties, FMRP levels were not ascertained limiting the veracity of its proposed role associated with the *FMR1* intron 1 methylation molecular mechanism identified. Finally, PM females are at risk of a multitude of hormonal irregularities, which have not been investigated and may influence the results herein.

8.4 FUTURE DIRECTIONS

This thesis provides compelling, yet preliminary, evidence for cortico-cerebellar network disruption amongst PM females without FXTAS. Further investigations should focus on identifying prodromal and risk-factors associated with FXTAS in young asymptomatic PM-carriers. Prospective longitudinal analysis, documenting changes in executive function (including saccadic and other ocular motor paradigms) and neural phenotypes, for both male and female PM-carriers together and separately, over time, would be advantageous. Such studies should include detailed molecular analysis to ascertain the role of epigenetic markers (particularly FREE2 methylation markers), FMRP, AS*FMR1*, and other downstream products of the *FMR1* gene locus over time, as well as cellular metabolism including iron, and their linkage to FXTAS.

This thesis was primarily concerned with executive dysfunction, and provides preliminary evidence of its biological correlates in PM females without FXTAS. To comprehensively examine disruption to cortico-cerebellar pathway, functional connectivity analysis during rest, as well as sophisticated analysis of white matter microstructure, would also be ideal. This could be achieved through i) independent component analysis of the seven key resting state networks identified by Yeo *et al.* (2011), ii) seed based analysis focusing on connections

projecting to and from the cerebellum, and iii) examination of the apparent fibre density and cross-section of specific fibre populations (Raffelt *et al.*, 2012; Raffelt *et al.*, 2015). Combining these MRI analytical approaches with genetic, molecular and executive function measures would add to the current data presented, and further delineate the structural and functional neurological phenotype of PM-carriers.

Finally, the majority of health concerns specific to PM females may stem from hormonal changes associated with FXPOI [see Wheeler *et al.* (2014) for full description]. Therefore, it may be crucial to integrate measures of these changes, as well as measures of psychological well-being, given the mediating effect of executive function (Cornish *et al.*, 2015) in phenotype studies of PM females without FXTAS.

8.5 CONCLUDING REMARKS

This thesis provides the *first* comprehensive integrative investigation of the biological correlates of executive dysfunction in PM females without FXTAS. Although preliminary, evidence of disrupted cortico-cerebellar processing in PM females without FXTAS is clear, both at a genetic, neurological and behavioural level. Whether or not these findings result from neurodevelopmental or neurodegenerative effect (separate or related to FXTAS) remains unclear. However, the results provide a solid foundation for future studies to track degeneration within this population. Ultimately, greater understanding of the genetic and neurological changes that predate FXTAS symptomology will provide a foundation for the development of targeted, and early, interventions to lessen the extent of FXTAS burden amongst PM carriers, their families and the wider community.

REFERENCES

Adams JS, Adams PE, Nguyen D, Brunberg JA, Tassone F, Zhang W*, et al.* Volumetric brain changes in females with fragile X-associated tremor/ataxia syndrome (FXTAS). Neurology 2007; 69: 851-9.

Adams PE, Adams JS, Nguyen DV, Hessl D, Brunberg JA, Tassone F*, et al.* Psychological symptoms correlate with reduced hippocampal volume in fragile X premutation carriers. American Journal of Medical Genetics 2009; 153B(3): 775-85.

Aguilar D, Sigford KE, Soontarapornchai K, Nguyen DV, Adams PE, Yuhas JM*, et al.* A quantitative assessment of tremor and ataxia in FMR1 premutation carriers using CATSYS. Am J Med Genet A 2008; 146a(5): 629-35.

Al-Mahdawi S, Virmouni SA, Pook MA. The emerging role of 5-hydroxymethylcytosine in neurodegenerative diseases. Frontiers in Neuroscience 2014; 8: 397.

Alahyane N, Salemme R, Urquizar C, Cotti J, Guillaume A, Vercher JL*, et al.* Oculomotor plasticity: are mechanisms of adaptation for reactive and voluntary saccades separate? Brain research 2007; 1135(1): 107-21.

Allen EG, Hunter JE, Rusin M, Juncos J, Novak G, Hamilton D*, et al.* Neuropsychological findings from older premutation carrier males and their noncarrier siblings from families with fragile X syndrome. Neuropsychology 2011; 25(3): 404-11.

Allen EG, Sherman S, Abramowitz A, Leslie M, Novak G, Rusin M*, et al.* Examination of the effect of the polymorphic CGG repeat in the FMR1 gene on cognitive performance. Behav Genet 2005; 35: 435-45.

Allen EG, Sullivan AK, Marcus M, Small C, Dominguez C, Epstein MP*, et al.* Examination of reproductive aging milestones among women who carry the FMR1 premutation. Hum Reprod 2007; 22(8): 2142-52.

Alvarez-Mora MI, Rodriguez-Revenga L, Feliu A, Badenas C, Madrigal I, Mila M. Skewed X Inactivation in Women Carrying the FMR1 Premutation and Its Relation with Fragile-X-Associated Tremor/Ataxia Syndrome. Neuro-degenerative diseases 2015.

Anderson EJ, Husain M, Sumner P. Human intraparietal sulcus (IPS) and competition between exogenous and endogenous saccade plans. NeuroImage 2008; 40(2): 838-51.

Andersson JL, Sotiropoulos SN. An integrated approach to correction for off-resonance effects and subject movement in diffusion MR imaging. Neuroimage 2016; 125: 1063-78.

Apartis E, Blancher A, Meissner WG, Guyant-Maréchal L, Maltête D, De Broucker T*, et al.* FXTAS: new insights and the need for revised diagnostic criteria. Neurology 2012; 79: 1898-907.

Ariza J, Steward C, Rueckert F, Widdison M, Coffman R, Afjei A*, et al.* Dysregulated iron metabolism in the choroid plexus in fragile X-associated tremor/ataxia syndrome. Brain research 2015; 1598: 88-96.

Arocena DG, Iwahashi CK, Won N, Beilina A, Ludwig AL, Tassone F*, et al.* Induction of inclusion formation and disruption of lamin A/C structure by premutation CGG-repeat RNA in human cultured neural cells. Human Molecular Genetics 2005; 14(23): 3661-71.

Atsma F, Bartelink ML, Grobbee DE, van der Schouw YT. Postmenopausal status and early menopause as independent risk factors for cardiovascular disease: a meta-analysis. Menopause (New York, NY) 2006; 13(2): 265-79.

Au J, Akins RS, Berkowitz-Sutherland L, Tang HT, Chen Y, Boyd A*, et al.* Prevalence and risk of migraine headaches in adult fragile X premutation carriers. Clin Genet 2013; 84(6): 546-51.

Baddeley AD. Working memory. New York, NY: Oxford University Press; 1986.

Bailey DB, Jr., Raspa M, Olmsted M, Holiday DB. Co-occurring conditions associated with FMR1 gene variations: findings from a national parent survey. Am J Med Genet A 2008; 146a(16): 2060-9.

Barbas H, Mesulam MM. Organization of afferent input to subdivisions of area 8 in the rhesus monkey. The Journal of comparative neurology 1981; 200(3): 407-31.

Barton JJS, Greenzang C, Hefter R, Edelman JA, Manoach DS. Switching, plasticity, and prediction in a saccade task-switch paradigm. Experimental brain research 2006a; 168: 76-87.

Barton JJS, Raoof M, Jameel O, Manoach DS. Task-switching with antisaccades versus no-go trials: a comparison of inter-trial effects. Experimental brain research 2006b; 172: 114-9.

Battistella G, Niederhauser J, Fornari E, Hippolyte L, Gronchi Perrin A, Lesca G*, et al.* Brain structure in asymptomatic FMR1 premutation carriers at risk for fragile X-associated tremor/ataxia syndrome. Neurobiology of Aging 2012; 34(6): 1700-7.

Battistella G, Niederhauser J, Fornari E, Hippolyte L, Gronchi Perrin A, Lesca G*, et al.* Brain structure in asymptomatic FMR1 premutation carriers at risk for fragile X-associated tremor/ataxia syndrome. Neurobiology of Aging 2013; 34(6): 1700-7.

Becker W. The neurobiology of saccadic eye movements. Metrics. Reviews of oculomotor research 1989; 3: 13-67.

Benton AL, de Hamsher SK, Sivan AB. Multillingual aplasia examination. 2nd ed. ed. Iowa City, IA: AJA Associates; 1983.

Berry-Kravis E, Goetz CG, Leehey MA, Hagerman RJ, Zhang L, Li L*, et al.* Neuropathic features in fragile X premutation carriers. Am J Med Genet A 2007; 143a(1): 19-26.

Bisley JW, Goldberg ME. Neuronal activity in the lateral intraparietal area and spatial attention. Science 2003; 299(5603): 81-6.

Blohm G, Missal M, Lefevre P. Processing of retinal and extraretinal signals for memory-guided saccades during smooth pursuit. J Neurophysiol 2005; 93(3): 1510-22.

Botta-Orfila T, Tartaglia GG, Michalon A. Molecular Pathophysiology of Fragile X-Associated Tremor/Ataxia Syndrome and Perspectives for Drug Development. Cerebellum 2016; 15(5): 599-610.

Bourgeois JA. Neuropsychiatry of fragile X-premutation carriers with and without fragile X-associated tremor-ataxia syndrome: implications for neuropsychology. The Clinical neuropsychologist 2016: 1-16.

Bourgeois JA, Cogswell JB, Hessl D, Zhang L, Ono MY, Tassone F*, et al.* Cognitive, anxiety and mood disorders in the fragile X-associated tremor/ataxia syndrome. General hospital psychiatry 2007; 29(4): 349-56.

Boxer AL, Garbutt S, Seeley WW, Jafari A, Heuer HW, Mirsky J*, et al.* Saccade abnormalities in autopsy-confirmed frontotemporal lobar degeneration and Alzheimer disease. Arch Neurol 2012; 69(4): 509-17.

Branco MR, Ficz G, Reik W. Uncovering the role of 5-hydroxymethylcytosine in the epigenome. Nature Reviews Genetics 2012; 13: 7-13.

Brasa S, Mueller A, Jacquemont S, Hahne F, Rozenberg I, Peters T*, et al.* Reciprocal changes in DNA methylation and hydroxymethylation and a broad repressive epigenetic switch characterize FMR1 transcriptional silencing in fragile X syndrome. Clinical Epigenetics 2016; 8(1): 1-15.

Brega AG, Goodrich G, Bennett RE, Hessl D, Engle K, Leehey MA*, et al.* The primary cognitive deficit among males with fragile X-associated tremor/ataxia syndrome (FXTAS) is a dysexecutive syndrome. Journal of Clinical and Experimental Neuropsychology 2008; 30(8): 853-69.

Brown L. The prevalence of Fragile X-Assoicated Disorders in Australia: The National Centre for Social and Economic Modelling; 2010.

Brown SSG, Stanfield AC. Fragile X premutation carriers: A systematic review of neuroimaging findings. Journal of the neurological sciences 2015; 352(1-2): 19-28.

Bruce CJ, Goldberg ME, Bushnell MC, Stanton GB. Primate frontal eye fields. II. Physiological and anatomical correlates of electrically evoked eye movements. J Neurophysiol 1985; 54(3): 714-34.

Brunberg JA, Jacquemont S, Hagerman RJ, Berry-Kravis EM, Grigsby J, Leehey MA*, et al.* Fragile X premutation carriers: characteristic MR imaging finding of adult male patients with progressive cerebellar and cognitive dysfunction. American Journal of Neuroradiology 2002; 23: 1757-66.

Brüuhl AB, Hänggi J, Baur V, Rufer M, Delsignore A, Weidt S*, et al.* Increased cortical thickness in a frontoparietal network in social anxiety disorder. Human Brain Mapping 2013; 35(7): 2966-77.

Burgess PW, Shallice T. The Hayling and Brixton Tests. Edmunds, England: Thames Valley Test Company Limited; 1997.

Callan MA, Zarnescu DC. Heads-up: New roles for the Fragile X Mental Retardation Protein in neural stem and progenitor cells. Genesis 2011; 49: 424-40.

Capelli LP, Gonçalves MR, Kok F, Leite CC, Nitrini R, Barbosa ER*, et al.* Fragile X-associated trmor/ataxia syndrome: intrafamiliar varaibility and size of the FMR1 premutation CGG repeat. Movement Disorders 2007; 22(6): 866-70.

Carpenter RHS. Movements of the eyes. 2nd edition ed. London: Pion; 1988.

Chan JL, DeSouza JFX. The effects of attentional load on saccadic task switching. Experimental brain research 2013; 227: 301-9.

Charlton RA, Barrick TR, Lawes IN, Markus HS, Morris RG. White matter pathways associated with working memory in normal aging. Cortex 2010; 46: 474-89.

Chatterjee S, Hadi AS. Influential Observations, High Leverage Points, and Outliers in Linear Regression. Statistical Science 1986; 1(3): 379-93.

Chen L, Hadd A, Sah S, Filipovic-Sadic S, Krosting J, Sekinger E*, et al.* An information-rich CGG repeat primed PCR that detects the full range of fragile X expanded alleles and minimizes the need for sourthern blot analysis. J Mol Diagn 2010; 12(5): 589-600.

Cheng Y, Bernstein A, Chen D, Jin P. 5-Hyroxymethylcytosine: a new player in brain disorders? Experimental neurology 2015; 268: 3-9.

Cherkasova M, Manoach DS, Intriligator J, Barton JJ. Antisaccades and task-switching: interactions in controlled processing. Experimental brain research 2002; 227: 301-9.

Chonchaiya W, Nguyen DV, Au J, Campos L, Berry-Kravis EM, Lohse K*, et al.* Clinical involvement in daughters of men with fragile X-associated tremor ataxia syndrome. Clin Genet 2010; 78(1): 38-46.

Cieslik EC, Seidler I, Laird AR, Fox PT, Eickhoff SB. Different involvement of subregions within dorsal premotor and medial frontal cortex for pro- and antisaccades. Neurosci Biobehav Rev 2016.

Clementz BA, Brahmbhatt SB, McDowell JE, Brown R, Sweeney JA. When does the brain inform the eye whether and when to move? An EEG study in humans. Cerebral Cortex 2007; 17(11): 2634-43.

Clifford S, Dissanayake C, Bui QM, Huggins R, Taylor AK, Loesch DZ. Autism spectrum phenotype in males and females with fragile X full mutation and premutation. Journal of autism and developmental disorders 2007; 37(4): 738-47.

Clough M, Mitchell L, Millist L, Lizak N, Beh S, Frohman TC*, et al.* Ocular motor measures of cognitive dysfunction in multiple sclerosis II: working memory. Journal of neurology 2015; 262(5): 1138-47.

Coffee B, Keith K, Albizua I, Malone T, Mowrey J, Sherman SL*, et al.* Incidence of Fragile X syndrome by newborn screening for methylated FMR1 DNA. American Journal of Human Genetics 2009; 85(4): 503-14.

Coffey SM, Cook K, Tartaglia N, Tassone F, Nguyen DV, Pan R*, et al.* Expanded clinical phenotype of women with the FMR1 premutation. American Journal of Medical Genetics 2008; 146A(8): 1009-16.

Cohen S, Masyn K, Adams J, Hessl D, Rivera S, Tassone F*, et al.* Molecular and imaging correlates of the fragile X-associated tremor ataxia syndrome. Neurology 2006; 67(8): 1426-31.

Colak D, Zaninovic N, Cohen MS, Rosenwaks Z, Yang WY, Gerhardt J*, et al.* Promoter-bound trinucleotide repeat mRNA drives epigenetic silencing in fragile X syndrome. Science 2014; 343(6154): 1002-5.

Collette F, Hogge M, Salmon E, Van Der Linden M. Exploration of the neural substrates of executive functioning by functional neuroimaging. Neuroscience 2006; 139: 209-21.

Conde V, Palomar FJ, Lama MJ, Martínez R, Carrillo F, Pintado E*, et al.* Abnormal GABA-mediated and cerebellar inhibition in women with the fragile X premutation. J Neurophysiol 2013; 109(5): 1315-22.

Corbetta M, Shulman GL. Control of goal-directed and stimulus-driven attention in the brain. Nature reviews Neuroscience 2002; 3(3): 201-15.

Cornish K, Turk J, Hagerman R. The fragile X continuum: new advances and perspectives. Journal of Intellectual Disability Research 2008a; 52(Pt 6): 469-92.

Cornish KM, Hocking DR, Moss SA, Kogan CS. Selective executive markers of at-risk profiles associated with the fragile X premutation. Neurology 2011; 77(7): 618-22.

Cornish KM, Kogan CS, Li L, Turk J, Jacquemont S, Hagerman RJ. Lifespan changes in working memory in fragile X premutation males. Brain and Cognition 2009; 69(3): 551-8.

Cornish KM, Kogan CS, Turk J, Manly T, James N, Mills A*, et al.* The emerging fragile X premutation phenotypes: evidence from the domain of social cognition. Brain and Cognition 2005; 57: 53-60.

Cornish KM, Kraan CM, Bui MQ, Bellgrove MA, Metcalfe SA, Troller JN*, et al.* Novel methylation markers of the dysexecutive-psychiatric phenotype in FMR1 premutation women. Neurology 2015; 84(16): 1631-8.

Cornish KM, Li L, Kogan CS, Jacquemont S, Turk J, Dalton A*, et al.* Age-dependent cognitive changes in carriers of the fragile X syndrome. Cortex 2008b; 44(6): 628-36.
Courtney SM, Ungerleider LG, Keil K, Haxby JV. Object and spatial visual working memory activate separate neural systems in human cortex. Cerebral Cortex 1996; 6(1): 39-49.
Curtis CE, D'Esposito M. Success and failure suppressing reflexive behaviour. J Cogn Neurosci 2003; 15(3): 409-18.
Curtis CE, D'Esposito M. Selection and maintenance of saccade goals in the human frontal eye fields. J Neurophysiol 2006; 95(6): 3923-7.
Curtis CE, Rao VY, D'Esposito M. Maintenance of spatial and motor codes during oculomotor delayed response tasks. Journal of Neuroscience 2004; 24: 3944-52.
Cynader M, Berman N. Receptive-field organization of monkey superior colliculus. J Neurophysiol 1972; 35(2): 187-201.
D'Esposito M. From cognitive to neural models of working memory. Philos Trans R Soc Lond: B Biol Sci 2007; 362(1481): 761-72.
De Pablo-Fernandez E, Doherty KM, Holton JL, Revesz T, Djamshidian A, Limousin P*, et al.* Concomitant fragile X-associated tremor ataxia syndrome and Parkinson's disease: a clinicopathological report of two cases. Journal of Neurology, Neurosurgery, and Psychiatry 2014; epub ahead of print.
DeSimone K, Weiler J, Aber GS, Heath M. The unidirectional prosaccade switch-cost: Correct and error antisaccades differentially influence the planning times for subsequent prosaccades. Vision research 2014; 96: 17-24.
Elizur SE, Dratviman-Storobinsky O, Derech-Haim S, Lebovitz O, Dor J, Orvieto R*, et al.* FMR6 may play a role in the pathogenesis of fragile X-associated premature ovarian insufficiency. Gynecological endocrinology 2015: 1-4.
Fatemi SH, Folsom TD. The role of fragile X mental retardation protein in major mental disorders. Neuropharmacology 2011; 60(7–8): 1221-6.
Fielding J, Corben L, Cremer P, Millist L, White O, Delatycki M. Disruption to higher order processes in Friedreich ataxia. Neuropsychologia 2010; 48(1): 235-42.
Fielding J, Georgiou-Karistianis N, Bradshaw J, Millist L, White O. No sequence dependent modulation of the Simon effect in Parkinson's disease. Brain Research Cognitive Brain Research 2005; 25(1): 251-60.
Fielding J, Georgiou-Karistianis N, Millist L, White O. Temporal variation in the control of goal-directed visuospatial attention in basal ganglia disorders. Neurosci Res 2006; 54(1): 57-65.
Fielding J, Kilpatrick T, Millist L, Clough M, White O. Longitudinal assessment of antisaccades in patients with multiple sclerosis. PLoS ONE 2012; 7(2): 1-4.
Filley CM. Fragile X tremor ataxia syndrome and white matter dementia. The Clinical neuropsychologist 2016: 1-12.
Filley CM, Brown MS, Onderko K, Ray M, Bennett RE, Berry-Kravis E*, et al.* White matter disease and cognitive impairment in FMR1 premutation carriers. Neurology 2015; 84(21): 2146-52.
Fischl B. FreeSurfer. NeuroImage 2012; 62(2): 774-81.
Fischl B, Dale AM. Measuring the thickness of the human cerebral cortex from magnetic resonance images. Proc Natl Acad Sci USA 2000; 97: 11050-5.
Fischl B, Salat DH, Busa E, Albert M, Dieterich M, Haselgrove C*, et al.* Whole brain segmentation: Automated labeling of neuroanatomical structures in the human brain. Neuron 2002; 2002(33): 341-55.

Fischl B, Salat DH, van der Kouwe AJ, Makris N, Segonne F, Quinn BT*, et al.* Sequence-independent segmentation of magnetic resonance images. NeuroImage 2004; 23(S1): S69-S84.

Fortea J, Sala-Llonch R, Bartres-Faz D, Bosch B, Llado A, Bargallo N*, et al.* Increased cortical thickness and caudate volume precede atrophy in PSEN1 mutation carriers. Journal of Alzheimer's disease : JAD 2010; 22(3): 909-22.

Franke C, Reuter B, Schulz L, Kathmann N. Schizophrenia patients show impaired response switching in saccade tasks. Biological psychology 2007; 76(1-2): 91-9.

Franke P, Leboyer M, Hardt J, Sohne E, Weiffenbach O, Biancalana V*, et al.* Neuropsychological profiles of FMR-1 premutation and full-mutation carrier females. Psychiatry Research 1999; 87(2–3): 223-31.

Fuchs AF, Robinson FR, Straube A. Role of the caudal fastigial nucleus in saccade generation. I. Neuronal discharge pattern. J Neurophysiol 1993; 70(5): 1723-40.

Gallagher JC. Effect of early menopause on bone mineral density and fractures. Menopause (New York, NY) 2007; 14(3 Pt 2): 567-71.

Gallego PK, Burris JL, Rivera SM. Visual motion processing deficits in infants with the fragile X premutation. Journal of Neurodevelopmental Disorders 2014; 6(1): 29.

Georgopoulos AP. Neural aspects of cognitive motor control. Current Opinion in Neurobiology 2000; 10: 238-41.

Girard B, Berthoz A. From brainstem to cortex: Computational models of saccade generation circuitry. Progress in neurobiology 2005; 77(4): 215-51.

Godijn R, Pratt J. Endogenous saccades are preceded by shifts of visual attention: evidence from cross-saccadic priming effects. Acta Psychologica 2002; 110: 83-102.

Godler DE, Inaba Y, Shi EZ, Skinner C, Bui QM, Francis D*, et al.* Relationships between age and epi-genotype of the FMR1 exon 1/intro 1 boundary are consistent with non-random X-chromosome inactivation in FM individuals, with the selection for the unmethylated state being most significant between birth ad puberty. Human Molecular Genetics 2013; 22(8).

Godler DE, Slater HR, Amor D, Loesch DZ. Methylation analysis of fragile X-related epigenetic elements may provide newborn screening test for fragile X syndrome. Genetics in Medicine 2010a; 12(9): 595.

Godler DE, Slater HR, Bui QM, Ono M, Gehling F, Francis D*, et al.* FMR1 intron 1 methylation predicts FMRP expression in blood of female carriers of expanded FMR1 alleles. Journal of Molecular Diagnostics 2011; 13(5): 528-36.

Godler DE, Slater HR, Bui QM, Storey E, Ono MY, Gehling F*, et al.* Fragile X mental retardation (FMR1) intro 1 methylation in blood predicts verbal cognitive impairment in female carriers of expanded FMR1 alleles: evidence from a pilot study. Clinical Chemistry 2012; 58(3): 590-8.

Godler DE, Tassone F, Loesch DZ, Taylor AK, Gehling F, Hagerman RJ*, et al.* Methylation of novel markers of fragile X alleles is inversely correlated with FMRP expression and FMR1 activation ratio. Human Molecular Genetics 2010b; 75(3): 255-60.

Goldberg ME, Bisley J, Powell KD, Gottlieb J, Kusunoki M. The role of the lateral intraparietal area of the monkey in the generation of saccades and visuospatial attention. Annals of the New York Academy of Science 2002; 956: 205-15.

Goldberg ME, Bisley JW, Powell KD, Gottlieb J. Saccades, salience and attention: the role of the lateral intraparietal area in visual behavior. Progress in brain research 2006; 155: 157-75.

Golden CJ. Stroop colour and word test: A manual for clinical and experimental uses. Illinois, USA: Stoelting; 1978.

Golden CJ, Freshwater SM. The stroop colour and word test: A manual for clinical and experimental uses. Illinois, USA: Stoelting Co.; 2002.

Goodrich-Hunsaker NJ, Wong LM, McLennan Y, Srivastava S, Tassone F, Harvey D*, et al.* Young adult female fragile X premutation carriers show age- and genetically-modulated cognitive impairments. Brain and Cognition 2011a; 75(3): 255-60.

Goodrich-Hunsaker NJ, Wong LM, McLennan Y, Tassone F, Harvey D, Rivera SM*, et al.* Adult female fragile X premutation carriers exhibit age- and CGG repeat length-related impairments on an attentionally based enumeration task. Frontiers of Human Neuroscience 2011b; 5.

Goto Y, Hatakeyama K, Kitama T, Sato Y, Kanemura H, Aoyagi K*, et al.* Saccade eye movements as a quantitative measure of frontostriatal network in children with ADHD. Brain Dev 2010; 32(5): 347-55.

Greco CM, Berman RF, Martin RM, Tassone F, Schwartz PH, Chang A*, et al.* Neuropathology of fragile X-associated tremor/ataxia syndrome (FXTAS). Brain 2006; 129(1): 243-55.

Greco CM, Hagerman RJ, Tassone F, Chudley AE, Del Bigio MR, Jacquemont S*, et al.* Neuronal intranuclear inclusions in a new cerebellar tremor/ataxia syndrome among fragile X carriers. Brain 2002; 125(8): 1769-71.

Grigsby J, Brega AG, Engle K, Leehey MA, Hagerman RJ, Tassone F*, et al.* Cognitive profile of fragile X premutation carriers with and without fragile X-associated tremor/ataxia syndrome. Neuropsychology 2008; 22(1): 48-60.

Grigsby J, Brega AG, Jacquemont S, Loesch DZ, Leehey MA, Goodrich GK*, et al.* Impairment in the cognitive functioning of men with fragile X-associated tremor/ataxia syndrome (FXTAS). Journal of the neurological sciences 2006; 248(1-2): 227-33.

Grigsby J, Brega AG, Leehey MA, Goodrich GK, Jacquemont S, Loesch DZ*, et al.* Impairment of executive cognitive functioning in males with fragile X-associated tremor/ataxia syndrome. Movement Disorders 2007; 22(5): 645-50.

Grigsby J, Cornish K, Hocking D, Kraan C, Olichney JM, Rivera SM*, et al.* The cognitive neuropsychological phenotype of carriers of the FMR1 premutation. Journal of Neurodevelopmental Disorders 2014; 6(1-8): 28.

Grigsby J, Kaye K. The behavioural dyscontrol scale: Manual. 2nd ed. Denver, CO.; 1996.

Gronwall DMA. Paced auditory serial-addition task: a measure of recovery from concussion. Percept Mot Skill 1977; 44(2): 367-73.

Grosbras MH, Lobel E, Van de Moortele PF, LeBihan D, Berthoz A. An anatomical landmark for the supplementary eye fields in human revealed with functional magnetic resonance imaging. Cereb Cortex 1999; 9(7): 705-11.

Gunning-Dixon FM, Raz N. The cognitive correlates of white matter abnormalities in normal aging: a quantitative review. Neuropsychology 2000; 14(2): 224-34.

Hadd AG, Filipovic-Sadic S, Zhou L, Williams A, Latham GJ, Berry-Kravis E*, et al.* A methylation PCR method determines FMR1 activation ratios and differentiates premutation allele mosaicism in carrier siblings. Clin Epigenetics 2016; 8: 130.

Hagerman R, Hagerman P. Advances in clinical and molecular understanding of the *FMR1* premutation and fragile X-associated tremor/ataxia syndrome. Lancet Neurology 2013; 12: 786-98.

Hagerman RJ, Coffey SM, Maselli R, Soontarapornchai K, Brunberg JA, Leehey MA*, et al.* Neuropathy as a presenting feature in fragile X-associated tremor/ataxia syndrome. Am J Med Genet A 2007; 143A(19): 2256-60.

Hagerman RJ, Hagerman P. Fragile X-associated tremor/ataxia syndrome - features, mechanisms and management. Nature reviews Neurology 2016; 12(7): 403-12.

Hagerman RJ, Leavitt BR, Farzin F, Jacquemont S, Greco CM, Brunberg JA*, et al.* Fragile-X-associated tremor/ataxia syndrome (FXTAS) in females with the FMR1 premutation. Am J Hum Genet 2004; 74(5): 1051-6.

Hagerman RJ, Leehey M, Heinrichs W, Tassone F, Wilson R, Hills J*, et al.* Intention tremor, parkinsonism, and generalised brain atrophy in male carriers of fragile X. Neurology 2001; 57: 127-30.

Hall D, Todorova-Koteva K, Pandya S, Bernard B, Ouyang B, Walsh M*, et al.* Neurological and endocrine phenotypes of fragile X carrier women. Clinical Genetics 2015; NA: NA.

Hall DA, Birch RC, Anheim M, Jonch AE, Pintado E, O'Keefe J*, et al.* Emerging topics in FXTAS. Journal of Neurodevelopmental Disorders 2014; 6(1): 31-41.

Hall DA, Robertson-Dick EE, O'Keefe JA, Hadd AG, Zhou L, Berry-Kravis E. X-inactivation in the clinical phenotype of fragile X premutation carrier sisters. Neurology Genetics February 2016a; 2: 1.

Hall DA, Robertson E, Shelton AL, Losh MC, Mila M, Moreno EG*, et al.* Update on the Clinical, Radiographic, and Neurobehavioral Manifestations in FXTAS and FMR1 Premutation Carriers. Cerebellum 2016b; 15(5): 578-86.

Hamlin A, Liu Y, Nguyen DV, Tassone F, Zhang L, Hagerman RJ. Sleep apnea in fragile X premutation carriers with and without FXTAS. Am J Med Genet B Neuropsychiatr Genet 2011; 156b(8): 923-8.

Hamlin A, Sukharev D, Campos L, Mu Y, Tassone F, Hessl D*, et al.* Hypertension in FMR1 premutation males with and without fragile X-associated tremor/ataxia syndrome (FXTAS). Am J Med Genet A 2012; 158a(6): 1304-9.

Hashimoto R, Backer KC, Tassone F, Hagerman RJ, Rivera SM. An fMRI study of the prefrontal activity during the performance of a working memory task in premutation carriers of the fragile X mental retardation 1 gene with and without fragile X-associated tremor/ataxia syndrome (FXTAS). J Psychiatr Res 2011a; 45(1): 36-43.

Hashimoto R, Javan AK, Tassone F, Hagerman RJ, Rivera SM. A voxel-based morphometry study of grey matter loss in fragile X-assocaited tremor/ataxia syndrome. Brain 2011b; 134(3): 863-78.

Hashimoto R, Srivastava S, Tassone F, Hagerman RJ, Rivera SM. Diffusion tensor imaging in male premutation carriers of the fragile X mental retardation gene. Movement Disorders 2011c; 26(7): 1329-36.

Heide W, Kompf D. Combined deficits of saccades and visuo-spatial orientation after cortical lesions. Exp Brain Res 1998; 123(1-2): 164-71.

Hellemans J, Mortier G, De Paepe A, Speleman F, Vandesompele J. qBase relative quantification framework and software for management and automated analysis of real-time quantitative PCR data. Genome Biology 2007; 8(2): R19-R.

Henderson T, Georgiou-Karistianis N, White O, Millist L, Williams DR, Churchyard A*, et al.* Inhibitory control during smooth pursuit in Parkinson's disease and Huntington's disease. Movement Disorders 2011; 26(10): 1893-9.

Herzfeld DJ, Kojima Y, Soetedjo R, Shadmehr R. Encoding of action by the Purkinje cells of the cerebellum. Nature 2015; 526(5753).

Hessl D, Rivera S, Koldewyn K, Cordeiro L, Adams J, Tassone F*, et al.* Amygdala dysfunction in men with the fragile X premutation. Brain 2007; 130(Pt 2): 404-16.

Hessl D, Wang JM, Schneider A, Koldewyn K, Le L, Iwahashi C*, et al.* Decreased Fragile X Mental Retardation Protein Expression Underlies Amygdala Dysfunction in Carriers of the Fragile X Premutation. Biological psychiatry 2011; 70(9): 859-65.

Hikosaka O, Sakamoto M, Usui S. Functional properties of monkey caudate neurons. III. Activities related to expectation of target and reward. J Neurophysiol 1989; 61(4): 814-32.

Hikosaka O, Takikawa Y, Kawagoe R. Role of the basal ganglia in the control of purposive saccadic eye movements. Physiological reviews 2000; 80(3): 953-78.

Hippolyte L, Battistell G, Perrin AG, Fornari E, Cornish KM, Beckmann JS*, et al.* Investigation of memory, executive functions and anatomical correlates in asymptomatic FMR1 premutation carriers. Neurobiology of Aging 2014; 35(8): 1939-46.

Hocking DR, Kogan CS, Cornish KM. Selective spatial processing deficits in an at-risk subgroup of the fragile X premutation. Brain Cogn 2012; 79(1): 39-44.

Hocking DR, Kraan CM, Godler DE, Bui QM, Li X, Bradshaw JL*, et al.* Evidence linking *FMR1* mRNA and attentional demands of stepping and postural control in women with the premutation. Neurobiology of Aging 2015; 36(3): 1400-8.

Hundscheid RD, Smits AP, Thomas CM, Kiemeney LA, Braat DD. Female carriers of fragile X premutations have no increased risk for additional diseases other than premature ovarian failure. Am J Med Genet A 2003; 117a(1): 6-9.

Hunsaker MR, Goodrich-Hunsaker NJ, Willemsen R, Berman RF. Temporal ordering deficits in female CGG KI mice heterozygous for the fragile X premutation. Behavioural Brain Research 2010; 213(2): 263-8.

Hunsaker MR, von Leden RE, Ta BT, Goodrich-Hunsaker NJ, Arque G, Kim K*, et al.* Motor deficits on a ladder rung task in male and female adolescent and adult CGG knock-in mice. Behavioural Brain Research 2011; 222(1): 117-21.

Hunter JE, Allen EG, Abramowitz A, Rusin M, Leslie M, Novak G*, et al.* No Evidence for a Difference in Neuropsychological Profile among Carriers and Noncarriers of the FMR1 Premutation in Adults under the Age of 50. The American Journal of Human Genetics 2008; 83(6): 692-702.

Hunter JE, Epstein MP, Tinker SW, Abramowitz A, Sherman SL. The FMR1 premutation and attention-deficit hyperactivity disorder (ADHD): evidence for a complex inheritance. Behav Genet 2012a; 42(3): 415-22.

Hunter JE, Leslie M, Novak G, Hamilton D, Shubeck L, Charen K*, et al.* Depression and anxiety symptoms among women who carry the FMR1 premutation: impact of raising a child with fragile X syndrome is moderated by CRHR1 polymorphisms. American Journal of Medical Genetics 2012b; 159B(5): 549-59.

Hunter JE, Sherman S, Grigsby J, Kogan C, Cornish K. Capturing the fragile X premutation phenotypes: a collaborative effort across multiple cohorts. Neuropsychology 2012c; 26(2): 156-64.

Hutton SB. Cognitive control of saccadic eye movements. Brain Cogn 2008; 68(3): 327-40.

Inaba Y, Herlihy AS, Schwartz CE, Skinner C, Bui QM, Cobb J*, et al.* Fragile X-related element 2 methylation analysis may provide a suitable option for inclusion of

fragile X syndrome and/or sex chromosome aneuploidy into newborn screening: a technical validation study. Genetics in Medicine 2013; 15(4): 290-8.

Inaba Y, Schwartz CE, Bui QM, Li X, Skinner C, Field M*, et al.* Early detection of fragile X syndrome: applications of a novel approach for improced quantitative methylation analysis in venous blood and newborn blood spots. Clinical Chemistry 2014; 60(7).

Jacquemont S, Hagerman RJ, Hagerman PJ, Leehey MA. Fragile-X syndrome and fragile X-assocaited tremor/ataxia syndrome: two faces of *FMR1*. Lancet Neurol 2007; 6(1): 45-55.

Jacquemont S, Hagerman RJ, Leehey M, Grigsby J, Zhang L, Brunberg JA*, et al.* Fragile X premutation tremor/ataxia syndrome: molecular, clinical, and neuroimaging correlates. Am J Hum Genet 2003; 72(4): 869-78.

Jacquemont S, Vingerhoets F, Maeder P, Battistella G, Gronchi A, Niederhauser J*, et al.* Early white matter alterations in men predisposed to FXTAS revealed by MT imaging. 16th Annual Meeting of the Organization for Human Brain Mapping; 2010; Barcelona, Spain; 2010.

Jäkälä P, Hänninen T, Ryynänen M, Laakso M, Partanen K, Mannermaa A*, et al.* Fragile-X: Neuropsychological test performance, CCG triplet repeat lengths, and hippocampal volumes. The journal of Clinical Invsetigation 1997; 100(2): 331-8.

Jamadar S, Fielding J, Egan G. Quantitative Meta-Analysis Reveals Consistent fMRI activation in fronto-striatal-parietal regions and cerebellum during antisaccades and prosaccades. Frontiers in Cognition 2013.

Jamadar S, Johnson BP, Clough M, Egan GF, Fielding J. Behavioural and neural plasticity of ocular motor control: changes in performance and fMRI activity following antisaccade training. Frontiers in Human Neuroscience 2015; 9.

Jeter CB, Patel SS, Sereno AB. Novel n-back spatial working memory task using eye movement response. Behavior Research Methosd 2011; 43(3): 879-87.

Johnston K, Everling S. Neurophysiology and neuroanatomy of reflexive and voluntary saccades in non-human primates. Brain Cogn 2008; 68(3): 271-83.

Jonides J, Smith EE, Koeppe RA, Awh E, Minoshima S, Mintun MA. Spatial working memory in humans as revealed by PET. Nature 1993; 363: 623-5.

Jubault T, Gagnon JF, Karama S, Ptito A, Lafontaine AL, Evans AC*, et al.* Patterns of cortical thickness and surface area in early Parkinson's disease. Neuroimage 2011; 55(2): 462-7.

Juncos JL, Lazarus JT, Graves-Allen E, Shubeck L, Rusin M, Novak G*, et al.* New clinical findings in the fragile X-associated tremor ataxia syndrome (FXTAS). Neurogenetics 2011; 12: 123-35.

Kalantaridou SN, Naka KK, Papanikolaou E, Kazakos N, Kravariti M, Calis KA*, et al.* Impaired endothelial function in young women with premature ovarian failure: normalization with hormone therapy. The Journal of clinical endocrinology and metabolism 2004; 89(8): 3907-13.

Kamali A, Kramer LA, Frye RE, Butler IJ, Hasan KM. Diffusion Tensor Tractography of the Human Brain Cortico-Ponto-Cerebellar Pathways: A Quantitative Preliminary Study. Journal of magnetic resonance imaging : JMRI 2010; 32(4): 809-17.

Kaufmann WE, Abrams MT, Chen W, Reiss AL. Genotype, molecular phenotype, and cognitive phenotype: correlations in fragile X syndrome. Am J Med Genet 1999; 83(4): 286-95.

Kelly RM, Strick PL. Cerebellar loops with motor cortex and prefrontal cortex of a nonhuman primate. The Journal of neuroscience : the official journal of the Society for Neuroscience 2003; 23(23): 8432-44.

Kemper MB, Hagerman RJ, Altshul-Stark D. Cognitive profiles of boys with the fragile X syndrome. American Journal of Medical Genetics 1988; 30: 191-200.

Keri S, Benedek G. Why is vision impaired in fragile X premutation carriers? The role of fragile X mental retardation protein and potential FMR1 mRNA toxicity. Neuroscience 2012; 206: 183-9.

Kéri S, Benedek G. Visual pathway deficit in female fragile X premutation carriers: a potential endophenotype. Brain Cogn 2009; 69(2): 291-5.

Kéri S, Benedek G. The perception of biological and mechanical motion in female fragile X premutation carriers. Brain Cogn 2010; 72(2): 197-201.

Khalil AM, Faghihi MA, Modarresi F, Brothers SP, Wahlestedt C. A Novel RNA Transcript with Antiapoptotic Function Is Silenced in Fragile X Syndrome. PLoS ONE 2008; 3(1): e1486.

Kheradmand A, Zee DS. Cerebellum and Ocular Motor Control. Frontiers in Neurology 2011; 2: 1-15.

Kim S-Y, Hashimoto R, Tassone F, Simon TJ, Rivera SM. Altered neural activity of magnitude estimation processing in adults with the fragile x premutation. J Psychiatr Res 2013; 47: 1909-16.

Kim S-Y, Tassone F, Simon TJ, Rivera SM. Altered neural activity in the 'when' pathway during temporal processing in fragile X premutation carriers. Behavioural Brain Research 2014; 261: 240-8.

Kogan CS, Cornish KM. Mapping self-reports of working memory deficits to executive dysfunction in fragile X mental retardation 1 (FMR1) gene premutation carriers asymptomatic for FXTAS. Brain Cogn 2010; 73(3): 236-43.

Kolbe S, Mitchell P, Kipatrick T, White O, Egan G, Fielding J. Dysfunctional inhibitory eye movements are associated with cerebellar injury in multiple sclerosis. Hum Brain Mapp in press April 2013.

Koldewyn K, Hessl D, Adams J, Tassone F, Hagerman PJ, Hagerman RJ*, et al.* Reduced hippocampal activation during recall is associated with elevated FMR1 mRNA and psychiatric symptoms in men with the fragile X premutation. Brain Imaging and Behaviour 2008; 2: 105-16.

Koukoui SD, Chaudhuri A. Neuroanatomical, molecular genetic, and behavioral correlates of fragile X syndrome. Brain Research Reviews 2007; 53(1): 27-38.

Koziol LF, Budding DE, Chidekel D. From movement to thought: exective function, embodied cognition, and the cerebellum. Cerebellum 2012; 11: 505-25.

Kraan CM, Cornish KM, Bui QM, Li X, Slater HR, Godler DE. Beta-glucuronidase mRNA levels are correlated with gait and working memory in premutation females: understanding the role of FMR1 premutation alleles. Scientific Reports 2016; 6: 29366.

Kraan CM, Hocking D, Georgiou-Karistianis N, Metcalfe S, Archibald A, Fielding J*, et al.* Age and CGG-repeat length are associated with neuromotor impairments in at-risk females with the *FMR1* premutation. Neurobiology of Aging 2014a; 35(9).

Kraan CM, Hocking DR, Bradshaw JL, Fielding J, Cohen J, Georgiou-Karistianis N*, et al.* Neurobehavioural evidence for the involvement of the FMR1 gene in female carriers of fragile X syndrome. Neurosci Biobehav Rev 2013a; 37(3): 522-47.

Kraan CM, Hocking DR, Bradshaw JL, Georgiou-Karistianis N, Metcalfe SA, Archibald AD*, et al.* Symbolic sequence learning is associated with cognitve-affective profiles in female FMR1 premutation carriers. Genes, Brain, and Behavior 2014b; 13(4): 385-93.

Kraan CM, Hocking DR, Georgiou-Karistianis N, Metcalfe SA, Archibald AD, Fielding J*, et al.* Cognitive-motor interference during postural control indicates at-risk cerebellar profiles in females with the FMR1 premutation. Behavioural Brain Research 2013b; 253: 329-36.

Kraan CM, Hocking DR, Georgiou-Karistianis N, Metcalfe SA, Archibald AD, Fielding J*, et al.* Impaired response inhibition is associated with self-reported symptoms of depression, anxiety, and ADHD in female FMR1 premutation carriers. American Journal of Medical Genetics: Part B Neuropsychiatric Genetics 2014c; 165(1): 41-51.

Krauzlis RJ. The control of voluntary eye movements: new perspectives. Neuroscientist 2005; 11(2): 124-37.

Kumari D, Usdin K. The distribution of repressive histone modifications on silenced FMR1 alleles provides clues to the mechanism of gene silencing in fragile X syndrome. Human Molecular Genetics 2010; 19(23): 4634-42.

Lachiewicz A, M., Dawson DV, Spiridigliozzi GA, McConkie-Rosell A. Arithmetic difficulties in females with the fragile X premutation. American Journal of Medical Genetics 2006; 140A(7): 65-672.

Ladd PD, Smith LE, Rabaia NA, Moore JM, Georges SA, Hansen RS*, et al.* An antisense transcript spanning the CGG repeat region of *FMR1* is upregulated in premutation carriers but silenced in full mutation individuals. Human Molecular Genetics 2007; 16(24): 3174-87.

Lasker AG, Mazzocco MM, Zee DS. Ocular motor indicators of executive dysfunction in fragile X and Turner syndromes. Brain Cogn 2007; 63(3): 203-20.

Leehey MA. Fragile X-associated tremor/ataxia syndrome; clinical phenotype diagnosis, and treatment. J Investig Med 2009; 57: 830-6.

Leehey MA, Berry-Kravis E, Goetz CG, Zhang L, Hall DA, Li L*, et al.* FMR1 CGG repeat length predicts motor dysfunction in premutation carriers. Neurology 2008; 70(16): 1397-402.

Leehey MA, Legg W, Tassone F, Hagerman R. Fibromyalgia in fragile X mental retardation 1 gene premutation carriers. Rheumatology (Oxford, England) 2011; 50(12): 2233-6.

Leigh RJ, Zee DS. The neurology of eye movements. 4th ed ed. New York: Oxford University Press; 2006.

Leow A, Harvey D, Goodrich-Hunsaker NJ, Gadelkarim J, Kumar A, Zhan L*, et al.* Altered structural brain connectome in young adult fragile X premutation carriers. Human Brain Mapping 2014; 35(9): 4518-30.

Linden DEJ, Bittner RA, Muckli L, Waltz JA, Kriegeskorte N, Goebel R*, et al.* Cortical capacity constraints for visual working memory: dissociation of fMRI load effects in a fronto-parietal network. NeuroImage 2003; 20: 1518-30.

Loesch D, Godler DE, Evans A, Bui QM, Gehling F, Kotschet K*, et al.* Evidence for the toxicity of bidirectional transcripts and mitochondrial dysfunction in blood associated with small CGG expansions in the FMR1 gene in patients with parkinsonism. . Genetics in Medicine 2011; 13: 392-9.

Loesch D, Hagerman R. Unstable mutations in the FMR1 gene and the phenotypes. Advances in Experimental Medicine and Biology 2012; 769: 78-114.

Loesch D, Litewka L, Brotchie P, Huggins RM, Tassone F, Cook M. Magnetic resonance imaging study in older fragile x premutation male carriers. Ann Neurol 2005a; 58(2): 326-30.

Loesch DZ, Bui QM, Dissanayake C, Clifford S, Gould E, Bulhak-Paterson D*, et al.* Molecular and cognitive predictors of the continuum of autistic behaviours in fragile X. Neuroscience & Biobehavioral Reviews 2007; 31(3): 315-26.

Loesch DZ, Bui QM, Grigsby J, Butler E, Epstein J, Huggins RM*, et al.* Effect of the fragile X status categories and the fragile X mental retardation protein levels on executive functioning in males and females with fragile X. Neuropsychology 2003; 17(4): 646-57.

Loesch DZ, Cook M, Litewka L, Gould E, Churchyard A, Tassone F*, et al.* A low symptomatic form of neurodegeneration in younger carriers of FMR1 premutation, manufesting typical radiological changes. Journal of Medical Genetics 2008; 45(3): 179-81.

Loesch DZ, Khaniani MS, Slater HR, Rubio JP, Bui QM, Kotschet K*, et al.* Small CGG repeat expansion alleles of FMR1 gene are associated with parkinsonism. Clin Genet 2009; 76: 471-6.

Loesch DZ, Litewka L, Brotchie P, Huggins RM, Tassone F, Cook M. Magnetic resonance imaging study in older fragile X premutation male carriers. Ann Neurol 2005b; 58(2): 326-30.

Losh M, Klusek J, Martin GE, Sideris J, Parlier M, Piven J. Defining genetically meaningful language and personality traits in relatives of individuals with fragile X syndrome and relatives of individuals with autism. Am J Med Genet B Neuropsychiatr Genet 2012; 159b(6): 660-8.

Luo Y, Shan G, Guo W, Smrt RD, Johnson EB, Li X*, et al.* Fragile x mental retardation protein regulates proliferation and differentiation of dult neural stem/progenitor cells PloS Genetics 2010; 6(4).

Lynch JC, Tian JR. Cortico-cortical networks and cortico-subcortical loops for the higher control of eye movements. Progress in brain research 2006; 151: 461-501.

Madden DJ, Bennett IJ, Song AW. Cerebral white matter integrity and cognitive aging: cntributions from diffusion tensor imaging. Neuropsychology Review 2009a; 19(4): 415-35.

Madden DJ, Bennett IJ, Song AW. Cerebral white matter integrity and cognitive aging: Contributions from diffusion tensor imaging. Neuropsychology review 2009b; 19(4): 415-35.

Madhyastha TM, Askren MK, Boord P, Zhang J, Leverenz JB, Grabowski TJ. Cerebral perfusion and cortical thickness indicate cortical involvement in mild Parkinson's disease. Mov Disord 2015; 30(14): 1893-900.

Martorell L, Tondo M, Garcia-Fructuoso F, Naudo M, Alegre C, Gamez J*, et al.* Screening for the presence of FMR1 premutation alleles in a Spanish population with fibromyalgia. Clinical rheumatology 2012; 31(11): 1611-5.

Mays LE, Sparks DL. Dissociation of visual and saccade-related responses in superior colliculus neurons. J Neurophysiol 1980; 43(1): 207-32.

McDowell JE, Dyckman KA, Austin BP, Clementz BA. Neurophysiology and neuroanatomy of reflexive and volitional saccades: evidence from studies of humans. Brain Cogn 2008; 68(3): 255-70.

McLennan Y, Polussa J, Tassone F, Hagerman R. Fragile X Syndrome. Current Genomics 2011; 12: 216-24.

Meguid NA, Fahim C, Sami R, Nashaat NH, Yoon U, Anwar M*, et al.* Cognition and lobar morphology in full mutation boys with fragile X syndrome. Brain and Cognition 2012; 78(1): 74-84.

Metcalfe S, Jacques A, Archibald A, Burgess T, Collins V, Henry A*, et al.* A model for offering carrier screening for fragile X syndrome to nonpregnant women: results from a pilot study. Genet Med 2008; 10(7): 525-35.

Middleton FA, Strick PL. Cerebellar projections to the prefrontal cortex of the primate. The Journal of neuroscience : the official journal of the Society for Neuroscience 2001; 21(2): 700-12.

Moore CJ, Daly EM, Schmitz N, Tassone F, Tysoe C, Hagerman RJ*, et al.* A neuropsychological investigation of male premutation carriers of fragile X syndrome. Neuropsychologia 2004a; 42(14): 1934-47.

Moore CJ, Daly EM, Tassone F, Tysoe C, Schmitz N, Ng V*, et al.* The effect of pre-mutation of X chromosome CGG trinucleotide repeats on brain anatomy. Brain 2004b; 127(12).

Mori S, Wakana S, van Zijl PCM, Nagae-Poetscher LM. MRI Atlas of Human White Matter. Amsterdam, The Netherlands: Elsevier; 2005.

Moutou C, Vincent MC, Biancalana V, Mandel JL. Transition from premtuation to full mutation in fragile X syndrome is likely to be prezygotic. Human Molecular Genetics 1997; 6(7): 971-9.

Munoz DP, Everling S. Look away: the anti-saccade task and the voluntary control of eye movement. Nature reviews Neuroscience 2004; 5(3): 218-28.

Munoz DP, Wurtz RH. Saccade-related activity in monkey superior colliculus. I. Characteristics of burst and buildup cells. J Neurophysiol 1995; 73(6): 2313-33.

Muri RM, Nyffeler T. Neurophysiology and neuroanatomy of reflexive and volitional saccades as revealed by lesion studies with neurological patients and transcranial magnetic stimulation (TMS). Brain Cogn 2008; 68(3): 284-92.

Murphy DGM, Mentis MJ, Pietrini P, Grady CL, Moore CJ, Horwitz B*, et al.* Premutation Female Carriers of Fragile X Syndrome: A Pilot Study on Brain Anatomy and Metabolism. J Am Acad Child Adolesc Psychiatry 1999; 38(10): 1294-301.

Murray A, Ennis S, MacSwiney F, Webb J, Morton NE. Reproductive and menstrual history of females and fragile X expansions. European Journal of Human Genetics 2000; 8(4): 247-52.

Muzar Z, Adams PE, Schneider A, Hagerman RJ, Lozano R. Addictive substances may induce a rapid neurological deterioration in fragile X-associated tremor ataxia syndrome: A report of two cases. Intractable & Rare Diseases Research 2014; 3(4): 162-5.

Nagel BJ, Ohannessian, A., Cummins, K. Performance dissociation during verbal and spatial working memory tasks. Perceptual and Motor Skills 2007; 105(1): 243-50.

Narcisa V, Aguilar D, Nguyen DV, Campos L, Brodovsky J, White S*, et al.* A Quantitative Assessment of Tremor and Ataxia in Female FMR1 Premutation Carriers Using CATSYS. Current gerontology and geriatrics research 2011; 2011: 484713.

Neidhart M. Chapter 3 - DNA Methylation and Epigenetic Biomarkers in Non-Neoplastic Diseases. DNA Methylation and Complex Human Disease. Oxford: Academic Press; 2016. p. 29-43.

Niendam TA, Laird AR, Ray KL, Dean YM, Clahn DC, Carter CS. Meta-analytic evidence for a superordinate cognitive control network subserving diverse executive functions. Cognitive Affective Behavioural Neuroscience 2012; 12(2): 241-68.

Niu YQ, Yang JC, Hall DA, Leehey MA, Tassone F, Olichney JM*, et al.* Parkinsonism in fragile X-associated tremor/ataxia syndrome (FXTAS): revisited. Parkinsonism Relat Disord 2014; 20(4): 456-9.

Noda H, Sugita S, Ikeda Y. Afferent and efferent connections of the oculomotor region of the fastigial nucleus in the macaque monkey. The Journal of comparative neurology 1990; 302(2): 330-48.

Nolin SL, Glicksman A, Ding X, Ersalesi N, Brown WT, Sherman SL*, et al.* Fragile X analysis of 1112 prenatal samples from 1991 to 2010. Prenatal diagnosis 2011; 31(10): 925-31.

Nolin SL, Sah S, Glicksman A, Sherman SL, Allen E, Berry-Kravis E*, et al.* Fragile X AGG analysis provides new risk predictions for 45-69 repeat alleles. Am J Med Genet A 2013; 161A(4): 771-8.

Nyffeler T, Egli A, Pflugshaupt T, von Wartburg R, Wurtz P, Mosimann U*, et al.* The role of the human posterior parietal cortex in memory-guided saccade execution: a double-pulse transcranial magnetic stimulation study. The European journal of neuroscience 2005; 22(2): 535-8.

O'Keefe J, Robertson-Dick E, Dunn EJ, Li Y, Deng Y, Fiutko AN*, et al.* Characterization and Early Detection of Balance Deficits in Fragile X Premutation Carriers with and without fragile X-assocaited tremor/ataxia syndrome (FXTAS). The Cerebellum 2015a.

O'Keefe JA, Robertson-Dick EE, Hall DA, Berry-Kravis E. Gait and functional mobility deficits in Fragile X-Associated tremor/ataxia syndrome. The Cerebellum 2015b.

Ohtsuka K, Noda H. Discharge properties of Purkinje cells in the oculomotor vermis during visually guided saccades in the macaque monkey. J Neurophysiol 1995; 74(5): 1828-40.

Oostra BA, Willemsen R. FMR1: a gene with three faces. Biochimica et biophysica acta 2009; 1790(6): 467-77.

Osaka N, Osaka M, Kondo H, Morishita M, Fukuyama H, Shibasaki H. The neural basis of executive function in working memory: an fMRI study based on individual differences. NeuroImage 2004; 21(2): 623-31.

Owen AM, McMillan KM, Laird AR, Bullmore E. N-back working memory paradigm: a meta-analysis of normative functional neuroimaging studies. Human Brain mapping 2005; 25: 46-59.

Oyama G, Umemura A, Shimo Y, Nishikawa N, Nakajima A, Jo T*, et al.* Posterior Subthalamic Area Deep Brain Stimulation for Fragile X-associated Tremor/Ataxia syndrome. Neuromodulation: Technology at the Neural Interface 2014.

Pastori C, Peschansky VJ, Barbouth D, Mehta A, Silva JP, Wahlestedt C. Comprehensive analysis of the transcriptional landscape of the human FMR1 gene reveals two new long noncoding RNAs differentially expressed in Fragile X syndrome and Fragile X-associated tremor/ataxia syndrome. Human Genetics 2014; 133(1): 59-67.

Peprah E, He W, Allen EG, Oliver T, Boyne A, Sherman SL. Examination of FMR1 transcipt and protein levels among 74 premutation carriers. J Hum Genet 2010; 55(1): 66-8.

Pierrot-Deseilligny C, Müri RM, Ploner CJ, Gaymard B, Rivaud-Péchoux S. Cortical control of ocular saccades in humans: a model for motricity. In: C. Prablanc DPYR, editor. Progress in brain research: Elsevier; 2003. p. 3-17.

Pierrot-Deseilligny C, Rivaud S, Gaymard B, Müri R, Vermersch AI. Cortical control of saccades. Annals of Neurology 1995; 37(5): 557-67.

Ptak R, Müri RM. The parietal cortex and saccade planning: lessons from human lesion studies. Frontiers in Human Neuroscience 2013; 7: 254.

Qiu L, Lui S, Kuang W, Huang X, Li J, Li J*, et al.* Regional increases of cortical thickness in untreated, first-episode major depressive disorder. Translational Psychiatry 2014; 4(4): e378.

Raffelt D, Tournier JD, Rose S, Ridgway GR, Henderson R, Crozier S*, et al.* Apparent Fibre Density: a novel measure for the analysis of diffusion-weighted magnetic resonance images. Neuroimage 2012; 59(4): 3976-94.

Raffelt DA, Smith RE, Ridgway GR, Tournier JD, Vaughan DN, Rose S*, et al.* Connectivity-based fixel enhancement: Whole-brain statistical analysis of diffusion MRI measures in the presence of crossing fibres. Neuroimage 2015; 117: 40-55.

Ramnani N. The primate cortico-cerebellar system: anatomy and function. Nature Reviews: Neuroscience 2006; 7: 511-22.

Ramnani N. Frontal lobe and posterior parietal contributions to the cortico-cerebellar system. Cerebellum 2012; 11: 366-83.

Renaud M, Fourcade G, Castelnovo G. Teaching NeuroImages: Corpus callosum splenium hyperintensity in fragile X-associated tremor ataxia syndrome. Neurology 2015a; 84(22): 194.

Renaud M, Perriard J, Coudray S, Sévin-Allouet M, Marcel C, Meissner WG*, et al.* Relevance of corpus callosum splenium versus middle cerebellar peduncle hyperintensity for FXTAS diagnosis in clinical practise. Journal of Neurology, Neurosurgery, and Psychiatry 2015b; 262: 435-42.

Reuter B, Kathmann N. Using saccade tasks as a tool to analyze executive dysfunctions in schizophrenia. Acta Psychol (Amst) 2004; 115(2-3): 255-69.

Rivera S, Stebbins GT, Grigsby J. Radiological Findings in FXTAS. In: Tassone F, Berry-Kravis EM, editors. The Fragile X-Associated Tremor Ataxia Syndrome (FXTAS): Springer Science; 2010. p. 55-66.

Robertson KD. DNA methylation and human disease. Nat Rev Genet 2005; 6(8): 597-610.

Rodriguez-Revenga L, Madrigal I, Blanch-Rubio J, Elurbe DM, Docampo E, Collado A*, et al.* Screening for the presence of FMR1 premutation alleles in women with fibromyalgia. Gene 2013; 512(2): 305-8.

Rodriguez-Revenga L, Madrigal I, Pagonabarraga J, Xuncla M, Badenas C, Kulisevsky J*, et al.* Penetrance of FMR1 premutation associated pathologies in fragile x syndrome families. European Journal of Human Genetics 2009; 17(10): 1359-62.

Rogers H, Ariza J, Monterrubio A, Hagerman P, Martínez-Cerdeño V. Cerebellar Mild Iron Accumulation in a Subset of FMR1 Premutation Carriers with FXTAS. The Cerebellum 2016: 1-4.

Schaffner SF. The X chromosome in population genetics. Nat Rev Genet 2004; 5(1): 43-51.

Schall JD, Morel A, Kaas JH. Topography of supplementary eye field afferents to frontal eye field in macaque: implications for mapping between saccade coordinate systems. Vis Neurosci 1993; 10(2): 385-93.

Schlag-Rey M, Amador N, Sanchez H, Schlag J. Antisaccade performance predicted by neuronal activity in the supplementary eye field. Nature 1997; 390(6658): 398-401.

Schneider A, Ballinger E, Chavez A, Tassone F, Hagerman RJ, Hessl D. Prepulse inhibition in patients with fragile X-associated tremor ataxia syndrome. Neurobiol Aging 2012; 33(6): 1045-53.

Schneider A, Hagerman RJ, Hessl D. Fragile X syndrome -- from genes to cognition. Developmental disabilities research reviews 2009; 15(4): 333-42.

Schubert MC, Zee DS. Saccade and vestibular ocular motor adaptation. Restorative neurology and neuroscience 2010; 28(1): 9-18.

Scudder CA. Role of the fastigial nucleus in controlling horizontal saccades during adaptation. Annals of the New York Academy of Sciences 2002; 978: 63-78.

Scudder CA, Kaneko CS, Fuchs AF. The brainstem burst generator for saccadic eye movements: a modern synthesis. Exp Brain Res 2002; 142(4): 439-62.

Scudder CA, Moschovakis AK, Karabelas AB, Highstein SM. Anatomy and physiology of saccadic long-lead burst neurons recorded in the alert squirrel monkey. II. Pontine neurons. J Neurophysiol 1996; 76(1): 353-70.

Sellier C, Usdin K, Pastori C, Peschansky VJ, Tassone F, Charlet-Berguer N. The multiple molecular facets of fragile X-associated tremor/ataxia syndrome. Journal of Neurodevelopmental Disorders 2014; 6(1).

Selmeczy D, Koldewyn K, Wang JM, Lee A, Harvey D, Hessl DR*, et al.* Investigation of amygdala volume in men with the fragile X premutation. Brain Imaging and Behaviour 2011; 5: 285-94.

Seltzer MM, Baker MW, Hong J, Maenner M, Greenberg J, Mandel D. Prevalence of CGG expansions of the FMR1 gene in a US population-based sample. American Journal of Medical Genetics 2012a; 159B(5): 589-97.

Seltzer MM, Barker ET, Greenberg JS, Hong J, Coe C, Almeida D. Differential sensitivity to life stress in FMR1 premutation carrier mothers of children with fragile X syndrome. Health psychology : official journal of the Division of Health Psychology, American Psychological Association 2012b; 31(5): 612-22.

Semenza C, Bonollo S, Polli R, Busana C, Pignatti R, Iuculano T*, et al.* Genetics and mathematics: FMR1 premutation female carriers. Neuropsychologia 2012; 50(14): 3757-63.

Seritan AL, Nguyen DV, Farias ST, Hinton L, Grigsby J, Bourgeois JA*, et al.* Dementia in fragile X-associated tremor/ataxia syndrome (FXTAS): comparison with Alzheimer's disease. American Journal of Medical Genetics 2008; 147B(7): 1138-44.

Sestieri C, Pizzella V, Cianflone F, Romani GL, Corbetta M. Sequential activation of human oculomotor centers during planning of visually-guided eye movements: a combined fMRI-MEG study. Frontiers of Human Neuroscience 2008; 1(1): 1-8.

Shafiq-Antonacci R, Maruff P, Masters C, Currie J. Spectrum of saccade system function in Alzheimer disease. Arch Neurol 2003; 60(9): 1272-8.

Shelton AL, Cornish K, Clough M, Gajamange S, Kolbe S, Fielding J. Disassociation between brain activation and executive function in fragile X premutation females. Human Brain Mapping 2016a, in press.

Shelton AL, Cornish K, Kraan C, Georgiou-Karistianis N, Metcalfe SA, Bradshaw JL*, et al.* Exploring inhibitory deficits in female premutation carriers of fragile X syndrome: through eye movements. Brain and Cognition 2014; 85: 201-8.

Shelton AL, Cornish KM, Godler DE, Clough M, Kraan C, Bui MQ*, et al.* Delineation of the working memory profile in female FMR1 premutation carriers: The effect of cognitive load on ocular motor responses. Behavioural Brain Research 2015; 282(1): 194-200.

Shelton AL, Cornish KM, Kolbe S, Clough MC, Slater HR, Li X*, et al.* Brain structure and intragenic DNA methylation are correlated, and predict executive dysfunction in Fragile X premutation females. Translational Psychiatry 2016b; 6(12).

Shelton AL, Cornish KM, Kraan CM, Lozano R, Bui M, Fielding J. Executive Dysfunction in Female FMR1 Premutation Carriers. Cerebellum 2016c; 15(5): 565-9.

Sherman SL. Premature ovarian failure among fragile X premutation carriers: Parent-of-origin effect? Am J Hum Genet 2000; 67(1): 11-3.

Sherman SL, Curnow EC, Easley CA, Jin P, Hukema RK, Tejada MI*, et al.* Use of model systems to understand the etiology of fragile X-associated primary ovarian insufficiency. Journal of Neurodevelopmental Disorders 2014; 6(1).

Shimo Y, Hikosaka O. Role of tonically active neurons in primate caudate in reward-oriented saccadic eye movement. The Journal of neuroscience : the official journal of the Society for Neuroscience 2001; 21(19): 7804-14.

Silk TJ, Bellgrove MA, Wrafter P, Mattingley JB, Cunnington R. Spatial working memory and spatial attention rely on common neural processes in the intraparietal sulcus. NeuroImage 2010; 53(2): 718-24.

Singer M, Kosti I, Pachter L, Mandel-Gutfreund Y. A diverse epigenetic landscape at human exons with implication for expression. Nucleic Acids Research 2015.

Smith A. Symbol Digit Modalities Test. Los Angeles: Western Psychological Services; 1973.

Smith SM, Jenkinson M, Johansen-Berg H, Rueckert D, Nichols TE, Mackay CE*, et al.* Tract-based spatial statistics: voxelwise analysis of multi-subject diffusion data. Neuroimage 2006; 31(4): 1487-505.

Smith SM, Jenkinson M, Woolrich MW, Beckmann CF, Behrens TE, Johansen-Berg H*, et al.* Advances in functional and structural MR image analysis and implementation as FSL. Neuroimage 2004; 23 Suppl 1: S208-19.

Soontarapornchair K, Maselli R, Renton-Farrell G, Tassone F, Hagerman PJ, Hessl D*, et al.* Abnormal nerve conduction features in fragile X premutation carriers. Arch Neurol 2008; 65(4): 495-8.

Spath MA, Nillesen WN, Smits AP, Feuth TB, Braat DD, van Kessel AG*, et al.* X chromosome inactivation does not define the development of premature ovarian failure in fragile X premutation carriers. Am J Med Genet A 2010; 152A(2): 387-93.

St Laurent G, Shtokalo D, Tackett MR, Yang Z, Eremina T, Wahlestedt C*, et al.* Intronic RNAs constitute the major fraction of the non-coding RNA in mammalian cells. BMC Genomics 2012; 13(1): 1-23.

Sterling AM, Mailick M, Greenberg J, Warren SF, Brady N. Language dysfluencies in females with the FMR1 premutation. Brain and Cognition 2013; 82: 84-9.

Stevenson RE, Rogers RC, Schwartz CE. Atlas of X-Linked Intellectual Disability Syndromes. New York: Oxford University Press; 2012.

Steyaert J, Legius E, Borghgraef M, Fryns JP. A distinct neurocognitive phenotype in female fragile-X premutation carriers assessed with visual attention tasks. American Journal of Medical Genetics 2003a; 116A(1): 44-51.

Steyaert J, Legius E, Borghgraef M, Fryns JP. A distinct neurocognitive phenotype in female fragile X premutation carriers assessed with visual attention tasks. American Journal of Medical Genetics 2003b; 116(1): 44-51.

Stoodley CJ. The Cerebellum and Cognition: Evidence from Functional Imaging Studies. The Cerebellum 2012; 11: 352-65.

Stoodley CJ, Schmahmann JD. Evidence for topographic organization in the cerebellum of motor control versus cognitive and affective processing. Cortex 2010; 46(7): 831-44.

Streuli I, Fraisse T, Ibecheole V, Moix I, Morris MA, de Ziegler D. Intermediate and premutation FMR1 alleles in women with occult primary ovarian insufficiency. Fertility and sterility 2009; 92(2): 464-70.

Sullivan AK, Marcus M, Epstein. MP, Allen EG, Anido AE, Paquin JJ*, et al.* Association of FMR1 repeat size and ovarian dysfunction. Human Reproduction 2005; 20(2): 402-12.

Summers SM, Cogswell J, Goodrich JE, Mu Y, Nguyen DV, Brass SD*, et al.* Prevalence of restless legs syndrome and sleep quality in carriers of the fragile X premutation. Clin Genet 2014; 86(2): 181-4.

Tassone F, Adams J, Berry-Kravis EM, Cohen SS, Brusco A, Leehey MA*, et al.* CGG repeat length correlates with age of onset of motor signs of the fragile X-associated tremor/ataxia syndrome (FXTAS). American Journal of Medical Genetics 2007a; 144B(4): 566-9.

Tassone F, Beilina A, Carosi C, Albertosi S, Bagni C, Li L*, et al.* Elevated FMR1 mRNA in premutation carriers is due to increased transcription. Rna 2007b; 13(4): 555-62.

Tassone F, Hagerman RJ, Garcia-Arocena D, Khandjian EW, Greco CM, Hagerman PJ. Intracellular inclusions in neural cells with premutation alleles in fragile X associated tremor/ataxia syndrome. Journal of Medical Genetics 2004a; 41(4): 43-5.

Tassone F, Hagerman RJ, Iklé DN, Dver PN, Lampe M, Willemsen R*, et al.* FMRP expression as a potential prognostic indicator in fragile X syndrome. American Journal of Medical Genetics 1999; 84(3): 250-61.

Tassone F, Hagerman RJ, Taylor AK, Gane LW, Godfrey TE, Hagerman PJ. Elevated levels of FMR1 mRNA in carrier males: a new mechanism of involvement in the fragile-X syndrome. Am J Hum Genet 2000; 66(1): 6-15.

Tassone F, Iwahashi C, Hagerman PJ. FMR1 RNA within the intranuclear inclusions of fragile X-associated tremor/ataxia syndrome (FXTAS). RNA biology 2004b; 1(2): 103-5.

Tassone F, Long KP, Tong TH, Lo J, Gane LW, Berry-Kravis E*, et al.* FMR1 CGG allele size and prevalence ascertained through newborn screening in the United States. Genome Med 2012; 4(12): 100-13.

Tehovnik EJ, Lee K, Schiller PH. Stimulation-evoked saccades from the dorsomedial frontal cortex of the rhesus monkey following lesions of the frontal eye fields and superior colliculus. Exp Brain Res 1994; 98(2): 179-90.

Tejada MI, Garcia-Alegria E, Bilbao A, Martinez-Bouzas C, Beristain E, Poch M*, et al.* Analysis of the molecular parameters that could predict the risk of manifesting premature ovarian failure in female premutation carriers of fragile X syndrome. Menopause (New York, NY) 2008; 15(5): 945-9.

Tervonen TA, Louhivuori V, Sun X, Hokkanen ME, Kratochwil CF, P. Z*, et al.* Aberrant differentiation of glutamatergic cells in neocortex of mouse model for fragile X syndrome. Neurobiology of Disease 2009; 33(2): 250-9.

Todd PK, Oh SY, Krans A, He F, Sellier C, Frazer M*, et al.* CGG Repeat Associated Translation Mediates Neurodegeneration in Fragile X Tremor Ataxia Syndrome. Neuron 2013; 78(3): 440-55.

Tournier JD, Calamante F, Connelly A. MRtrix: diffusion tractography in crossing fiber regions. International Journal of Imaging Systems 2012; 22(1): 53-66.

Turken AU, Whitfield-Gabrieli S, Bammer R, Baldo J, Dronkers NF, Gabrieli JDE. Cognitive processing speed and the structure of white matter pathways: Convergent evidence from normal variation and lesion studies. NeuroImage 2008; 42(2): 1032-44.

van der Knaap LJ, van der Ham IJ. How does the corpus callosum mediate interhemispheric transfer? A review. Behav Brain Res 2011; 223(1): 211-21.

Van der Stigchel S, Van Koningsbruggen M, Nijboer TCW, List A, Rafal RD. The role of the frontal eye fields in the oculomotor inhibition of reflecive saccades: Evidence from lesion patients. Neuropsychologia 2012; 50: 198-203.

Van Gisbergen JA, Robinson DA, Gielen S. A quantitative analysis of generation of saccadic eye movements by burst neurons. J Neurophysiol 1981; 45(3): 417-42.

Van Opstal J, Hepp K, Suzuki Y, Henn V. Role of monkey nucleus reticularis tegmenti pontis in the stabilization of Listing's plane. The Journal of neuroscience : the official journal of the Society for Neuroscience 1996; 16(22): 7284-96.

Vandenberghe R, Molenberghs P, Gillebert CR. Spatial attention deficits in humans: the critical role of superior compared to inferior parietal lesions. Neuropsychologia 2012; 50(6): 1092-103.

Wang JM, Koldewyn K, Hashimoto R, Schneider A, Le L, Tassone F*, et al.* Male carriers of the FMR1 premutation show altered hippocampal-prefrontal function during memory encoding. Frontiers in Human Neuroscience 2012a; 6.

Wang JY, Hessl D, Iwahashi C, Cheung K, Schneider A, Hagerman RJ*, et al.* Influence of the fragile X mental retardation (FMR1) gene on the brain and working memory in men with normal FMR1 alleles. NeuroImage 2013a; 65: 288-98.

Wang JY, Hessl D, Schneider A, Tassone F, Hagerman RJ, Rivera SM. Fragile X-associated tremor/ataxia syndrome: influence of the FMR1 gene on motor fiber tracts in males with normal and premutation alleles. JAMA Neurol 2013b; 70(8): 1022-9.

Wang Y, Hessl D, Hagerman R, Tassone F, Rivera SM. Age-dependent structural connectivity effects in fragile x premutation. Archive of Neurology 2012b; 69(4): 482-9.

Wechsler D. WAIS-III administration and scoring manual. San Antonio, Texas, USA: Psychological Corportation; 1997.

Wechsler D. Wechsler abbreviated scale of intelligence (WASI). San Antonio: Pearson Inc 1999.

Wheeler AC, Bailey DB, Berry-Kravis E, Greenberg J, Losh M, Mailick M*, et al.* Associated features in females with an FMR1 premutation. Journal of Neurodevelopmental Disorders 2014; 6(1).

Willemsen R, Hoogeveen-Westerveld M, Reis S, Holstege J, Severijnen L-A, W. F. M., Nieuwenhuizen IM*, et al.* The *FMR1* CGG repeat mouse displays ubiquitin-positive intranuclear neuronal inclusions; implications for the cerebellar tremor/ataxia syndrome. Human Molecular Genetics 2003; 12(9): 949-59.

Willemsen R, Levenga J, Oostra BA. CGG repeat in the FMR1 gene: size matters. Clinical Genetics 2011; 80(3): 214-25.

Willemsen R, Oostra BA, Bassell GJ, Dictenberg J. The fragile X syndrome: from molecular genetics to neurobiology. Mental Retardation and Development Disabilities Research Reviews 2004; 10: 60-7.

Wilson LB, Tregellas JR, Hagerman RJ, Rogers SJ, Rojas DC. A voxel-based morphometry comparison of regional gray matter between fragile X syndrome and autism. Psychiatry Research: Neuroimaging 2009; 174(2): 138-45.

Winarni TI, Chonchaiya W, Sumekar TA, Ashwood P, Morales GM, Tassone F*, et al.* Immune-mediated disorders among women carriers of fragile X premutation alleles. Am J Med Genet A 2012; 158A(10): 2473-81.

Winkler AM, Ridgway GR, Webster MA, Smith SM, Nichols TE. Permutation inference for the general linear model. NeuroImage 2014; 92: 381-97.

Wittenberger MD, Hagerman RJ, Sherman SL, McConkie-Rosell A, Welt CK, Rebar RW*, et al.* The FMR1 premutation and reproduction. Fertility and sterility 2007; 87(3): 456-65.

Wong LM, Goodrich-Hunsaker NJ, McLennan Y, Tassone F, Harvey D, Rivera SM*, et al.* Young adult male carriers of the fragile X premutation exhibit genetically modulated impairements in visuospatial tasks controlled for psychomotor speed. Journal of Developmental Disorders 2012; 4(1).

Wong LM, Goodrich-Hunsaker NJ, McLennan Y, Tassone F, Zhang M, Rivera SM*, et al.* Eye movements reveal impaired inhibitory control in adult male fragile x premutation carriers asymptomatic for FXTAS. Neuropsychology 2014; in press.

Wong LM, Goodrich-Hunsaker NJ, McLennan YA, Tassone F, Rivera SM, Simon TJ. A cross-sectional analysis of orienting of visuospatial attention in child and adult carriers of the fragile X premutation. Journal of Neurodevelopmental Disorders 2015; 6(45).

Yang J-C, Simon C, Niu Y-Q, Bogost M, Schneider A, Tassone F*, et al.* Phenotypes of hypofrontality in older female fragile x premutation carriers. Ann Neurol 2013; 74(2): 275-83.

Yao B, Lin L, Street RC, Zalewski ZA, Galloway JN, Wu H*, et al.* Genome-wide alteration of 5-hydroxymethylcytosine in a mouse model of fragile X-associated tremor/ataxia syndrome. Human Molecular Genetics 2014; 23(4): 1095-107.

Yeo BT, Krienen FM, Sepulcre J, Sabuncu MR, Lashkari D, Hollinshead M*, et al.* The organization of the human cerebral cortex estimated by intrinsic functional connectivity. J Neurophysiol 2011; 106(3): 1125-65.

Yrigollen CM, Durbin-Johnson B, Gane L, Nelson DL, Hagerman R, Hagerman PJ*, et al.* AGG interruptions within the maternal FMR1 gene reduce the risk of offspring with fragile X syndrome. Genet Med 2012; 14(8): 729-36.

Yrigollen CM, Martorell L, Durbin-Johnson B, Naudo M, Genoves J, Murgia A*, et al.* AGG interruptions and maternal age affect FMR1 CGG allele stability during transmission. Journal of Neurodevelopmental Disorders 2014a; 6(1).

Yrigollen CM, Sweha S, Durbin-Johnson B, Zhou L, Berry-Kravis E, Fernandez-Carvajal I*, et al.* Distribution of AGG interruption patterns within nine world populations. Intractable & Rare Diseases Research 2014b; 3(4): 153-61.

Yugeta A, Terao Y, Fukuda H, Hikosaka O, Yokochi F, Okiyama R*, et al.* Effects of STN stimulation on the initiation and inhibition of saccade in Parkinson disease. Neurology 2010; 74(9): 743-8.

Zangenehpour S, Cornish KM, Chaudhuri A. Whole-brain expression analysis of FMRP in adult monkey and its relationship to cognitive deficits in fragile X syndrome. Brain research 2009; 1264(0): 76-84.

Zannas AS, West AE. Epigenetics and the regulation of stress vulnerability and resilience. Neuroscience 2014; 264: 157-70.

Zee DS, Walker M. Cerebellum and Oculomotor Control. In: Editor-in-Chief: Larry RS, editor. Encyclopedia of Neuroscience. Oxford: Academic Press; 2009. p. 729-36.